

# **Understanding the Arctic marine carbon cycle under changing climate: a reconstruction of productivity and biogenic carbon burial on the West Greenland margin of the Baffin Bay**

Dissertation

zur Erlangung des akademischen Grades eines Doktors der Naturwissenschaften

-Dr. rer. nat.-

am Fachbereich Geowissenschaften der Universität Bremen/

submitted for the doctoral degree in natural sciences -Dr. rer. nat.-

at the faculty of Geosciences of Bremen University

vorgelegt von/

by

**Sabrina Hohmann**

born on 10 January 1985 in Bremen

submitted on 21 February 2023

**Gutachter/ Reviewers:**

Prof. Dr. Michal Kucera, MARUM – Zentrum für Marine Umweltwissenschaften, Universität Bremen  
Prof. Dr. Audrey Limoges, UNB – University of New Brunswick

**Datum des Kolloquiums/ Date of colloquium:** 20 June 2023





## Versicherung an Eides Statt

gem. § 5 Abs. 5 der Promotionsordnung vom 18.06.2018

Ich Sabrina Hohmann, versichere an Eides Statt durch meine Unterschrift, dass ich die vorliegende Dissertation selbständig und ohne fremde Hilfe angefertigt und alle Stellen, die ich wörtlich dem Sinne nach aus Veröffentlichungen entnommen habe, als solche kenntlich gemacht habe, mich auch keiner anderen als der angegebenen Literatur oder sonstiger Hilfsmittel bedient habe und die zu Prüfungszwecken beigelegte elektronische Version (PDF) der Dissertation mit der abgegebenen gedruckten Version identisch ist.

Ich versichere an Eides Statt, dass ich die vorgenannten Angaben nach bestem Wissen und Gewissen gemacht habe und dass die Angaben der Wahrheit entsprechen und ich nichts verschwiegen habe.

Die Strafbarkeit einer falschen eidesstattlichen Versicherung ist mir bekannt, namentlich die Strafandrohung gemäß § 156 StGB bis zu drei Jahren Freiheitsstrafe oder Geldstrafe bei vorsätzlicher Begehung der Tat bzw. gemäß § 161 Abs. 1 StGB bis zu einem Jahr Freiheitsstrafe oder Geldstrafe bei fahrlässiger Begehung.

Bremen, 21. February 2023

---

Sabrina Hohmann





To Ludvig, Lilly & Livinus

“Aim for the stars.”



## **Table of Contents**

Abstract.....	9
Zusammenfassung.....	12
<b><u>Chapter 1</u></b>	
<b>Introduction .....</b>	<b>16</b>
1.1 The marine carbon cycle: interaction with climate change.....	16
1.2 Baffin Bay: where change hits hard.....	19
1.3 Primary productivity: the troublemaker .....	23
1.4 Dinoflagellate cysts and a transfer function: saviours of the day? .....	25
1.5 Thesis objectives outline .....	27
<b><u>Chapter 2</u></b>	
<b>Description of own contributions.....</b>	<b>31</b>
<b><u>Chapter 3</u></b>	
<b>Identifying the signature of sea-surface properties in dinocyst assemblages: Implications for quantitative palaeoceanographical reconstructions by transfer functions and analogue techniques (Manuscript I).....</b>	<b>33</b>
Abstract .....	33
3.1 Introduction .....	34
3.2 Data .....	36
3.3. Data analysis .....	38
3.3.1 <i>Data treatment</i> .....	38
3.3.2 <i>Transfer functions and analogue techniques</i> .....	43
3.3.3 <i>Transfer function and analogue technique performance statistics</i> .....	45
3.4 Results.....	46
3.5 Discussion .....	55
3.6 Conclusion .....	63
3.7 Data availability.....	64
3.8 Acknowledgements.....	64
3.9 References (Chapter 3).....	64
3.10 Supplementary material .....	70
<b><u>Chapter 4</u></b>	
<b>Disentangling environmental drivers of Subarctic dinocyst assemblage compositional change during the Holocene (Manuscript II) .....</b>	<b>71</b>
Abstract .....	71
4.1 Introduction .....	72
4.2 Material and methods .....	77
4.2.1 <i>Data</i> .....	77
4.2.2 <i>Data analysis</i> .....	80
4.3. Results.....	84
4.3.1 <i>Multiple factor analysis</i> .....	84
4.3.2 <i>Redundancy analysis</i> .....	87
4.3.3 <i>Spatial autocorrelation</i> .....	89
4.3.4 <i>Cross-validation</i> .....	89

4.3.5 <i>Transfer function significances in sediment core reconstructions</i> .....	91
4.4 Discussion .....	95
4.5 Conclusion .....	100
4.6 Data availability .....	101
4.7 Acknowledgements .....	101
4.8 References (Chapter 4).....	101
4.9 Supplementary material .....	108
<b>Chapter 5</b>	
<b>Holocene biogenic carbon production and deposition on the West Greenland margin of the Baffin Bay (Manuscript III).....</b>	<b>112</b>
Abstract .....	112
5.1 Introduction .....	113
5.2 Regional setting .....	117
5.3 Material and methods .....	118
5.3.1 <i>Sediment core</i> .....	118
5.3.2 <i>Proxy selection</i> .....	119
5.3.3 <i>Foraminifera analysis</i> .....	121
5.4 Results.....	121
5.4.1 <i>Dinocysts</i> .....	121
5.4.2 <i>Foraminifera</i> .....	126
5.4.3 <i>Bulk parameters and biomarkers</i> .....	127
5.5 Discussion .....	127
5.5.1 <i>Primary productivity</i> .....	127
5.5.2 <i>Export productivity</i> .....	130
5.5.3 <i>Burial flux</i> .....	132
5.5.4 <i>Burial efficiency</i> .....	134
5.5.5 <i>Carbonate preservation</i> .....	135
5.5.6 <i>Palaeoceanography</i> .....	137
5.6 Conclusion .....	142
5.7 Data availability .....	143
5.8 Acknowledgements.....	143
5.9 References (Chapter 5).....	143
<b>Chapter 6</b>	
<b>Conclusions and outlook.....</b>	<b>154</b>
6.1 Conclusion .....	154
6.2 Implications and outlook.....	154
Acknowledgements .....	<b>159</b>
Datasets .....	<b>160</b>
References (Chapters 1,2 and 6) .....	<b>162</b>

# Abstract

The continued input of anthropogenic carbon dioxide (CO<sub>2</sub>) since the start of the Industrial Revolution has increased the atmospheric carbon dioxide content by around 100 ppm and is supposedly the highest experienced for at least the past 800,000 years and the fastest for millions of years. This increase presumably reflects only about 70% of the total additionally added CO<sub>2</sub> as the rest has supposedly been taken up by the ocean, acting as a reservoir for carbon and buffering the climatic feedback. The Earth's climate and the ocean's carbon reservoir interact through the marine carbon cycle and its driving factors have a substantial impact on carbon storage and atmospheric CO<sub>2</sub> concentrations.

The additional uptake of atmospheric CO<sub>2</sub> by the ocean changes marine chemistry. These changes, known as ocean acidification, negatively affect especially calcifying marine organisms and actively enhance calcium carbonate dissolution, implying changes in biological productivity and ecosystem dynamics with significant effects on carbon storage and sequestration from the atmosphere.

In the Arctic, increasing temperatures supposedly triggered by the increase in atmospheric CO<sub>2</sub>, led to an accelerating reduction in sea ice cover and ice sheet extent during the past three to four decades. As ice coverage controls nutrient release and light distribution, these changes will also trigger shifts in biological productivity and ecosystem processes. Furthermore, cold high-latitude oceans are already naturally more "acidic", condemning the Arctic realm to experience a greater-than-average response to a changing climate with profound effects on the marine carbon cycle. Therefore, a better understanding of biogeochemical processes in surface waters and in the sediment is of critical importance to understand the role of the future Arctic realm as a potential atmospheric carbon sink.

The ongoing rapid changes in terrestrial, coastal and offshore environments in the Arctic will have immense consequences for socio-ecological systems, requiring adequate information for governments of future developments in this region. However, projections of future twenty-first century changes in the behaviour of the marine carbon cycle from biogeochemical models differ strongly across models and their constraints, demanding sustainable constraints to improve projections of future Arctic climate and carbon cycling. The geological record provides an opportunity to provide observational constraints by assessing past interactions between changing climate conditions and the marine carbon cycle. The Baffin Bay area is a particular suitable region as it has experienced large changes in sea ice cover and its associated parameters during the Holocene (11.7 kyrs BP – present). The Holocene may serve as an example to estimate the direction and magnitude of possible future developments and as an equivalent for the recent environmental changes leading to a warmer climate.

Understanding the Arctic marine carbon cycle in the context of a changing climate requires the quantification of key constraints like primary productivity, export productivity and carbon burial. However, primary productivity being a fundamental driver of the marine carbon cycle fixing dissolved CO<sub>2</sub> into biomass, is notoriously difficult to quantify, since it does not leave a direct trace in the sediment. It has to be reconstructed indirectly from the signature of plankton community composition, which is associated with difficulties. Parameters commonly used to estimate past productivity from the geological record seem to be mostly influenced by other signals induced by diagenetic processes or other environmental parameters obliterating the signal of productivity.

With the aim to contribute to the understanding of the marine carbon cycle as a requirement for the provisioning of sustainable model constraints, the main prerequisite of this thesis was to establish a method for a nuisance free quantification of past primary productivity.

The new dinoflagellate cyst (dinocyst) database (n=1968), including modern dinocyst assemblage compositions from 1968 sites of top sediment samples from the Northern Hemisphere and the corresponding environmental parameters, provides a good opportunity for a nuisance free primary productivity quantification, especially in high latitudes. Dinocyst assemblages appear to reflect multiple parameters of the surface-ocean environment under which they were produced, including primary productivity. The specific interest in the first study (chapter 3) was to test if dinocyst assemblage compositions are significantly and independently driven by primary productivity. The study re-evaluates the regional impact of sea surface properties in dinocyst assemblages in general, not focussing solely on primary productivity and addresses the impact of diagenetically induced nuisance variables on the assemblages in the dinocyst database. Region specific primary drivers for assemblage compositions (including primary productivity) were identified, implying that primary productivity can be quantified independently from other drivers if it drives the composition in the certain area of interest and suggesting an advantage for nuisance-free quantification when local datasets are applied.

The interest in the second study (chapter 4) was to determine if the relationship between dinocyst assemblage composition and primary productivity is significant in the Baffin Bay area and if this relationship was significant in Holocene fossil assemblage compositions in the area. The study uses a locally calibrated dinocyst dataset and four Holocene sediment cores from a North-South transect throughout the Baffin Bay area to evaluate the impact of primary productivity on modern and Holocene assemblage compositions. Results imply that primary productivity is a less important driver for modern and Holocene assemblages in the area as they are/were primarily driven by hydrography changes. In Southern Melville Bay off the coast of West Greenland however, primary productivity played a major role in driving dinocyst compositions, posing the opportunity to reconstruct a nuisance-depleted primary productivity record for the Holocene in Southern Melville Bay.

With the potential of adequately quantifying primary productivity, the interest in the third study (chapter 5) was to evaluate the sensitivity of key components driving the marine carbon cycle to changing environmental boundary conditions. A sediment core from Southern Melville Bay (GeoB19927-3) served as generalisation to evaluate what drove these key components' (primary productivity, export productivity and burial) variability in time, conjecturing that this is what drives the variability across space and to provide constraints for future model projections. Results imply that during the ongoing effects of interglacial warming primary productivity, export productivity and organic carbon burial were decoupled during the Holocene in Melville Bay. This was probably caused by changes in export efficiency, induced by a combination of an increase in the efficiency of organic matter recycling in the productive zone and a decrease in preservation due to longer oxygen exposure times induced by low sedimentation rates and suggests that during meltwater-influenced warming conditions the efficiency of organic carbon burial is decreasing resulting in a weakening of the organic carbon pump .

These results advance the understanding of parameter quantification through the application of dinocyst assemblage compositions and can be used to refine palaeoceanographic reconstructions and interpretations. These results also enhance the understanding of the Arctic marine carbon cycle and can help to improve projections of its future behavior and future climate change.

# Zusammenfassung

Der kontinuierliche Eintrag von anthropogen erzeugtem Kohlenstoffdioxid ( $\text{CO}_2$ ) seit Beginn der industriellen Revolution hat den atmosphärischen Kohlenstoffdioxidgehalt um etwa 100 ppm erhöht und ist mutmaßlich der höchste Wert seit mindestens 800.000 Jahren und der schnellste Anstieg seit Millionen von Jahren. Dieser Anstieg spiegelt vermutlich nur etwa 70 % des zusätzlich anthropogen erzeugten  $\text{CO}_2$  wider, da der Rest mutmaßlich vom Ozean aufgenommen wurde, der als Kohlenstoffspeicher fungiert und die klimatischen Rückkopplungseffekte puffert. Das Klima der Erde und das Kohlenstoffreservoir des Ozeans stehen durch den marinen Kohlenstoffkreislauf in Wechselwirkung, und dessen treibende Faktoren haben einen erheblichen Einfluss auf die Kohlenstoffspeicherung und die atmosphärischen  $\text{CO}_2$ -Konzentrationen.

Die zusätzliche Aufnahme von atmosphärischem  $\text{CO}_2$  durch den Ozean verändert die chemische Zusammensetzung des Meerwassers. Diese als Ozeanversauerung bezeichneten Veränderungen wirken sich insbesondere auf kalkbildende Meeresorganismen negativ aus und fördern aktiv die Lösung von Kalziumkarbonat. Das führt zu Veränderungen der biologischen Produktivität und der Dynamik des Ökosystems und hat erhebliche Veränderungen in der Speicherung und Bindung von Kohlenstoff aus der Atmosphäre zur Folge.

In der Arktis hat der, vermutlich durch den Anstieg des atmosphärischen  $\text{CO}_2$  ausgelöste Temperaturanstieg in den letzten drei bis vier Jahrzehnten, zu einem beschleunigten Rückgang der Meereisbedeckung und der Ausdehnung der Eisschilde geführt. Da die Eisbedeckung die Freisetzung von Nährstoffen und die Lichtverteilung steuert, werden diese Veränderungen auch zu Verschiebungen der biologischen Produktivität und der Prozesse innerhalb des Ökosystems führen. Darüber hinaus sind die kalten Ozeane in hohen Breitengraden bereits von Natur aus "saurer", was dazu führt, dass die Arktis überdurchschnittlich stark auf den Klimawandel reagieren wird. Dies wird tiefgreifende Auswirkungen auf den marinen Kohlenstoffkreislauf haben. Aus diesem Grund ist ein besseres Verständnis der biogeochemischen Prozesse in Oberflächengewässern und im Ozean-sediment von entscheidender Bedeutung, um die zukünftige Rolle der Arktis als potenzielle atmosphärische Kohlenstoffsенke zu verstehen.

Die andauernden raschen Veränderungen der terrestrischen und küstennahen Gebiete als auch der Schelfgebiete in der Arktis werden immense Auswirkungen auf die sozio-ökologischen Systeme haben. Die Regierungen werden angemessene Informationen über die künftigen Entwicklungen in dieser Region benötigen. Vorhersagen zum Verhalten des marinen Kohlenstoffkreislaufs, das von biogeochemischen Modellen prognostiziert wird, unterscheiden sich jedoch stark zwischen den einzelnen Modellen und ihren definierten Randbedingungen. Um die Vorhersagen für das zukünftige arktische Klima und den Kohlenstoffkreislauf zu



verbessern ist es erforderlich, verlässliche Randbedingungen zu definieren. Geologische Daten bieten die Möglichkeit vergangene Wechselwirkungen zwischen sich ändernden Klimabedingungen und dem marinen Kohlenstoffkreislauf zu bewerten und durch Beobachtungsstudien Randbedingungen zu liefern. Das Gebiet der Baffin Bucht ist eine besonders gut geeignete Region für diese Studien, da es während des Holozäns (11.700 Jahre BP - heute) große Veränderungen in der Meereisbedeckung und den damit einhergehenden Parametern erfahren hat. Das Holozän kann als Beispiel zur Abschätzung der Richtung und des Ausmaßes einer möglichen zukünftigen Entwicklungen und als Äquivalent für die momentanen Umweltveränderungen dienen.

Das Verständnis des arktischen marinen Kohlenstoffkreislaufs im Kontext eines sich verändernden Klimas erfordert die Quantifizierung von Schlüsselparametern wie Primärproduktion, Exportproduktion und Kohlenstoffablagerung. Die Primärproduktion, die gelöstes CO<sub>2</sub> in Biomasse umwandelt und damit ein wesentlicher Faktor des marinen Kohlenstoffkreislaufs ist, ist jedoch bekanntermaßen schwer zu quantifizieren, da sie keine direkten Spuren im Sediment hinterlässt. Sie muss indirekt anhand der Zusammensetzung von Planktongemeinschaften rekonstruiert werden, was mit Schwierigkeiten verbunden ist. Die Parameter, die üblicherweise verwendet werden um vergangene Produktivität aus den geologischen Daten abzuschätzen, scheinen meist durch andere Signale beeinflusst zu werden, die durch diagenetische Prozesse oder andere Umweltparameter hervorgerufen werden und das Produktivitätssignal überlagern.

Mit dem Ziel, einen Beitrag zum Verständnis des marinen Kohlenstoffkreislaufs als Voraussetzung für die Definition verlässlicher Randbedingungen zu leisten, bestand die Hauptvoraussetzung dieser Arbeit darin, eine Methode für eine störungsfreie Quantifizierung von vergangener Primärproduktion zu entwickeln.

Die neue Datenbank für Dinoflagellatenzysten (Dinozysten) (n=1968) enthält die Zusammensetzung moderner Dinozysten-Gesellschaften und die entsprechenden Umweltparameter aus Oberflächensedimentproben von 1968 Standorten der nördlichen Hemisphäre. Sie bietet eine gute Möglichkeit um vergangene Primärproduktion störungsfrei zu quantifizieren, besonders in hohen Breitengraden. Dinozysten-Gesellschaften scheinen mehrere Umweltparameter der Meeresoberfläche widerzuspiegeln, in der sie entstanden sind, einschließlich Primärproduktion. Das besondere Interesse der ersten Studie (Kapitel 3) bestand darin, zu prüfen, ob die Zusammensetzung der Dinozysten-Gesellschaften signifikant und unabhängig von der Primärproduktion gesteuert wird. In dieser Studie wurden die regionalen Auswirkungen der Umweltparameter auf die Dinozysten-Gesellschaften im Allgemeinen neu bewertet, wobei der Schwerpunkt nicht nur auf Primärproduktion lag. Die Auswirkungen diagenetisch bedingter Störvariablen auf die Vergesellschaftung der Dinozysten wurden untersucht. Es wurden regionalspezifische primäre Steuerfaktoren für die

Zusammensetzung der Dinozysten-Gesellschaften (einschließlich Primärproduktion) identifiziert. Dies bedeutet, dass Primärproduktivität unabhängig von anderen Einflussfaktoren quantifiziert werden kann, wenn sie die Zusammensetzung der Vergesellschaftung in einem bestimmten Gebiet gesteuert haben. Dies legt nahe, dass lokal kalibrierte Dinozysten-Datensätze für eine störungsfreie Quantifizierung von Vorteil sind.

In der zweiten Studie (Kapitel 4) sollte festgestellt werden, ob die Zusammensetzungen der Dinozysten-Gesellschaften im Gebiet der Baffin Bucht von Primärproduktion gesteuert wird und ob die Zusammensetzung der fossilen Vergesellschaftungen im Holozän in diesem Gebiet ebenfalls von Primärproduktion gesteuert wurde. Die Studie verwendete einen lokal kalibrierten Dinozysten-Datensatz und vier holozäne Sedimentkerne aus einem Nord-Süd-Transekt im Gebiet der Baffin Bucht, um die Auswirkungen der Primärproduktion auf die Zusammensetzung moderner und holozäner Dinozysten-Gesellschaften zu untersuchen. Die Ergebnisse deuten darauf hin, dass die Primärproduktivität für die modernen und holozänen Vergesellschaftungen in diesem Gebiet eine weniger wichtige Rolle spielte, da sie in erster Linie durch Veränderungen der Hydrographie gesteuert werden bzw. wurden. In der südlichen Melville-Bucht vor der Küste Westgrönlands spielte Primärproduktion jedoch eine wichtige Rolle für die Zusammensetzung der Dinozysten-Gesellschaft. Dies bietet die Möglichkeit, Primärproduktion störungsarm für das Holozän in der südlichen Melville-Bucht zu rekonstruieren.

Angesichts des Potenzials, die Primärproduktivität angemessen zu quantifizieren, bestand das Interesse in der dritten Studie (Kapitel 5) darin, die Reaktion der Schlüsselkomponenten des marinen Kohlenstoffkreislaufs gegenüber veränderten Umweltbedingungen zu bewerten. Ein Sedimentkern aus der südlichen Melville-Bucht (GeoB19927-3) diente als Verallgemeinerung, um zu bewerten, was die zeitliche Variabilität dieser Schlüsselkomponenten (Primärproduktion, Exportproduktion und Ablagerung) antreibt. Dies sollte als Annahme dienen, dass diese Veränderungen auch die räumliche Variabilität antreiben um somit Randbedingungen für künftige Modellprognosen zu liefern. Die Ergebnisse deuten darauf hin, dass während der anhaltenden Auswirkungen der interglazialen Erwärmung Primärproduktivität, Exportproduktivität und Ablagerung von organischem Kohlenstoff während des Holozäns in der Melville-Bucht entkoppelt waren. Dies wurde vermutlich durch Veränderungen in der Exporteffizienz verursacht, die durch eine Kombination aus einem Anstieg der Effizienz des Recyclings organischer Stoffe in der produktiven Zone und einer Abnahme der Erhaltung aufgrund längerer Sauerstoffaussetzung durch niedrige Sedimentationsraten, hervorgerufen wurden. Dies deutet darauf hin, dass während einer schmelzwasserbegleitenden Erwärmung die Effizienz der Ablagerung organischen Kohlenstoffs abnimmt, was zu einer Schwächung der organischen Kohlenstoffpumpe führt.

Die Ergebnisse dieser Arbeit erweitern das Verständnis der Parameterquantifizierung mit Hilfe von Zusammensetzungen der Dinozysten-Gesellschaften und können zur Verfeinerung paläozeanographischer Rekonstruktionen und Interpretationen verwendet werden. Diese Ergebnisse verbessern auch das Verständnis des arktischen marinen Kohlenstoffkreislaufs und können dazu beitragen, Prognosen über dessen künftiges Verhalten und künftige Klimaänderungen zu verbessern.

# Chapter 1

## Introduction

### 1.1 The marine carbon cycle: interaction with climate change

During the last century an analysis of trapped air inside polar ice cores revealed, that the carbon dioxide (CO<sub>2</sub>) content of the Earth's atmosphere was on average lower during glacial times (180 ppm) than during the Holocene (280 ppm) (Berner et al. 1980; Delmas et al. 1980; Barnola et al. 1987). The continued input of anthropogenic CO<sub>2</sub> since the start of the Industrial Revolution has additionally increased the atmospheric carbon dioxide content by around 100 ppm (e.g. Jones et al. 1987; IPCC 2013). As further studies suggest that this increase is the highest experienced for at least the past 800,000 years (Lüthi et al., 2008) and the fastest for millions of years (Doney and Schimel, 2007), the concerns about consequences for future climate increase.

The increase in atmospheric CO<sub>2</sub> presumably reflects only about 70% of the total additionally added carbon dioxide as the rest has supposedly been taken up by the ocean (IPCC, 2013; Le Quéré et al., 2010; Mikaloff Fletcher et al., 2006), acting as a reservoir for carbon (Sabine et al., 2004). Consequently, changes in this reservoir or its driving factors might have a substantial impact on the concentration of CO<sub>2</sub> in the atmosphere.

The ocean's carbon reservoir is controlled by the marine carbon cycle, which is a part of the global carbon cycle. In the oceans, three forms of carbon exist: dissolved inorganic carbon (DIC), dissolved organic carbon (DOC) and particulate organic matter (POC). The carbon is transported by and transferred between three mechanisms called the solubility pump, the organic carbon pump and the carbonate pump (Heinze et al., 1991; Volk and Hoffert, 1985). The two latter once can be summarised as the biological pump. While the solubility pump transports CO<sub>2</sub> from the atmosphere into the ocean interiors (i.e. DIC), the biological pump transports biogenic carbon, i.e. DOC and POC (Ducklow et al., 2001) (Fig. 1.1).

Within the processes of the organic carbon pump and the carbonate (counter-) pump, marine microorganisms fix dissolved inorganic carbon into biomass but also release CO<sub>2</sub> due to the biomineralisation of carbonate. After their death, remineralisation and degradation of organic material generates new dissolved carbon whilst carbonate dissolution takes up dissolved carbon (Ducklow et al., 2001; Heinze et al., 1991; Volk and Hoffert, 1985). In general, less than 1% of the net primary production and hence fixed carbon is stored for millennia in the sediment

after it reaches the deep seafloor (Ducklow et al. 2001). More than 99% of the organic matter is hydrolysed, remineralised and utilised in the water column (e.g. Iversen, 2023).

The anthropogenically induced additional uptake of atmospheric  $\text{CO}_2$  by the ocean through the solubility pump influences marine chemistry, decreasing the pH and the carbonate ion concentration  $[\text{CO}_3^{2-}]$ , reducing the saturation state  $\Omega$  of calcium carbonate ( $\text{CaCO}_3$ ) (Haugan and Drange, 1996; Orr et al., 2005). These changes, known as ocean acidification, have been shown to negatively affect especially calcifying marine organisms, impairing their growth, reproduction and survival (Fabry et al., 2009; Kroeker et al., 2010; Orr et al., 2005). Studies revealed that as  $\Omega$  decreases, calcification rates at organism and community level decline (Albright et al., 2016; Bednarsek et al., 2014; Kroeker et al., 2010; Langdon and Atkinson, 2005). Additionally, the dissolution of  $\text{CaCO}_3$  is actively enhanced under undersaturated conditions.

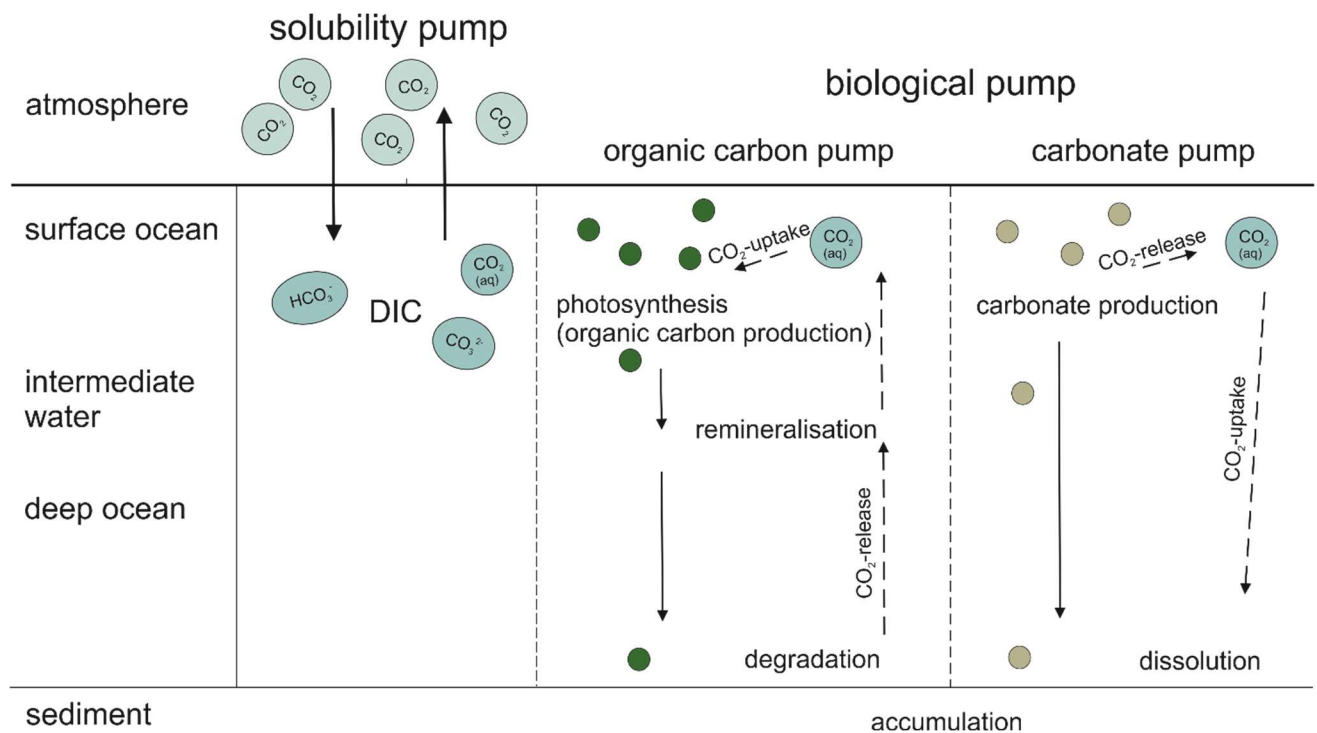


**Figure 1.1:** The marine carbon cycle (modified after Heinze et al. (1991)).

As cold water absorbs more  $\text{CO}_2$ , high-latitude oceans have naturally low saturation states of calcium carbonate (Orr et al., 2005; Steinacher et al., 2009). Given this natural state and the amplifying effect of increased  $\text{CO}_2$  input, the Arctic Ocean is suspected to experience the lowest pH and  $\Omega$  conditions in the coming decades (Steinacher et al., 2009) with adverse consequences for many calcifying organisms, resulting in changes to bioproductivity, biodiversity, trophic interactions, and other ecosystem processes (Baes, 1982; Falkowski et al., 1998).

The accelerating reduction in sea-ice cover and ice sheet extent for the past three to four decades in the Arctic, triggered supposedly by increasing temperatures due to the increase in atmospheric CO<sub>2</sub> (e.g. IPCC 2013), will also result in changes of bioproductivity, as it controls light distribution and timing of nutrient release to surface-waters (e.g. Copin-Montegut and Copin-Montegut, 1983; Redfield, 1934 Meir 2011). Palaeoceanographic studies have shown that Arctic marine ecosystems react quickly to changing environmental conditions, especially when sea-ice cover and light conditions are involved (Cormier et al., 2016; Matishov, 1999; W.N. Meir, 2011).

Although sea-ice cover mitigates the uptake of CO<sub>2</sub> into the ocean, at present the Arctic Ocean CO<sub>2</sub> uptake is in the order of  $-66$  to  $-199 \cdot 10^{12} \text{gC year}^{-1}$ , contributing 5–14% to the global balance of the global carbon reservoir (Bates and Mathis, 2009). As sea-ice cover further decreases inducing enhanced bioproductivity, an increase in the uptake of CO<sub>2</sub> by Arctic Ocean surface waters can be expected. Considering the ongoing changes in sea-ice cover, bioproductivity and acidification (Fig. 1.2), the processes happening currently in the Arctic realm increase the uptake of atmospheric CO<sub>2</sub>, suggesting the Arctic to act as a potential carbon sink for the rising atmospheric CO<sub>2</sub>-concentration.

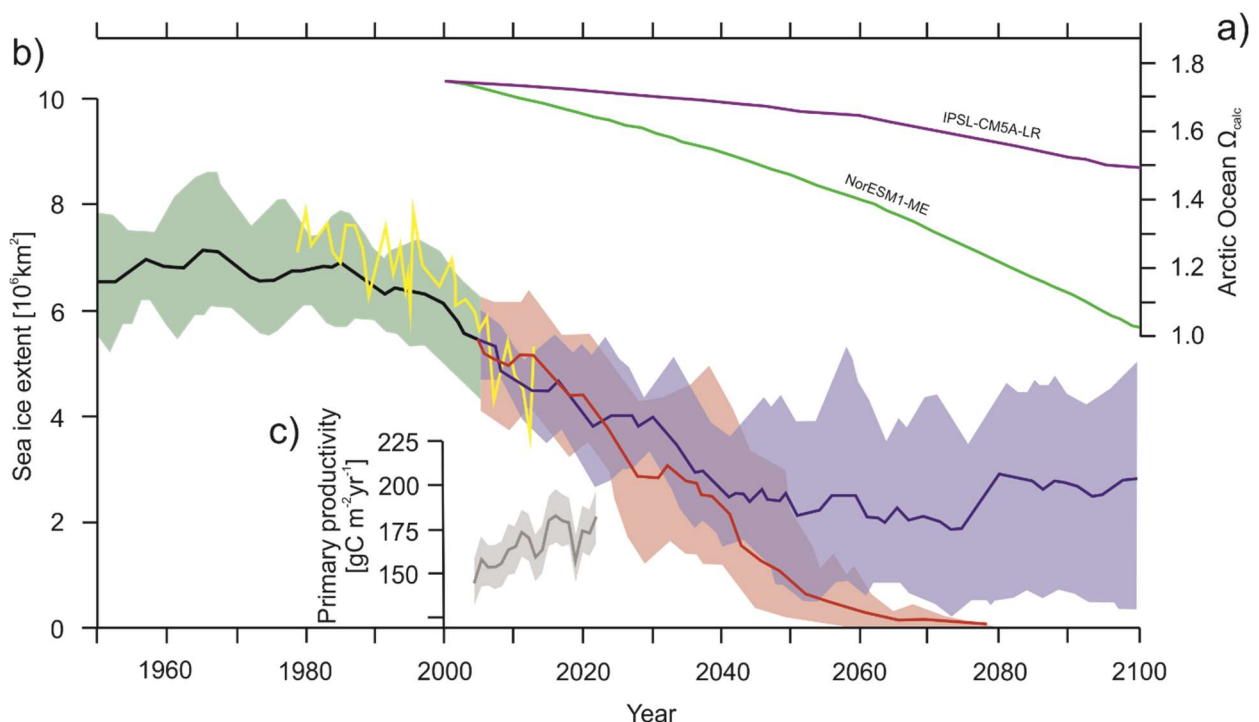


**Figure 1.2:** Changes in the Arctic. a) Projected saturation state of calcium carbonate (calcite) of the twenty-first century Arctic Ocean basin (averaged) with highest and lowest constraints (Terhaar et al., 2020). b) Projections of Northern Hemisphere sea-ice extent in September for this century based on 5<sup>th</sup> assessment of IPCC AR5 report that best captures recent sea-ice changes until 2013 (yellow). High (red) and very low emissions (blue) scenarios are shown as shaded bands with solid as mean. c)

Average primary productivity (2003-2021, March-September) from nine Arctic and Subarctic regions. (Sources for b) and c): website accessed in 2023: <https://arctic.noaa.gov/Report-card>).

## **1.2 Baffin Bay: where change hits hard**

The ongoing rapid changes in terrestrial, coastal and offshore environments in the Arctic will have immense consequences for socio-ecological systems (Burrows et al., 2011; Carmack and Wassmann, 2006; Lafrenière and Lamoureux, 2019; Meier et al., 2014; Ruscio et al., 2015). The present understanding of the Arctic climatic system is not sufficient enough to give adequate information to the managements across the region. Biogeochemical models can be applied to project future changes in e.g. sea-ice cover, carbonate saturation and bioproductivity and to predict the future behaviour of the marine carbon cycle. However, the magnitudes of the projected twenty-first century changes differ strongly across models and their constraints. Providing sustainable constraints for modelling is essential to improve projections of future Arctic climate and carbon cycling. The geological record provides an opportunity to assess the sensitivity of ecological processes to changing boundary conditions and to provide observational constraints. During the Holocene (11.7 kyrs BP – present) the Baffin Bay region is known to have experienced large changes in sea-ice cover and its associated parameters (de Vernal et al., 2013; Knudsen et al., 2008; Perner et al., 2013), rendering it a particular suitable region to assess past interactions between changing climate conditions and the marine carbon cycle.

Baffin Bay is a 1300 km long and 450 km wide oceanic basin between Canada and Greenland, stretching from 67°N to 76°N and covering a total area of 690,000 km<sup>2</sup> (Fig. 1.3). The basin is connected with the North Atlantic via the Davis Strait (with a water depth of 650 m) and with the Arctic Ocean via the Nares Strait (with a water depth of 600 m) and various channels of the Canadian Arctic Archipelago. Baffin Bays central abyssal plain is about 2500 m deep and is adjoined in the east by steep continental slopes extending from the Greenland shelf by more than 250 km. While these slopes are characterised by submarine fans and cross-shelf troughs, the continental slopes adjacent to Baffin Island are marked by narrower shelves of less than 50 km and smaller fjord outlets (Cofaigh et al., 2013).

Hydrographic conditions in the Baffin Bay are dominated by the Baffin Island current (BIC) and the West Greenland Current (WGC) generating an anti-cyclonic circulation. The BIC delivers cold polar waters from the Arctic Ocean and flows southward along the coast of east Baffin Island. The WGC is fed by the East Greenland Current (EGC) and the Irminger Current (IC). The EGC consists of polar waters and flows southward along the coast of east Greenland,

where it is met by the warmer and more saline northward flowing Irminger Current (IC), which is an offshoot of the North Atlantic Current, which flows beneath the EGC. These currents continue to follow the Greenland coastline and enter into Baffin Bay, becoming the WGC that is increasingly mixed as it travels up the west Greenland coast (Buch, 1981; Tang et al., 2004).

The WGC forms a subsurface water layer between 150 and 600 metre (West Greenland Intermediate Water) water depth which caps the cool and saline Baffin Bay deep water ( $\sim 0^{\circ}\text{C}$ ) (Tang et al., 2004).

The top 150 metre of the water column are predominantly affected by meltwater input from the Greenland Ice Sheet (GIS) and the southward flow of the BIC, keeping the surface layer cool and fresh and rendering Baffin Bays water column relatively well stratified. The inflow of Atlantic waters via the IC causes an asymmetric distribution of sea-ice in Baffin Bay, where sea-ice cover is more persistent and extensive in the western part of Baffin Bay than along the west Greenland margins although, sea-ice is persistent throughout most of the year with the exception of September and August (Tang et al., 2004).

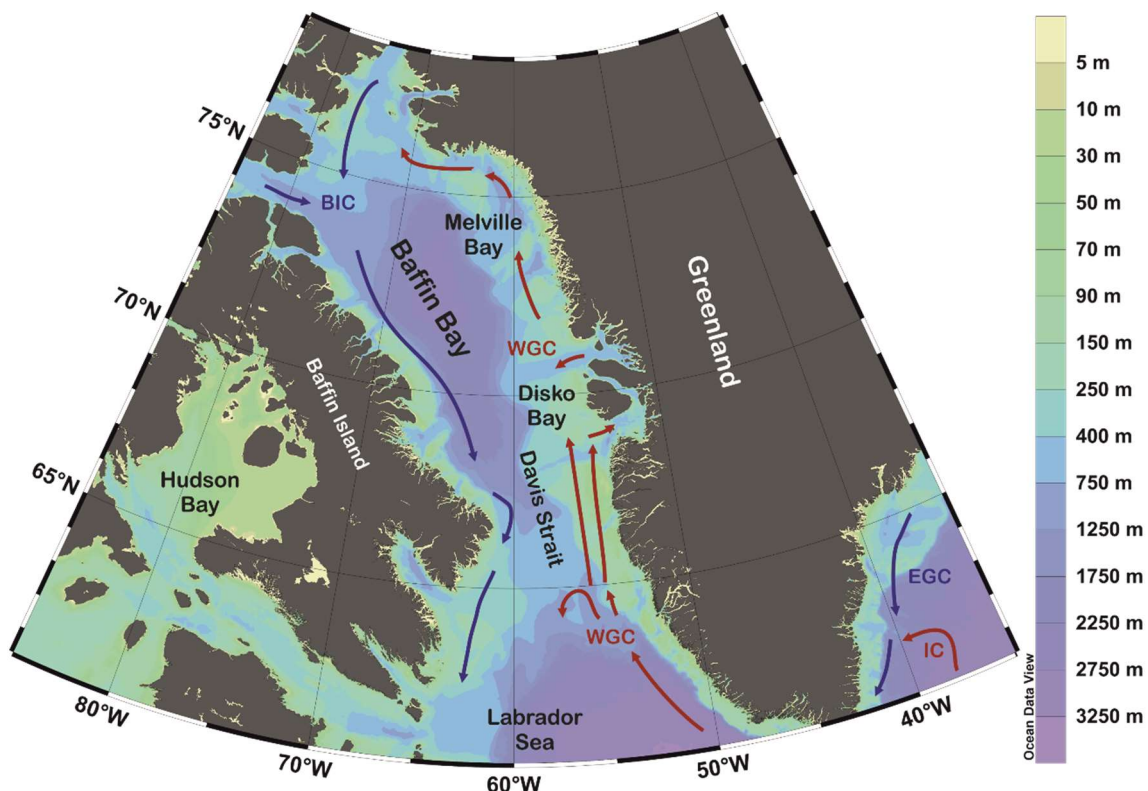


**Figure 1.3:** Modern Oceanography in Baffin Bay. Colours indicates modern bathymetry (Ocean Data View (Schlitzer 2018)). Arrows indicate schematically the modern surface circulation system in Baffin Bay (EGC - East Greenland Current, IC - Irminger Current, WGC - West Greenland Current, BIC - Baffin Island Current).



The interaction of the Baffin Bay currents with the GIS meltwater discharge collectively affect local stratification, sea-ice conditions and light supply generating strong feedback mechanisms (e.g. Bamberg et al., 2010). Modelling results and fossil proxy records suggest that the GIS and the Baffin Bay circulation have been tightly coupled in the past and appear to be strongly linked at present (Kaufman et al., 2004; Renssen et al., 2012). Data from marine sediment cores indicate that ocean conditions in the Baffin Bay in general have been highly variable and sensitive on millennial to decadal time scales even during the last 10,000 years (Briner et al., 2016) during the onset of the Holocene.

With the beginning of the Holocene, around 11.7 ka, reduced sea-ice and high thermal maximum conditions characterised its onset after the colder and drier conditions throughout the Younger Dryas (Rasmussen et al., 2006) (Fig. 1.4). The early (11.7-7.8 ka) to mid (7.8-3 ka) Holocene is generally characterized by high atmospheric temperatures, termed as the Holocene Thermal Maximum (HTM) (e.g. Kaufman et al., 2004; Axford et al., 2013; Axford et al., 2021; Andresen et al., 2022). This warm period has been suggested to be associated with high summer insolation and an increased advection of Atlantic water masses and an enhanced north-westward retreat of sea-ice in the Arctic (Koc et al., 1993; Svendsen et al., 2004). The late Holocene (3 ka-present) is characterised by a decreasing solar insolation and increasing sea-ice and glacier re-advances, referred to as Neoglacial cooling trend (e.g. Wanner et al., 2011; Weidick et al., 2012) and is supposedly associated with an enhanced influence of Arctic Waters into the Baffin Bay (Perner et al., 2013). Interleaved with this general cooling trend several short-time climate fluctuations i.e. the Roman Warm Period (2250-1600 a) (Lamb, 2002), the Dark Ages Cold Period (DACP) (1600-1150 a) (e.g. Helama et al., 2017), the Medieval Climatic Optimum (1100-700 a) (Lamb, 1965; Mann, 2002a) and the Little Ice Age (700 – 150 a) (Mann, 2002b; Matthews and Briffa, 2005) were recorded in the North Atlantic regions, supposedly driven by the retreat or advance of Atlantic waters towards the Arctic (Ljungqvist, 2010).

In recent years, the Greenland Ice Sheet has undergone significant changes. Satellite data covering the last 50 years reveal an extensive decrease in sea-ice in this area (Walsh and Chapman, 2001) and especially the contribution of the Greenland Ice Sheet to the global sea level and the freshening of ocean water is a reason for serious concern (Alley and Agustsdottir, 2005). While the reconstruction of the interglacial history of the Baffin Bay during the last millennia and hence the understanding of the feedback mechanisms between ocean and cryosphere is constantly advancing, the ecology and population dynamics driving the marine carbon cycle and possible feedback mechanisms with ocean and cryosphere are not yet fully understood. In general, oceanographic conditions in Baffin Bay during spring, when the sea-ice starts to break up, promote phytoplankton spring blooms, which tend to follow the sea-ice margin (Arrigo et al., 2012). Phytoplankton blooms in summer-fall have been associated with

freshwater inputs due to meltwater runoff from the GIS, triggering upwelling of nutrient-rich waters and high productivity (Juul-Pedersen et al., 2015; Krawczyk et al., 2015, 2018). Along most of the West Greenland margin, sea-ice melt and meltwater runoff from the GIS result in seasonal stratification of surface waters, which is amplified in summer by solar heat leading to relatively mild conditions (Juul-Pedersen et al., 2015; Tremblay et al., 2015) also enhancing primary productivity.

The impact of a fast changing environment in the Baffin Bay region on marine productivity remains unclear. But considering the fact that Arctic marine ecosystems are known to react quickly to changing environmental conditions (Cormier et al., 2016; Matishov, 1999; W.N. Meir, 2011), the Baffin Bay region can be expected to experience a greater-than-average response to the present climate change (de Vernal et al., 2013; Knudsen et al., 2008; Perner et al., 2013).

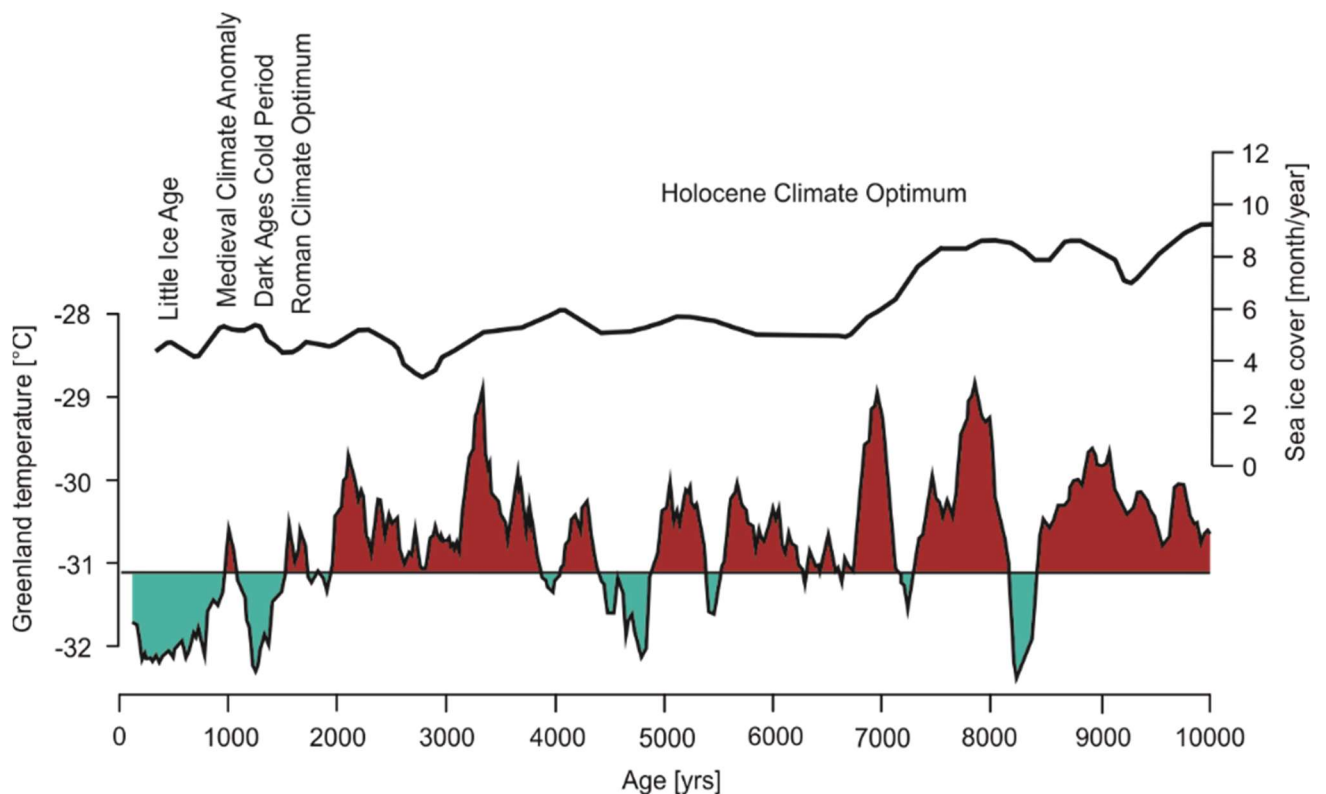


**Figure 1.4:** Holocene Greenland temperatures based on  $\delta^{18}\text{O}$  from the GISP ice core (Alley et al., 2010) and sea ice cover in Baffin Bay ( $68^\circ\text{N}$ ) reconstructed from dinoflagellate cyst assemblages (5-point running mean) (Gibb et al., 2015).

### 1.3 Primary productivity: the troublemaker

To understand the role of the Arctic marine carbon cycle in the context of a changing climate the key components driving the cycle have to be quantified to constrain their responses to a changing physical environment (Fig. 1.5). The Holocene geological record poses the opportunity to quantify these parameters under changing physical conditions so that the past may serve as an example to estimate the direction and magnitude of possible future developments and as an equivalent for the recent environmental changes leading to a warmer climate.

Some of these parameters like organic and inorganic carbon burial are relatively easy to reconstruct, although their interpretation in the context of the marine carbon cycle is potentially complicated by terrestrial carbon and detrital carbonate deposition (e.g. Saini, 2021). Other parameters like primary productivity and export productivity notoriously difficult to quantify as they do not leave a direct trace in the sediment. These parameters have to be reconstructed indirectly from the signature of plankton community composition (e.g. Radi and de Vernal, 2008) and benthic biomass approximated by the abundance of shelled organisms (e.g. Gooday, 2003; Jorissen et al., 2007), which are both associated with difficulties.

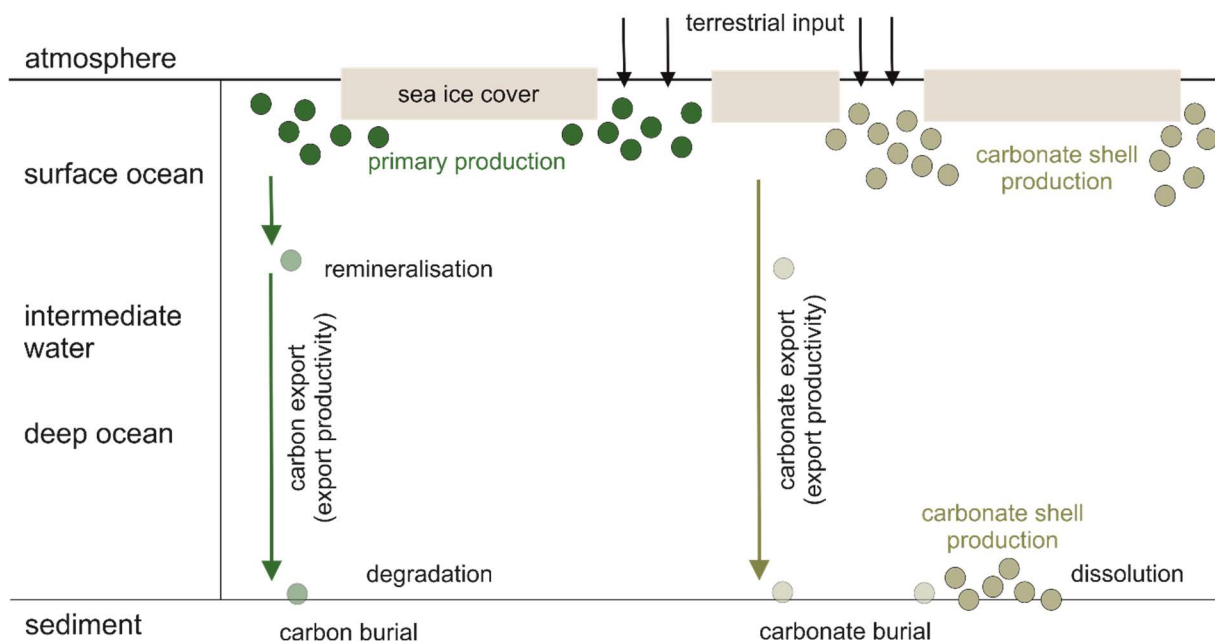


**Figure 1.5:** Key components of the Arctic marine carbon cycle.

However, especially primary productivity in the upper ocean plays a dominant role in the carbon cycle fixing the dissolved CO<sub>2</sub> into long-term storable organic carbon and needs detailed investigation as it accounts for about half of the global biosphere productivity (Behrenfeld et al., 2001; Field et al., 1998). Marine primary productivity refers to the production

of organic matter by phytoplankton through photosynthesis, converting inorganic to organic carbon. These photoautotrophic algae supply organic carbon to heterotrophic organisms like zooplankton, nekton and benthos. Productivity processes in coastal ecosystems are often more complex than in the open ocean. Along coastlines the seafloor is shallower and often sunlight can penetrate through the water column to the bottom, supporting photosynthesis of benthic organisms and nutrient supply through sinking organic carbon resulting in thriving benthic faunal communities (Bender et al., 1987; Sigman et al., 2012). While in general, marine productivity depends strongly on the availability of light and nutrients rendering it a function of water depth, in the Arctic bioproductivity is simultaneously a function of sea ice cover and latitude (Ardayna et al., 2017; Leu et al., 2015; Wassmann et al., 2020). Hence, during the seasons of a year, beside the spatial and temporal light variability caused by latitude, the melting/retreat and freezing/advance of sea-ice affects phytoplankton activity leading to phytoplankton blooms that supposedly develop faster than in areas of open waters (Wassmann et al., 2011). The recent changing climate and its resulting reduction in sea-ice and increase in nutrients will presumably result in more persistent algae blooms enhancing primary productivity in the Arctic (Hill et al., 2018; Lewis et al., 2020; Wassmann et al., 2020). Present marine primary productivity can be calculated from remotely sensed information. Satellite-based estimates of chlorophyll-a, based on the selective absorption of blue and blue-green wavelengths of this photosynthetic pigment, allow the quantification of phytoplankton biomass and hence organic carbon production (Behrenfeld and Falkowski, 1997).

To assess the role of marine bioproductivity within the climate system, it is required to understand past productivity changes over longer geological time scales. The application of fossil marine sediment records poses the possibility to quantify past productivity changes. However, former studies revealed that the reconstruction of paleoproductivity from sediments gives different results depending on the measurement used. Commonly, the content of organic carbon in sediments has been used as an index for palaeoproductivity assuming that organic carbon production in the surface layer correlates with organic carbon export through the water column and organic carbon burial in the sediment (e.g. Müller and Suess 1979, Muller et al. 1983, Sarnthein et al. 1992, Fischer et al. 2000). However, estimating palaeoproductivity from burial of sedimentary organic carbon is complicated by sedimentary processes that may imply lateral transport, focusing or winnowing and remineralisation within the water column and at the seafloor, even within anoxic sediments (Emerson and Hedges 1988, 2003, Meyers 1997, Rühlemann et al. 1999). Additionally, primary productivity, export productivity, and carbon burial may be fundamentally decoupled under scenarios of large-scale climate change, challenging the assumption of their covariance (Lopes et al. 2015). Some abiotic proxies like total sedimentary barium (e.g. Jeandel et al., 2000) and the isotopic composition of thorium and protactinium (Bradtmitter et al., 2006) have been used but presented limitations due to

their physical and chemical behaviours (Dymond et al., 1992; Francois et al., 2004, 1995; Klump et al., 2000; Paytan et al., 1996; Von Breymann et al., 1992). Proxies based on inorganic remains of planktonic and benthic microorganisms like foraminifera shells, diatom frustules or coccoliths are based on their isotopic or chemical composition or their abundances (e.g. Abrantes et al., 1994; Almogi-Labin et al., 2000; Beaufort et al., 1997, 1999, 2001; Berger et al., 1989; Fischer and Wefer, 1999; Loubere, 1991, 1994, 1999; Loubere and Fariduddin, 1999; Mackensen et al., 2000; Naidu and Malmgren, 1996; Vénec-Peyré and Caulet, 2000; Wefer et al., 1999). The application of assemblages of foraminifera or coccoliths together with recent productivity estimates from satellite measurements has led to the calibration of some regional transfer functions for past reconstructions (Beaufort et al., 2001; Cayre et al., 1999; Ivanova et al., 2003; Loubere, 1999; Loubere and Fariduddin, 1999). Inorganic remains however, consisting of carbonate and silicate, are prone to dissolution (e.g. Gallinari et al., 2002; Nelson et al., 1995; Ragueneau et al., 2000), especially in high latitudes (e.g. Aksu, 1983). Moreover benthic foraminifera show vital effects where the dissolution seems to remove preferentially  $^{13}\text{C}$  from the tests (McCorkle et al., 1995). In summary, the quantification of bioproductivity in the past is largely hampered by the difficulty to separate past productivity signals from those induced by early diagenetic processes.

#### **1.4 Dinoflagellate cysts and a transfer function: saviours of the day?**

Dinoflagellates are eukaryotic, unicellular organisms, forming a major group of planktonic marine primary producers besides coccolithophorids and diatoms. They include diverse autotrophic, mixotrophic and heterotrophic forms that all thrive in the upper layers of the oceans (e.g. de Vernal & Marret 2007). During sexual reproduction some dinoflagellate species (about 20%) produce fossilisable organic-walled cysts (=dinocysts) (Dale, 1983; Taylor, 1987; Wall and Dale, 1968). The cyst walls are composed of a condensed macromolecular structure that is predominantly aromatic in composition (Kokinis et al., 1998). Resistance of the cyst wall to degradation facilitates a relatively good preservation in seafloor sediments (e.g. Zonneveld et al. 2008). Unlike calcareous (e.g. foraminifera) or siliceous (e.g. diatoms) microfossils, dinocysts are not susceptible to dissolution after death (Koc et al., 1993; Matthiessen et al., 2001; Schröder-Adams and van Rooyen, 2011; Seidenkrantz et al., 2007; Zamelczyk et al., 2012). While a particularly high species diversity is observed in intertropical regions, even in polar environments with an extensive sea-ice cover a relatively high number of species is found (Matthiessen et al., 2005). Palynological studies from recent marine environments revealed that modern assemblages of dinocysts appear to reflect multiple parameters of the surface-ocean environment where the cysts were produced like sea surface temperature, sea surface

salinity, seasonal duration of sea-ice cover and primary productivity (Mudie 1992; Rochon & Vernal 1994; Matthiessen 1995; de Vernal et al. 1997, 2000, 2001, 2013; Radi et al. 2001; Radi & de Vernal 2004, 2008; Rochon et al. 2008). Therefore, sedimentary remains of dinocyst assemblages have been used to reconstruct past environmental parameters including primary productivity (e.g. Bringué et al., 2016; de Vernal et al., 2001a; Pospelova et al., 2008; Radi and de Vernal, 2008; Rochon et al., 1999a). A commonly used method for this reconstructions is the application of a transfer function developed by de Vernal et al. (1997). This transfer function is based on the Modern Analogue Technique (MAT) which is an approach assuming that similar modern assemblages have developed under similar environmental conditions as in the past (Guiot, 1990). It requires a calibration dataset that, after several updates throughout the last years includes now census counts of recent dinocyst assemblages linked with modern environmental data from surface sediments at 1968 sites from the Northern Hemisphere (de Vernal et al., 2020). The dinocyst Dataset is archived at GEOTOP (<http://www.geotop.uqam.ca>).

In general, the application of transfer functions assumes that the species assemblage responds to environmental forcing and that the main environmental driving factors are known (Birks, 1995). This is a challenging assumption and requires a combination of prior ecological knowledge and objective variable selection approaches (Guiot and de Vernal, 2007). Using multivariate techniques such as canonical correspondence analyses (CCA) (ter Braak, 1986) an assessment of the relationship between environmental parameters and the distribution in species assemblages can be made and help to identify driving variables. In a palaeoceanographic context, the variable selection however, is often complicated by a high degree of collinearity among candidate oceanographic factors: even if the number of mutually orthogonal factors (directions of compositional change) in the calibration dataset can be identified, their attribution to specific (seasonal) environmental variables remains difficult (Lopes et al., 2010). While in theory, dinocyst assemblage distribution appears to be related to multiple variables of the sea-surface environment, there is evidence that the exact number and kind of factors affecting dinocyst assemblages varies regionally (Radi and de Vernal, 2008; Zonneveld and Siccha, 2016), challenging the presumption that all variables can be reconstructed in all regions covered by the calibration dataset.

While dinocysts still appear to be good tracers of environmental parameters, especially in high latitudes where carbonate and silicate dissolution plays a dominant role, they may be affected by oxidation during exposure on the seafloor, resulting in a selective organic matter degradation that leaves a distinct fingerprint in the assemblage composition (Zonneveld et al., 2010), affecting the reliability of reconstructions.

Nuisance in the calibration dataset may also be caused by other factors. Not to be disregarded is the possibility of lateral transport of the dinocysts during sinking and sedimentation

processes (Nooteboom et al. 2019). While sediment trap studies indicate that dinocysts produced in the upper water column are in general rapidly transported to the sea floor and that there is no evidence for a species-selective lateral transport (Marret and Zonneveld, 2003; Susek et al., 2005; Zonneveld and Brummer, 2000), long distance cyst transport by bottom waters and sediment flows was suggested based on sediment trap studies in the central and North Atlantic Oceans (Dale, 1992; Dale and Dale, 1992). Model simulations suggest major lateral transport when ocean currents are strong (Nooteboom et al. 2019).

Within the calibration dataset census counts of recent dinocyst assemblages from surface sediments are linked with modern environmental data. The environmental data is provided by recent observations while the dinocyst assemblages were collected in the uppermost centimetre of box or gravity cores and represent a few tens of years to centuries, depending upon sedimentation rates and mixing due to bioturbation (Radi and de Vernal, 2008), not precisely accounting for modern environmental conditions.

However, the latest calibration dataset (de Vernal et al., 2020), covering 1968 sample sites, is large and therefore adequate to represent well the environmental gradients to cover the fossil assemblage compositions emerging from larger scale climate change in the past. It suggests that the reconstruction of palaeoproductivity is possible if nuisance variables are tended to appropriately. Moreover, especially in the Baffin Bay area, where carbonate and silicate dissolution poses a major issue, it offers a powerful tool, when the challenge of identifying region-specific environmental factors driving the compositional change of dinocyst assemblages is mastered adequately.

## **1.5 Thesis objectives outline**

Complex interactions between the marine carbon cycle and the Earth's climate will supposedly result in feedback mechanisms regarding CO<sub>2</sub> concentrations, changes in the physical environment and biological productivity in the oceans, especially in the Arctic regime. The linkages between carbon fixation (primary productivity), carbon long-term storage (carbon burial) and changes in the physical environment however, is incompletely understood in the present and over longer geological time scales.

Understanding these linkages is of paramount importance for model projections estimating future developments of the marine carbon cycle. Therefore, a reliable quantification of processes within the cycle, especially primary productivity and burial representing major drivers, is needed. As parameters commonly used to estimate past primary productivity from the geological record seem to be mostly influenced by other signals induced by diagenetic processes or other environmental parameters obliterating the signal of primary productivity,

The main prerequisite of this thesis is to establish a method for a nuisance free quantification of past primary productivity.

The aim of this thesis is to contribute to the understanding of the sensitivity of marine biological productivity and burial to a changing physical environment by constraining key components of the Arctic marine carbon cycle, so that model projections can enhance. This work is a cumulative thesis consisting of three manuscripts:

- ◆ Manuscript I: Identifying the signature of sea-surface properties in dinocyst assemblages: Implications for quantitative palaeoceanographical reconstructions by transfer functions and analogue techniques
- ◆ Objective: Is primary productivity a significant independent driver of dinocyst assemblage compositions? Is it possible to reconstruct primary productivity, where the estimation is predominantly free of diagenetic imprints and/or nuisance of other driving parameters?

The dinocyst database from de Vernal et al. (2020) provides the best possibility for primary productivity reconstructions in Arctic environments as other indicators are subjected to dissolution processes and are not preserved in high latitudes. Despite some nuisance inducing factors and the evidence of spatial differences in driving variables for dinocyst assemblages a robust quantification of primary productivity should be possible if the identification of the region-specific environmental driving factors for the assemblage composition is feasible and if primary productivity is a driving factor. The specific interest in the first manuscript was to test if dinocyst assemblage compositions are significantly and independently driven by primary productivity. To this end, this manuscript contains a study that re-evaluates the regional impact of sea surface properties in dinocyst assemblages in general, not focussing solely on primary productivity and addresses the impact of diagenetically induced nuisance variables on the assemblages in the dinocyst database. Region specific primary drivers for assemblage compositions (including primary productivity) have been identified, posing the opportunity to estimate primary productivity independently from other drivers if the parameter drives the composition in the area of interest.

- ◆ Manuscript II: Disentangling environmental drivers of Subarctic dinocyst assemblage compositional change during the Holocene
- ◆ Objective: Is primary productivity a primary driver of dinocyst assemblage composition in the (sub-) Arctic? Was primary productivity a significant driver during the Holocene?



The first study implies that dinocyst assemblages provide the opportunity for an independent and nuisance depleted reconstruction of primary productivity, in case that primary productivity is a primary driver in the study area. The interest in the second manuscript was to determine if the relationship between dinocyst assemblage composition and primary productivity can be used to estimate productivity in the (sub-) Arctic and if the relationship was also significant in Holocene fossil assemblage compositions.

A local dinocyst dataset is calibrated for the Baffin Bay area to test which environmental parameters are independent primary drivers in this region and if primary productivity is one of them. Statistical significances of reconstructions derived from fossil dinocyst assemblage compositions within four Holocene sediment cores from a North-South transect throughout the Baffin Bay area are tested to determine primary drivers during the Holocene. The analyses imply that present-day and Holocene dinocyst assemblages in the Baffin Bay area are in general primarily driven by salinity changes. Primary productivity being less important with exception of one core in Southern Melville Bay.

- ◆ Manuscript III: Holocene biogenic carbon production and deposition on the West Greenland Margin of the Baffin Bay
- ◆ Objective: How much did biogenic carbon production and burial change in the Subarctic during the Holocene? What environmental factors drove primary productivity and burial variability in the Holocene? How was the variability in burial related to changes in production?

The first manuscript proposes that dinocyst assemblage compositions are independently driven by primary productivity changes in certain regions. The second study suggests that within Southern Melville Bay present and fossil assemblages have also been significantly driven by primary productivity. This poses the opportunity to reconstruct a nuisance depleted primary productivity record during the Holocene and to constrain the responses of Arctic marine carbon cycle's key components to a changing physical environment. In the third manuscript, a multi-proxy study reconstructing variabilities of several parameters of the marine carbon cycle from a sediment core from Southern Melville Bay serves as a past example for the direction and magnitude of change that may occur in the future. Estimates of marine primary productivity, export productivity, carbon burial, carbonate preservation and terrigenous input are **compared** with reconstructed environmental conditions like sea ice, sea surface salinity and Greenland temperature.

Increased primary productivity seems to be induced by continuous melting conditions with reduction in ice cover and ice-sheet retreat fostering a longer growth season, upwelling conditions and mild surface waters due to enhanced stratification. An increase in primary

productivity supposedly leads to increasing efficiency of organic matter recycling in the productive zone resulting in a decreasing burial efficiency and a decoupling between carbon production and carbon burial.

# Chapter 2

## Description of own contributions

This thesis has been carried out within the framework of the International Research Training Group ArcTrain under the supervision of Prof. Dr. Michal Kucera. Funding was provided by the Deutsche Forschungsgemeinschaft (DFG). The Center of Marine Environmental Sciences (MARUM) at the University of Bremen, working group Marine Micropalaeontology-Palaeoceanography provided laboratories and technical support. The thesis is written cumulatively, composed of three joint-authorship manuscripts that have been or will be published in peer-reviewed journals. The manuscripts were written by myself with contributions from the co-authors.

The first study has been designed by the candidate and M. Kucera with the contribution of A. de Vernal. The candidate revised all data in the calibration dataset (de Vernal et al., 2020), designed and performed all statistical analyses, wrote all scripts, produced all figures and prepared the first draft of the manuscript. The evaluation of the analyses benefitted from contributions from all co-authors, providing insights regarding the interpretation of the data, and helped to structure the manuscript. All authors reviewed the results and approved the final version of the manuscript.

The second study has been designed by the candidate and M. Kucera with the contribution of A. de Vernal. The working half of sediment core GeoB19927-3, that was collected on board the RV Maria S. Merian on cruise MSM44, has been sampled by the candidate and the help of colleagues L. Madaj, J. Saini and J. Weiser at 1 cm intervals. The entirety of the working halves were sampled. The candidate conducted the freeze-drying and weighting of samples, performed the sample preparation and laboratory work for palynomorph analysis. The candidate did the microscope work of counting and identifying dinoflagellate cysts at UQAM, Montréal with consultation from M. Henry. The candidate assembled the local calibration dataset, subsetting the Northern Hemisphere dataset, designed and performed all statistical analyses, wrote the scripts, produced all figures and prepared the first draft of the manuscript. The analyses benefitted from contributions from all co-authors that provided insights regarding the interpretation of the data, and helped to structure the manuscript. All authors reviewed the results and approved the final version of the manuscript.

The third study has been designed by the candidate and M. Kucera. From aforementioned freeze-dried samples of sediment core GeoB19927-3 the candidate performed foraminifera

analyses. The candidate washed, wet sieved, oven-dried and weighted the samples. Because of the large amount of samples a student assistant helped with the wet sieving and non-species-specific picking. The candidate counted the foraminifera and in the case of benthic foraminifers identified the species after the taxonomy learned at Aarhus University with M.S. Seidenkrantz. The candidate performed all statistical analyses, produced all figures and prepared the first draft of the manuscript. The analyses benefitted from contributions from M. Kucera and A. de Vernal providing insights regarding the interpretation of the data, and helped to structure the manuscript. All authors reviewed the results and approved the final version of the manuscript.

# Chapter 3

## **Identifying the signature of sea-surface properties in dinocyst assemblages: Implications for quantitative palaeoceanographical reconstructions by transfer functions and analogue techniques (Manuscript I)**

Published

Hohmann, S., Kucera, M., de Vernal, A., 2020. Identifying the signature of sea-surface properties in dinocyst assemblages: Implications for quantitative palaeoceanographical reconstructions by transfer functions and analogue techniques. *Mar. Micropaleontol.* 159, 101816. <https://doi.org/https://doi.org/10.1016/j.marmicro.2019.101816>

### **Abstract**

Dinoflagellate cyst (=dinocyst) assemblages are widely used for the reconstruction of multiple oceanographic variables through the application of transfer functions. There is evidence that the number and kind of variables driving compositional changes in dinocyst assemblages vary regionally and that the selection of driving factors and the evaluation of transfer function performances are method-specific and complicated by spatial autocorrelation. Here, we used two new modern datasets from the Northern Hemisphere Atlantic-Arctic and the Northern Hemisphere Pacific oceans to re-evaluate the impact of sea-surface properties in dinocyst assemblages. We determined the dimensionality of the dinocyst ecological response and identified the main drivers for both regions. We calibrated and evaluated transfer function methods for the prediction of these variables and estimated their performances considering spatial autocorrelation. In both datasets, multiple environmental variables mutually and independently affect assemblage compositions, but the number and kind of these variables differ between datasets. We detected spatial autocorrelation, which was often due to environmental similarity, but some variables appeared to reflect geographical closeness, implying that spatial independence between sample sites depends upon the variables. We identified different primary drivers in both areas, highlighting the merit of regional calibrations and the necessity to carry out variable selection for each region separately. The multiple gradients

identified imply that potentially multiple parameters could be reconstructed from the same fossil dinocyst assemblages. However, as the multiple gradients reflect geographical structuring, we propose that regional calibrations, even at the expense of generalisation, could improve the reliability and interpretation of transfer function reconstructions.

### **3.1 Introduction**

The application of transfer functions and analogue methods for quantitative reconstructions of environmental variables from microfossil assemblages is widely used in palaeoceanography (Imbrie and Kipp, 1971). During the last decades, the growing interest in changing climate has led to numerous studies documenting short- and long-term oceanographic variations at multi-decadal to multi-millennial time scales based on the application of these techniques. A range of mathematical methods (Guiot and de Vernal, 2007) has been used to reconstruct environmental variables from a variety of marine microfossils, including planktonic foraminifera (e.g., Kucera et al., 2005), diatoms (e.g., Sha et al., 2014) and dinoflagellate cysts (e.g., de Vernal et al., 2005a, 2005b). The application of transfer functions is subject to a number of assumptions (Birks, 1995). Some of these are methodological, such as the success of the numerical methods to capture the environmental dependency of species composition and the adequacy and coverage of the calibration dataset. Others are related to the preservation of the signal in the sediment, making it difficult to separate the environmental signal imprinted within the assemblages during their lifetime (Birks, 1995), from diagenetic processes altering the assemblages after their deaths, such as dissolution (e.g., Berger, 1970) or organic matter degradation (e.g., Zonneveld et al., 1997, 2019). On a more fundamental level, however, the application of transfer functions assumes that the species composition of the analysed group responds to environmental forcing and that the main driving factors are known (Birks, 1995). This is by far the most challenging assumption, requiring a combination of prior ecological knowledge and objective variable selection approaches (e.g., Guiot and de Vernal, 2007). In a palaeoceanographic context, variable selection is often complicated by a high degree of collinearity among candidate oceanographic factors: even if the number of mutually orthogonal factors (directions of compositional change) in the calibration dataset can be identified, their attribution to specific (seasonal) environmental variables remains difficult (Lopes et al., 2010).

The challenge in identifying the most relevant environmental factors driving compositional change in microfossil assemblages is well exemplified by the application of organic-walled dinoflagellate cyst assemblages in quantitative environmental reconstructions. Dinoflagellates form a major group of planktonic marine primary producers and include diverse autotrophic, mixotrophic and heterotrophic forms that all thrive in the upper layers of the oceans (e.g., de

Vernal and Marret, 2007). Many dinoflagellate species (about 20%) produce fossilisable organic-walled cysts during their life cycle (Dale, 1983; Taylor, 1987; Wall and Dale, 1968; Head, 1996). The cyst walls are composed of a condensed macromolecular structure that is predominantly aromatic in composition (Kokinos et al., 1998). Resistance of the cyst wall to degradation facilitates a relatively good preservation in seafloor sediments (e.g., Zonneveld et al., 2008). Unlike calcareous (e.g., foraminifera and nannoplankton) or siliceous (e.g., diatoms and radiolarians) microfossils, dinocysts are not susceptible to dissolution after death like mineralised fossils (Koç et al., 1993; Matthiessen et al., 2001; Schröder-Adams and van Rooyen, 2011; Seidenkrantz et al., 2007; Zamelczyk et al., 2012). However, they may be affected by oxidation during exposure on the seafloor, resulting in a selective organic matter degradation that may leave a fingerprint in the assemblage composition (Zonneveld et al., 2010). However, since  $\text{SiO}_2$  and  $\text{CaCO}_3$  dissolution and organic matter degradation reflect different diagenetic processes, in settings with carbonate or opal dissolution, dinocyst-based transfer functions are potentially a powerful approach if organic matter degradation is negligible.

Palynological studies of surface sediment samples from marine environments of the Northern Hemisphere revealed that dinocyst assemblage distribution appears to be related to multiple variables of the sea-surface environment, with most commonly inferred drivers being sea-surface temperature and salinity, seasonal duration of sea-ice cover and primary productivity (Mudie, 1992; Rochon and de Vernal, 1994; Matthiessen, 1995; de Vernal et al., 1997, 2000, 2001, 2013; Radi et al., 2001; Radi and de Vernal, 2004, 2008; Rochon et al., 2008). However, there is evidence that the exact number and kind of factors affecting dinocyst assemblages varies regionally (e.g., Zonneveld and Siccha, 2016) and that the selection of driving factors and the evaluation of performance is method-specific and complicated by spatial autocorrelation (Telford and Birks, 2005, 2009).

In this study, we take advantage of the newly developed enhanced and taxonomically harmonised dataset of dinocyst assemblages in surface sediment samples from the Northern Hemisphere (de Vernal et al., 2020) to re-evaluate the signature of sea-surface properties in dinocyst assemblages. To this end, we analyse the dimensionality of the dinocyst ecological response separately for assemblages from the Pacific and the Atlantic-Arctic regions and use canonical correspondence analysis to identify the optimal seasonal representations of the forcing environmental variables in each region. We then calibrate and evaluate multiple transfer-function methods for predicting these environmental variables and estimate their performances in the light of spatial autocorrelation. With a rigorous statistical analysis of the relationship between assemblage data and multiple candidate controlling parameters, we aim

to provide a guidance on the sequences of steps that have to precede an application of dinocysts as indicators of past sea-surface properties.

### **3.2 Data**

The calibration dataset includes most of the data from the updated dataset (de Vernal et al., 2020), except for the samples from Price et al. (2016, 2018), which were added at a later stage. It comprises census counts of recent organic-walled dinoflagellate cyst assemblages from core-top sediments at 1826 sites from the Northern Hemisphere (Fig. 3.1). In poor samples, minimum counts of 60 specimens were accepted, while the mean count was 415 specimens per sample. The core-top samples were collected from the uppermost 1 cm of box or gravity cores and represent a few tens of years to centuries, depending upon sedimentation rates and mixing due to bioturbation (Radi and de Vernal, 2008). Palynological sample processing followed the standardised procedures for palynological preparation (de Vernal et al., 2010), which exclude the use of oxidation techniques to avoid selective degradation of more sensitive cyst taxa such as those produced by the Protoperidinales (Marret, 1993). The taxonomy used corresponds to that presented in Rochon et al. (1999) and updated in Van Nieuwenhove et al. (2020).

For the purpose of the analysis, the original taxonomic resolution of the dataset (71 dinocyst taxa) was reduced to 58 taxa (Table 3.1). This is because we discarded taxa which occur in too few samples (<10) and we grouped taxa whose distinction at species level is equivocal or because they represent groups with debatable taxonomy and/or undistinguishable ecological affinities. The relationships between dinocyst assemblage composition and environmental variables are complex as shown by Radi and de Vernal (2008) pointing to different relationships between assemblages and environmental conditions in the Pacific and Atlantic-Arctic regions. For example, whereas temperature and salinity gradients are determinant in the Atlantic-Arctic region, primary productivity explains a large portion of the variability in the Pacific. Therefore, the relationship between dinocyst assemblages and environmental variables was studied in two regional subsets. This also resulted in further reduction of taxa number, reflecting the presence of endemic taxa. The final Atlantic and Arctic Ocean (AAO) dataset includes 1436 samples and 56 dinocyst taxa and the Pacific Ocean (PO) dataset includes 390 samples and 51 taxa (Fig. 3.1). The original dinocyst dataset holding taxon percentages is archived at GEOTOP (<http://www.geotop.uqam.ca>); the regional data matrices with reduced taxonomy used in this analysis are available as supplementary material (Excel-file S3.1).



We chose to carry out a canonical-ordination based parameter selection (ter Braak, 1986) to characterise the relationship between environmental variables and dinocyst assemblage composition. We began by defining a broad set of potential controlling variables. These included all oceanographic variables that are commonly considered (e.g., Radi and de Vernal, 2008) to affect dinocyst distribution: surface layer (here represented by conditions at 0 m depth) temperature and salinity, sea-ice cover and productivity. For the variable selection, we considered separately the warm and cold-season temperature and salinity, as they are the most climatologically relevant variables with diverse gradients in summer and in winter. This is especially important along the continental margins of mid latitudes, which are characterised by large freshwater discharge and low surface salinity leading to strong stratification and low thermal inertia of the surface water layer (de Vernal et al., 1994). For productivity, we considered seasonal averages, considering the complex productivity regimes in the calibration dataset, including upwelling regions and high-latitude ocean (Sathyendranath et al., 1995). The initial variable selection included the variables listed in Table 3.2.

SST and SSS data were compiled from World Ocean Atlas “WOA V2 2013” (Locarnini et al., 2013; Zweng et al., 2013) covering measurements between 1955 and 2012 with a resolution of  $1/4^\circ$ . Sea-ice cover data were compiled from the “Gridded Monthly Sea Ice Extent and Concentration” dataset spanning 1950–2013 as provided by the National Snow and Ice Data Center (NSIDC) with a  $1/4^\circ$  resolution (Walsh et al., 2015). Sea-ice cover is expressed as the average number of months per year with  $>50\%$  sea-ice concentration, derived from the monthly concentration data. This definition, which has been used in earlier studies, correlates well with other measures of annual sea ice concentration as it derives from the same data (de Vernal et al., 2005b, 2013). Finally, the primary productivity data was calculated with the Vertical Generalized Production Model (VGPM) described by Behrenfeld and Falkowski (1997) using chlorophyll data to estimate carbon uptake. The data were provided by the NASA's moderate resolution imaging spectroradiometer (MODIS) program (<https://modis.gsfc.nasa.gov/data/dataproduct>). Annual and monthly productivity data as HDF files were downloaded from the Oregon State University web site (O'Malley, 2018). Those data are structured on a basis of  $1/6$  degree of spatial resolution. PPannual covers measurements between 2002 and 2007, while PPwinter, PPspring, PPsummer and PPautumn means were calculated from measurements between 2002 and 2016, which have better temporal resolution, but on the cost of including more measurements from the recent years, which are marked by the ongoing warming. The ranges of environmental variables in the regional datasets are listed in Table 3.2, their spatial distribution is shown in Fig. 3.1.

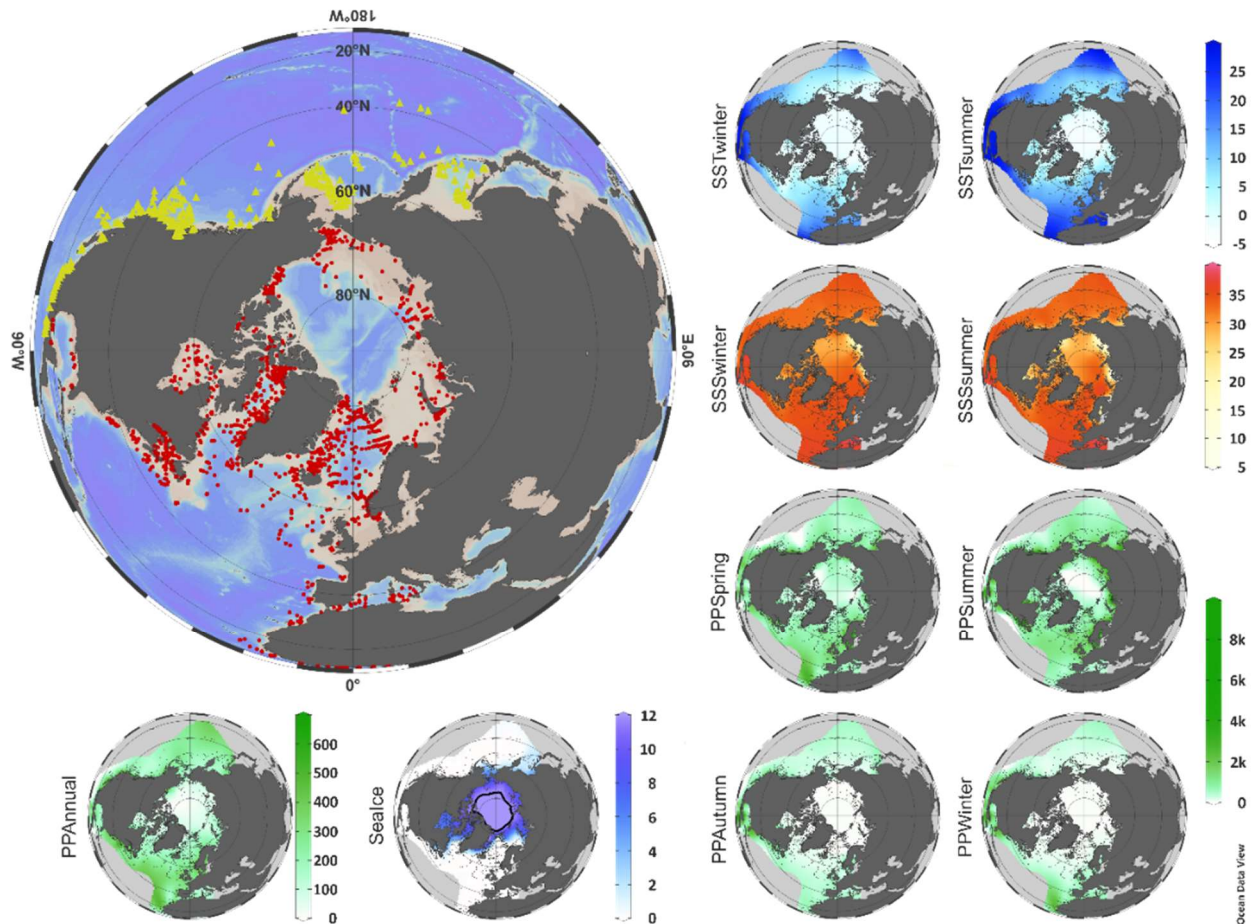


**Figure 3.1:** Location of surface sediment samples used in this study (top left) with sample sites included in the AAO calibration dataset (red dots) and sample sites included in the PO calibration dataset (yellow triangles). Initial environmental variable gradients (units listed in Table 3.2) were gridded using DIVA gridding with Ocean Data View (Schlitzer, 2018). The perennial sea-ice edge in the sea-ice gradient map is indicated by the twelve-month sea-ice cover line.

### 3.3. Data analysis

#### 3.3.1 Data treatment

To explore the relationship between dinocyst assemblage data and environmental forcing variables, we used statistical ordination to detect continuous patterns and highlight taxon variances contained in the multivariate calibration datasets (McGarigal et al., 2000). We first determined which types of ordination techniques are adequate for our taxa datasets. We performed detrended correspondence analysis (DCA) (Birks, 1995) on each dataset to evaluate the gradient lengths, expressed as standard deviation (SD) units in the first DCA axis to decide whether to apply linear ( $SD < 3$ ) or unimodal ordination ( $SD > 4$ ;  $SD > 3$  to  $< 4$  both methods possible but unimodal ordination is advised) (Lepš and Šmilauer, 2003). For DCA

and further analyses we used the vegan package (Oksanen et al., 2017) in R (R Core Team, 2017). Both analysed datasets were found to have an SD > 3 (Fig. S3.1 - Supplementary data) (AAO - SD 3.7, PO - SD 3.7) using log-transformed (log (x + 1)) dinocyst assemblage per mil data. We thus continued using unimodal techniques for statistical ordination.

**Table 3.1:** List of dinocyst taxa in the two calibration datasets with abbreviations and maximum ratios (minimum is always zero). Asterisks indicate heterotrophic dinocyst taxa.

Taxa name	Abbreviation	Notes	Maximum % AAO	Maximum % PO
<i>Achomosphaera andalousiense</i>	Aand		2.2	-
<i>Ataxiodinium choane</i>	Atax		4.0	1.2
<i>Bitectatodinium tepikiense</i>	Btep		30.0	1.6
<i>Bitectatodinium spongium</i>	Bspo		9.3	51.6
<i>Impagidinium aculeatum</i>	Iacu		83.7	60.3
<i>Impagidinium pallidum</i>	Ipal		40.0	9.8
<i>Impagidinium paradoxum</i>	Ipar		14.0	8.6
<i>Impagidinium patulum</i>	Ipat		28.2	27.2
<i>Impagidinium sphaericum</i>	Isph		8.8	1.6
<i>Impagidinium strialatum</i>	Istr		6.8	25.2
<i>Impagidinium plicatum</i>	Ipli		3.8	0.3
<i>Impagidinium velorum</i>	Ivel		1.5	6.5
<i>Impagidinium japonicum</i>	Ijap	Grouped with Ivel	-	-
<i>Lingulodinium machaerophorum</i>	Lmac		80.5	73.0
<i>Melitasphaeridium choanophorum</i>	Mcho		6.3	-
<i>Nematosphaeropsis labyrinthus</i>	Nlab		71.5	80.0
<i>Nematosphaeropsis rigida</i>	Nrig		5.6	-
<i>Operculodinium centrocarpum</i>	Ocen	Group including: <i>Operculodinium centrocarpum</i> , <i>O. centrocarpum</i> —short processes, <i>O. centrocarpum</i> —Arctic morphotype	93.5	90.5
<i>Operculodinium israelianum</i>	Oisr		12.8	0.3
<i>Operculodinium cf. janduchenei</i>	Ojan		7.0	0.8
<i>Operculodinium longispinigerum</i>	Olon		4.1	-
<i>Polysphaeridium zoharyi</i>	Pzoh		70.6	40.5
<i>Pyxidinopsis reticulata</i>	Pret		3.6	43.4
<i>Spiniferites membranaceus</i>	Smem		29.9	0.4
<i>Spiniferites delicatus</i>	Sdel		73.6	57.8
<i>Spiniferites elongatus</i>	Selo		48.0	17.7
<i>Spiniferites ramosus</i>	Sram		44.7	42.9
<i>Spiniferites belerius</i>	Sbel	Grouped with Sspp	-	-
<i>Spiniferites bentorii</i>	Sben		10.8	0.4
<i>Spiniferites bulloideus</i>	Sbul	Grouped with Sspp	-	-
<i>Spiniferites lazus</i>	Slaz		2.2	-
<i>Spiniferites mirabilis-hyperacanthus</i>	Smir		77.0	17.4
<i>Spiniferites</i> type granular	Sgra		5.7	4.5

<i>Spiniferites pachydermus</i>	Spac	Grouped with Sgra	-	-
<i>Spiniferites</i> spp.	Sspp		27.3	24.0
<i>Tectatodinium pellitum</i>	Tpel		1.7	1.6
Cyst of <i>Pentapharsodinium dalei</i>	Pdal		95.9	80.5
Cyst of <i>Scrippsiella trifida</i>	Stri		17.2	1.6
<i>Tuberculodinium vancampoae</i>	Tvan		6.9	0.7
<i>Dalella chathamense</i>	Dcha		1.3	1.6
<i>Gymnodinium</i> sp.	Gymn		49.0	-
<i>Islandinium minutum</i> *	Imin		96.8	67.9
<i>Islandinium ? cezare</i> *	Imic	Grouped with Imin	-	-
<i>Islandinium brevispinosum</i> *	Ibre	Grouped with Imin	-	-
<i>Echinidinium karaense</i> spp.*	Ekar		19.6	29.4
<i>Brigantedinium</i> spp.*	Bspp	Group including: <i>Brigantedinium</i> spp., <i>Brigantedinium cariaeoense</i> , <i>Brigantedinium simplex</i>	99.0	88.6
<i>Lejeunecysta</i> spp.*	Lspp		12.7	2.4
<i>Selenopemphix nephroides</i> *	Snep		10.0	5.9
<i>Xandarodinium xanthum</i> *	Xxan		2.4	-
<i>Selenopemphix quanta</i> *	Squa		21.5	12.0
Cyst of <i>Protoperidinium nudum</i> *	Pnud	Grouped with Squa	-	-
<i>Trinovantedinium applanatum</i> *	Tapp		20.2	1.5
<i>Trinovantedinium variabile</i> *	Tvar		-	1.5
<i>Votadinium calvum</i> *	Vcal		2.8	1.9
<i>Votadinium spinosum</i> *	Vspi		3.4	2.5
Cyst of <i>Protoperidinium americanum</i> *	Pame	Grouped with Bspp	-	-
<i>Quinquecupis concreta</i> *	Qcon		8.4	33.3
Cyst of <i>Polykrikos schwartzii</i> *	Psch		71.5	4.1
Cyst of <i>Polykrikos</i> sp. – Arctic*	Parc		23.1	0.5
Cyst of <i>Polykrikos kofoidii</i> *	Pkof		39.0	15.9
<i>Echinidinium aculeatum</i> *	Eacu		3.5	19.9
<i>Echinidinium granulatum</i> *	Egra		3.2	39.2
<i>Echinidinium delicatum</i> *	Edel		5.9	23.8
<i>Echinidinium transparantum</i> *	Etra	Grouped with Edel	-	-
<i>Echinidinium</i> spp.*	Espp		8.9	31.2
<i>Stelladinium stellatum</i> *	Sste		26.5	1.7
<i>Stelladinium bifurcatum</i> *	Sbif	Grouped with Sste	-	-
Cyst A*	Cysa		-	5.2

As we aimed to study relationships between assemblage variance and specific ecological variables, we applied constrained ordination (McGarigal et al., 2000). This method is applied to quantify the strength of the relationship between taxon variances and the tested environmental variables in the AAO and PO assemblage datasets by performing Canonical Correspondence Analysis (CCA). CCA was performed after ter Braak (1986) with log-transformed ( $\log(x + 1)$ ) dinocyst assemblage data (taxa ratios in per mil) in order to increase the weight of taxa that usually have narrower tolerances to environmental variables than

ubiquitous taxa that often dominate the assemblages (de Vernal et al., 2001; Radi and de Vernal, 2008). In the CCA, we ranked the importance of environmental variables by the amount of variance they explain in the taxon dataset and applied Monte Carlo permutation tests (ter Braak and Smilauer, 2002) assessing if the variation explained by an environmental variable is larger than a random contribution. Since the tested variables are affected by collinearity, we proceeded by selecting the smallest number of oceanographic variables that express the essential variance contained in the taxon datasets by maximising eigenvalues and minimising the residual random noise (McCune, 1997). To this end, we calculated Variance Inflation Factors (VIF), expressing how much of the variance explained by an environmental variable is already explained by another variable in the dataset. The VIF of a variable is calculated from the multiple correlations ( $r$ ) among the environmental variables (ter Braak and Smilauer, 2002), using the equation  $VIF = 1 / (1 - r^2)$ . We chose a cut-off value of  $VIF \leq 2$  for all oceanographic factors as also suggested in other studies (e.g., Lopes et al., 2010). Such a VIF value only allows collinearities of  $r^2 \leq 0.5$  and thus not more than half of the variance in the data explained by one variable to also be explained by another variable. A low cut-off value, might lead to the exclusion of an important oceanographic factor explaining a significant variance in the taxa and might also give a suboptimal model. However, as this exclusion would be due to collinearity with the remaining variables, the variance explained by this excluded oceanographic factor would still be explained by one of the remaining factors, implementing no loss of explained taxa inertia. In this study, pursuing the approach of a low cut-off value allows us to identify the largest number of variables that will explain essential variances in the taxon dataset independently of each other. In order to test the significance of each variable and to avoid VIFs  $> 2$ , we carried out a manual forward selection ranking variables after their importance in explaining variance in the data (Manly, 1991; ter Braak, 1992; ter Braak and Verdonschot, 1995). First, we performed CCA with each environmental variable as the only variable to obtain their eigenvalues and ranked them according to the amount of variance they explain exclusively. Second, we selected the best variable with the highest eigenvalue and added the other variables step-by-step according to their rank. During the process, environmental variables resulting in VIFs  $> 2$  were excluded. If there was more than one variable with a VIF  $> 2$ , we performed the analysis by removing one variable at a time, performing a CCA for each remaining dataset determining their variations explained and pursued a final solution that maximised the total variance explained. In this way, we obtained independently a set of environmental variables for the AAO and PO datasets, which we used for final CCAs and further analyses.

**Table 3.2:** Environmental variables used in the canonical-ordination based parameter selection and their ranges within the two calibration datasets.

Environmental variable	AAO			PO		
	Minimum	Maximum	Range	Minimum	Maximum	Range
SSTsummer [°C]	-1.56	29.95	31.51	6.70	30.55	23.85
SSTwinter [°C]	-1.88	28.92	30.80	-1.20	28.25	29.44
SSSummer [psu]	6.67	38.18	31.51	16.41	35.90	19.49
SSSwinter [psu]	19.49	38.09	18.61	27.07	35.07	8.00
Sealce [months/yr]	0	12	12	0	4.74	4.74
PPannual [gC/m <sup>2</sup> /yr]	10.67	620.77	610.10	119.64	658.93	539.29
PPwinter [mgC/m <sup>2</sup> /day]	0	3485.67	3485.67	28.33	4570.00	4541.67
PPspring [mgC/m <sup>2</sup> /day]	64.33	5659.67	5595.33	342.67	5255.39	4912.72
PPsummer [mgC/m <sup>2</sup> /day]	123.00	10331.67	10208.67	292.00	5734.21	5443.21
PPfall [mgC/m <sup>2</sup> /day]	0	4085.00	4085.00	97.00	2105.00	2008.00

Prior to the development and evaluation of transfer functions, we determine the extent and type of autocorrelation in the two calibration datasets. As pointed out by Telford and Birks (2009), a simple evaluation of transfer function performance is possible only if the residual of the environmental variable of interest at one training set site is independent of its value at other sites. In case of dependence, the calibration dataset would be spatially autocorrelated, and the estimates of transfer function performance will be over-optimistic to a different degree for different methods, which could result in inappropriate choices of transfer function models and variables and make oceanographical factors with no ecological relevance appear to be “reconstructable”. To assess spatial autocorrelation in the AAO and PO datasets we applied the test developed by Telford and Birks (2009), which is based on the assumption that in a spatially autocorrelated calibration dataset deleting geographically close sites would preferentially delete the best analogues and therefore be more damaging to performance statistics than a random site deletion. If the observations are independent, deleting a given proportion of samples should have the same effect regardless of how they are selected.

Comparing the performances ( $r^2$ ) of random or neighbourhood deletion of sites is a simple method to evaluate autocorrelation within a dataset, but it does not differentiate between the mechanisms responsible for the autocorrelation (Telford and Birks, 2009). Similar dinocyst assemblages exist, in theory, because of geographical proximity and/or similar environmental conditions with similar taxon-environment relationships. In a spatial autocorrelation scenario where similar assemblages exist due to similar environmental conditions regarding the variable of interest, the assumptions of transfer functions are still met, because the spatial similarity reflects environmental similarity. A spatial autocorrelation where similar assemblages exist due to geographical proximity and/or taxon-environment relationships of other variables than that of interest would violate the assumption of a transfer function as the spatial similarity does not

reflect environmental similarity for the tested transfer function. It is therefore important to test for the mechanism responsible for the spatial autocorrelation. In a spatially autocorrelated dataset, the transfer function performance will be worse when geographically close sites are deleted than when environmentally similar sites are removed, and vice versa. For autocorrelation tests and further analyses we used R packages *fields* (Nychka et al., 2017), *palaeoSig* (Telford, 2015) and *rioja* (Juggins, 2017) implementing the routines developed in Telford and Birks (2009).

### ***3.3.2 Transfer functions and analogue techniques***

The evaluation of transfer function techniques solely on the basis of their performance favours efficient interpolation over efficient generalisation (Kucera et al., 2005). For this reason, the evaluation is carried out by various leaving-out approaches. However, since calibrations are bound to samples from the same time frame (modern surface sediment samples) whereas the application of transfer functions is made on older samples, the trade-off between efficient interpolation and generalisation (the overfitting problem) remains. A possible solution is to use several transfer function techniques based on different computational logics to assess to what degree the reconstructions are method-sensitive (Kucera et al., 2005). Here we adopt this approach and test the performance of three distinctly different transfer function approaches: the Maximum Likelihood (ML) calibration technique, the Weighted Averaging Partial Least Square (WA-PLS) calibration technique, which are based on the idea that a taxon assemblage can be expressed as a function of certain environmental variable(s) (ter Braak, 1987) and the Modern Analogue Technique (MAT), which is an approach assuming that similar past assemblages have developed under similar environmental conditions to those today (Guiot, 1990).

In the ML method, the ecological response curves are modeled from the relationship between the percentage of each taxon and a specific environmental variable, consisting of systematic and random (error) components. The resulting curves are fitted to the modern dataset by non-linear regression and determine jointly which percentages are expected at a given value of the environmental variable. Using this model the likelihood that a particular value for the environmental variable would occur with a given taxon assemblage can be calculated, and the value that gives the highest probability is the ML estimate (Birks et al., 1990). Birks (1995) suggested this model as the most unbiased statistical technique for ecological reconstructions because, in theory, it minimises the influence of non-climatic nuisance variance as the sample size increases. However, ML estimates can be heavily biased for small samples and the

method is liable to find sub-optimal solutions (local minima), especially when the taxon tolerances are unequal (Birks et al., 1990).

An alternative approach following a similar logic as ML but being computationally simpler as it describes an approximation of ML is WA (ter Braak and Van Dam, 1989; ter Braak and Prentice, 1988). WA assumes that taxa have unimodal responses to the reconstructed environmental variables with each taxon abundance decreasing away from the ecological optimum. The optimum of a taxon is defined as the average of all the values for a certain environmental variable at sites where the taxon occurs, weighted by the taxon's percentage (ter Braak, 1987). An estimate of the environmental variable for an unknown sample is then the average of the optima of individual taxa weighted by their percentage and/or the widths of their environmental tolerances. In a WA model, averages of the response are taken twice having the effect of shrinking the range of possible estimates. This issue is addressed by different deshrinking approaches: classical (WA<sub>cla</sub>), inverse (WA<sub>inv</sub>) and monotonic (WA<sub>mono</sub>) deshrinking, while monotonic deshrinking often outperforms the others depending on the calibration dataset (Birks and Simpson, 2013). One important limitation of WA is that it considers the taxa individually and thus often ignores correlations among the assemblage data that remain after fitting the environmental variable of interest. To overcome this problem, weighted averaging partial least squares regression (WA-PLS) was developed (ter Braak and Juggins, 1993). WA-PLS performs inverse deshrinking and incorporates information from secondary gradients in the calibration dataset (ter Braak and Juggins, 1993). It uses the residual correlation structure in the data by using further components (two-way weighted averages for the residual of the variable) utilising the residual structure in the assemblage data, to improve the fit between the assemblage data and the environmental variable of interest in the modern calibration dataset (Birks, 1995). As former studies of surface sediment samples from marine environments revealed that dinocyst assemblage distribution appears to be related to multiple variables of the sea-surface environment (e.g., Mudie, 1992; Rochon and de Vernal, 1994; Matthiessen, 1995; de Vernal et al., 1997, 2000, 2001, 2013; Radi et al., 2001; Radi and de Vernal, 2004, 2008; Rochon et al., 2008) we chose WA-PLS over WA<sub>cla</sub>, WA<sub>inv</sub> and WA<sub>mono</sub>, to ensure the incorporation of secondary environmental variable information in the WA model. The number of retained components was determined by selecting a model for each reconstructed environmental variable that yielded the lowest root mean square error of prediction (leaving-one-out) and highest coefficient of correlations between observations and reconstruction, while reducing the prediction error significantly ( $p \leq .01$ ), using a randomisation t-test for testing the significance of cross-validated components after van der Voet (1994).



While ML and WA-PLS are unimodal taxon-environment response models, MAT is a strict interpolator, sorting samples in the calibration dataset by their (dis)similarity to a fossil assemblage using the conditions under which the best modern analogue(s) were formed to estimate the environmental variable for the fossil assemblage (e.g., Hutson, 1980; Prell, 1985; Overpeck et al. 1985; Morley, 1989; Guiot, 1990). Applying MAT for quantitative reconstructions requires a large calibration dataset covering well the environmental gradient and representing well the compositions of all fossil assemblages. It allows a simple and objective identification of fossil assemblages that have no modern analogue in the modern calibration dataset (Hutson, 1977). Such situations (i.e. having no analogues) are a major problem in MAT because no realistic environmental reconstruction is possible in such cases. An advantage of MAT, however, is that there is no assumption about the kind of the quantitative relationships between assemblages and reconstructed variables (e.g., Guiot and de Vernal, 2007). The MAT estimates were determined using a log-transformed distance calculation for the analogue selection as in de Vernal et al. (2005a). The optimal number of analogues for each environmental variable was determined by calculating the root mean square error of prediction (by leaving one out) as a function of the number of analogues used. For the reconstructions, analogues were only selected if their distance was lower than a threshold value above which the analogy between two samples is considered insignificant. This threshold value was calculated based on the average distance between randomly taken pairs of samples (Monte-Carlo procedure) from the assemblage dataset and its standard deviation and corresponds to the average random distance minus the standard deviation (de Vernal et al., 2001). We chose the Monte-Carlo procedure as it is a common way to proceed, so that the statistical properties of independence are respected when there is no probabilistic model for pairs of samples. Thus, the number of analogues used for each reconstruction lies between the determined optimum number of analogues (as maximum) and the maximum number of “below-the-threshold” analogues (as minimum). For MAT calculations we used the R package *bioindic* (Guiot et al., 2014).

### ***3.3.3 Transfer function and analogue technique performance statistics of the calibration datasets***

In order to assess the performance of the tested reconstruction approaches, cross-validation tests were performed using the leave-one-out (LOO) (cf. Efron and Gong, 1983) method as well as the h-block method (Burman et al., 1994; Telford and Birks, 2005, 2009). For ML and WA-PLS, we applied LOO on the AAO and the PO datasets as a whole and for MAT we applied LOO on both datasets two times – once on a calibration and once on a verification dataset. The procedure of splitting the whole datasets in a calibration and a verification dataset is

applied to evaluate the coverage of the AAO and PO datasets. If the sample coverage of assemblages in space and along the range of the tested environmental variables is oversaturated, the performance within the calibration dataset and within the verification dataset should be similar. In our application, we used a calibration subset containing 5/6 of the original database and a verification subset containing 1/6 of the original database. The subsets were generated by random selection and a subsequent test for representativeness to avoid a non-representative random selection. Then, one sample is left out and treated as a potential fossil sample. The transfer function is constructed on the remaining samples and the environmental variable for the sample left out is estimated. This procedure is repeated until all samples have been estimated and the differences between the known values and the estimates for the individual samples are used to calculate the coefficient of correlation ( $r^2$ ) between predicted and observed values and the standard deviation of the residuals between reconstructed and observed values, as an approximation of the RMSEP (ter Braak and Juggins, 1993). This procedure is carried out separately for the calibration and the verification subsets.

The LOO method assumes that all observations within a dataset are independent, which is not true in case of autocorrelation or other types of pseudo-replication, and in such situations, performance statistics based on LOO applied as described above will be over-optimistic (Payne et al., 2012; Telford and Birks, 2005). Since the distribution of microfossil assemblages in marine sediments is likely affected by spatial autocorrelation, we also applied the h-block method (Burman et al., 1994) following Telford and Birks (2009). In h-block cross-validation, the LOO procedure is supplemented by a step in which all samples within h kilometres of the tested observation are omitted from the calibration (Burman et al., 1994; Telford and Birks, 2009). To estimate h we fitted a spherical variogram to detrended residuals of a WA model as suggested by Telford and Birks (2009) as well as Trachsel and Telford (2016) and then performed h-block cross-validation using additionally R packages *gstat* (Pebesma, 2004) and *sp*. (Pebesma and Bivand, 2005) following R code developed by Trachsel and Telford (2016).

### **3.4 Results**

The first step of the variable selection procedure, a CCA carried out individually for single variables, revealed that when considered individually, each of the ten environmental variables appeared to explain a significant ( $p < .01$ ) amount of variation in the assemblage composition dataset (Table 3.3). Together, the ten variables explained 29% of the total inertia in the AAO dataset and 30% in the PO dataset. We then evaluated the collinearity of the tested environmental variables through a manual forward selection which uncovered no collinearity (independence;  $VIF < 2$ ) between SSTwinter, Sealce and PPsummer in the AAO dataset and

no collinearity ( $VIF < 2$ ) between SSSwinter, Sealce, PPannual and PPspring in the PO dataset, while explaining the largest possible amount of inertia when taken together. The remaining variables were identified as collinearly related to these variables and were excluded from further analyses.

When only the non-correlated environmental variables are used, the constrained parts of the CCA explain about 20% of the taxa inertia within the AAO and 17% within the PO dataset (Table 3.4) and, as expected, all environmental variables have significant correlations with CCA-axes (Table 3.5). In the AAO dataset, the first CCA axis explains 74% of the constrained variance and is positively correlated with SSTwinter, whereas in the PO dataset, the first CCA axis explains 49% of the constrained variance and is correlated with SSSwinter and Sealce (Fig. 3.2, Tables 3.4 and 3.5). Within the AAO dataset Sealce is apparently correlated to axis 2, while PPsummer is correlated with axis 3. In the PO dataset axis 2 is correlated to PPannual and PPspring, while axis 3 is also apparently correlated to Sealce. Axis 4 is not significant (ANOVA test; threshold  $p < .01$ ) and shows no correlation to any of the environmental variables. This indicates that despite the selection of four variables, the PO dataset likely only has three significant independent environmental gradients.

Regarding taxon-environment relationships within the AAO dataset, we find that variances in some heterotrophic taxa (cyst of *Polykrikos* sp. – Arctic, *E. karaense* and *I. minutum*) are related to changes in Sealce, while variances in some phototrophic cysts (*B. spongium*, *O. longispinigerum*, *D. chathamense* and *T. vancampoae*) can be associated with changes in SSTwinter. A higher PPsummer seems to be correlated to lower phototrophic cyst percentages and higher heterotrophic cyst fractions in general. Within the PO dataset, Sealce is correlated to axes 1 and 3 and shows a strong relationship with cyst of *Polykrikos* sp. – Arctic. Variances in *S. bentorii* and *O. israelianum* are related to variances in PPannual and PPspring, while in general, a higher productivity seem to correlate to lower phototrophic cyst percentages and higher heterotrophic cyst percentages in the AAO dataset.

However, we observe an Arch Effect within the ordination diagrams of the AAO (Figs. 3.2 and 3.3), a mathematical artefact known in ordination techniques (Gauch et al., 1977), in which the second axis is curved relative to the first axis resulting from sampling units covering a long ecological gradient while those samples at each end of the gradient having only few taxa in common (Minchin, 1987). In Fig. 3.2 some taxa and in Fig. 3.3 some sites which are located at the ends of the arch appear to be near to each other and therefore appear to be rather similar (ecologically), which is not necessarily true.

**Table 3.3:** Explained inertia and variance inflation factors of the tested environmental variables in the CCA models when all variables are considered (VIF(A)) and after manual forward selection for variables without redundancy (VIF(B)).

Environmental variable	AAO			PO		
	% inertia explained	VIF(A)	VIF(B)	% inertia explained	VIF(A)	VIF(B)
SSTsummer	13.8	8.50		13.4	17.21	
SSTwinter	14.5	6.55	1.58	14.0	16.80	
SSSummer	7.3	7.38		4.5	16.62	
SSSwinter	7.8	6.36		6.2	21.09	1.50
Sealce	8.2	4.31	1.58	4.8	1.73	1.23
PPannual	2.8	4.08		4.5	2.73	1.80
PPwinter	9.7	8.18		9.8	10.73	
PPspring	1.4	7.13		4.1	16.71	1.80
PPsummer	1.5	8.22	1.04	4.5	13.92	
PPautumn	5.5	8.79		6.9	5.60	

**Table 3.4:** CCA results and results of permutation test for the significance of CCA-axes after manual forward selection. A) Results for the AAO dataset and B) for the PO dataset.

A) AAO	CCA-axis 1	CCA-axis 2	CCA-axis 3		Total inertia	Proportion of total variance explained
Eigenvalues	0.450	0.115	0.043		3.094	0.196
Constrained proportion explained	0.741	0.189	0.070			
Constrained cumulative proportion	0.741	0.930	1.000			
F-value	259.084	66.020	24.492			
B) PO	CCA-axis 1	CCA-axis 2	CCA-axis 3	CCA-axis 4	Total inertia	Proportion of total variance explained
Eigenvalues	0.195	0.127	0.067	0.011	2.349	0.170
Constrained proportion explained	0.487	0.318	0.167	0.028		
Constrained cumulative proportion	0.487	0.804	0.972	1.000		
F-value	38.470	25.142	13.228	2.235		

**Table 3.5:** Intraset correlation for non-redundant variables and the first three/four CCA-axes and correlation coefficients ( $r^2$ ) between the variables themselves. A) Results for the AAO dataset and B) for the PO dataset.

A) AAO	CCA-axis 1	CCA-axis 2	CCA-axis 3		SSTwinter	Sealce	PPsummer	
<b>SSTwinter</b>	0.99	0.01	0.00		1	0.35	0.00	
<b>Sealce</b>	0.44	0.71	0.02			1	0.01	
<b>PPsummer</b>	0.01	0.00	0.99				1	
B) PO	CCA-axis 1	CCA-axis 2	CCA-axis 3	CCA-axis 4	SSSwinter	Sealce	PPannual	PPspring
<b>SSSwinter</b>	0.46	0.15	0.23	0.01	1	0.00	0.20	0.25
<b>Sealce</b>	0.50	0.00	0.58	0.17		1	0.15	0.07
<b>PPannual</b>	0.04	0.66	0.23	0.03			1	0.38
<b>PPspring</b>	0.00	0.72	0.02	0.32				1

The observed Arch Effect indicates either that the second axis may show no real ecological gradient and that we could assume that the dataset only has a single dominant gradient represented by axis 1 or that the second axis should only be interpreted together with the first axis as there might be no strong second dimension in the data and that a folded version of the first axis – represented by axis 2 - explains more inertia than another direction in the data. This assumption might be true as in the AAO dataset, Sealce which is represented by axis 2 is basically a truncated temperature variable (represented by axis 1). However, it might also be that the second axis represents a real ecological gradient as we observe VIF's <math>< 1.5</math>, implying that SSTwinter and Sealce variances are explained by different dimensions of species variances in the AAO dataset.

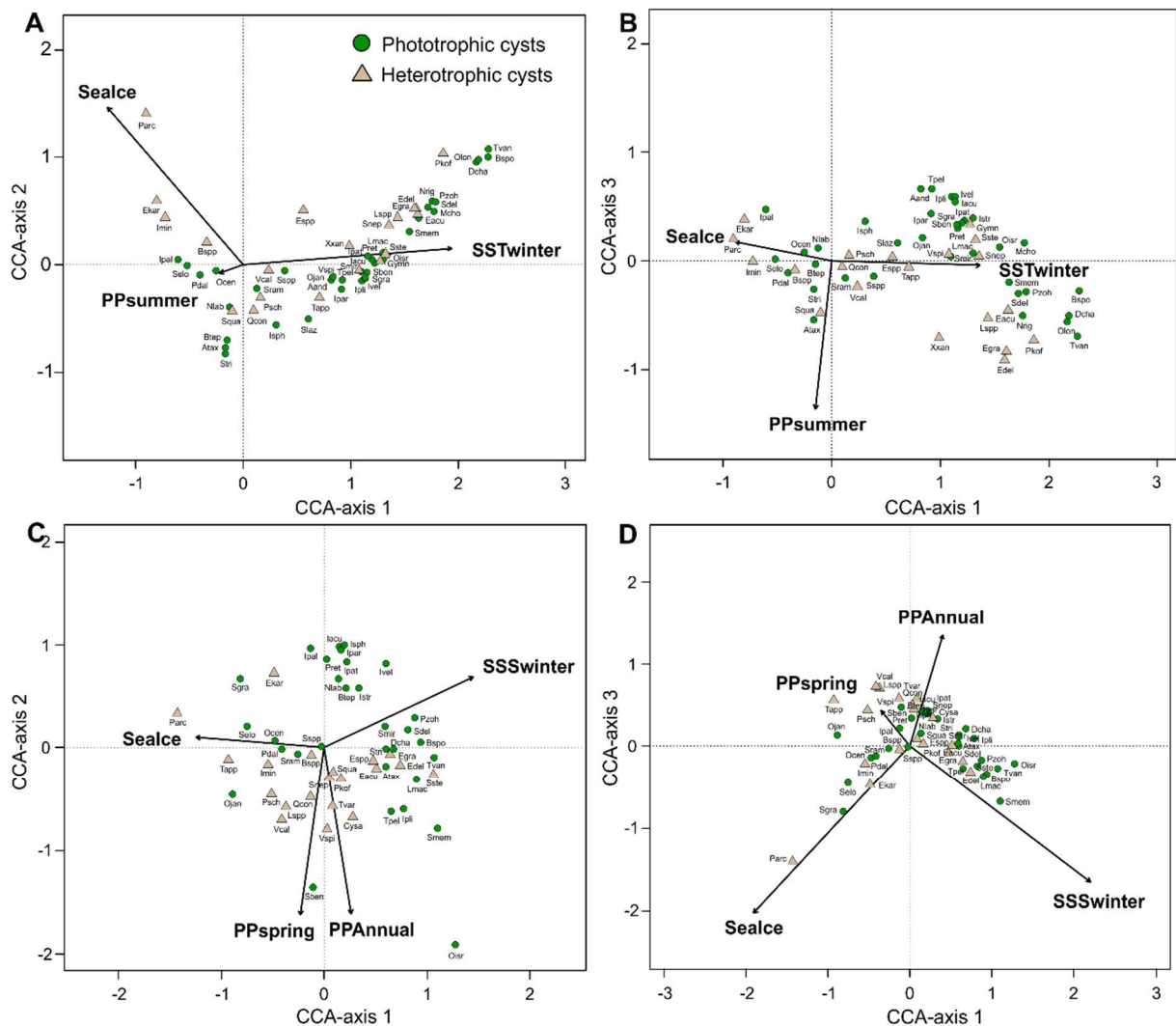


**Figure 3.2:** CCA ordination diagrams of the dinocyst taxa (see Table 3.1 for abbreviations) (taxon-environment relations), constrained by non-redundant environmental variables in AAO (A–B) and PO

(C–D) datasets. A) AAO axis 1 vs 2, B) AAO axis 1 vs 3, C) PO axis 1 vs 2 and D) PO axis 1 vs 3. Environmental variables (arrows) are displayed by their correlation with the axes (direction of arrows) and by their importance in explaining the dinocyst distribution (length of arrows).

After assessing which environmental variables can theoretically be reconstructed while being independent from each other within the two datasets, we tested for the presence of spatial and environmental autocorrelation, considering only the non-redundant variables. Like in the procedure described by Telford and Birks (2009) we used MAT with five analogues as the test reconstruction technique. In both datasets, inevitably, the performance ( $r^2$ ) of the analogue technique deteriorates with increasing fraction of sites deleted (Fig. 3.4). We find that the deterioration of performance is much worse with neighbourhood deletion than with random deletion. For example, deleting sites from the PO dataset within a 200 km neighbourhood of each site reduces the amount of analogues available on average only by 5%, but the performance of Sealce reconstruction deteriorates from 0.63 to 0.40 ( $r^2$ ). In a random site deletion, the same performance decline requires a deletion of 90% of available sites. Clearly, deleting nearby sites is not equivalent to deleting random sites, indicating the presence of spatial autocorrelation. When deleting environmentally similar sites, we find a pattern of performance loss that is worse for neighbourhood deletion than for environmental deletion (Fig. 3.4). This is especially the case for Sealce in both datasets and PPsummer in the AAO dataset. For SSSwinter and PPspring in the PO dataset removing environmentally similar sites causes a similar decline in performance of the analogue technique as when the same fraction of geographically close sites is removed (Fig. 3.4). Thus, there is evidence for spatial autocorrelation due to environmental similarity for at least those two variables but it seems that spatial similarity does not reflect environmental similarity for most other tested environmental variables. Environmental variables showing exclusively a strong signal of spatial autocorrelation because of spatial similarity might not have been the primary drivers for dinocyst assemblage composition at most sites within the calibration dataset. This is because, in these instances, assemblages are similar only due to geographical proximity rendering any environmental variable to appear reconstructable as long as it varies in space with a similar spatial autocorrelation structure as the assemblage composition. However, for those variables where performances drop below 0.65 when samples within a 200 km radius are deleted, we can assume that the transfer function might not be deemed robust.

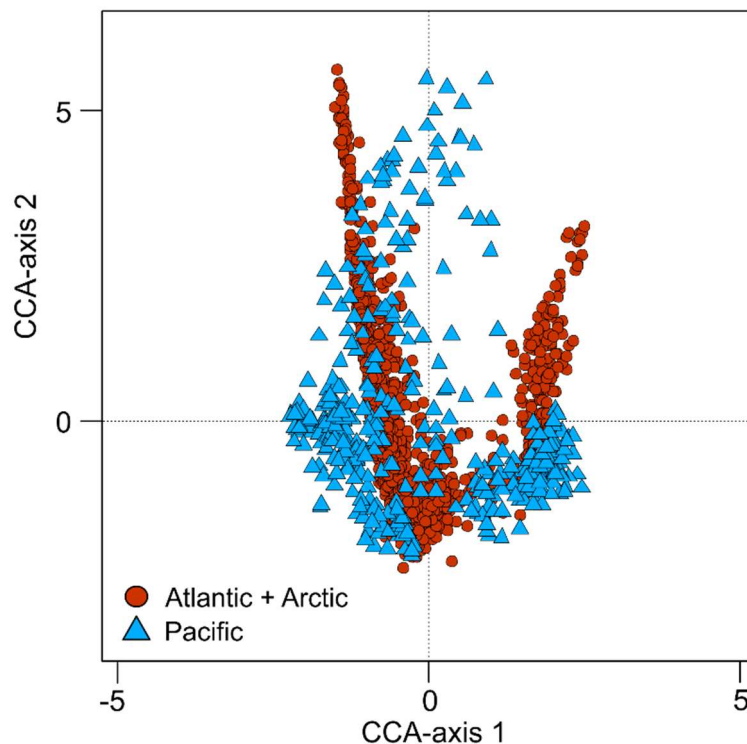


**Figure 3.3:** Sample ordination for CCA constrained by non-redundant environmental variables for axes 1 and 2 in the AAO and PO datasets (analysed separately but shown in the same diagram).

Next, we apply ML, WA-PLS and MAT for transfer function development for the non-redundant variables as these appear to be suitable for a calibration of independent transfer functions, while together explaining the maximum amount of inertia. Performance analyses of MAT indicate that the optimum number of analogues varied between two and seven depending on the variable and the dataset (Table 3.6). For WA-PLS the number of retained components varied between two and five (Table 3.7). The requirement of few analogues or many components might be on account of the found spatial autocorrelation, hinting to the necessity of an h-block cross-validation for model selection.

The LOO-cross-validation indicates best performance for MAT, with WA-PLS RMSEP values on average higher by >50% and ML RMSEP values on average higher by >80% (Table 3.7). In contrast, the differences in RMSEP between the calibration and verification subsets are on average <5%, indicating similar performance between the larger calibration subset and the small verification subset. In the AAO dataset, SSTwinter appears to be better reconstructed than Sealce, which appears better reconstructed than PPsummer, following the ranking of the variables in the CCA (Table 3.3). In the PO dataset, the differences among the variables are smaller, corresponding to their more similar F-values in the CCA test (Table 3.3). Nevertheless, for all methods, productivity appears more difficult to reconstruct than SSSwinter and Sealce.

The h-block cross-validation reveals a markedly different result, with MAT RMSEP increasing two- to fourfold, but the RMSEP of the WA-PLS and ML remained largely unaffected by the applied site deletion (Table 3.7). H-values, estimated by fitting a spherical variogram to detrended residuals of a WA model (Fig. S3.2 - Supplementary material), range between 165 and 1626 km depending upon the variable (Table 3.7).

An inspection of the distribution of residuals of the tested variables along their environmental gradient reveals symmetrical and even residual distribution for SSTwinter and SSSwinter (Fig. 3.5). For all transfer function methods, the spatial structure of the residuals is complex and large residual values are observed on the geographical edges of the two regions. Sealce residuals show for all methods and both datasets a distinct bias, which is the manifestation of a systematic underestimation of sea-ice cover in the polar Arctic and subpolar North Pacific (Fig. 3.5). The apparent truncation of the spread of the residuals is simply reflecting the constrained range of the variable between 0 and 12. Reconstructions of PP also show a clear structure in the residuals, especially in WA-PLS reconstruction for the AAO dataset, where they reflect systematic errors over the Siberian shelf and in the Arctic. The PP productivity residuals for both seasons in the PO dataset are more biased for WA-PLS and ML, where they appear to follow an east-west dipole across the North Pacific.

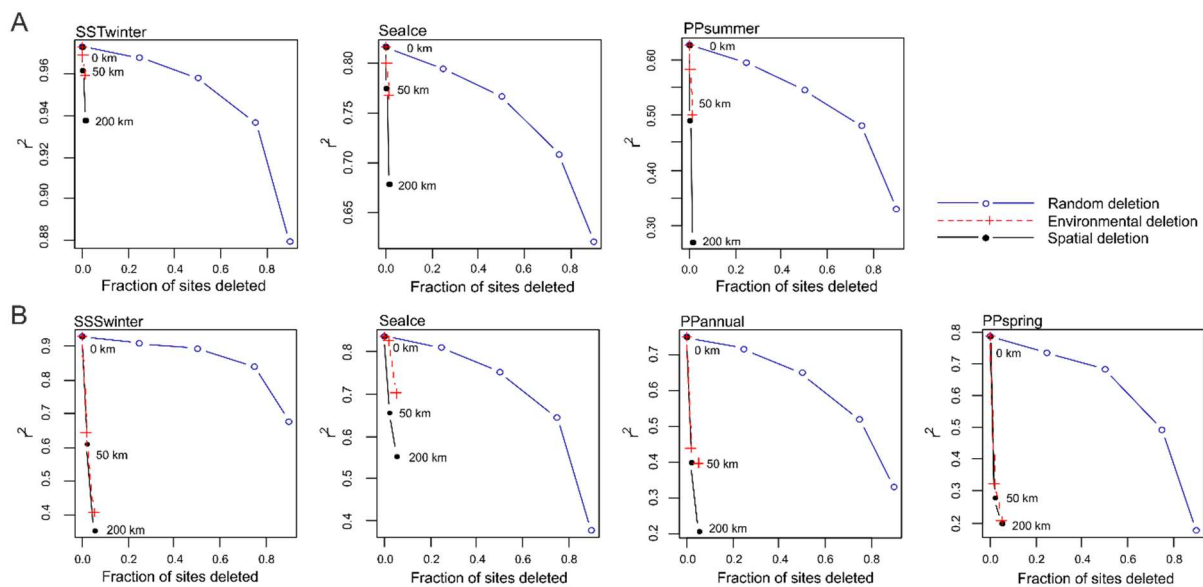


**Figure 3.4:** The effect of site deletion on the performance of a test transfer function (leaving-one-out  $r^2$  between observed and predicted values), comparing random site deletion, neighbourhood deletion (testing three distances) and environmental deletion for A) AAO and B) PO non-redundant variables. Note that the scale for  $r^2$  is different for each tested variable depending on its performance at the beginning.



**Table 3.6:** Performance of MAT reconstructions for different number of analogues used. Best performance/used number of analogues in cross-validation tests in bold.

No. of analogues used	A) AAO						B) PO							
	SSTwinter		Sealce		PPsummer		SSSwinter		Sealce		PPannual		PPspring	
	RMSE	r <sup>2</sup>	RMSE	r <sup>2</sup>	RMSE	r <sup>2</sup>	RMSE	r <sup>2</sup>	RMSE	r <sup>2</sup>	RMSE	r <sup>2</sup>	RMSE	r <sup>2</sup>
1	1.37	0.97	1.91	0.78	867.94	0.38	0.68	0.88	0.58	0.71	84.79	0.66	619.28	0.72
2	1.17	0.98	1.69	0.82	769.25	0.51	<b>0.49</b>	<b>0.94</b>	0.51	0.78	70.67	0.76	534.10	0.79
3	1.10	0.98	1.62	0.84	723.93	0.57	0.51	0.93	<b>0.50</b>	<b>0.78</b>	72.93	0.75	529.79	0.79
4	<b>1.08</b>	<b>0.98</b>	<b>1.57</b>	<b>0.85</b>	700.07	0.60	0.51	0.93	0.51	0.78	71.94	0.75	<b>527.32</b>	<b>0.80</b>
5	1.08	0.98	1.57	0.85	691.56	0.61	0.54	0.93	0.50	0.78	<b>71.52</b>	<b>0.76</b>	535.72	0.79
6	1.09	0.98	1.58	0.85	683.27	0.62	0.54	0.93	0.50	0.78	71.59	0.76	534.65	0.79
7	1.09	0.98	1.58	0.85	<b>681.96</b>	<b>0.62</b>	0.55	0.92	0.51	0.78	72.48	0.75	550.58	0.78
8	1.11	0.98	1.60	0.84	682.19	0.62	0.55	0.92	0.52	0.77	73.04	0.75	564.28	0.77
9	1.10	0.98	1.62	0.84	687.02	0.61	0.57	0.92	0.52	0.77	73.95	0.74	580.45	0.75
10	1.11	0.98	1.62	0.84	688.56	0.61	0.57	0.91	0.52	0.77	75.06	0.73	590.39	0.74

**Table 3.7:** Cross-validation performance for MAT (c - calibration dataset, v – verification dataset) with the number of analogues used (#ana.), for WA-PLS with the number of components used (#comp.) and for ML, applying LOO-cross-validation and h-block cross-validation on the AAO and PO datasets. The number of analogues and components that will perform best during reconstructions (#ana. and #comp.) have been determined calculating the RMSE of prediction as a function of the number of analogues used and a randomisation t-test for testing the significance of cross-validated components used after van der Voet (1994), respectively.

Method	LOO													
	MAT					WA-PLS					ML			
	RMSEP	r <sup>2</sup> <sub>c</sub>	RMSEP	r <sup>2</sup> <sub>v</sub>	#ana.	RMSE	r <sup>2</sup>	RMSEP	r <sup>2</sup>	#comp.	RMSE	r <sup>2</sup>	RMSEP	r <sup>2</sup>
A) AAO														
SSTwinter	1.10	0.98	1.15	0.98	4	2.82	0.87	2.95	0.86	4	2.99	0.86	3.00	0.86
Sealce	1.62	0.84	1.58	0.84	4	2.61	0.58	2.65	0.57	4	3.31	0.48	3.32	0.48
PPsummer	687.93	0.61	710.13	0.59	7	934.71	0.28	948.11	0.26	3	1472.35	0.21	1501.40	0.19
B) PO														
SSSwinter	0.54	0.92	0.42	0.96	2	0.89	0.79	0.94	0.77	4	1.79	0.24	1.78	0.25
Sealce	0.53	0.77	0.56	0.63	3	0.76	0.50	0.79	0.46	3	1.02	0.51	1.05	0.49
PPannual	72.58	0.75	75.77	0.74	5	102.51	0.50	105.42	0.47	2	133.27	0.41	133.69	0.40
PPspring	554.93	0.78	499.69	0.81	4	872.60	0.44	903.08	0.40	3	1121.74	0.19	1131.50	0.18
Method	h-block													
	MAT			WA-PLS			ML		h [km]	Variogram model				
	RMSEP	r <sup>2</sup>	#ana.	RMSEP	r <sup>2</sup>	#comp.	RMSEP	r <sup>2</sup>						
A) AAO														
SSTwinter	3.60	0.80	4	2.79	0.88	5	3.02	0.86	1307	Spherical				
Sealce	2.92	0.50	4	2.60	0.58	4	3.31	0.48	588	Spherical				
PPsummer	1243.21	0.01	7	922.98	0.32	5	1403.36	0.23	1089	Spherical				
B) PO														
SSSwinter	2.25	0.02	2	0.95	0.81	5	1.96	0.32	1626	Spherical				
Sealce	0.74	0.58	3	0.71	0.56	4	1.02	0.51	165	Spherical				
PPannual	134.87	0.20	5	96.51	0.56	5	133.50	0.41	208	Spherical				
PPspring	1823.37	0.02	4	831.78	0.48	4	1210.95	0.16	795	Spherical				

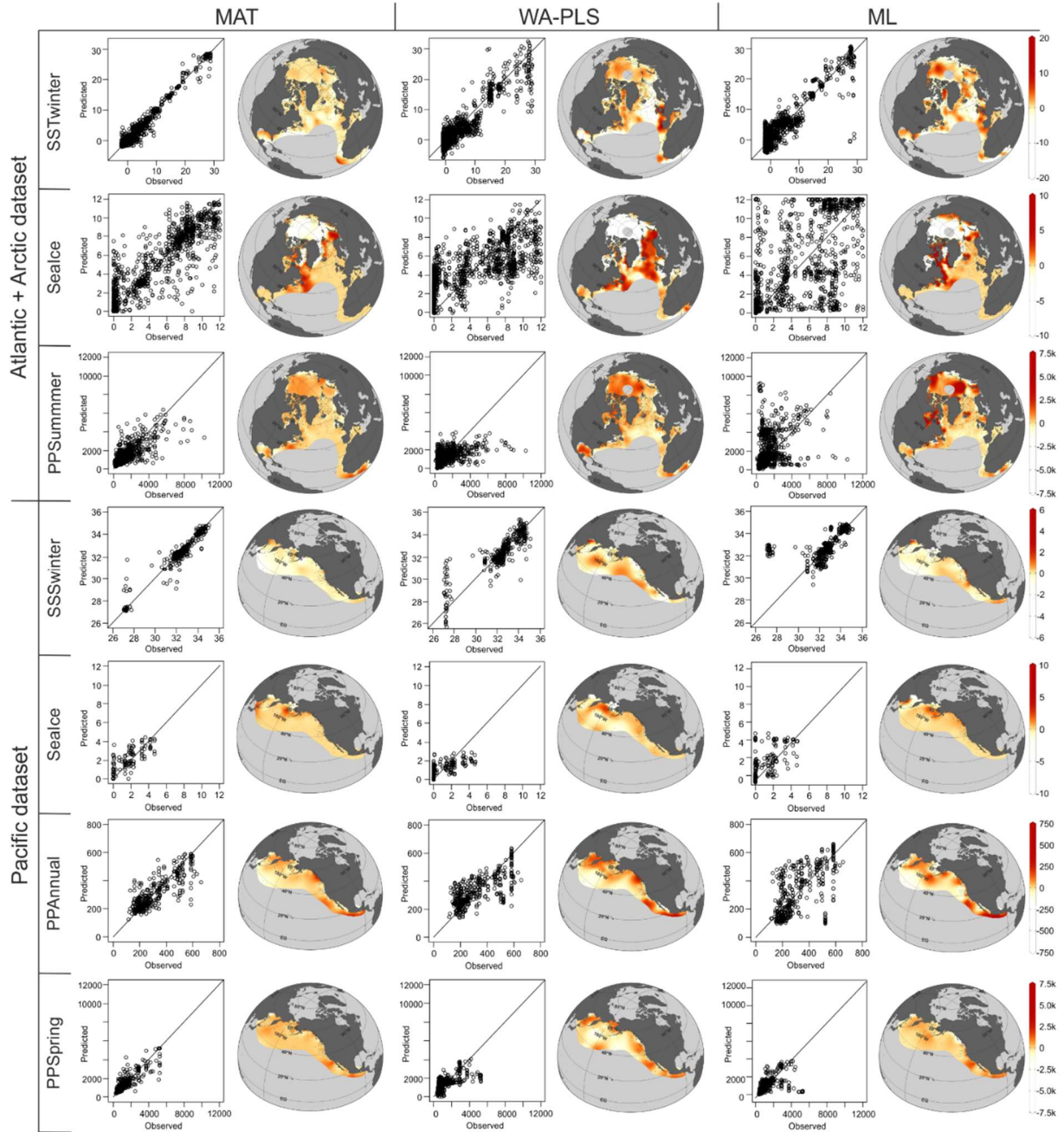


**Figure 3.5:** Residuals from the leave-one-out cross-validation for all tested transfer functions shown in cross-plots of predicted vs. observed environmental variables and in maps, indicating overestimation through red colours and underestimation through white colours. Orange colours indicate none or little residuals.

### 3.5 Discussion

Inevitably, the distribution and composition of dinocyst assemblages in the calibration dataset could carry an imprint of non-oceanographic factors and post-depositional alteration. Therefore, prior to a discussion of the analysed oceanographic variables, we first consider the effect of two potential non-oceanographical factors: the dinoflagellate life-cycle (e.g., Bravo and Figueroa, 2014) and organic matter degradation (Zonneveld et al., 2019). The encystment of dinoflagellates is related to the sexual reproduction and the function of dinocysts is to protect the diploid cell during dormancy of variable length after which the cell excysts and re-establishes metabolic activities and cellular divisions within the pelagic ecosystem (Taylor and Pollinger, 1987). For many dinoflagellate taxa, the cycle includes settlement of the cyst on the seafloor and the completion of the life cycle is thus favoured where the seafloor is not too deep to prevent excystment and migration of the cells towards surface waters. This is already reflected in the bias towards samples from marginal marine settings in the calibration dataset (Fig. 3.1).

Nevertheless, many of the calibration samples were taken further offshore and we therefore tested for the potential effect of life-cycle processes on the observed dinocyst distribution by carrying out a CCA constrained in addition to the oceanographic variables also by water depth (1 m – 5655 m; pooled data) and distance from shore (0.02 km–1493.44 km; pooled data). Both variables were shown to explain a significant amount of variance in a pooled analysis as well as in an analysis for the AAO and PO datasets separately ( $p < .01$ ). The variables are collinear, but appear to describe in each dataset a separate dimension of variability, independent of the oceanographic factors. Thus, the dinocyst distribution appears to be affected by life-cycle processes, at least at the analysed sites further away from shorelines. On the other hand, distance from shore and water depth could also describe a gradient in some unconsidered primary driving variable, such as predation or other biotic interaction, and further work is required to elucidate the nature of the apparent relationship of dinocyst assemblages to depth and distance from shore.

In the hypothesis that post-depositional processes, such as organic matter degradation, affect the dinocyst assemblage composition at some sites, the residuals of the transfer functions should be disproportionately large for the affected samples. However, we observe no systematic relationship between the residuals for any of the tested variables and the ratio between cysts of heterotrophic and autotrophic/ phototrophic taxa (none of the correlation coefficients is significant; Fig. 3.6), which should systematically decrease with increasing degradation due to the different composition of the wall polymer of the heterotrophic taxa (e.g., Zonneveld et al., 1997). We observe similar relationships between residuals and heterotrophic

cyst abundances for MAT, WA-PLS and ML, contradicting the hypothesis of regional organic matter degradations for geographically close assemblages. Additionally, objecting a general degradation issue within the calibration datasets is the relative high abundance ratio of Brigantedinium spp. (> 900 samples > 5% for AAO, > 320 samples > 5% for PO), a very sensitive taxon in regard of organic aerobic degradation (e.g., Zonneveld et al., 2008).

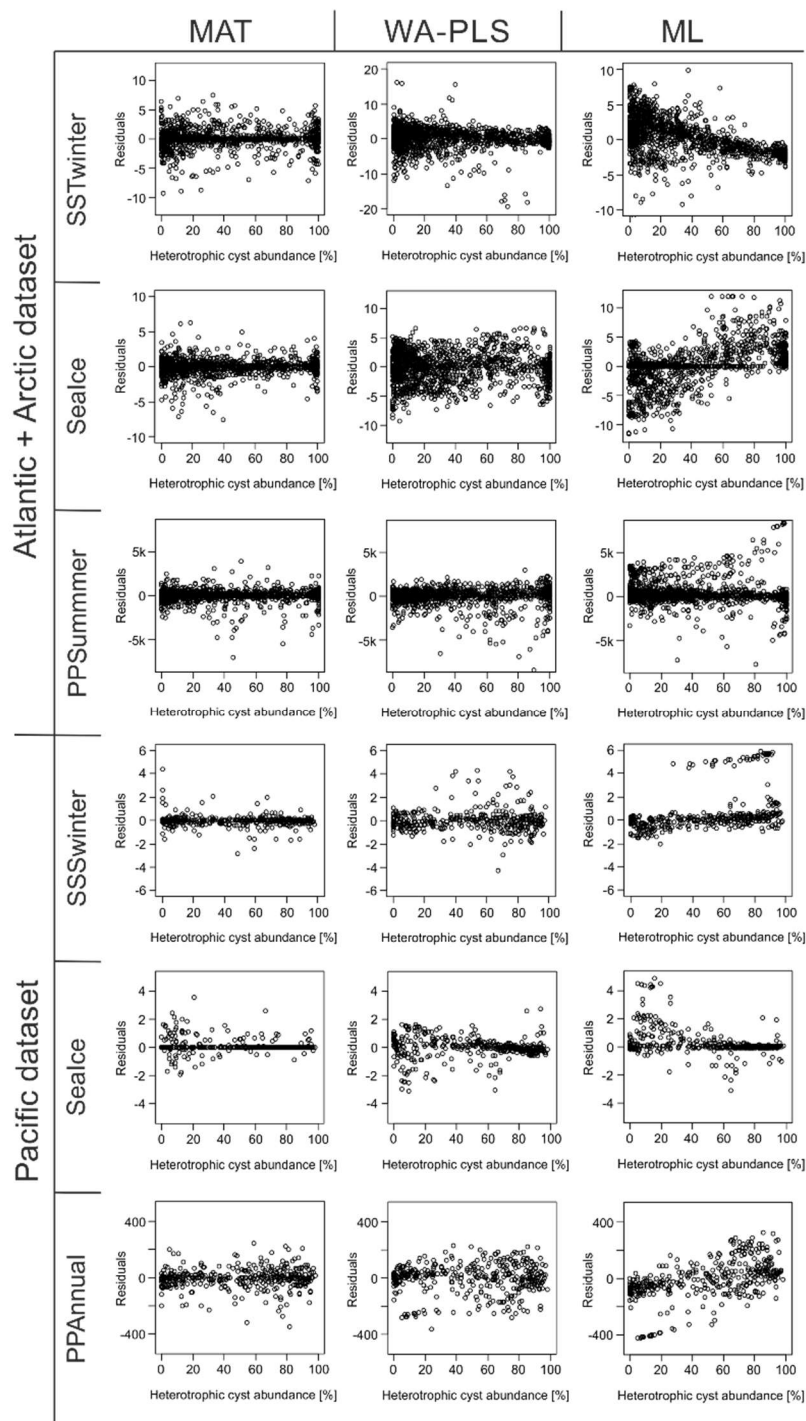
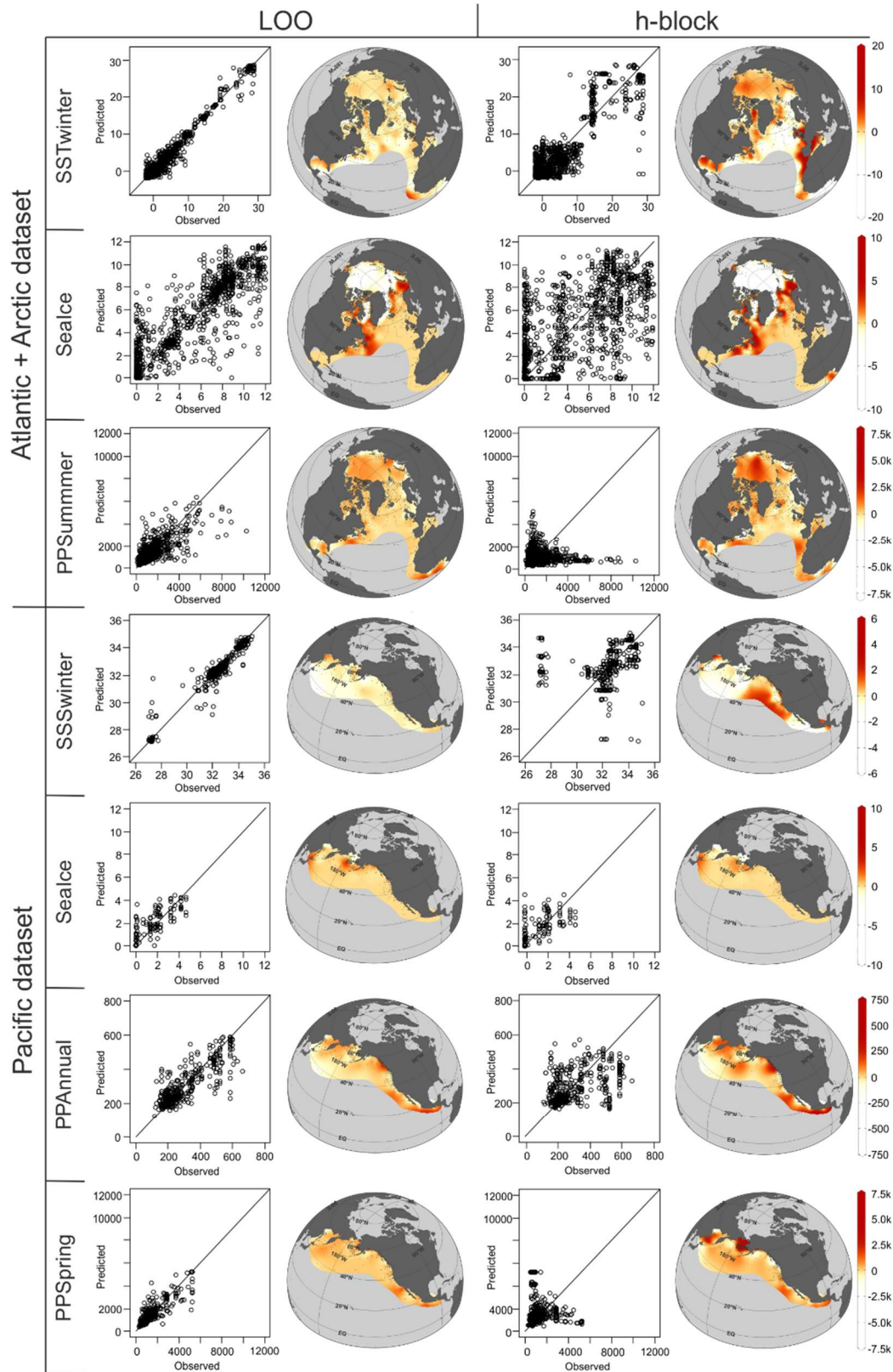


Figure 3.6: Residuals from leave-one-out cross-validation and heterotrophic cyst ratio.

Having excluded the substantial effect of selective degradation as a secondary factor and showing that life-cycle factors explain an independent dimension of the variance, we can consider the distribution of dinocyst assemblages in the calibration datasets as being driven by environmental (oceanographic) factors. First, we consider the significance of the observation that each of the two datasets contains at least three mutually independent ecological gradients, which can be attributed to different environmental factors. This result contrasts with the distribution of zooplankton microfossils, such as planktonic foraminifera and radiolarians, which seems to be controlled by temperature alone (Morey et al., 2005; Hernández-Almeida et al., 2017). However, it is comparable to an analysis of diatom distribution in the North Pacific, which also showed the control of multiple environmental factors (Lopes et al., 2010). It is reasonable to conclude that phytoplankton has a more complex relationship to the environment than zooplankton, reflecting the independent imprint of hydrography and nutrient availability. In the case of dinoflagellates, this is further accentuated by their proliferation in marginal marine environments, where the environmental gradients are more pronounced compared to the dominantly open ocean habitat of planktonic foraminifera and radiolaria. The confirmation that dinocyst assemblages reflect multiple environmental gradients is in line with previous findings (de Vernal et al., 2000, 2001, 2005a); Dale et al., 2002; Holzwarth et al., 2007; Radi and de Vernal, 2008; Ribeiro and Amorim, 2008) and appears to suggest that it should be possible to extract information from the same fossil dinocyst assemblage on past variability for more than one of the environmental drivers. However, we have to caution against such generalisation, because the presence of multiple environmental gradients in the tested dinocyst datasets is clearly associated with spatial structuring of their environment. For example, in the PO dataset, a large portion of the salinity and sea-ice gradient only affects the northwestern margin (Fig. 3.5). In other words, it seems that the environmental variables that are deemed significant in the redundancy analysis are significant because they drive dinocyst distribution in a certain region within the dataset, where the gradient in the given variables is strong. This is consistent with the observed strong spatial autocorrelation of the environmental variables (Fig. 3.4) and leads to a large decrease in the performance of MAT in h-block validation (Fig. 3.7) and strong spatial structure of the residuals in all methods (Fig. 3.5). The existence of regionally different environmental drivers on dinocyst distribution is also reflected by the different outcome of variable selection in the PO and AAO datasets (Table 3.3). Collectively, these observations indicate that the detected mutually independent signature of multiple environmental factors in each dataset is likely a result of agglomeration of information from regions with different environmental drivers and specific (endemic) taxon-environment relationships. A more powerful characterisation of each gradient would require more localised analysis, which comes, inevitably, at the cost of loss of

generalisation of the resulting ecological models and their limited applicability to past oceanographic states.

Irrespective of the effect of the spatial structuring of the environmental gradients on the dinocyst data, a large portion of variance in the two datasets (around 70%) cannot be explained by any combination of the tested environmental variables even when water depth and distance from shore are included. There are several potential explanations for this lack of determinism in dinocyst assemblage composition, some of which could act in combination. Firstly, it is possible that the applied taxonomic concepts, often combining taxa to achieve higher consistency, hide a finer taxonomic level, which is ecologically relevant. This process is very likely active, as evidenced by the existence of cryptic species in modern dinoflagellates (Montresor et al., 2003; Parkinson et al., 2016; Wang et al., 2019), but unavoidable because it is unlikely that the current taxonomic concepts as applied in the practice can be substantially refined in routine analyses (de Vernal et al., 2020). Secondly, it is possible that we left out one or several important environmental variables in the analysis. If such variables occur, and act independently of (are not collinear with) the tested variables, then the result of the variable selection (Table 3.3) may be biased. Such a situation is unlikely for variables describing the physical aspects of the environment, as those would likely covary with temperature or sea ice, but we have of course no control on variables related to biotic interactions, such as the presence of specific prey, predator or competitor. The effect of biotic interactions on marine plankton (Lima-Mendez et al., 2015) is likely a major contributor to the unexplained portion of the variance. Thirdly, immobile particles as dinocysts sinking within the water column are subjected to some transport by three-dimensional currents. This might, in some areas in the open ocean where gyres are in place, result in a lateral relocation and deviant sedimentation of the cysts from their region of origin (Nooteboom et al., 2019), resulting in transport biases between deposited dinocysts and the overlying environmental variables. Finally, there may be another bias regarding the way we assign environmental variables to sedimentary assemblages. These represent average fluxes over different time intervals and the resulting assemblages may be to a different degree affected by anthropogenic effects, such as local pollution or global warming. Conversely, assemblages from sites with low sediment accumulation may represent averages over millennia and contain microfossils deposited during distinct oceanographic events of the late Holocene (e.g., Wigley et al., 1981; Bradley and Jonest, 1993). Since most sites in the database likely integrate over longer periods (centuries), there should be a systematic bias caused by offsetting the taxon-environment relationship towards conditions induced by anthropogenic global change, which are reflected in the values of the environmental variables derived from instrumental records.



**Figure 3.7:** Residuals from MAT for leave-one-out and h-block cross-validation shown in cross-plots of predicted vs. observed environmental variables and in maps, indicating overestimation through red colours and underestimation through white colours. Orange colours indicate none or little residuals.



A specific reason for the complicated relationship between dinocyst assemblage composition and environmental variables could be the presence of samples with unusual composition, distorted by some secondary (e.g., depositional) or primary (e.g., biotic) factor. The existence of such heterogeneity in the calibration dataset can be easily detected by diagnosing the distribution of the residuals from the transfer function models. Such assemblages should lack good analogues and a correlation between the dissimilarity to the nearest analogue and the residual would be expected. This is unlikely a significant effect in our case, since we do not observe any such relationship (Fig. 3.8). It seems, on the contrary, that all assemblages are sufficiently represented and that the geographical range of the dataset is not an issue. This is also reflected by the remarkable performance of SSTwinter transfer functions (Table 3.7). A no-analogue assemblage situation should also lead to a predictable pattern in the distribution of transfer-function residuals for different variables reconstructed from the same assemblage. If a given assemblage lacked analogues, then it should more likely cause a large deviation from the actual value of all the reconstructed environmental variables. This is also not the case (Fig. 3.6), but we observe that the residuals show a different diagnostic pattern. Large residuals are usually mutually exclusive between pairs of reconstructed variables (Fig. 3.9). Apparently, where it seems difficult to reconstruct productivity, temperature residuals are small and a similar pattern holds for all pairs of variables. This is very likely a signature of spatially structured environmental gradients driven by different dominant processes in each region.

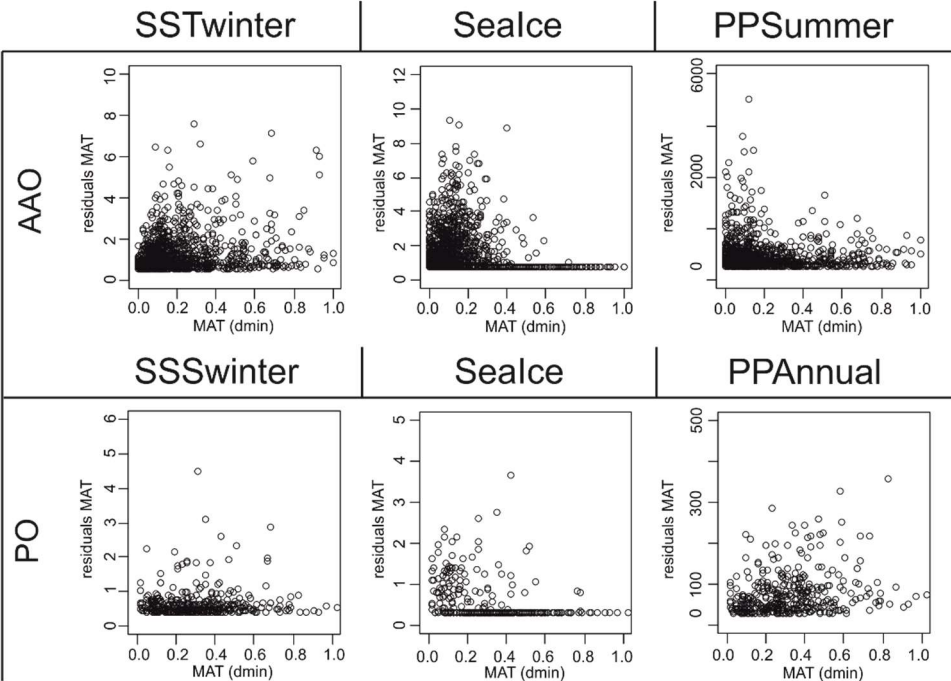


**Figure 3.8:** Residuals from MAT leave-one-out cross-validation and the dissimilarities to the closest analogue.



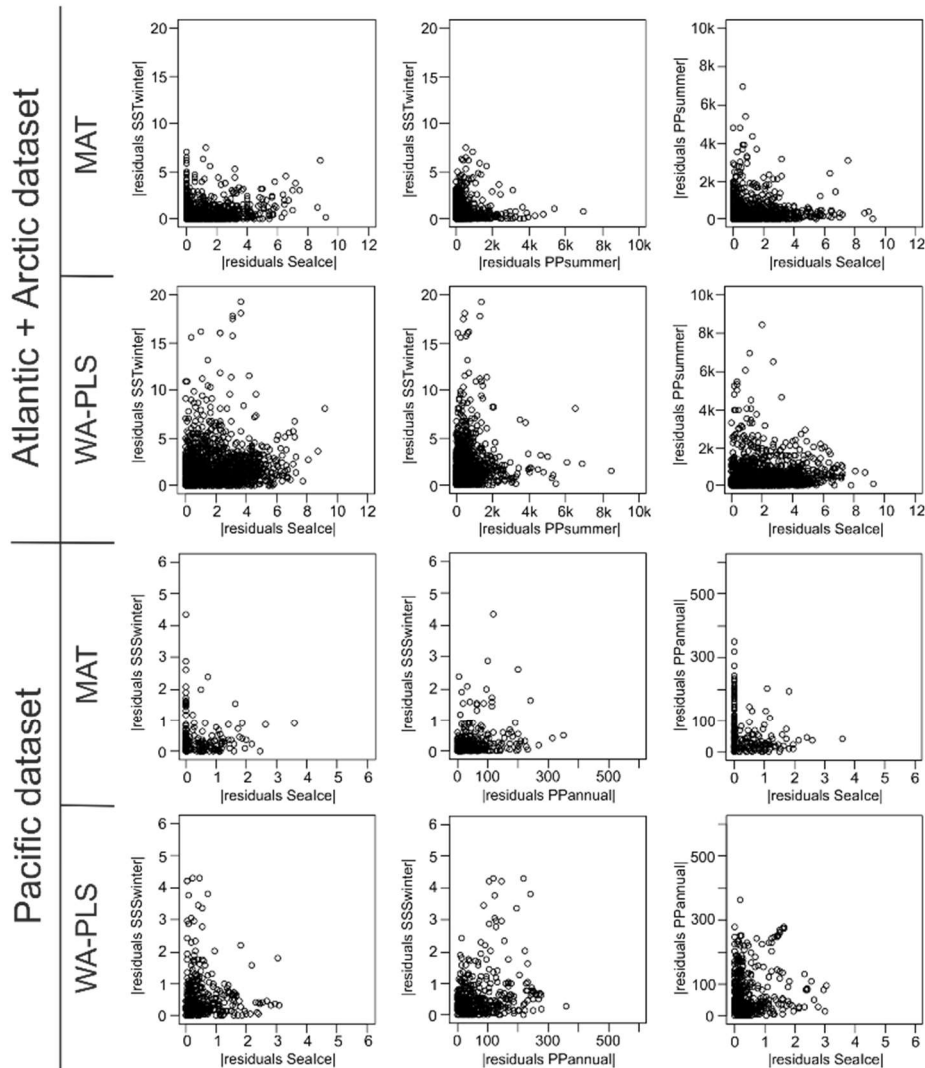


**Figure 3.9:** Correlation between residuals from the tested variables from MAT and WA-PLS leave-one-out cross-validation.

The potential effects of non-oceanographic variables, the spatial structuring of the datasets and the regionally different dominant environmental drivers would all affect our ability to produce environmental reconstruction models reflecting the most general aspect of the taxon-environment relationship, which has the best prospect to yield meaningful palaeoenvironmental reconstructions. In theory, these factors should affect different transfer function approaches based on different fundamental principles in different ways (Kucera et al., 2005). This was the reason for the selection of the three specific methods in this study. Indeed, our analyses reveal that they are affected by the properties of the datasets in different ways. The ML approach appears unable to effectively (with low RMSEP and high  $r^2$ ) extract the taxon-environment relationship in the presence of multiple gradients. In contrast, the same approach,

together with WA, is less affected by the spatial autocorrelation of the tested environmental variables. When this is considered by using the h-block validation, the performance of WA and ML remains essentially the same, but the performance of MAT plummets, returning not only higher RMSEP and lower  $r^2$  than ML and WA (Table 3.7), but also replicating the regional structure of the residuals as shown by ML and WA irrespective of how validated (Fig. 3.10). This is not to say that MAT is not suited for transfer function development with dinocyst assemblage data, but it indicates that the performance indicators for this method based on LOO are more optimistic than for ML and WA (Telford and Birks, 2005). Regardless of the approach, the threshold of change in a reconstructed variable that can be safely interpreted is large and one must consider this inherent uncertainty when interpreting dinocyst transfer function reconstructions with low amplitude of inferred past variability.

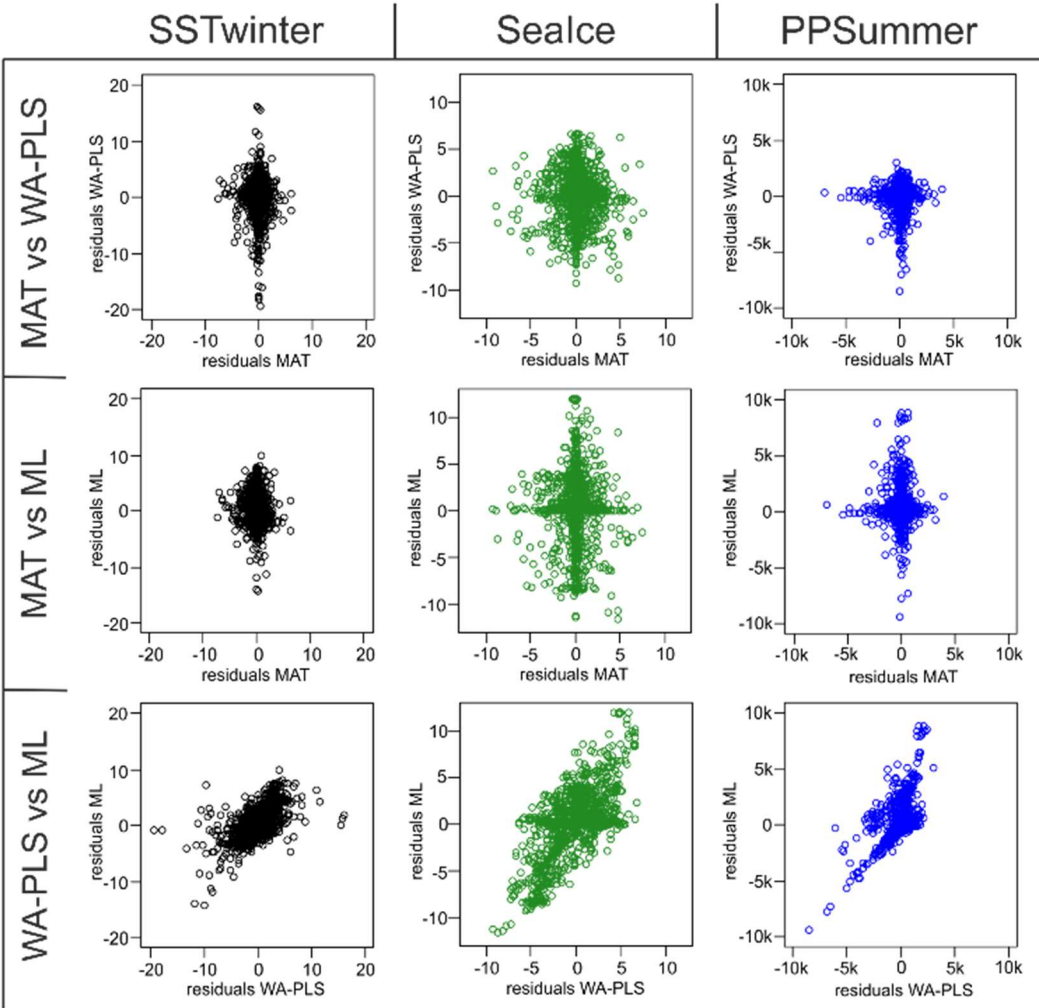


**Figure 3.10:** Correlations between leave-one-out residuals from the considered three transfer function approaches for the AAO dataset.

### 3.6 Conclusion

By analysing the relationship between dinocyst distribution in surface sediment samples and a range of potential driving environmental variables in two new regional calibration datasets, we highlight the complexity of this relationship and review the statistical considerations involved in the application of analogue technique and transfer functions to obtain quantitative palaeoenvironmental reconstructions from fossil dinocyst assemblages.

For the tested AAO and PO dinocyst datasets, among the ten considered environmental variables three (AAO) or four (PO) explained significant amounts of the variance independently of each other, indicating that multiple variables independently affect the assemblage composition and thus could, in theory, be reconstructed. In both datasets, seasonal values of the same variable were found to be too highly correlated to be reconstructed independently.

Both datasets show significant spatial autocorrelation, which leads to underestimation of prediction uncertainty in leave-one-out cross-validation tests, especially for the analogue technique. For some variables, the spatial autocorrelation resonates with environmental autocorrelation (close sites are similar because they are affected by similar conditions), but we also observed for some variables a signature of only spatial autocorrelation (close sites are similar only because they are close), with consequences for variable selection in transfer function models. Either way, in both of the tested datasets, the spatial and environmental gradients are sufficiently covered and the performance of transfer function models is unlikely to improve by adding more samples to the datasets.

Between the two regional datasets, different variables were found to explain different amounts of the taxa variance and different variables were found to be independent, suggesting different primary driving factors for taxa assemblages for different areas. These observations point to the necessity of separate variable selection depending upon the region of the calibration dataset. We conclude that regional calibrations, even at the expense of generalisation, could improve the reliability of dinocyst-based quantitative palaeoenvironmental reconstructions, particularly by a more realistic identification of the main controlling environmental variables that can be reconstructed.

Supplementary data to this article can be found online at [https:// doi.org/10.1016/j.marmicro.2019.101816](https://doi.org/10.1016/j.marmicro.2019.101816).

### 3.7 Data availability

Supplementary data associated with this article can be found online at <https://doi.org/10.1016/j.marmicro.2019.101816>. This material includes the matrices of taxa abundances with all tested environmental (oceanographic and non-oceanographic) variables for the PO and AAO datasets, DCA analyses plots and variogram plots. The R codes applied for analyses can be accessed on Zenodo.org (<https://zenodo.org/record/3594160>).

### 3.8 Acknowledgements

This study is a contribution of the International Research Training Group “Processes and Impacts of Climate Change in the North Atlantic Ocean and the Canadian Arctic” (ArcTrain), which was supported jointly by the German Research Foundation (DFG) (IRTG 1904 ArcTrain) and by the Natural Sciences and Engineering Research Council of Canada (NSERC). We also acknowledge the support from the Fonds de recherche du Québec – Nature et Technologie (FRQNT). We are grateful to Taoufik Radi and Sebastien Zaragozi for their help in the preparation of the reference oceanographical data set.

### 3.9 References (Chapter 3, according to the journal’s style)

- Behrenfeld, M.J., Falkowski, P.G., 1997. Photosynthetic rates derived from satellite-based chlorophyll concentration. *Limnol. Oceanogr.* 42, 1–20. <https://doi.org/10.4319/lo.1997.42.1.0001>.
- Berger, W.H., 1970. Planktonic Foraminifera: selective solution and the lysocline. *Mar. Geol.* 8, 111–138.
- Birks, J.B., 1995. Quantitative palaeoenvironmental reconstructions. In: Maddy, D., Brew, I.S. (Eds.), *Statistical Modelling of Quaternary Science Data*. Quaternary Research Association, Cambridge (271 pp).
- Birks, H.J.B., Line, J.M., Juggins, S., Stevenson, A.C., ter Braak, C.J.F., 1990. Diatoms and pH reconstruction. *Phil. Trans. R. Soc. B* 3, 263–278.
- Birks, H.J.B., Simpson, G.L., 2013. ‘Diatoms and pH reconstruction’ (1990) revisited. *Paleolimnology* 49, 363–371. <https://doi.org/10.1007/s10933-013-9697-7>.
- Bradley, R.S., Jonest, P.D., 1993. ‘Little Ice Age’ summer temperature variations: their nature and relevance to recent global warming trends. *Holocene* 3, 367–376.
- Bravo, I., Figueroa, R., 2014. Towards an ecological understanding of dinoflagellate cyst functions. *Microorganisms* 2, 11–32. <https://doi.org/10.3390/microorganisms2010011>.
- Burman, P., Bhow, E., Nonal, D., 1994. A cross-validators method for dependent data. *Biometrika* 81, 351–358.
- Dale, B., 1983. *Dinoflagellate Resting Cysts: “Benthic Plankton,” Survival Strategies of the Algae*. Cambridge University Press.
- Dale, B., Dale, A.L., Jansen, J.H.F., 2002. Dinoflagellate cysts as environmental indicators in surface sediments from the Congo deep-sea fan and adjacent regions. *Palaeogeogr. Palaeoclimatol. Palaeoecol.* 185, 309–338. [https://doi.org/10.1016/S0031-0182\(02\)00380-2](https://doi.org/10.1016/S0031-0182(02)00380-2).

- de Vernal, A., Eynaud, F., Henry, M., Hillaire-Marcel, C., Londeix, L., Mangin, S., Matthiessen, J., Marret, F., Radi, T., Rochon, A., Solignac, S., Turon, J.L., 2005a. Reconstruction of sea-surface conditions at middle to high latitudes of the Northern Hemisphere during the last Glacial Maximum (LGM) based on dinoflagellate cyst assemblages. *Quat. Sci. Rev.* 24, 897–924. <https://doi.org/10.1016/j.quascirev.2004.06.014>.
- de Vernal, A., Hillaire-Marcel, C., Darby, D.A., 2005b. Variability of sea ice cover in the Chukchi Sea (western Arctic Ocean) during the Holocene. *Paleoceanography* 20. <https://doi.org/10.1029/2005PA001157>.
- de Vernal, A., Henry, M., Bilodeau, G., 2010. Micropaleontological preparation techniques and analyses. In: *Les Cahiers du GEOTOP*.
- de Vernal, A., Henry, M., Matthiessen, J., Mudie, P.J., Rochon, A., Boessenkool, K., Eynaud, F., Grøsfjeld, K., Guiot, J., Hamel, D., Harland, R., Head, M.J., Kunz-Pirrung, M., Levac, E., Loucheur, V., Peyron, O., Pospelova, V., Radi, T., Turon, J.-L., Voronina, E., 2001. Dinoflagellate cyst assemblages as tracers of sea-surface conditions in the northern North Atlantic, Arctic and sub-Arctic seas: the new “n= 677” data base and its application for quantitative palaeoceanographic reconstruction. *J. Quat. Sci.* 16, 681–698. <https://doi.org/10.1002/jqs.659>.
- de Vernal, A., Hillaire-Marcel, C., Turon, J.-L., Matthiessen, J., 2000. Reconstruction of sea-surface temperature, salinity, and sea-ice cover in the northern North Atlantic during the last glacial maximum based on dinocyst assemblages. *Can. J. Earth Sci.* 37, 725–750.
- de Vernal, A., Marret, F., 2007. Organic-walled dinoflagellate cysts: tracers of sea-surface conditions. *Dev. Mar. Geol.* 1, 371–408. [https://doi.org/10.1016/S1572-5480\(07\)01014-7](https://doi.org/10.1016/S1572-5480(07)01014-7).
- de Vernal, A., Radi, T., Zaragosi, S., Van Nieuwenhove, N., Rochon, A., Allan, E., De Schepper, S., Eynaud, F., Head, M.J., Limoges, A., Londeix, L., Marret, F., Matthiessen, J., Penaud, A., Pospelova, V., Price, A., Richerol, T., 2020. Distribution of common modern dinoflagellate cyst taxa in surface sediments of the Northern Hemisphere in relation to environmental parameters: The new n=1968 database. *Mar. Micropaleontol* this volume.
- de Vernal, A., Rochon, A., Fréchette, B., Henry, M., Radi, T., Solignac, S., 2013. Reconstructing past sea ice cover of the Northern Hemisphere from dinocyst assemblages: status of the approach. *Quat. Sci. Rev.* 79, 122–134. <https://doi.org/10.1016/j.quascirev.2013.06.022>.
- de Vernal, A., Rochon, A., Turon, J.-L., Matthiessen, J., 1997. Organic-walled dinoflagellate cysts: palynological tracers of sea-surface conditions in middle to high latitude marine environments. *Geobios* 30, 905–920. [https://doi.org/10.1016/S0016-6995\(97\)80215-X](https://doi.org/10.1016/S0016-6995(97)80215-X).
- de Vernal, A., Turon, J.-L., Guiot, J., 1994. Dinoflagellate cyst distribution in high-latitude marine environments and quantitative reconstruction of sea-surface salinity, temperature, and seasonality. *Can. J. Earth Sci.* 31, 48–62. <https://doi.org/10.1139/e94-006>.
- Efron, B., Gong, G., 1983. A Leisurely look at the Bootstrap, the Jackknife, and Cross-Validation. *Am. Stat.* 37, 36–48. <https://doi.org/10.1080/00031305.1983.10483087>.
- Gauch, H.G., Whittaker, R.H., Wentworth, T.R., 1977. A comparative study of reciprocal averaging and other ordination techniques. *J. Ecol.* 65, 157–174.
- Guiot, J., 1990. Methodology of the last climatic cycle reconstruction in France from pollen data. *Palaeo-geogr. Palaeoclimatol. Palaeoecol.* 80, 49–69. [https://doi.org/10.1016/0031-0182\(90\)90033-4](https://doi.org/10.1016/0031-0182(90)90033-4).
- Guiot, J., Brewer, S., Gally, Y., ECCOREV, 2014. Bioindic: Statistic Analyses for Environmental Bioindicators. R package version 4.0.9. <https://www.eccorev.fr/spip.php?rubrique55>.
- Guiot, J., de Vernal, A., 2007. Transfer functions: methods for quantitative paleoceanography based on microfossils. *Dev. Mar. Geol.* 1, 523–563. [https://doi.org/10.1016/S1572-5480\(07\)01018-4](https://doi.org/10.1016/S1572-5480(07)01018-4).
- Head, M.J., 1996. Modern dinoflagellate cysts and their biological affinities. In: Jansonius, J., McGregor, D.C. (Eds.), *Palynology: Principles and Applications*. American Association of Stratigraphic Palynologists Foundation, pp. 1197–1248.
- Hernández-Almeida, I., Cortese, G., Chen, M.-T., Kucera, M., 2017. Environmental determinants of radiolarian assemblages in the western Pacific since the last deglaciation. *Paleoceanography* 830–847. <https://doi.org/10.1002/2017PA003159>.

- Holzwarth, U., Esper, O., Zonneveld, K.A.F., 2007. Distribution of organic-walled dinoflagellate cysts in shelf surface sediments of the Benguela upwelling system in relationship to environmental conditions. *Mar. Micropaleontol.* 64, 91–119. <https://doi.org/10.1016/j.marmicro.2007.04.001>.
- Hutson, W.H., 1977. Transfer functions under no-analog conditions: experiments with Indian Ocean Planktonic Foraminifera. *Quat. Res.* 8, 355–367. [https://doi.org/10.1016/0033-5894\(77\)90077-1](https://doi.org/10.1016/0033-5894(77)90077-1).
- Hutson, W.H., 1980. The Agulhas current during the late pleistocene: analysis of modern faunal analogs. *Science (80-.)* 207, 64–67.
- Imbrie, J., Kipp, N.G., 1971. A new micropaleontological method for quantitative paleoclimatology: application to a late Pleistocene Caribbean core. In: Turekian, K.K. (Ed.), *The Late Cenozoic Glacial Ages*. Yale University Press, New Haven, pp. 71–181.
- Juggins, S., 2017. rioja: Analysis of Quaternary Science Data, R package version (0.9-21). <http://cran.r-project.org/package=rioja>.
- Koç, N., Jansen, E., Hafliðason, H., 1993. Paleoceanographic reconstruction of surface ocean conditions in the Greenland, Iceland, and Norwegian seas through the last 14,000 years based on diatoms. *Quat. Sci. Rev.* 12, 115–140.
- Kokinos, J.P., Eglinton, T.I., Gon, M.A., 1998. Characterization of a highly resistant biomacromolecular material in the cell wall of a marine dinoflagellate resting cyst. *Organic* 28, 265–288.
- Kucera, M., Weinelt, Mara, Kiefer, T., Pflaumann, U., Hayes, A., Weinelt, Martin, Chen, M., Mix, A.C., Barrows, T.T., Cortijo, E., Duprat, J., Juggins, S., Waelbroeck, C., 2005. Reconstruction of sea-surface temperatures from assemblages of planktonic foraminifera: multi-technique approach based on geographically constrained calibration data sets and its application to glacial Atlantic and Pacific Oceans. *Quat. Sci. Rev.* 24, 951–998. <https://doi.org/10.1016/j.quascirev.2004.07.014>.
- Lepš, J., Šmilauer, P., 2003. *Multivariate Analysis of Ecological Data Using CANOCO*. Cambridge university press.
- Lima-Mendez, G., Faust, K., Henry, N., Colin, S., Carcillo, F., Chaffron, S., Cesar, J., Roux, S., Vincent, F., Bittner, L., Darzi, Y., Wang, J., Audic, S., Berline, L., Cabello, A., Cornejo-castillo, F.M., Ovidio, F., De, L., Ferrera, I., Guidi, L., Pesant, S., Royo-lonch, M., Salazar, G., Sebastian, M., Souffreau, C., Dimier, C., Searson, S., Kandels-Lewis, S., Gorsky, G., Not, F., Ogata, H., Speich, S., Wincker, P., Bontempi, G., Acinas, S.G., Sunagawa, S., Bork, P., Sullivan, M.B., Bowler, C., 2015. Determinants of community structure in the global plankton interactome. *Science (80-.)* 348. <https://doi.org/10.1126/science.1262073>.
- Locarnini, R.A., Mishonov, A.V., Antonov, J.I., Boyer, T.P., Garcia, H.E., Baranova, O.K., Zweng, M.M., Paver, C.R., Reagan, J.R., Johnson, D.R., Hamilton, M., Seidov, D., 2013. Temperature. In: *World Ocean Atlas 2013*. 1 NOAA Atlas NESDIS 73.
- Lopes, C., Mix, A.C., Abrantes, F., 2010. Environmental controls of diatom species in northeast Pacific sediments. *Palaeogeogr. Palaeoclimatol. Palaeoecol.* 297, 188–200. <https://doi.org/10.1016/j.palaeo.2010.07.029>.
- Manly, B.F.J., 1991. *Randomization and Monte Carlo Methods in Biology*. NewYork Chapman Hall (281 pp).
- Marret, F., 1993. Les effets de l'acétolyse sur les assemblages des kystes de dinoflagellés. *Palynosciences* 2, 267–272.
- Matthiessen, J., 1995. Distribution patterns of dinoflagellate cysts and other organic-walled microfossils in recent Norwegian-Greenland Sea sediments. *Mar. Micropaleontol.* 24, 307–334. [https://doi.org/10.1016/0377-8398\(94\)00016-G](https://doi.org/10.1016/0377-8398(94)00016-G).
- Matthiessen, J., Baumann, K.H., Schröder-Ritzrau, A., Hass, C., Andruleit, H., Baumann, A., Jensen, S., Kohly, A., Pflaumann, U., Samtleben, C., Schäfer, P., Thiede, J., 2001. Distribution of calcareous, siliceous and organic-walled planktic microfossils in surface sediments of the nordic seas and their relation to surface-water masses. In: Schäfer, P., Ritzrau, W., Schlüter, M., Thiede, J. (Eds.), *The Northern North Atlantic*. Springer Berlin Heidelberg, pp. 105–127.
- McCune, B., 1997. Influence of noisy environmental data on canonical correspondence analysis. *Ecology* 78, 2617–2623.

- McGarigal, K., Stafford, S., Cushman, S., 2000. Discriminant analysis. In: *Multivariate Statistics for Wildlife and Ecology Research*. Springer New York, New York, NY, pp. 129–187. [https://doi.org/10.1007/978-1-4612-1288-1\\_4](https://doi.org/10.1007/978-1-4612-1288-1_4).
- Minchin, P.R., 1987. An evaluation of the relative robustness of techniques for ecological ordination. In: Prentice, I.C., van der Maarel, E. (Eds.), *Theory and Models in Vegetation Science: Proceedings of Symposium*, Uppsala, July 8–13, 1985. Springer Netherlands, Dordrecht, pp. 89–107. [https://doi.org/10.1007/978-94-009-4061-1\\_9](https://doi.org/10.1007/978-94-009-4061-1_9).
- Montresor, M., Sgroso, S., Procaccini, G., Wiebe, H.C.F., 2003. Intraspecific diversity in *Scrippsiella trochoidea* (Dinophyceae): evidence for cryptic species. *Phycologia* 42, 56–70. <https://doi.org/10.2216/i0031-8884-42-1-56.1>.
- Morey, A.E., Mix, A.C., Pisias, N.G., 2005. Planktonic foraminiferal assemblages preserved in surface sediments correspond to multiple environment variables. *Quat. Sci. Rev.* 24, 925–950. <https://doi.org/10.1016/j.quascirev.2003.09.011>.
- Morley, J.J., 1989. Variations in high-latitude oceanographic fronts in the southern Indian Ocean: an estimation based on faunal changes. *Paleoceanography* 4, 547–554.
- Mudie, P.J., 1992. Circum-Arctic Quaternary and Neogene marine palynofloras: paleoecology and statistical analysis. In: *Neogene Quat. Dinoflag. Cysts Acritarchs*. 10. pp. 347–390.
- Nooteboom, P.D., Bijl, P.K., Van Sebille, E., Von Der Heydt, A.S., Dijkstra, H.A., 2019. Transport bias by ocean currents in sedimentary microplankton assemblages: implications for paleoceanographic reconstructions. *Paleogeogr. Paleoclimatology*. <https://doi.org/10.1029/2019PA003606>.
- Nychka, D., Furrer, R., Sain, S., 2017. *Fields: Tools for Spatial Data*. R package version 9.7. <https://doi.org/10.5065/D6W957CT>. [github.com/NCAR/Fields](https://github.com/NCAR/Fields).
- Oksanen, J., Blanchet, F.G., Friendly, M., Kindt, R., Legendre, P., McGlinn, D., Minchin, P.R., O'Hara, R.B., Simpson, G.L., Solymos, P., Stevens, M.H.H., Szoecs, E., Wagner, H., 2017. *vegan: Community Ecology Package*.
- O'Malley, R., 2018. Online Data: Standard VGPM [WWW Document]. Ocean Product. <http://orca.science.oregonstate.edu/2160.by.4320.monthly.xyz.vgpm.m.chl.m.sst.php>.
- Overpeck, J.T., Webb, T., Prentice, I.C., 1985. Quantitative interpretation of fossil pollen spectra: dissimilarity coefficients and the method of modern analogs. *Quat. Res.* 23, 87–108. [https://doi.org/10.1016/0033-5894\(85\)90074-2](https://doi.org/10.1016/0033-5894(85)90074-2).
- Parkinson, J.E., Baumgarten, S., Michell, C.T., Baums, I.B., Lajeunesse, T.C., Voolstra, C.R., 2016. Gene expression variation resolves species and individual strains among coral-associated dinoflagellates within the genus *Symbiodinium*. *Genome Biol. Evol.* 8, 665–680. <https://doi.org/10.1093/gbe/evw019>.
- Payne, R.J., Telford, R.J., Blackford, J.J., Blundell, A., Booth, R.K., Charman, D.J., Lamentowicz, Ł., Lamentowicz, M., Mitchell, E.A.D., Potts, G., Swindles, G.T., Warner, B.G., Woodland, W., 2012. Testing peatland testate amoeba transfer functions: appropriate methods for clustered training-sets. *Holocene* 22, 819–825. <https://doi.org/10.1177/0959683611430412>.
- Pebesma, E.J., 2004. Multivariable geostatistics in R: the gstat package. *Comput. Geosci.* 30, 683–691.
- Pebesma, E.J., Bivand, R.S., 2005. Classes and methods for spatial data in R. *R News* 5 (2). <https://cran.r-project.org/doc/Rnews/>.
- Prell, W.L., 1985. Stability of low-latitude sea-surface temperatures: an evaluation of the CLIMAP reconstruction with emphasis on the positive SST anomalies. In: *Final report, Technical Report*, Washington DC.
- Price, A.M., Baustian, M.M., Turner, R.E., Rabalais, N.N., Chmura, G.L., Price, A.M., 2018. Dinoflagellate cysts track eutrophication in the Northern Gulf of Mexico. *Estuar. Coasts* 41, 1322–1336.
- Price, A.M., Pospelova, V., Coffin, M.R.S., Latimer, J.S., Chmura, G.L., 2016. Biogeography of dinoflagellate cysts in northwest Atlantic estuaries. *Ecol. Evol.* 6, 5648–5662. <https://doi.org/10.1002/ece3.2262>.
- R Core Team, 2017. *R: A Language and Environment for Statistical Computing*. R Foundation for Statistical Computing, Vienna, Austria. <https://www.R-project.org/>.

- Radi, T., de Vernal, A., 2004. Dinocyst distribution in surface sediments from the northeastern Pacific margin (40-60°N) in relation to hydrographic conditions, productivity and upwelling. *Rev. Palaeobot. Palynol.* 128, 169–193. [https://doi.org/10.1016/S0034-6667\(03\)00118-0](https://doi.org/10.1016/S0034-6667(03)00118-0).
- Radi, T., de Vernal, A., 2008. Dinocysts as proxy of primary productivity in mid-high latitudes of the Northern Hemisphere. *Mar. Micropaleontol.* 68, 84–114. <https://doi.org/10.1016/j.marmicro.2008.01.012>.
- Radi, T., de Vernal, A., Peyron, O., 2001. Relationships between dinoflagellate cyst assemblages in surface sediment and hydrographic conditions in the Bering and Chukchi seas. *J. Quat. Sci.* 16, 667–680. <https://doi.org/10.1002/jqs.652>.
- Ribeiro, S., Amorim, A., 2008. Environmental drivers of temporal succession in recent dinoflagellate cyst assemblages from a coastal site in the North-East Atlantic (Lisbon Bay, Portugal). *Mar. Micropaleontol.* 68, 156–178. <https://doi.org/10.1016/j.marmicro.2008.01.013>.
- Rochon, A., de Vernal, A., 1994. Palynomorph distribution in recent sediments from the Labrador Sea. *Can. J. Earth Sci.* 31, 115–127.
- Rochon, A., de Vernal, A., Turon, J.-L., Matthießen, J., Head, M.J., 1999. Distribution of recent dinoflagellate cysts in surface sediments from the North Atlantic Ocean and adjacent seas in relation to sea-surface parameters. *Am. Assoc. Stratigr. Palynol. Contrib. Ser.* 35, 1–146.
- Rochon, A., Eynaud, F., de Vernal, A., 2008. Dinocysts as tracers of hydrographical conditions and productivity along the ocean margins: Introduction. *Mar. Micropaleontol.* 68, 1–5. <https://doi.org/10.1016/j.marmicro.2008.04.001>.
- Sathyendranath, S., Longhurst, A., Caverhill, C.M., Platt, T., 1995. Regionally and seasonally differentiated primary production in the North Atlantic. *Deep-Sea Res.* 42, 1773–1802.
- Schlitzer, R., 2018. Ocean Data View. <https://odv.awi.de/>.
- Schröder-Adams, C.J., van Rooyen, D., 2011. Response of recent benthic foraminiferal assemblages to contrasting environments in Baffin Bay and the northern Labrador Sea, Northwest Atlantic. *Arctic* 64, 317–341. <https://doi.org/10.14430/arctic4122>.
- Seidenkrantz, M.S., Aagaard-Sørensen, S., Sulsbrück, H., Kuijpers, A., Jensen, K.G., Kunzendorf, H., 2007. Hydrography and climate of the last 4400 years in a SW Greenland fjord: implications for Labrador Sea palaeoceanography. *Holocene* 17, 387–401. <https://doi.org/10.1177/0959683607075840>.
- Sha, L., Jiang, H., Seidenkrantz, M.S., Knudsen, K.L., Olsen, J., Kuijpers, A., Liu, Y., 2014. A diatom-based sea-ice reconstruction for the Vaigat Strait (Disko Bugt, West Greenland) over the last 5000yr. *Palaeogeogr. Palaeoclimatol. Palaeoecol.* 403, 66–79. <https://doi.org/10.1016/j.palaeo.2014.03.028>.
- Taylor, F.J.R., 1987. The biology of dinoflagellates. *Syst. Bot. Monogr.* 21, 723–731.
- Taylor, F.J.R., Pollinger, U., 1987. The ecology of Dinoflagellates. In: Taylor, F.J.R. (Ed.), *The Biology of Dinoflagellates*. Blackwell Scientific Publications, Oxford, pp. 398–529.
- Telford, R.J., 2015. palaeoSig: Significance Tests of Quantitative Palaeoenvironmental Reconstructions, R package version (1.1-3). <https://cran.r-project.org/package=palaeoSig>.
- Telford, R.J., Birks, H.J.B., 2005. The secret assumption of transfer functions: Problems with spatial autocorrelation in evaluating model performance. *Quat. Sci. Rev.* 24, 2173–2179. <https://doi.org/10.1016/j.quascirev.2005.05.001>.
- Telford, R.J., Birks, H.J.B., 2009. Evaluation of transfer functions in spatially structured environments. *Quat. Sci. Rev.* 28, 1309–1316. <https://doi.org/10.1016/j.quascirev.2008.12.020>.
- ter Braak, C.J.F., 1986. Canonical Correspondence analysis: a new eigenvector technique for multivariate direct gradient analysis. *Ecology* 67, 1167–1179.
- ter Braak, C.J.F., 1987. Ordination. In: Jongman, R.H., ter Braak, C.J.F., van Tongeren, O.F.R. (Eds.), *Data Analysis in Community and Landscape Ecology*. Center for Agricultural Publishing and Documentation, Wageningen, The Netherlands, pp. 91–169.
- ter Braak, C.J.F., 1992. Permutation versus bootstrap significance tests in multiple regression and anova. In: Jöckel, K.-H., Rothe, G., Sandler, W. (Eds.), *Bootstrapping and Related Techniques*. Springer Berlin Heidelberg, Berlin, Heidelberg, pp. 79–85.



- ter Braak, C.J.F., Juggins, S., 1993. Weighted averaging partial least squares regression (WA-PLS): an improved method for reconstructing environmental variables from species assemblages. *Hydrobiologia* 269/270, 485–502. <https://doi.org/10.1007/BF00028046>.
- ter Braak, C.J.F., Prentice, I.C., 1988. A theory of gradient analysis. In: *Advances in Ecological Research*. 18. Elsevier, pp. 271–317.
- ter Braak, C.J.F., Smilauer, P., 2002. *CANOCO Reference Manual and User's Guide to Canoco for Windows: Software for Canonical Community Ordination (Version 4.5)*. Microcomputer Power, Ithaca, New York, USA.
- ter Braak, C.J.F., Van Dam, H., 1989. Inferring pH from diatoms: a comparison of old and new calibration methods. *Hydrobiologia* 178, 209–223.
- ter Braak, C.J.F., Verdonschot, P.F.M., 1995. Canonical correspondence analysis and related multivariate methods in aquatic ecology. *Aquat. Sci.* 57, 255–289. <https://doi.org/10.1007/BF00877430>.
- Trachsel, M., Telford, R.J., 2016. Technical note: estimating unbiased transfer-function performances in spatially structured environments. *Clim. Past* 12, 1215–1223. <https://doi.org/10.5194/cp-12-1215-2016>.
- van der Voet, H., 1994. Comparing the predictive accuracy of models using a simple randomization test. *Chemom. Intell. Lab. Syst.* 25, 313–323. [https://doi.org/10.1016/0169-7439\(94\)85050-X](https://doi.org/10.1016/0169-7439(94)85050-X).
- Van Nieuwenhove, N., Head, M.J., Limoges, A., Pospelova, V., Mertens, K.N., Matthiessen, J., de Schepper, S., de Vernal, A., Eynaud, F., Londeix, L., Marret, F., Penaud, A., Radi, T., Rochon, A., 2020. An overview and brief description of common marine organic-walled dinoflagellate cyst taxa occurring in surface sediments of the Northern Hemisphere. *Mar. Micropaleontol.* this volume.
- Wall, D., Dale, B., 1968. Modern dinoflagellate cysts and evolution of the peridinales. *Micropaleontology* 14, 265–304.
- Walsh, J.E., Chapman, W.L., Fetterer, F., 2015. *Gridded Monthly Sea Ice Extent and Concentration, 1850 Onward, Version 1*. <https://doi.org/10.7265/N5833PZ5>.
- Wang, N., Mertens, K.N., Krock, B., Luo, Z., Derrien, A., Pospelova, V., Liang, Y., Bilien, G., Smith, K.F., De Schepper, S., Wietkamp, S., Tillmann, U., Gu, H., 2019. Cryptic speciation in *Protoceratium reticulatum* (Dinophyceae): evidence from morphological, molecular and ecophysiological data. *Harmful Algae*. <https://doi.org/10.1016/j.hal.2019.05.003>.
- Wigley, T.M.L., Ingram, M.J., Farmer, G., 1981. Past climates and their impact on man: a review. In: Wigley, T.M.L., Ingram, M.J., Farmer, G. (Eds.), *Climate and History*. Cambridge University Press, New York, pp. 3–50.
- Zamelczyk, K., Rasmussen, T.L., Husum, K., Hafliðason, H., de Vernal, A., Ravna, E.K., Hald, M., Hillaire-Marcel, C., 2012. Paleooceanographic changes and calcium carbonate dissolution in the central Fram Strait during the last 20ka. *Quat. Res. (United States)* 78, 405–416. <https://doi.org/10.1016/j.yqres.2012.07.006>.
- Zonneveld, K.A.F., Gray, D., Kuhn, G., Versteegh, G.J.M., 2019. Post-depositional aerobic and anaerobic particulate organic matter degradation succession reflected by dinoflagellate cysts: the Madeira Abyssal Plain revisited. *Mar. Geol.* 408, 87–109.
- Zonneveld, K.A.F., Siccha, M., 2016. Dinoflagellate cyst based modern analogue technique at test - a 300 year record from the Gulf of Taranto (Eastern Mediterranean). *Palaeogeogr. Palaeoclimatol. Palaeoecol.* 450, 17–37. <https://doi.org/10.1016/j.palaeo.2016.02.045>.
- Zonneveld, K.A.F., Versteegh, G.J.M., De Lange, G.J., 1997. Preservation of organic-walled dinoflagellate cysts in different oxygen regimes: a 10,000 year natural experiment. *Mar. Micropaleontol.* 29, 393–405.
- Zonneveld, K.A.F., Versteegh, G.J.M., Kasten, S., Eglinton, T.I., Emeis, K., Huguet, C., Koch, B.P., 2010. Selective preservation of organic matter in marine environments; processes and impact on the sedimentary record. *Biogeosciences* 7, 483–511.
- Zonneveld, K.A.F., Versteegh, G., Kodrans-Nsiah, M., 2008. Preservation and organic chemistry of late Cenozoic organic-walled dinoflagellate cysts: a review. *Mar. Micropaleontol.* 68, 179–197. <https://doi.org/10.1016/j.marmicro.2008.01.015>.

Zweng, M., Reagan, J.R., Antonov, J.I., Locarnini, R.A., Mishonov, A.V., Boyer, T.P., Garcia, H.E., Baranova, O.K., Johnson, D.R., Seidov, D., Biddle, M.M., 2013. Salinity. In: World Ocean Atlas 2013. 2 NOAA Atlas NESDIS 73.

### 3.10 Supplementary material

**Dataset S3.1:** Matrices of taxa abundances with all tested environmental (oceanographic and non-oceanographic) variables for the PO and AAO datasets can be found at <https://doi.org/10.1016/j.marmicro.2019.101816>.

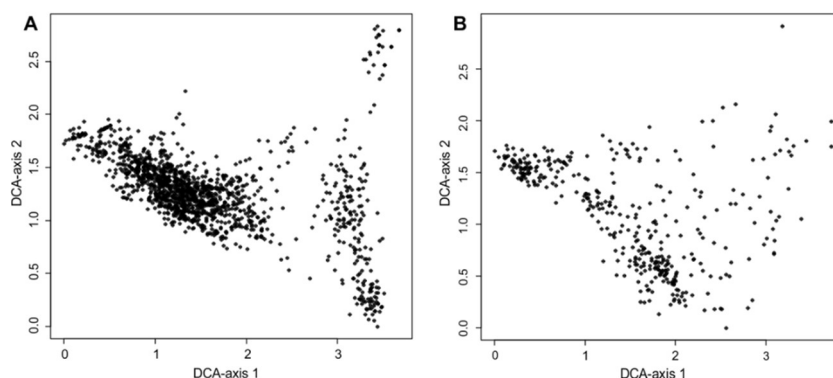


**Figure S3.2:** DCA analyses plots for the Atlantic-Arctic (A) and the Pacific (B) calibration datasets.

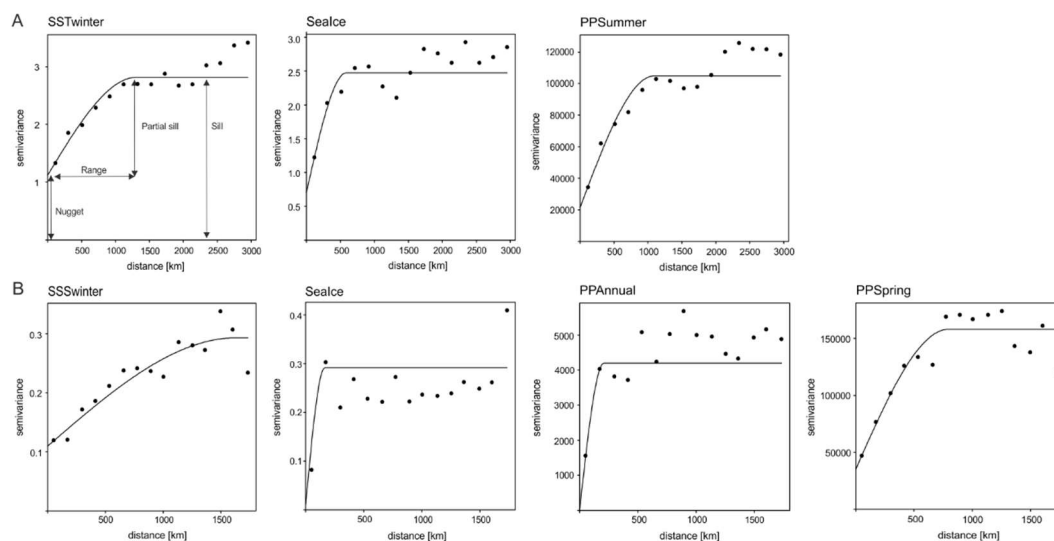


**Figure S3.3:** Variogram plots for the estimation of  $h$  in the  $h$ -block cross-validation for the Atlantic-Arctic (A) and the Pacific (B) calibration datasets.

# Chapter 4

## **Disentangling environmental drivers of Subarctic dinocyst assemblage compositional change during the Holocene (Manuscript II)**

Published as preprint in *Climate of the Past* (under review)

Hohmann, S., Kucera, M. and de Vernal, A., 2023. Disentangling environmental drivers of subarctic dinocyst assemblage compositional change during the Holocene. *EGUsphere* 2023, 1-46. 10.5194/egusphere-2023-561

### **Abstract**

Analysis of compositional changes in fossil organic-walled dinoflagellate cyst (dinocysts) assemblages is a widely used tool for the quantitative reconstruction of past environmental parameters. This approach assumes that the assemblage composition is significantly and independently related to the reconstructed environmental parameters. Theoretically, dinocyst assemblages can be used to reconstruct multiple environmental variables. However, there is evidence that primary and subordinate drivers for assemblage compositions differ regionally and it remains unclear whether a significant relationship to specific parameters in the present ocean always implies that this relationship is significant in fossil assemblages, questioning if past changes in these multiple parameters can be reconstructed simultaneously from fossil assemblages. Here, we analysed a local subset of the Northern Hemisphere dinocyst calibration dataset ( $n = 1968$ ), including samples from the Baffin Bay area ( $n = 421$ ), and evaluated the benefits of a local versus a more regional or global calibration for the environmental reconstruction of Baffin Bay oceanography during the Holocene. We determined the dimensionality of the dinocyst ecological response and identified environmental drivers in the Baffin Bay area for the modern dataset. We analysed four existing Holocene records along a North-South transect in the area and evaluated the statistical significance of downcore reconstructions by applying the local and global datasets with different techniques: the modern analogue technique (MAT), the weighted average partial least square (WA-PLS), and maximum likelihood (ML). Our analyses imply that present-day and Holocene dinocyst

assemblages in the Baffin Bay area are primarily driven by salinity and temperature; other parameters were less important in driving assemblage compositions and their contribution differed among the studied records. We show that the objectively occurring and temporally coherent shifts in dinocyst assemblages in the Holocene of Baffin Bay can be interpreted robustly only by transfer functions that are calibrated locally. Transfer functions based on the broad North Hemisphere calibration yielded many insignificant environmental reconstructions. At the same time, we show that even in the local calibration, not all parameters that appear to significantly affect dinocyst assemblages in the calibration dataset can be meaningfully reconstructed in the fossil record. A thorough evaluation of the calibration dataset and the significance of downcore applications is necessary to reveal the region-specific information contained in dinocyst assemblage composition.

#### **4.1 Introduction**

During the last decades, the growing interest in changing climate and environment has led to many studies documenting short- and long-term climate variations at multi-decadal to multi-millennial time scales based on reconstructions making use of marine microfossils (Muller et al., 1983; Sarnthein et al., 1988; Berger et al., 1989; Meyers, 1997; Rühlemann et al., 1999; Fischer et al., 2000). Next to analyses of the chemical and isotopic signals locked in microfossils skeletons, quantitative analyses of changes in the taxonomic composition of microfossil assemblages by means of ecological models is a widely used tool in palaeoceanography since Imbrie & Kipp (1971). This approach assumes that the composition of marine plankton and benthos communities reflects the environmental regime under which they grew and that this information is transferred into the sediment by their fossils. The hypothesis that an assemblage of taxa can be expressed as a function of (a) certain environmental variable(s) (ter Braak, 1987), allows for quantitative modelling applying transfer functions and analogue methods (from now on called transfer functions). A range of transfer function methods has been used to reconstruct environmental variables from a variety of microfossils, including planktonic foraminifera (e.g. Kucera et al., 2005), diatoms (e.g. Sha et al., 2014) and dinoflagellate cysts (dinocysts) (e.g. de Vernal et al., 2005).

However, the key assumption of this approach requires that the assemblage composition is significantly related to the given environmental parameter to reconstruct both at present for the purpose of calibration and in the past for the purpose of reconstruction. In the presence of multiple environmental parameters affecting assemblage composition, it is challenging to disambiguate the effect of each parameter and determine which one(s) acted on the analysed fossil assemblages in the past.

Assemblages of zooplankton microfossils, such as planktonic foraminifera and radiolarians that are exclusively oceanic, seem to be controlled primarily by temperature (Morey et al., 2005; Hernández-Almeida et al., 2017), while analyses of phytoplankton distributions, such as diatoms and dinocysts, indicate that their assemblages are affected by multiple environmental factors (de Vernal et al., 2000, 2001; Dale et al., 2002; Holzwarth et al., 2007; Radi and de Vernal, 2008; Ribeiro and Amorim, 2008; Lopes et al., 2010; Hohmann et al., 2020). It seems that phytoplankton communities have a more complex relationship to the environment than zooplankton, reflecting independently the imprint of hydrography and nutrient availability, rendering reconstruction of multiple environmental factors possible. It is tempting to explore whether such dependency on multiple factors can be used to reconstruct changes in all the driving factors in the past.

Many dinoflagellate species (about 20 %) produce fossilisable organic-walled cysts during their life cycle (Wall and Dale, 1968; Dale, 1983; Taylor and Pollinger, 1987; Head, 1996). The cyst walls are composed of a condensed macromolecular structure that is predominantly aromatic in composition (Kokinos et al., 1998), facilitating relatively good preservation in seafloor sediments (e.g. Zonneveld et al., 2008). While mineralised fossils like calcareous (e.g. foraminifera and nannoplankton) or siliceous (e.g. diatoms and radiolarians) microfossils are susceptible to dissolution after death, the organic-walled dinocysts are resistant to dissolution (Koç et al., 1993; Matthiessen et al., 2001; Seidenkrantz et al., 2007; Schröder-Adams and van Rooyen, 2011; Zamelczyk et al., 2012). On the other hand, dinocysts may be affected by oxidation during exposure on the seafloor, resulting in a selective organic matter degradation that may leave a fingerprint in the assemblage composition (Zonneveld et al., 2010). Nevertheless, if organic matter degradation is negligible, in settings with carbonate or opal dissolution, dinocyst-based transfer functions are often the best means to reconstruct past surface ocean properties.

Dinoflagellates form a major group of planktonic marine primary producers and include diverse autotrophic, mixotrophic, and heterotrophic forms that all thrive in the upper layers of the oceans (e.g. de Vernal and Marret, 2007). Palynological studies of surface sediment samples from marine environments of the Northern Hemisphere revealed that dinocysts are excellent tracers of hydrological and biological conditions (Mudie, 1992; Rochon and Vernal, 1994; Matthiessen, 1995; de Vernal et al., 1997, 2000, 2001, 2013; Radi et al., 2001; Radi and de Vernal, 2004, 2008; Rochon et al., 2008). While dinocyst assemblages can theoretically be applied to quantify multiple environmental drivers, it is challenging to identify the most relevant environmental factor(s) driving the compositional change in microfossil assemblages. Relationships between the assemblages and environmental parameters are complex, pointing to regionally different relationships between assemblages and environmental conditions. For example, whereas temperature and salinity gradients are determinants in the Atlantic-Arctic

region, primary productivity seems to explain a large portion of taxa variability in the Pacific (Radi and de Vernal, 2008; Hohmann et al., 2020). There is evidence that the number and kind of the main driving factor(s) affecting dinocyst assemblages vary regionally (Zonneveld and Siccha, 2016; Hohmann et al., 2020) and that the evaluation of transfer function performance is method-specific (Hohmann et al., 2020) and complicated by spatial autocorrelation (Telford and Birks, 2005, 2009).

Hohmann et al. (2020) analysed the dimensionality of the dinocyst ecological response separately for assemblages from the Pacific and the Atlantic-Arctic regions, calibrated and evaluated multiple transfer-function methods for predicting environmental variables and estimated their performances in the light of spatial autocorrelation. This study identified different primary drivers for two areas affecting dinocyst assemblage composition, highlighting the merit of local calibrations and the necessity to carry out variable selections of main driving factors for each study area separately. Defining a local calibration dataset has the advantage of reducing the complexity of the assemblage to environment composition. However, this comes at the cost of reducing the pool of compositional variability, leading to the risk of biasing the results. For example, in Holocene cores off West Greenland, some of the best compositional analogues have been found in the Gulf of St. Lawrence (e.g. Allan et al., 2018). However, because factor(s) driving microfossil assemblages differ between regions, it is possible that the same fossil assemblages may find equally good compositional analogues representing different combinations of environmental parameters. Hence, while local calibrations limit the range of compositional variability available to derive the transfer function, they are more likely to disambiguate the main driving variable in a certain region, which may render reconstructions in that region more robust assuming the driving factors remain the same.

By calibrating locally, we can exclude areas where dinocysts are susceptible to lateral transport during sinking and sedimentation processes. There is evidence that a dinocyst could be displaced up to thousands of kilometres from the location at the surface where it was produced (Nooteboom et al., 2019). Long-distance cyst transport by bottom waters and sediment flows was also suggested based on sediment trap studies in the central and North Atlantic Oceans (Dale, 1992; Dale and Dale, 1992). This implies that in areas with strong ocean currents, the surface above the sedimentation area does not necessarily mirror the environmental conditions under which the plankton was produced, generating a nuisance in the calibration dataset.

The aim of this study is to investigate if a local dinocyst-based transfer function calibration on samples covering the Baffin Bay and surrounding regions allows a robust disambiguation of the factors that affected the assemblage variation in this region during the Holocene. Baffin Bay is a climate-sensitive region characterised by strong seasonal sea ice variability and

meltwater discharge from the Greenland Ice Sheet (GIS). In view of the current rapid warming in the Arctic, it is relevant to understand how this marine basin reacted to climate changes during the Holocene. Indeed, to this end, many Holocene reconstructions based on fossil dinocyst assemblages were made and could serve as a basis for a comprehensive analysis of factors affecting the assemblage composition (e.g. Levac et al., 2001; Ouellet-Bernier et al., 2014; Allan et al., 2018; Caron et al., 2019).

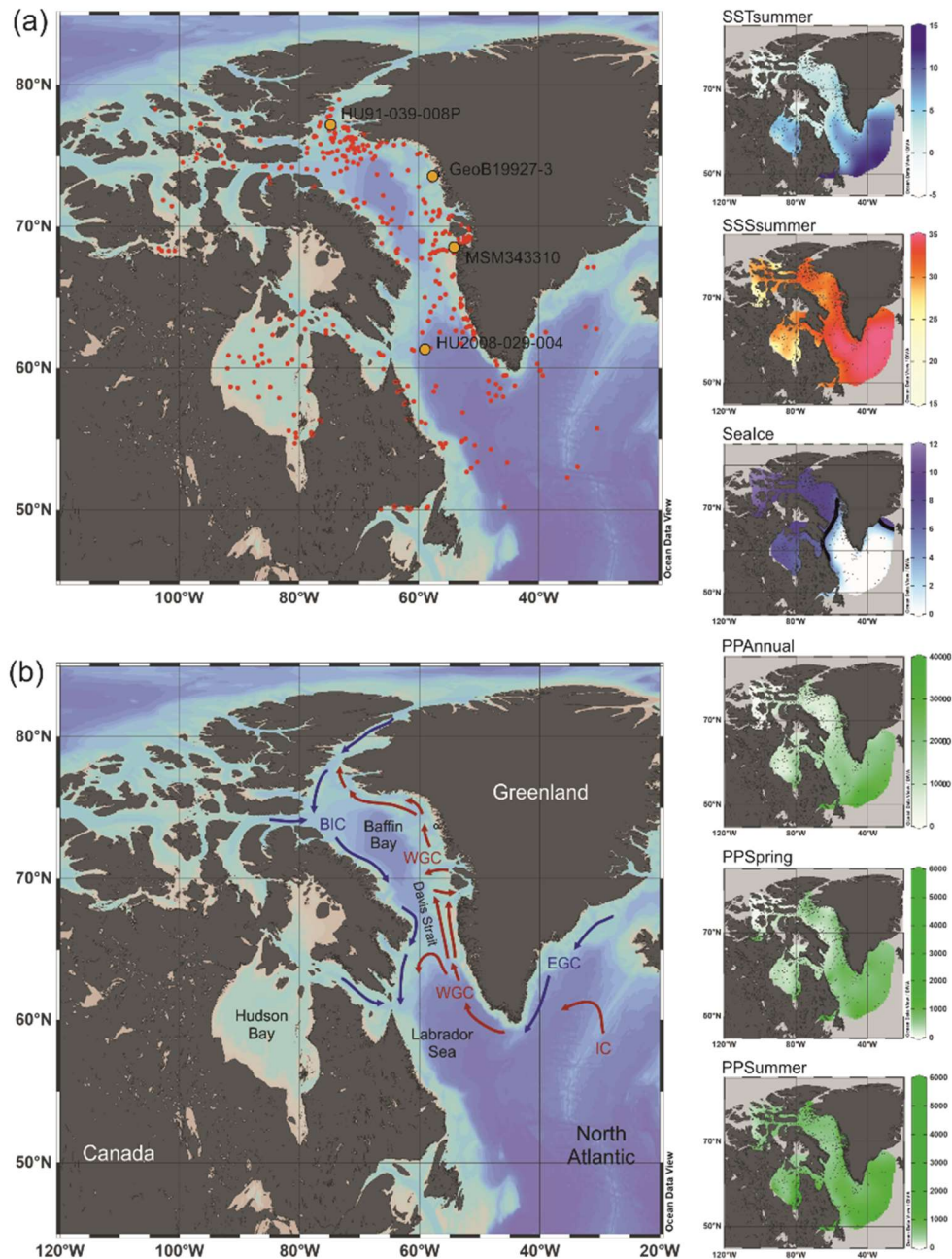


**Figure 4.1:** Map of the study area. (a) Location of surface sediment samples (red dots) from the calibration dataset and cores (orange dots; see Table 4.1) used in this study; (b) Schematic modern surface water circulation in the Baffin Bay area and around Greenland (BIC – Baffin Island Current,

WGC – West Greenland Current, EGC – East Greenland Current, IC – Irminger Current). On the right, modern environmental parameter gradients gridded using DIVA gridding with Ocean Data View (Schlitzer 2018). Units are listed in Table 4.3. The six-month sea-ice edge in the sea-ice gradient map is indicated by the thick black line.

We begin by carrying out an objective variable selection, guided by canonical ordination, and investigate the data structure of the resulting designed local transfer functions. We proceed by testing their ability to interpret assemblage changes recorded in Holocene sediments by their applications on four records covering a North-South transect throughout the Baffin Bay area. To this end, we used data from three existing records and added new data from a core located in Southern Melville Bay (see Fig. 4.1a) and Table 4.1). We specifically focus on Holocene sections, assuming that the magnitude of environmental change in the Holocene was relatively small for the local calibration to be sufficient to capture the range of past environments recorded in the cores. To estimate the significance of the reconstructions we apply a test designed by Telford and Birks (2011), evaluating if reconstructions explain more of the variation in the fossil taxa data than random environmental variables assigned to the same fossil data. To assess the merit of a local versus a larger regional calibration, we compared local transfer function results to regional transfer functions based on a Northern Hemisphere calibration dataset.

**Table 4.1:** List of cores used in this study. Including core location and water depth (m), the modern sea surface conditions: sea surface temperature (SST) in summer, sea surface salinity (SSS) in summer, months per year of sea ice cover, and annual productivity of organic carbon for each location provided by the WOA and NSIDC.

Core ID	Core location	Latitude (° N)	Longitude (° W)	Water depth (m)	Modern sea surface conditions				Time interval covered (yrs BP)	References for dinocyst records
					SST summer (°C)	SSS summer (psu)	Sealce (month yr <sup>-1</sup> )	PPannual (mgC m <sup>-2</sup> day <sup>-1</sup> )		
HU91-039-008P	Nares Strait	77.16	74.19	663	1.42	31.93	7.64	4635.00	1549-6756	Levac et al. 2001
GeoB19927-3	Southern Melville Bay	73.35	58.05	932	3.89	32.74	7.22	4179.00	0-7677	This paper and Saini et al. 2020
MSM343310	Disco Bugt	68.38	53.49	855	5.45	32.54	3.84	6374.00	135-3578	Allan et al. 2018
HU2008-029-004	Northwest Labrador Sea	61.46	58.03	2674	7.31	34.16	0.72	4497.00	0-9936	Gibb et al. 2015



## 4.2 Material and methods

### 4.2.1 Data

The calibration dataset includes a local subset of the data from the Northern Hemisphere dataset (n=1968) in de Vernal et al. (2020). The local subset comprises census counts of recent organic-walled dinoflagellate cyst assemblages from core-top sediments at 421 sites from Baffin Bay with Kane Basin, Norwegian Bay, and Lancaster Sound (n=233), Davis Strait (n=103), Labrador Sea (n=30) and Hudson Bay with Hudson Strait and Foxe Basin (n=55) (Fig.4.1a). In samples containing low dinocyst concentrations, minimum counts of 60 specimens were accepted. The core-top samples were collected in the uppermost 1 cm of box or gravity cores and represent a few tens of years to centuries, depending upon sedimentation rates and mixing due to bioturbation (Radi and de Vernal, 2008). Palynological sample processing followed the procedures for palynological preparation described in de Vernal et al. (2010), which exclude the use of oxidation techniques to avoid selective degradation of more sensitive cyst taxa such as those produced by *Protoperidinales* (Marret, 1993). The Northern Hemisphere dataset from (de Vernal et al., 2020) served also as the regional reference dataset which we use to compare the results of the local dataset to. With exception of the samples from Price et al. (2016, 2018), which were added at a later stage, the Northern Hemisphere dataset and therefore all samples included in the local dataset have been tested negative for a significant selective organic matter degradation (Zonneveld et al., 1997) in Hohmann et al. (2020). The taxonomy used corresponds to that presented in Rochon et al. (1999) and updated in van Nieuwenhove et al. (2020). The taxonomic resolution of the local dataset was reduced to 33 dinocyst taxa after grouping following Hohmann et al. (2020) (Table 4.2, List of taxa). The original dinocyst dataset holding taxon percentages is archived at PANGAEA (de Vernal et al., 2019); the local data matrices with reduced taxonomy used in this analysis are available as supplementary material (S4.1).

**Table 4.2:** List of dinocyst taxa in the local calibration dataset. Including abbreviations and highest relative abundances (minimum is always zero). Asterisks indicate heterotrophic taxa.

Taxa name	Abbreviation	Notes	Maximum %
<i>Ataxiodinium choane</i>	Atax		1.2
<i>Bitectatodinium tepikiense</i>	Btep		3.3
<i>Impagidinium aculeatum</i>	lacu		2.1
<i>Impagidinium pallidum</i>	lpal		7.5
<i>Impagidinium paradoxum</i>	lpar		8.8
<i>Impagidinium patulum</i>	lpat		1.8
<i>Impagidinium sphaericum</i>	lsph		6.2
<i>Nematosphaeropsis labyrinthus</i>	Nlab		71.6

<i>Operculodinium centrocarpum</i>	Ocen	Group including: <i>Operculodinium centrocarpum</i> , <i>O. centrocarpum</i> —short processes, <i>O. centrocarpum</i> —Arctic morphotype	93.5
<i>Pyxidinoopsis reticulata</i>	Pret		1.5
<i>Spiniferites elongatus</i>	Selo		27.3
<i>Spiniferites ramosus</i>	Sram		14.6
<i>Spiniferites lazus</i>	Slaz		0.3
<i>Spiniferites mirabilis-hyperacanthus</i>	Smir		0.6
<i>Spiniferites</i> spp.	Sspp		4.4
Cyst of <i>Pentapharsodinium dalei</i>	Pdal		95.3
Cyst of <i>Scrippsiella trifida</i>	Stri		4.2
<i>Islandinium minutum</i> *	Imin	Group including: <i>Islandinium minutum</i> *, <i>Islandinium ? cezare</i> *, <i>Islandinium brevispinosum</i> *	96.8
<i>Echinidinium karaense</i> spp.*	Ekar		19.6
<i>Brigantedinium</i> spp.*	Bspp	Group including: <i>Brigantedinium</i> spp., <i>Brigantedinium cariacense</i> , <i>Brigantedinium simplex</i> , Cyst of <i>Protopteridinium americanum</i> *	99.0
<i>Dubridinium</i> spp.*	Dubr		3.4
<i>Protopteridinioid</i> cyst*	Peri		1.3
<i>Lejeunecysta</i> spp.*	Lspp		0.7
<i>Selenopemphix nephroides</i> *	Snep		2.2
<i>Xandarodinium xanthum</i> *	Xxan		0.9
<i>Selenopemphix quanta</i> *	Squa	Group including: <i>Selenopemphix quanta</i> *, Cyst of <i>Protopteridinium nudum</i> *	20.8
<i>Trinovantedinium applanatum</i> *	Tapp		5.2
<i>Votadinium calvum</i> *	Vcal		0.5
<i>Votadinium spinosum</i> *	Vspi		0.6
<i>Quinquecuspis concreta</i> *	Qcon		0.7
Cyst of <i>Polykrikos kofoidii</i> *	Pkof		8.6
Cyst of <i>Polykrikos</i> sp. – Arctic*	Parc		23.1
<i>Echinidinium</i> spp.*	Espp		2.5

We chose to carry out a canonical-ordination-based parameter selection (Lopes et al., 2010) to characterise the relationship between environmental variables and dinocyst assemblage composition. We defined a set of potential environmental controlling variables for dinocyst distributions in the Baffin Bay region: surface layer (here represented by conditions at 0 m depth) temperature and salinity in summer, sea ice cover and productivity in spring and summer as well as for the whole year. We did not consider temperature, salinity, and productivity parameters for the cold seasons since most of the area is covered by sea ice and there is hardly any productivity and hence no dinocyst production. Apart from environmental factors, some life-cycle factors (e.g., Fensome et al., 1993) such as water depth and distance from shore seem to affect dinocyst assemblages. But as they represent a separate independent dimension of variance (Hohmann et al., 2020), we do not include them in the local calibration dataset. The initial variable selection is listed in Table 4.3 and includes some of the

variables considered in Hohmann et al. (2020) (c.f. for more detail). Their spatial distribution is shown in Fig. 4.1.

We used four sediment sequences to test the ability of the locally calibrated transfer functions to interpret assemblage changes during the Holocene. These sediment cores cover a North-South transect throughout the Baffin Bay region (Fig. 4.1a, Table 4.1) including intervals within the last 10 ka.

**Table 4.3:** Environmental variables used in the canonical-ordination based parameter selection and their ranges within the local calibration dataset.

Environmental variable	Minimum	Maximum	Range
SSTsummer [°C]	-0.81	13.24	14.05
SSSummer [psu]	17.51	34.98	17.47
SeaIce [months yr <sup>-1</sup> ]	0	12	12
PPAnnual [mgC m <sup>-2</sup> day <sup>-1</sup> ]	824	33047	32223
PPSpring [mgC m <sup>-2</sup> day <sup>-1</sup> ]	64	3626	3562
PPSummer [mgC m <sup>-2</sup> day <sup>-1</sup> ]	202	6021	5819

We analysed dinocyst assemblages in core GeoB19927-3 (73°35,26' N, 58°05,66' W), which was taken at 932 meters of water depth by gravity coring during cruise MSM44 in 2015 (Dorschel et al., 2015). This core is from southern Melville Bay, an area where the relatively warm high-salinity West Greenland Current (WGC) interacts with the cold polar water of the Baffin Current (BC) originating from the Arctic Ocean and meltwater from glaciers of the North-West Greenland region. It is located optimally and offers a high resolution and continuous sedimentation (Dorschel et al., 2016). A high-resolution radiocarbon-based chronology and organic biomarker proxies for sea ice and primary productivity have already been presented by Saini et al. (2020). The core consists of 1147 cm of sediment. The working half of the core was sampled and divided into four sets of samples. One set was freeze-dried for dinocyst analysis. The other three sets were stored for other multi-proxy analyses and chronology (i.e., biomarker, foraminifera, and provenance studies). In reference to summer temperature anomalies during the Holocene for the Northern Hemisphere (Marcott et al., 2013; Kaufman et al., 2020), we expected a possible trend towards the last 2000 years and sampled at a higher resolution within the top 270 cm. We sub-sampled every centimetre within the top 25 cm, every 5 cm within the 25 cm to 280 cm interval, and every 10 cm within the 280 cm to 760 cm interval covering the last 7677 years, including 124 samples (see Table 4.1). Sample processing followed the procedure for palynological preparation described in de Vernal et al. (2010), which consists of repeated HCl and HF treatment. The taxonomy of dinocysts used here was based on Rochon et al. (1999) and de Vernal et al. (2020), considering all taxonomic categories that were resolved in the calibration dataset. To obtain statistically reliable assemblage counts, at

least 300 dinocyst specimens were counted per sample when possible. For samples with low dinocyst abundance as many specimens as possible were enumerated. For the sample with the lowest dinocyst abundance, we counted 89 specimens. The raw assemblage dataset for GeoB19927-3 will be available on time via the PANGAEA database.

In addition, we re-evaluated three existing sediment records that have already been studied in detail and have been analysed for their palynological content and dinocyst assemblages. HU91-039-008P (Levac et al., 2001) was sampled every 20 cm from the top to 820 cm which corresponds to 1549-6756 years BP and includes 41 samples. MSM343310 (Allan et al., 2018) includes 194 samples taken around every 8 cm from top to 925 cm (135-3578 years BP), while HU2008-029-004 (Gibb et al., 2015) includes 30 samples from every 4 cm from top to 116,5 cm (0- 9936 years BP) (see Table 4.1).

#### **4.2.2 Data analysis**

To explore the local relationship between dinocyst assemblages and environmental variables, we followed the procedure schematically illustrated in Fig. 4.2 and used statistical ordination (McGarigal et al., 2000). We performed detrended correspondence analysis (DCA) (Birks, 1995) to evaluate the gradient length, expressed as standard deviation (SD) units in the first DCA axis to decide whether to apply linear ( $SD < 3$ ) or unimodal ordination ( $SD > 4$ ;  $SD > 3$  to  $< 4$  both methods possible but unimodal ordination is advised) (Lepš and Šmilauer, 2003). For DCA and further analyses, we used the vegan package (Oksanen et al., 2019) in R (R Core Team, 2017). The dataset was found to have an SD of 3.0 (S4.2 - supplementary data) using log-transformed ( $\log(x+1)$ ) dinocyst assemblage per mil data. As the SD of our dataset is biased towards the linear threshold, we proceeded with linear techniques.

In the first step, we used multiple factor analysis (MFA), an integration of multivariate matrices, to simultaneously couple several groups of variables that are defined on the same objects (Escofier and Pagès, 1984, 1990, 1994) with the aim of identifying a common or representative structure in the whole data matrix. MFA proposes a symmetrical, exploratory point of view, where correlative structures are exposed without any reference to the directionality of possible causal relationships. It is a simple co-inertia analysis that finds common structures in all or some of the data groups (Dray et al., 2003) and has previously been used in ecological studies (e.g. Beamud et al., 2010; Carlson et al., 2010; Lamentowicz et al., 2010). As all variables in this study are numerical, the MFA can be seen as a principal component analysis (PCA), wherein the first step each data group is analysed, weighted, and normalised by dividing all its elements by the first eigenvalue obtained from the PCA. In the second step, the normalised data groups are merged into a common matrix and a global PCA is performed.

We defined three data groups: One community dataset holding dinocyst taxa ratios (33 taxa) and two groups holding abiotic variables describing productivity (PPAnnual, PPSpring, PPSummer) and physical water properties (SSTsummer, SSSsummer, Sealce). All three groups hold exclusively quantitative variables. Hellinger-transformation (Rao, 1995) was applied to the dinocyst ratios in the community data set. This transformation, as proposed by Legendre & Gallagher (2001) for a PCA with community data containing many double-zero abundances, allows using PCA without considering the common absence of species as a resemblance between communities and preserves the Euclidean distance of a PCA when unimodal data is used, which might be possible as the SD of 3.0 might imply unimodal data.

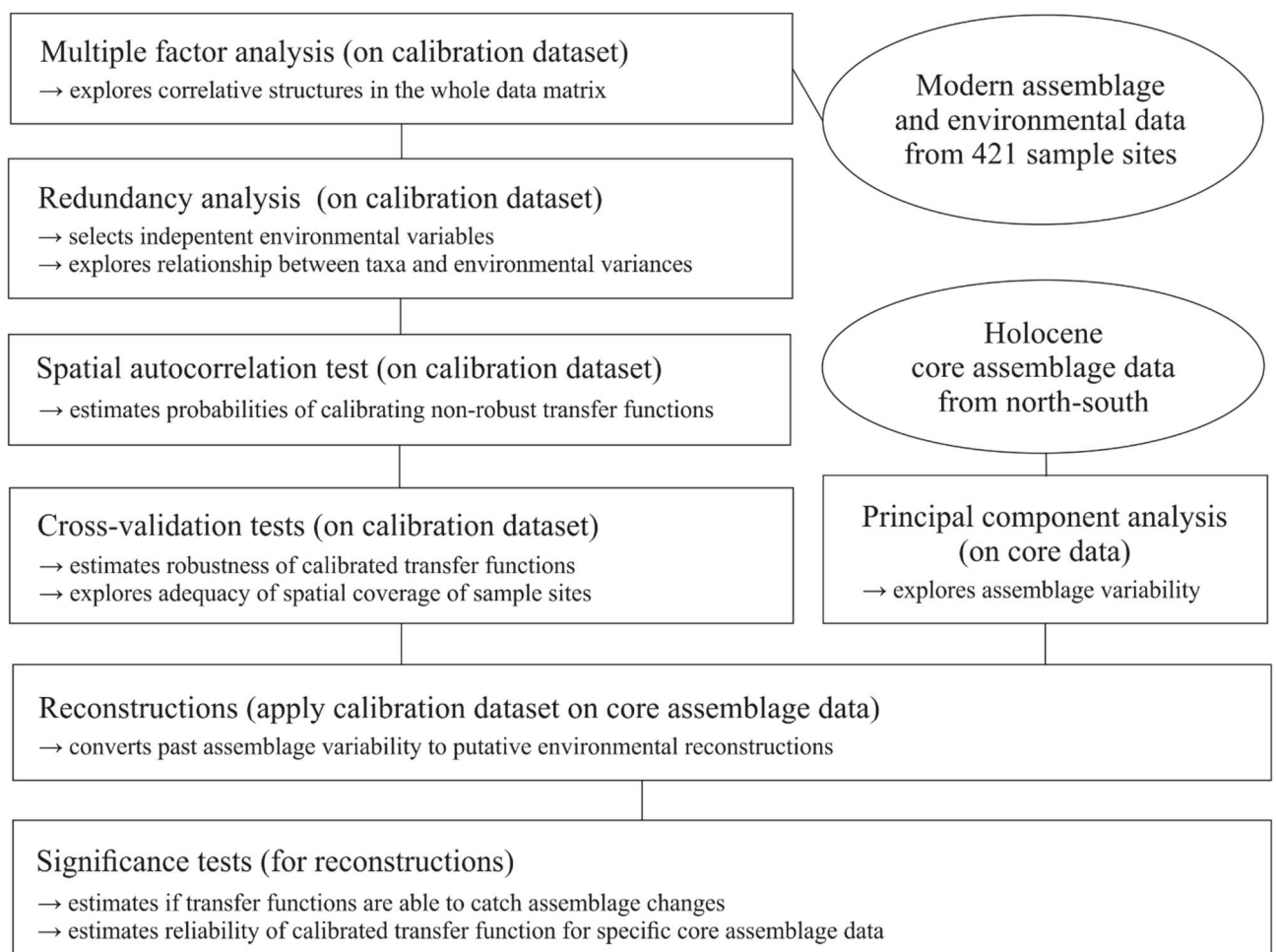


**Figure 4.2:** Flowchart describing the approach and sequence of analyses in this study.

After Hellinger-transformation, the data from all three groups was standardised by scaling variables to a standard deviation of 1 and a mean of 0. The affinity between the group derived from the MFA is measured by their RV coefficient, ranging from 0 to 1 (Robert and Escoufier, 1976), which is tested by a Pearson type III approximation (Josse et al., 2008). MFA

computations were performed with the FactoMineR (Lê et al., 2008) and factoextra (Kassambara and Mundt, 2017) R packages.

We continued selecting the main drivers affecting compositional changes in the dinocyst assemblages. We applied Redundancy Analysis (RDA), a constrained ordination (McGarigal et al., 2000) for linear data, to quantify the strength of the relationship between species variances and the tested forcing parameters. Again, we applied Hellinger-transformation (Rao, 1995) to the taxa ratios to ensure the preservation of Euclidean distance in the linear ordination as our species data SD did not indicate strongly linear data. Hellinger-transformation also gives less weight to species with low counts and many zeros, focussing more on the composition of common species, as we assume that local datasets unlike global ones do not include indicators or inter-regional endemic species. Environmental data were standardised as described above to ensure the compatibility of variables for comparisons.

RDA was performed after ter Braak (1986) using the software R (R Core Team, 2017). For the variable selection, we followed the procedure described in Hohmann et al. (2020), which includes a variable selection considering Variance Inflation Factors (VIFs)  $\leq 2$  with the objective to extricate independent variables that show no collinearity between each other and explaining a significant amount of the variance in the species data. Following this procedure, we obtained a set of three independent forcing variables, meaning that each of these three parameters explains a separate dimension of variance in the taxa data (for more explanation see S4.3 – supplementary data). These three independent variables, that revealed to be summer sea-surface temperature (SSTsummer), summer sea-surface salinity (SSSsummer), and spring productivity (PPSpring) (see section 4.3.2), were used for a final RDA and further analyses.

We determined the extent and type of autocorrelation in the independent data set, as an accurate evaluation of transfer function performances is only possible in case of spatial independence between sample sites in the data set (Telford and Birks, 2009). In the case of spatial autocorrelation, the transfer function performances can be overestimated, which could result in inappropriate choices of transfer function models and parameters, possibly including environmental variables with no ecological relevance as “reconstructable”. Autocorrelation could occur due to spatial interdependence of proxy variables, which would render the main requirement of spatial independence for adequate transfer functions violated. It could also be due to an environmental similarity of nearby sample sites. A spatial autocorrelation due to environmentally similar sites, as found in data sets from the North Pacific as well as the North Atlantic and Arctic (Hohmann et al., 2020), may meet the requirement of transfer functions. For autocorrelation tests and further analyses, we additionally used R packages fields (Nychka et al., 2017), palaeoSig (Telford, 2015), and rioja (Juggins, 2017) implementing the routines developed in Telford and Birks (2009).

For the transfer functions remaining in the independent calibration dataset, we did calibration and cross-validation based on the leave-one-out (LOO) (cf. Efron and Gong, 1983) and h-block technique (Burman et al., 1994; Telford and Birks, 2005, 2009) for three distinctly different transfer function approaches: the Maximum Likelihood (ML), the Weighted Averaging Partial Least Square (WA-PLS) and the Modern Analogue Technique (MAT). For calibration and cross-validation tests we additionally used R packages *bioindic* (Guiot and Gally, 2014), *gstat* (Pebesma, 2004), and *sp* (Pebesma and Bivand, 2005) and followed the R code developed by Trachsel and Telford (2016) for h-block cross-validation and the estimation of *h* (for more details see Hohmann et al., 2020).

We reconstructed the three independent variables (SSTsummer, SSSsummer, and PPSpring) within four sediment sequences collected along a north-south transect through the Baffin Bay area. To determine assemblage zones in each core we performed principal component analysis (PCA) on percentages of downcore dinocyst assemblages.

We tested the ability of the calibrated transfer functions to interpret the assemblage changes recorded in the sediments by applying the Telford and Birks method (2011). To estimate the significance of the reconstructions, this method evaluates if reconstructions explain more of the variance in the fossil data than most reconstructions derived from transfer functions trained on random environmental data. It also determines the best reconstruction when reconstructing several environmental variables and if there is sufficient information in the proxy data to support multiple independent reconstructions. We use redundancy analysis (RDA) to estimate the proportion of variance in the fossil data explained by a single reconstruction. Then, using the same taxa data from the calibration dataset, reconstructions are inferred from transfer functions trained on random environmental variables drawn from a uniform distribution. The proportion of the variance explained by these random reconstructions is then estimated. If the tested variable explains more of the taxa variance than 95 % of the random reconstructions, the reconstruction is deemed statistically significant (cf. Telford and Birks, 2011). Reconstructions that fail this test should be interpreted with caution.

Reconstructions and significance tests within the four cores were performed by applying the calibrated local dataset ( $n=421$ ) and the regional Northern Hemisphere dataset ( $n=1968$ ), aiming to assess the advantages and disadvantages of using the local dataset.

## 4.3. Results

### 4.3.1 Multiple factor analysis

The MFA provides an informative view of the two main gradients and the relationship among the three defined groups of variables. The first two axes represent about 31 % of the total variance. Figure 4.3 illustrates the correlation between the three defined groups and the first two dimensions of the MFA. Temperature variables (SSTsummer and Sealce) from the group of physical water properties contribute the most to the first dimension followed by productivity and some dinocyst species. Within the second dimension, salinity contributes the most, followed by productivity and some dinocyst species. The correlation circle (Fig. 4.3a) shows the relationship between single variables, their quality of representation within the first two dimensions, as well as the correlation between single variables and dimensions.

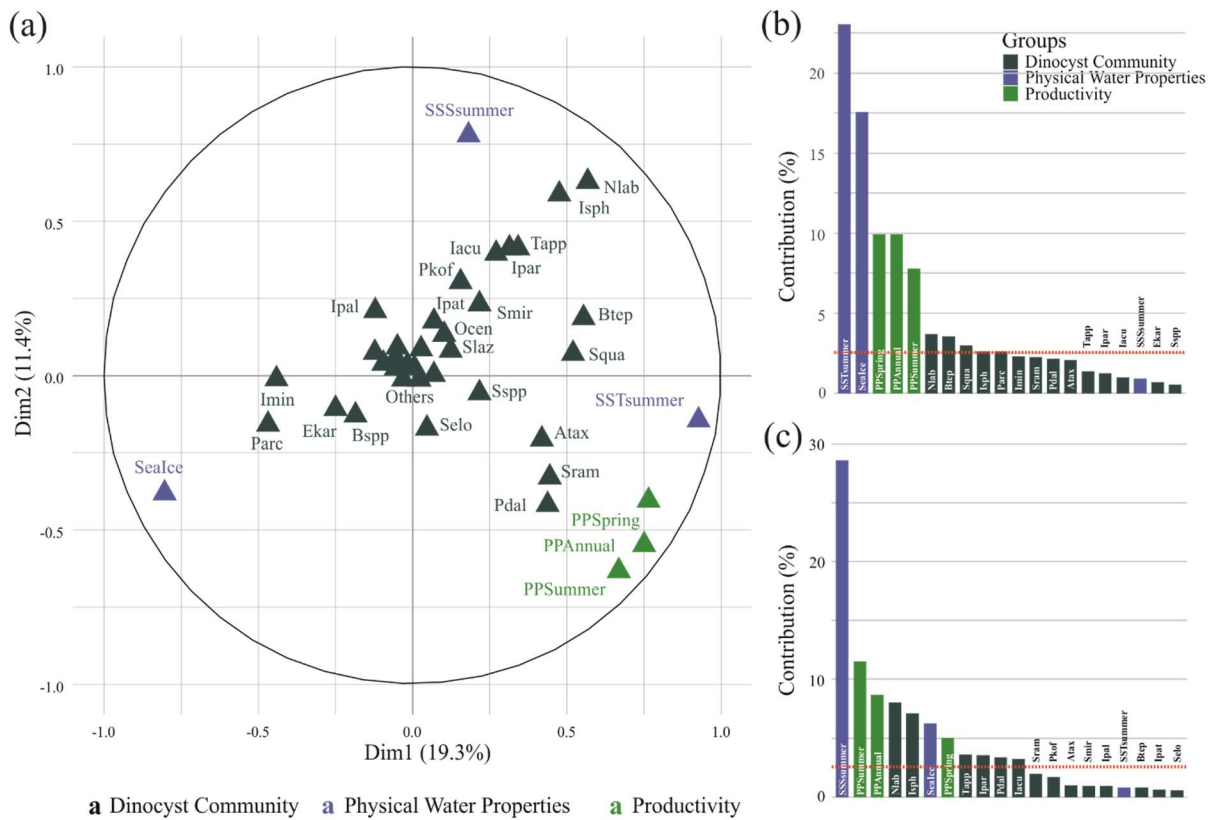
The first dimension mainly represents the negatively correlated physical water properties, SSTsummer and Sealce, while the second dimension is mostly represented by SSSsummer. Hence, we recognise the main gradient to be described by a transition from warmer and lesser sea-ice conditions to colder and exceeding sea-ice conditions with *Islandinium minutum* and the Cyst of *Polykrikos* sp. – Arctic characterising the colder end and *Bitectatodinium tepikiense* and *Selenopemphix quanta* the warmer end. The patterns of species vs environment relationships are further illustrated by the RV coefficients (Table 4.4).

Figure 4.4b illustrates sample site scores by their regional origins from the global PCA. Sample sites from the Labrador Sea and some sites from the Davis Strait mainly describe the first dimension. As emerged earlier, the first axis represents primarily a temperature gradient, pointing to a higher influence of temperature-related variables within the samples located along the first axis. The second dimension, thus salinity, is essentially associated with sample sites in Hudson Bay. Samples from Baffin Bay do not contribute much to the variance in the data matrix.

**Table 4.4:** RV coefficients. The coefficients appear in the lower-left triangle below the diagonal, while the upper-right triangle contains the p values among the four groups of variables used in the MFA.

	<b>Dinocyst Community</b>	<b>Physical Water Properties</b>	<b>Productivity</b>
<b>Dinocyst Community</b>	1.000	< 0.01	< 0.01
<b>Physical Water Properties</b>	0.338	1.000	< 0.01
<b>Productivity</b>	0.117	0.327	1.000





**Figure 4.3:** Contribution of the groups to the first two dimensions of the global PCA. a) Correlation circle of variables after MFA. The distance between the variable points and their origins represents the weight of the variable within the first two dimensions. The variables the most correlated with a dimension lie close to the dimension's axis. Positively correlated variables are grouped together, while negatively correlated ones lie on opposite sides. b) and c) Contribution of the variables to the first and second dimensions, respectively.

Figure 4.4a represents each sample site score with respect to the three groups. Larger black dots represent the site scores for the pooled MFA, while coloured dots connected with the black dots by coloured lines represent the separate PCA scores for each group. The highest contribution to productivity variances comes from sample sites in the Davis Strait, while the variance in dinocyst communities can be attributed mainly to the Labrador Sea. Sample sites from the Labrador Sea, Hudson Bay, and some from Baffin Bay contribute to the variance in physical water property variables.

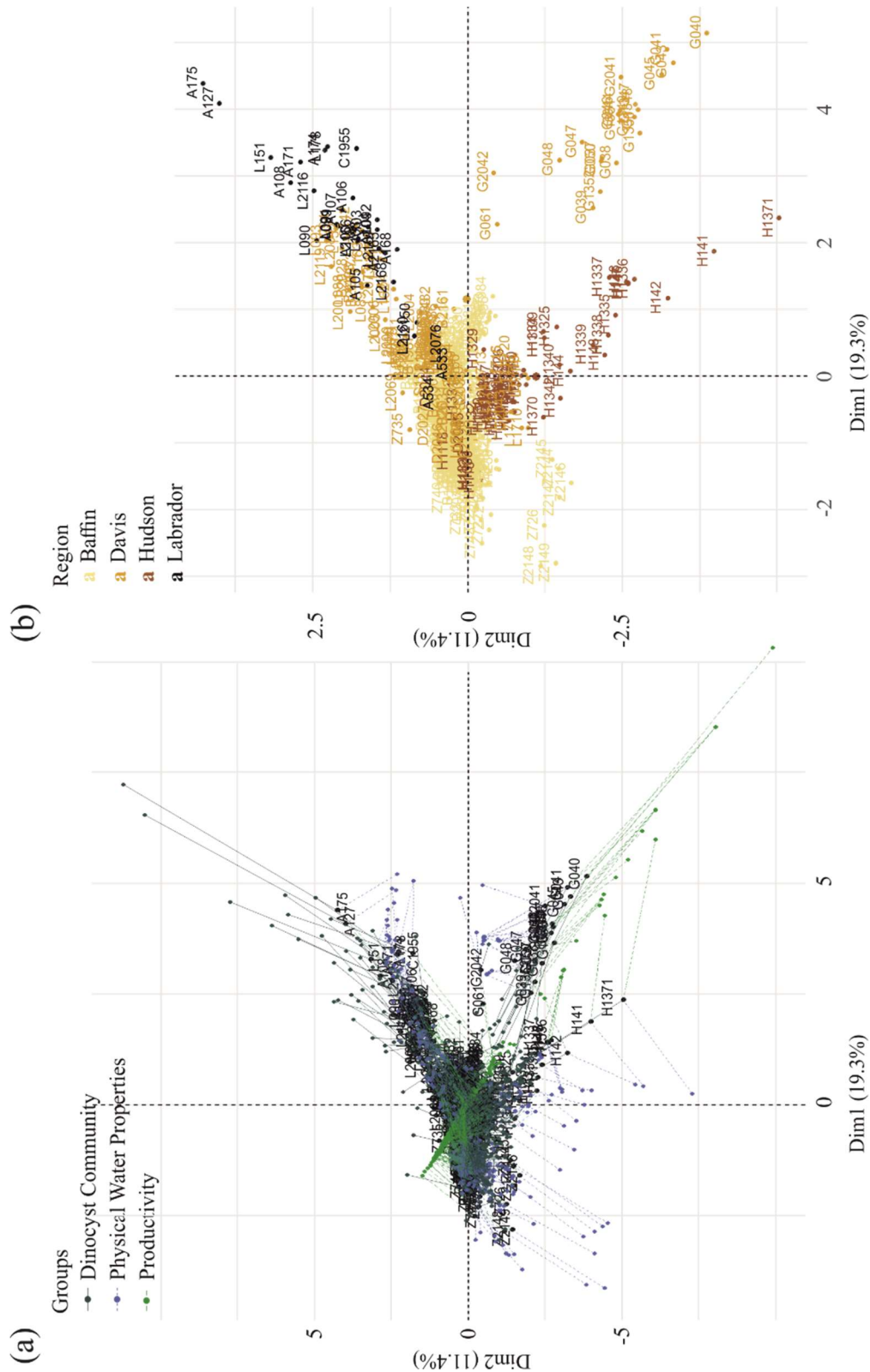


**Figure 4.4:** Sample sites within the first two dimensions of the MFA. a) Sample site scores according to the pooled MFA with 421 data points (large black dots) and single PCAs depicting how much sample sites contribute to the variance in the data matrix in respect to the three groups. b) Sample site scores relative to the first two dimensions of the global PCA. Sites with similar profiles are close to each other on the factor map.

### 4.3.2 Redundancy analysis

The first step of the variable selection is based on RDA carried out for single variables. It revealed that, when considered individually, each of the six environmental variables appeared to explain a significant ( $p \leq .01$ ) amount of variation in the assemblage composition in the dataset (Table 4.5). Together, they explain 32 % of the total inertia in the taxa dataset. We then evaluated the independence of the tested environmental variables through a selection, excluding variables with  $VIF > 2$ . This successive forward selection uncovered three separate dimensions in the taxa variance driven by SSTsummer, SSSsummer and PPSpring respectively. The remaining variables were excluded from further analyses due to their collinearity with SSTsummer, SSSsummer, or PPSpring.

When only the independent environmental variables are used, the constrained part of the RDA explains about 24 % of the taxa variance (Table 4.6) with environmental variables having significant correlations with RDA-axes (Table 4.7). The first axis explains 66 % of the constrained variance and is positively correlated with SSTsummer, while axes 2 and 3 explain 27 % and 7 % are positively correlated with SSSsummer and PPSpring, respectively (Fig. 4.5, Table 4.6). Regarding species-environment relationships, we find that the variance of *I. minutum* is strongly related to changes in SSTsummer, while the abundance of *N. labyrinthus* is related to SSSsummer. The cyst of *P. dalei* shows correlations with SSTsummer and PPSpring. Phototrophic cysts are generally associated with higher summer temperatures and heterotrophic cysts with lower temperatures (Figs. 4.5a-c). Sample-environment relationships (Figs. 4.5d-e) reveal that all samples contribute to the variance in SSTsummer. The variance for PPSpring is high for samples from Labrador Sea, Baffin Bay and Hudson Bay, while SSSsummer variance is highest in samples from Davis Strait and Hudson Bay.

**Table 4.5:** Explained inertia (as a single variable) and variance inflation factors of the tested environmental variables in the RDA model. VIF(a) when all variables are considered; VIF(b) after manual forward selection for variables without dependence.

Environmental variable	% inertia explained	VIF (a)	VIF (b)
SSTsummer	12.4	3.9	1.8
SSSsummer	6.9	2.0	1.0
Sealce	9.7	2.9	
PPAnnual	4.2	394.7	
PPSpring	2.5	72.7	1.8
PPSummer	4.6	137.5	

**Table 4.6:** RDA results and results of permutation tests for the significance of RDA-axes after manual forward selection ( $p \leq .01$ ).

	RDA-axis 1	RDA-axis 2	RDA-axis 3	Total inertia	Proportion of total variance explained
Eigenvalues	0.057	0.024	0.005	0.365	0.236
Constrained proportion explained	0.660	0.284	0.056		
Constrained cumulative proportion	0.660	0.944	1.000		
F-value	85.2	36.6	7.3		

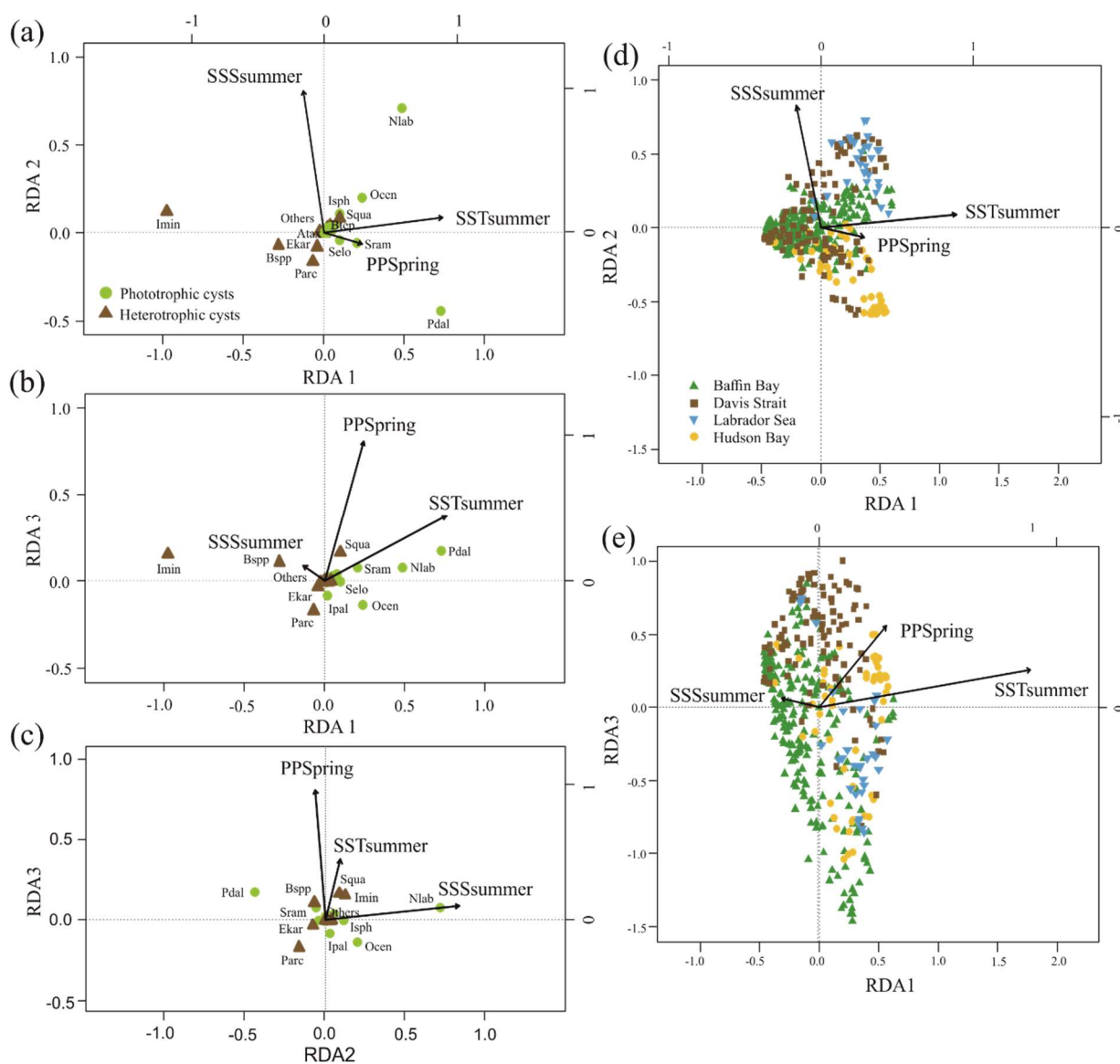


**Figure 4.5:** RDA scores. a, b and c): RDA ordination diagrams of dinocyst taxa (see Table 4.1 for abbreviations) vs environmental variables (arrows) showing the correlation with the axes (direction of arrows) and the strength of the dinocyst vs environmental variable relationship (length of arrows). Species in the centre region are without abbreviations. d and e): Sample ordination for RDA constrained by independent environmental variables for axes 1, 2 and 3.

**Table 4.7:** Intraset correlation coefficients ( $r^2$ ) between independent variables and RDA-axes and between the variables themselves.

	RDA-axis 1	RDA-axis 2	RDA-axis 3	SSTsummer	SSSsummer	PPSpring
SSTsummer	0.79	0.01	0.20	1	0.01	0.45
SSSsummer	0.02	0.96	0.01		1	0.01
PPSpring	0.08	0.01	0.91			1

### 4.3.3 Spatial autocorrelation

We tested spatial and environmental autocorrelation, considering only the independent variables and following the procedure described by Telford and Birks (2009). Inevitably, the performance ( $r^2$ ) deteriorates with increasing fraction of sites deleted (S4.4 - supplementary data). We find that the deterioration of performance is much worse with neighbourhood deletion than with random deletion, indicating the presence of spatial autocorrelation. When deleting environmentally similar sites, we find a pattern of performance loss that is slightly worse for neighbourhood deletion than for environmental deletion. Hence, removing geographically close sites causes a higher decline in performance than when the same fraction of environmentally similar sites is removed, indicating spatial autocorrelation over environmental autocorrelation. Variable performances drop below 0.55 when samples within a 200 km radius are deleted, implying that calibrated transfer functions need to be interpreted with caution.

### 4.3.4 Cross-validation

For transfer function development, LOO-cross-validation results indicate the best performances for MAT, with WA-PLS RMSEP values on average around 40 % higher and ML RMSEP values on average by around 100 % higher, depending upon the variable (Table 4.8). The differences in LOO-RMSEPs between the calibration and the verification subsets for MAT show differences of 25 % for SSSsummer and 8% for PPSpring, indicating an inadequate spatial coverage for some areas within the regional subset for these parameters. For SSTsummer reconstructions the spatial coverage in the dataset seems to be sufficient. All three environmental parameters show similar performances within each reconstruction method. The h-block cross-validation shows MAT RMSEP increasing by 60 %, 60 % and 95 % for SSTsummer, SSSsummer and PPSpring, respectively. RMSEPs of WA-PLS and ML remain largely unaffected by site deletion within the applied radius  $h$  for SSTsummer (1 %) and SSSsummer (7 %) (Table 4.8). For PPSpring RMSEPs increase by about 25 %.

**Table 4.8:** Cross-validation performances. Performance for n = 421 applying LOO-cross-validation and h-block cross-validation for MAT (c - calibration dataset, v – verification dataset) with the number of analogues used (#ana.), for WA-PLS with the number of components used (#comp.) and for ML. The number of analogues and components that will perform best during reconstructions (#ana. and #comp.) have been determined calculating the RMSE of prediction as a function of the number of analogues used and a randomisation t-test for testing the significance of cross-validated components used after van der Voet (1994), respectively. h-values have been estimated by fitting a spherical variogram to detrended residuals of a WA model (S4.5 - supplementary material) following Telford and Birks (2009) as well as Trachsel and Telford (2016).

Cross-validation	LOO													
Method	MAT					WA-PLS					ML			
	RMSEP <sub>c</sub>	r <sup>2</sup> <sub>c</sub>	RMSEP <sub>v</sub>	r <sup>2</sup> <sub>v</sub>	#ana.	RMSE	r <sup>2</sup>	RMSEP	r <sup>2</sup>	#comp.	RMSE	r <sup>2</sup>	RMSEP	r <sup>2</sup>
SSTsummer	1.38	0.76	1.35	0.80	5	1.90	0.58	2.03	0.52	4	2.73	0.41	2.75	0.40
SSSummer	1.35	0.68	1.01	0.78	5	1.55	0.56	1.60	0.53	2	2.34	0.49	2.37	0.47
PPSpring	324.16	0.61	298.14	0.75	7	446.20	0.30	466.17	0.24	3	748.44	0.04	750.99	0.04
Cross-validation	h-block										h [km]	Variogram model		
Method	MAT			WA-PLS			ML							
	RMSEP	r <sup>2</sup>	#ana.	RMSEP	r <sup>2</sup>	#comp.	RMSEP	r <sup>2</sup>						
SSTsummer	2.25	0.42	5	1.93	0.59	4	2.74	0.43	256	Spherical				
SSSummer	2.14	0.22	5	1.68	0.64	4	2.48	0.57	623	Spherical				
PPSpring	636.67	0.01	7	536.96	0.36	5	958.37	0.02	745	Spherical				

An inspection of the distribution of residuals from cross-validation tests of the variables along their environmental gradient reveals uneven residual distributions for all independent variables. (S4.6 - supplementary material). For all transfer function methods, the spatial structure of the residuals is complex and large residual values emerge regionally. For ML large over- and underestimations suggest that the method is inaccurate for reconstructions. For MAT and WA-PLS, we observe a systematic underestimation in the Labrador Sea, especially for SSTsummer and PPSpring and an overestimation in parts of Baffin Bay and Hudson Bay with especially large overestimations for PPSpring in Hudson Bay. However, residuals for SSSsummer reconstructions regarding MAT and WA-PLS are quite small, suggesting solid transfer functions.

#### **4.3.5 Transfer function significances in sediment core reconstructions**

Having established the transfer functions, we applied them to the selected four sediment cores covering the N-S transect. First, for each record, we identified the interval characterised by the largest changes in assemblage composition, which we assumed to be related to the most important environmental change. PC analysis of downcore dinocyst assemblages revealed one to two assemblage changes within each of the four cores (Fig. 4.6). The first component (PC1) of the PCA identified three assemblage zones in the northernmost record HU91-039-008P, which account for 74.5 % of the total variance, while PC2 accounted for 17.0 %. In Southern Melville Bay (GeoB19927-3) and Disko Bugt (MSM343310) PC1 identified two assemblage zones accounting for 76.6 % and 77.7 % of the total variance, while PC2 identified at least three assemblage zones accounting for 17.0 % and 18.3 % respectively. Within the most southern record from the Labrador Sea (HU2008-029-004) PC1 revealed four zones (69.3 %) and PC2 three zones (21.3 %).

The reconstructions based on the local calibration dataset for the northern core HU91-039-008P (Fig. 4.6a) show modest changes but SSTsummer resonates with the facies shifts. In core GeoB19927-3 (Fig. 4.6b), assemblage zone shifts correspond to variations in SSSsummer and PPSpring reconstructions based on ML and WA-PLS. In core MSM343310 (Fig. 4.6c), the facies shift is caught in SSSsummer and SSTsummer reconstructions based on ML and WA-PLS. In core HU2008-029-004 (Fig. 4.6d), we identify shifts based on WA-PLS and ML reconstructions. Cross-correlations between PCA-axis 1 and reconstructed SSTsummer, SSSsummer and PPSpring point to high correlation coefficients ( $r^2 \geq 0.70$ ) applying ML and WA-PLS followed by MAT with lower correlation coefficients (S4.7 - supplementary material).

The different degree of correspondence between the environmental reconstructions inferred by the transfer functions and the principal community change trends in the dinocyst records is echoed in the significance tests made after the approach of Telford and Birks (2011) for downcore reconstructions. Here a significant reconstruction should explain more of the variance in the fossil dinocyst assemblage than a random transfer function calibrated using the same assemblages but random environmental data. These tests reveal that different transfer function methods and environmental variables produce significant reconstructions for each core. Significance test results of transfer function applications with the local dataset and the regional Northern Hemisphere dataset reveal the same pattern (Table 4.9).



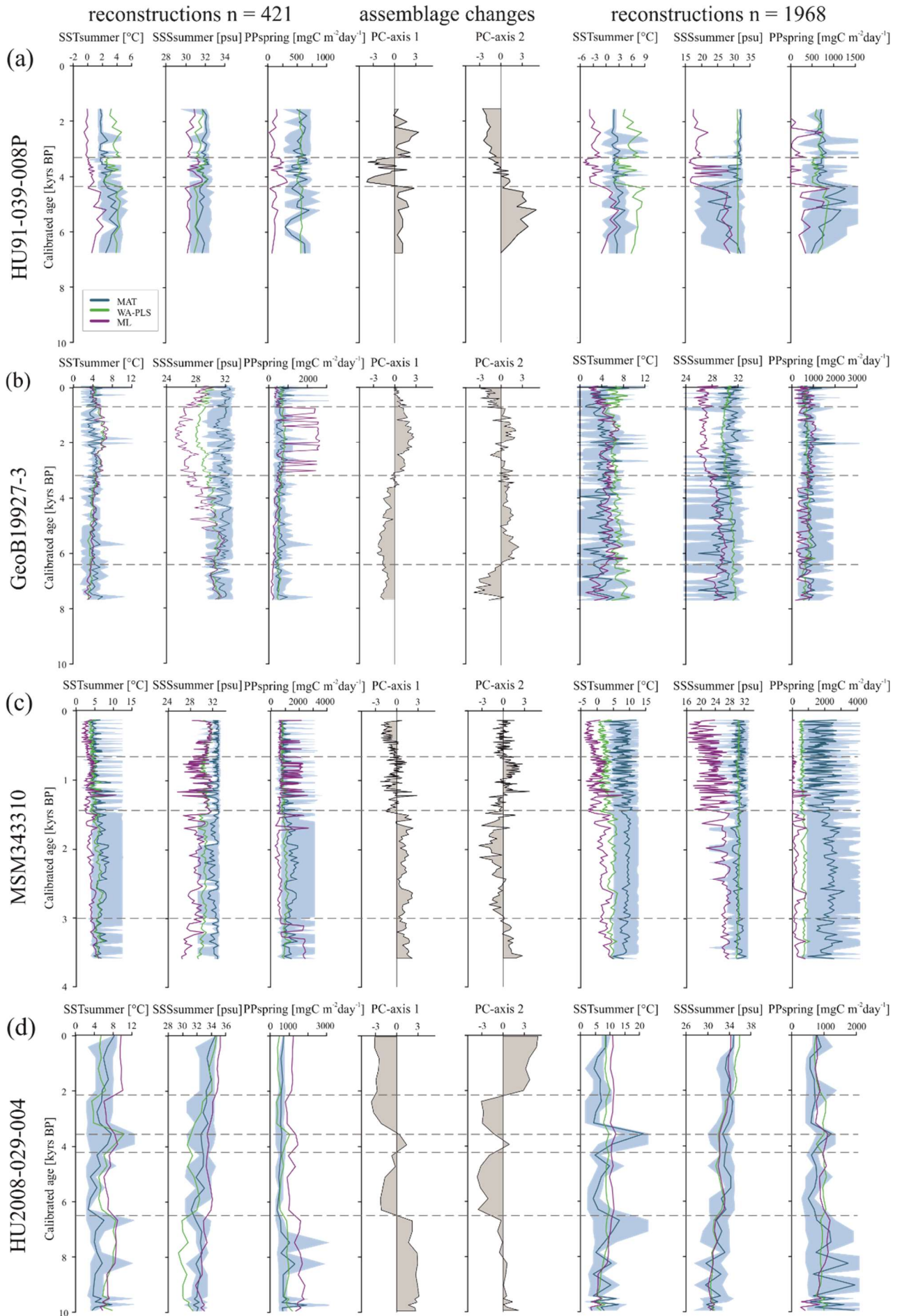




**Figure 4.6:** Downcore reconstructions based on the local dataset (n = 421) and the Northern Hemisphere dataset (n = 1968) using three transfer function techniques. MAT, WA-PLS and ML are represented by blue, green and purple curves respectively. The lighter blue curves correspond to maximum and minimum possible values calculated from a set of five modern analogues. The ecostratigraphic zones are determined from PC analyses. a) HU91-039-008P, b) GeoB19927-3, c) MSM343310 and d) HU2008-029-004.

When the Northern Hemisphere dataset (n=1968) is used for reconstructions of the four downcore assemblages (Fig. 4.6), we find that 17 % of all the tested transfer functions produce significant estimates (SSSsummer – 25 %, SSTsummer – 17 %, PPSpring – 8 %) (Fig. 4.7, Table 4.9).

However, when applying the local calibration dataset (n=421), most transfer functions produce significant reconstructions for SSSsummer (75 %) and SSTsummer (50 %), and some for PPSpring (8 %) (Fig. 4.7, Table 4.9). For the northern core HU91-039-008P, summer salinity estimates are significant with all three transfer function methods (Fig. 4.7a). In the Southern Melville Bay core GeoB19927-3, the WA-PLS transfer function has been tested as significant for PPSpring, as well as SSSsummer and SSTsummer (Fig. 4.7b). For records in Disko Bugt (MSM343310), both MAT and WA-PLAS produce significant estimates for SSSsummer, while WA-PLS shows additional significance for SSTsummer (Fig. 4.7c). Further south, the record from Labrador Sea (HU2008-029-004) yields significant estimates for SSSsummer and SSTsummer based on MAT and ML (Fig. 4.7d).

**Table 4.9:** Significances for downcore reconstructions after the approach of Telford and Birks (2011) using the local dataset (n = 421) and the regional Northern Hemisphere dataset (n = 1968). Significant reconstructions are marked by a green check mark, and the not significant ones by a red cross.

Transfer function significances		n = 421			n = 1968		
		SSTsummer	SSSsummer	PPspring	SSTsummer	SSSsummer	PPspring
HU91-039-008P	MAT	✓	✓	×	×	✓	✓
	WA-PLS	✓	✓	×	×	×	×
	ML	×	✓	×	×	×	×
GeoB19927-3	MAT	×	×	×	×	×	×
	WA-PLS	✓	✓	✓	×	✓	×
	ML	×	✓	×	×	×	×
MSM343310	MAT	×	✓	×	×	✓	×
	WA-PLS	✓	✓	×	×	×	×
	ML	×	×	×	✓	×	×
HU2008-029	MAT	✓	✓	×	✓	×	×
	WA-PLS	×	×	×	×	×	×
	ML	✓	✓	×	×	×	×

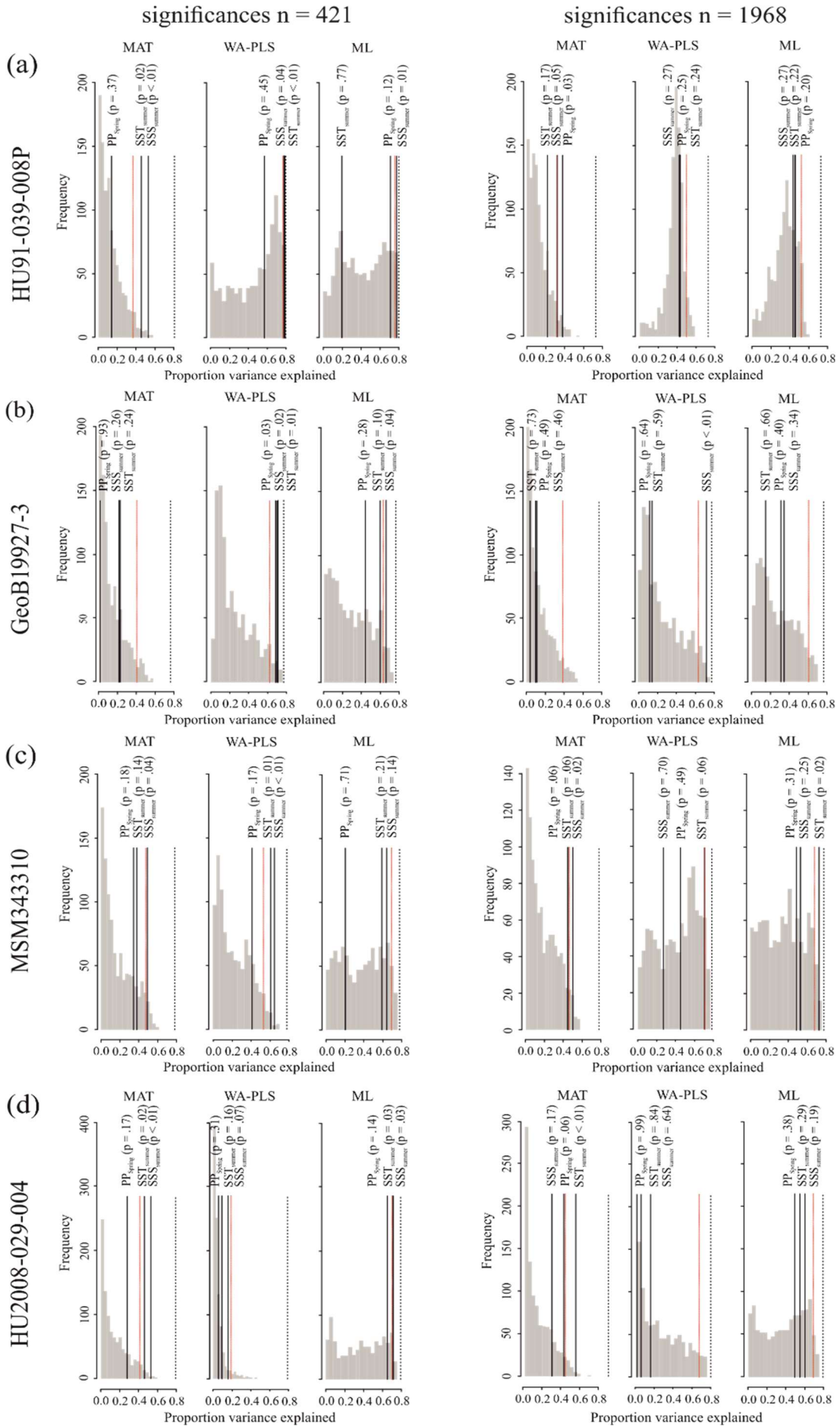


**Figure 4.7:** Results of the significance tests for downcore reconstructions. a) HU91-039-008P, b) GeoB19927-3, c) MSM343310 and d) HU2008-029-004. For all significance tests, 999 random environmental variables were generated to produce the null distribution (grey bars). Black lines mark the variances explained by observed variables. Red dotted lines mark the 95<sup>th</sup> percentile of the random distribution ( $p \leq .05$ ) above which reconstructions are deemed as significant. The proportion of the variance explained by the first axis of a principal component analysis (PCA) is also recorded (black dotted line), as this represents the maximum proportion of the variance in the fossil data that a reconstruction could possibly explain. For significance test analysis we applied the number of analogues (MAT) and components (WA-PLS) resulting in highest significances respecting all three variables.

#### 4.4 Discussion

The ecological models and transfer functions derived in this study rely on a few assumptions. Foremost is that the composition of dinocyst assemblages was primarily affected by the selected environmental parameters and that the set of parameters is comprehensive and includes all the relevant parameters. Indeed, there might be circumstances under which a sedimentary assemblage reflects other processes than the considered parameters. For example, the distribution and composition of dinocyst assemblages in the local calibration dataset could carry an imprint of non-oceanographic factors such as those related to the dinoflagellate life cycle (Bravo and Figueroa, 2014) and post-depositional organic matter degradation (Zonneveld et al., 2019). The encystment of dinoflagellates is related to sexual reproduction and the cyst plays a role as it protects the diploid cell during dormancy of variable length after which the cell excysts to re-establish metabolic activities and cellular divisions within the pelagic ecosystem (Taylor and Pollinger, 1987). For many dinoflagellate taxa, the cycle includes settlement of the cyst on the seafloor and the completion of the life cycle is thus favoured where the seafloor is not too deep to prevent excystment and migration of the cells towards surface waters. Hohmann et al. (2020) showed that water depth and distance from shore explain a significant amount of compositional variance in dinocyst assemblages ( $p < .01$ ). However, these variables were shown to describe a separate dimension of variability, orthogonal to the tested oceanographic and primary productivity factors. Also, when applied to a sedimentary record, factors such as the distance from shore and water depth should be mostly constant for the downcore record. The effect of organic matter degradation on the dinocyst assemblage composition can be detected independently of the ecological model because the ratio between cysts of autotrophic/phototrophic taxa should systematically decrease with increasing degradation due to the different composition of the wall polymer of the heterotrophic taxa (Zonneveld et al., 1997). In the Northern Hemisphere calibration dataset, there is no evidence of a pervasive effect of degradation, as no systematic relationship

between the residuals of the tested variables and the ratio between the cysts of heterotrophic and autotrophic/ phototrophic taxa was observed (Hohmann et al., 2020). This also holds for sample sites included within the local calibration dataset tested in this study.

Excluding the substantial effect of selective degradation as a secondary factor and showing that life-cycle factors explain an independent dimension of the variance, we can consider the distribution of dinocyst assemblages in the calibration dataset as being primarily driven by environmental factors. However, a large proportion of variance in the calibration dataset cannot be explained by any combination of the tested environmental drivers even when water depth and distance from shore are included. First, it is possible that the applied taxonomic concepts, often combining taxa to achieve higher consistency, hide a finer taxonomic level, which is ecologically relevant. This process is very likely, as evidenced by the existence of cryptic species in modern dinoflagellates (Montresor et al., 2003; Parkinson et al., 2016; Wang et al., 2019) and by the fact that we voluntarily group some taxa. It is, however, unavoidable because it is unlikely that the current taxonomic concepts as applied in the practice can be substantially refined in routine analyses (de Vernal et al., 2020).

Further, cyst-producing dinoflagellates lose their mobility at cyst formation, from which time onwards they are subject to ocean current transport until they reach the ocean floor. Although we excluded sample sites areas with strong oceanographic currents, small-size dinocyst particles might still be subject to transport by moderate currents when not incorporated in marine snow or faecal pellets (e.g. Turner 2002, 2015) or bottom water currents and sediment flows (Dale, 1992; Dale and Dale, 1992). This may result in a lateral relocation and sedimentation from a cysts formation environment and thus in an additional nuisance in the calibration dataset (Nooteboom et al., 2019).

Additional noise may also emerge from modern assemblages in the calibration dataset, which represent average fluxes over different time intervals. Assemblages may be to a different degree affected by anthropogenic effects, such as local pollution or global warming. Assemblages from sites with low sediment accumulation may represent averages over millennia and contain a mixture of microfossils deposited during distinct oceanographic events of the late Holocene (e.g. Wigley et al., 1981; Bradley and Jonest, 1993) or be affected by cysts deposited during conditions induced by modern anthropogenic global change.

Alternatively, it is possible that the tested parameters are not the most determinant ones or that the assemblage composition is to a certain degree driven by biotic interactions rather than by environmental factors. It is also possible that environmental factors, not yet considered, play an important role. These could include turbulence, micronutrients, stratification, or any other parameters that might be difficult to quantify for data treatment purposes.

Regardless of the limitations that can be due to missing or unidentified driving parameters, we find three mutually independent ecological gradients driving dinocyst assemblages in the local

calibration dataset. This confirms previous findings that phytoplankton (Lopes et al., 2010) and hence dinocyst assemblages reflect multiple environmental drivers (e.g. Radi and de Vernal, 2008; Ribeiro and Amorim, 2008; Hohmann et al., 2020).

The existence of multiple environmental gradients affecting the dinocyst assemblage composition implies that it should be possible to extract information from the same fossil dinocyst assemblage on past variability for more than one environmental driver. Whilst this is correct theoretically, one must consider the (small) amount of variance constrained by the tested parameters against the (large) portion of the variance that remains unconstrained. For example, primary productivity, which represents the third gradient after SST and SSS, explains a maximum of 6 % of the constraint variability in the RDA (Table 4.6 and 4.7). This parameter does not contribute to the first two dimensions of the MFA and the RDA (see also Radi and de Vernal, 2008; de Vernal et al., 2020) and although the extracted relationship appears statistically significant, it may well be overwhelmed by factors that are responsible for the unconstrained portion of the variance in assemblage composition.

Additionally, we note that the presence of multiple environmental gradients in the local calibration dataset is associated with spatial structuring of the environment (S4.6 – supplementary material), suggesting that some environmental variables are deemed significant in the RDA because they drive taxa distribution in a certain area within the local dataset, where the gradient of the given variable is strong. This is consequential with spatial autocorrelation of the variables (S4.4 – supplementary material) and leads to a performance decrease of MAT in the h-block cross-validation (Table 4.8) and to a strong spatial structure of the residuals in all methods (S4.6 – supplementary material). These observations are coherent with findings in Hohmann et al. (2020), where the detected mutually independent signatures of multiple environmental factors in two larger regional datasets are likely a result of the agglomeration of information from regions with different environmental drivers and specific (endemic) taxon-environment relationships. To test this effect quantitatively, we performed a q-mode factor analysis for the local dataset, where taxa were clustered into factors to analyse interrelationships among their large number and to explain them in terms of their common underlying dimensions with respect to assemblage driving parameters. The information contained in individual taxa was condensed into a smaller set of information. We found that most taxa showed correlation coefficients  $< 0.3$  with the retained factors, suggesting that driving parameters for taxa do not remain the same even throughout the region of the local Baffin Bay dataset. Hence, our results suggest even more localised driving mechanisms for dinocyst assemblage compositions in very specific areas. This implies that generating locally calibrated transfer functions will come at the cost of loss of generalisation and limited applicability to past oceanographic states.

Spatial structuring of the local dataset and the regionally different dominant environmental drivers seem to affect different transfer function approaches, which are based on different fundamental principles (Kucera et al., 2005). Our analyses reveal that the ML approach appears unable to effectively extract the taxon-environment relationship in the presence of multiple gradients. In contrast, the same approach, together with WA-PLS, is less affected by the spatial autocorrelation of the tested environmental variables. When this is considered by using the h-block validation, the performance of WA-PLS and ML remains essentially the same, but the performance of MAT plummets, returning higher RMSEP and lower  $r^2$  than ML and WA-PLS (Table 4.8). The similarity of cross-validated RMSEP for both ML and WA-PLS confirms that these methods are more robust with regard to the detected spatial structure in the data than MAT (Telford and Birks, 2005). While MAT finds the local structure in the assemblage data, ML and WA-PLS, which are based on a unimodal species-environment response model, find the general component of the variation in the assemblage data that is correlated with a specific environmental forcing. This is not to say that MAT is not suited for transfer function development with dinocyst assemblage data, but it indicates that the performance indicators for this method based on LOO are more optimistic than for ML and WA-PLS (Telford and Birks, 2005), especially in a strongly spatially structured dataset. Cross-validation of the local dataset applying a calibration and verification dataset results in a 25 % lower  $RMSEP_v$  for the verification dataset compared to the calibration dataset for SSSsummer, while  $RMSEP_v$  are < 10 % lower for SSTsummer (2 %) and PPSpring (8 %). This indicates that additional sample sites might benefit performances for SSSsummer transfer functions as with an adequate, hence representative, spatial coverage  $RMSEP$  should be similar for both datasets (Table 4.8).

Regardless of the statistical approach, a theoretical high-performance transfer function for one of the independent driving variables for assemblage composition in the local calibration dataset does not necessarily produce a reliable reconstruction applied to fossil downcore dinocyst assemblages. This is because we can never be sure that the main drivers for past assemblages were identical in the modern calibration dataset. To assess if the main past drivers resemble the main modern drivers, we compared the transfer function reconstructions to the major compositional trends in fossil dinocyst assemblages as revealed by multivariate analyses.

Across the four records throughout Baffin Bay, the main pattern of dinocyst assemblage change during the Holocene can be identified as two biofacies shifts occurring around 4.0 ka and 6.7 ka (Fig. 4.6 and 4.8). Despite the presence of this clear pattern, most transfer functions based on the local ( $n = 421$ ) and regional ( $n = 1968$ ) data sets reconstruct modest changes close to uncertainty for SSTsummer, SSSsummer and PPSpring (Fig. 4.6), likely reflecting the difficulty in attributing the taxa assemblage change to specific factors. Alternatively, one may

argue that we have not retained the correct determinant parameters during the manual forward selection. For example, the Holocene records could reflect changes that were due to large shifts in sea ice coverage. Indeed, during the selection process, the analysis suggested that Sealce does not explain a separate dimension of variance in the taxa assemblages within the local Baffin Bay dataset (S4.3 – supplementary material), as it revealed high collinearity with SSTsummer (Fig. 4.3). This means that regionally Sealce and SSTsummer explain a similar taxa variance and while reconstructing one, we reconstruct a mixture of both parameters. It is also possible that the parameterisation of sea ice cover used here is not ideal to describe the relationship with dinocyst assemblages. In the context of Baffin Bay, SSSsummer, which is the parameter that appears to be best reconstructed, is likely a reflection of the regional hydrography closely related to the sea ice cover that matters for productivity. Therefore, we can only conclude that the environmental regime shifts around 4.0 ka and 6.7 ka appear to be driven by changes in local hydrography that were associated with salinity changes but considering the magnitude of the salinity changes implied by the transfer functions, it is unlikely that the dinocyst composition responded to salinity directly.

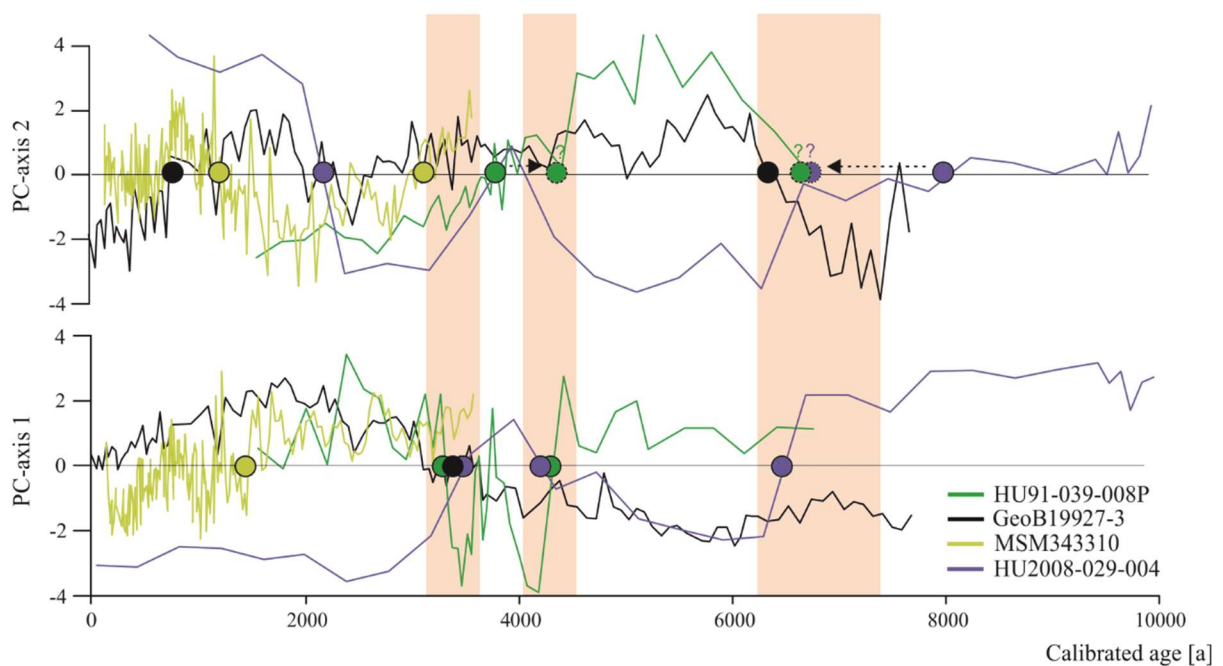


**Figure 4.8:** Dinocyst assemblage changes according to the first two PC-axes. Coloured dots represent PC transitions pointing to regime shifts around 4.0 ka (3.4 ka and 4.3 ka) and 6.7 ka in the three cores encompassing the middle and late Holocene (orange shaded).

In contrast to the results of the local calibration, only a few of the reconstructions were identified as significant when applying the regional Northern Hemisphere dataset (SSTsummer = 16 %, SSSsummer = 25 %, PPspring = 8 %) (Table 4.9, Fig. 4.7). This suggests that transfer

functions based on broad regional or even global calibration datasets are affected by nuisance variables, which makes it difficult to identify the driving mechanisms of dinocyst assemblages when the amplitude of environmental change is relatively small, as it is the case during the middle and late Holocene. For longer time intervals with large amplitude changes, global calibrations may work better and would be even necessary as larger datasets contain a wider range of analogues. Hence, we suggest a thorough evaluation of the calibration dataset and the significance of fossil applications ensuring that the driving mechanisms of dinocyst assemblages are caught through time and space.

#### **4.5 Conclusion**

Understanding past natural variability of ecosystem drivers in Arctic regions requires reliable reconstructions. We calibrated local transfer functions from Baffin Bay samples for three independent parameters driving dinocyst assemblages in this area. We estimated how well these local functions were able to estimate past environmental parameters in the Baffin Bay region during the Holocene, comparing them to estimates derived from regional transfer functions from Northern Hemisphere samples.

Statistical analyses of surface sediment samples and transfer function application on downcore samples from a Holocene transect along the Baffin Bay indicate that salinity is the main driver of present-day and Holocene dinocyst assemblage composition in the region, with temperature being an important but minor driver.

Analyses of four Holocene records in a North-South transect along the Baffin Bay show two regime shifts that occurred throughout the region. The main environmental parameter to which the dinoflagellate communities seem to have reacted during regime shifts is salinity, but further minor drivers may have differed regionally.

We show that the relationship between dinocyst assemblage composition and multiple environmental drivers can be modelled by MAT and WA-PLS transfer functions. In our study, the identification of main driving variables and regime shifts was achieved through the application of a local calibration dataset, while through the application of the Northern Hemisphere dataset, we did not succeed in extracting this information from the taxa variability. While our results reinforce the assumption of counteracting nuisance in spatially large calibration datasets, suggesting the application of local datasets, regions with spatially or temporarily broader environmental gradients might supposedly benefit from larger calibration datasets regardless of a certain nuisance.

We suggest a thorough evaluation of transfer function performances and significances for downcore applications to disclose the specific drivers for present and fossil dinocyst assemblages in a studied core location. To this end, a local calibration dataset, which reduces



several nuisances, is presumably beneficial when the amplitude of parameter change is relatively small, like during the middle and late Holocene.

#### **4.6 Data availability**

This study contains supplementary material. This material includes the matrices of taxa abundances with all tested environmental (oceanographic and non-oceanographic) variables from the local  $n = 421$  dataset (S1), DCA analysis plot (S2), script of manual forward selection (S3), spatial autocorrelation analysis plots (S4), variogram plots for the estimation of  $h$  in the  $h$ -block cross-validation (S5), residual plots from cross-validation tests (S6) and cross-correlation plots from reconstructions (S7). The R codes applied for analyses can be accessed on ZENODO ([link](#)). Dinocyst assemblage data from the newly analysed core GeoB19927-3 were uploaded to PANGAEA and will be available soon.

#### **4.7 Acknowledgements**

This study is a contribution of the International Research Training Group “Processes and Impacts of Climate Change in the North Atlantic Ocean and the Canadian Arctic” (ArcTrain), which was supported jointly by the German Research Foundation (DFG) (IRTG 1904) and by the Natural Sciences and Engineering Research Council of Canada (NSERC). We also acknowledge the support from the Fonds de recherche du Québec – Nature et Technologie (FRQNT). We are grateful to Taoufik Radi and Sebastien Zaragosi for their help in the preparation of the reference oceanographical data set and we especially thank Maryse Henry for her extraordinary support during sample analyses.

#### **4.8 References (Chapter 4, according to the journal’s style)**

- Allan, E., de Vernal, A., Knudsen, M.F., Hillaire-Marcel, C.: Late Holocene sea-surface instabilities in the Disko Bugt area, west Greenland, in phase with  $d^{18}O$ -oscillations at Camp Century, *Paleogeography and Paleoclimatology*, 33, 227-224, <https://doi.org/10.1002/2017PA003289>, 2018.
- Beamud, S.G., Diaz, M.M., Baccala, N.B., Pedrozo, F.L.: Limnological analysis of patterns of vertical and temporal distribution of phytoplankton using multifactorial analysis: Acidic Lake Caviahue, Patagonia, Argentina, *Limnologia*, 40, 140–147, <https://doi.org/10.1016/j.limno.2009.11.003>, 2010.
- Berger, W.H., Smetacek, V., Wefer, G.: Ocean productivity and paleoproductivity - an overview, in: *Productivity of the Ocean: Present and Past*, John Wiley & Sons Limited, 1–34, 1989.
- Birks, J.B.: Quantitative palaeoenvironmental reconstructions, in: *Statistical Modelling of Quaternary Science Data*, Maddy, D., Brew, I.S. (Eds.), Quaternary Research Association, Cambridge, 271, 1995.
- Bradley, R.S., Jonest, P.D.: ‘ Little Ice Age ’ summer temperature variations: their nature and

- relevance to recent global warming trends, *Holocene*, 3, 367–376, <https://doi.org/10.1177/095968369300300>, 1993.
- Bravo, I., Figueroa, R.: Towards an ecological understanding of dinoflagellate cyst functions, *Microorganisms*, 2, 11–32, <https://doi.org/10.3390/microorganisms2010011>, 2014.
- Burman, P., Bhow, E., Nonal, D.: A cross-validatory method for dependent data, *Biometrika*, 81, 351–358, <https://doi.org/10.1093/biomet/81.2.351>, 1994.
- Carlson, M.L., Flagstad, L.A., Gillet, F., Mitchell, E.A.D.: Community development along a proglacial chrono-sequence: are above-ground and below-ground community structure controlled more by biotic than abiotic factors?, *J. Ecol.*, 98, 1084–1095, <https://doi.org/10.1111/j.1365-2745.2010.01699.x>, 2010.
- Caron, M., Rochon, A., Carlos, J., Serrano, M., Onge, G.S.T.: Evolution of sea-surface conditions on the northwestern Greenland margin during the Holocene, *J. Quat. Sci.*, 34, 569–580, <https://doi.org/10.1002/jqs.3146>, 2019.
- Dale, B.: *Dinoflagellate resting cysts: “benthic plankton,” survival strategies of the algae*, Cambridge University Press, 1983.
- Dale, B.: Dinoflagellate contributions to the open ocean sediment flux, in: *Dinoflagellate Contributions to the Deep Sea*, Dale, B., Dale, A.L. (Eds.), *Ocean Biocoenosis Ser.*, 1–31, 1992.
- Dale, B., Dale, A.L.: Dinoflagellate contributions to the sediment flux of the Nordic Seas, in: *Dinoflagellate Contributions to the Deep Sea*, Dale, B., Dale, A.L. (Eds.), *Ocean Biocoenosis Ser.*, 45–75, 1992.
- Dale, B., Dale, A.L., Jansen, J.H.F.: Dinoflagellate cysts as environmental indicators in surface sediments from the Congo deep-sea fan and adjacent regions, *Palaeogeogr. Palaeoclimatol. Palaeoecol.*, 185, 309–338, [https://doi.org/10.1016/S0031-0182\(02\)00380-2](https://doi.org/10.1016/S0031-0182(02)00380-2), 2002.
- de Vernal, A., Marret, F.: Organic-walled dinoflagellate cysts: Tracers of sea-surface conditions, in: *Developments in Marine Geology*, Elsevier B.V., 371–408, [https://doi.org/10.1016/S1572-5480\(07\)01014-7](https://doi.org/10.1016/S1572-5480(07)01014-7), 2007.
- de Vernal, A., Rochon, A., Turon, J.-L., Matthiessen, J.: Organic-walled dinoflagellate cysts: Palynological tracers of sea-surface conditions in middle to high latitude marine environments, *Geobios.*, 30, 905–920, [https://doi.org/10.1016/S0016-6995\(97\)80215-X](https://doi.org/10.1016/S0016-6995(97)80215-X), 1997.
- de Vernal, A., Hillaire-Marcel, C., Turon, J.-L., Matthiessen, J.: Reconstruction of sea-surface temperature, salinity, and sea-ice cover in the northern North Atlantic during the last glacial maximum based on dinocyst assemblages, *Can. J. Earth Sci.*, 37, 725–750, 2000.
- de Vernal, A., Henry, M., Matthiessen, J., Mudie, P.J., Rochon, A., Boessenkool, K., Eynaud, F., Grøsfjeld, K., Guiot, J., Hamel, D., Harland, R., Head, M.J., Kunz-Pirrung, M., Levac, E., Loucheur, V., Peyron, O., Pos-pelova, V., Radi, T., Turon, J.-L., Voronina, E.: Dinoflagellate cyst assemblages as tracers of sea-surface conditions in the northern North Atlantic, Arctic and sub-Arctic seas: the new “n= 677” data base and its application for quantitative palaeoceanographic reconstruction, *J. Quat. Sci.*, 16, 681–698, <https://doi.org/10.1002/jqs.659>, 2001.
- de Vernal, A., Eynaud, F., Henry, M., Hillaire-Marcel, C., Londeix, L., Mangin, S., Matthiessen, J., Marret, F., Radi, T., Rochon, A., Solignac, S., Turon, J.L.: Reconstruction of sea-surface conditions at middle to high latitudes of the Northern Hemisphere during the Last Glacial Maximum (LGM) based on dinoflagellate cyst assemblages, *Quat. Sci. Rev.*, 24, 897–924, <https://doi.org/10.1016/j.quascirev.2004.06.014>, 2005.
- de Vernal, A., Henry, M., Bilodeau, G.: *Micropaleontological preparation techniques and analyses*, *Cahiers du Geotop*, 3, 2010.
- de Vernal, A., Rochon, A., Fréchette, B., Henry, M., Radi, T., Solignac, S.: Reconstructing past sea ice cover of the Northern Hemisphere from dinocyst assemblages: Status of the approach, *Quat. Sci. Rev.*, 79, 122–134, <https://doi.org/10.1016/j.quascirev.2013.06.022>, 2013.
- de Vernal, A., Radi, T., Zaragosi, S., Van Nieuwenhove, N., Rochon, A., Allan, E., De Schepper, S., Eynaud, F., Head, M.J., Limoges, A., Londeix, L., Marret, F., Matthiessen, J., Penaud, A., Pospelova, V., Price, A., Richerol, T.: Percentages of common modern dinoflagellate cyst taxa in surface sediments of the Northern Hemisphere and corresponding environmental parameters, *PANGAEA*,

<https://doi.org/10.1594/PANGAEA.908494>, 2019.

de Vernal, A., Radi, T., Zaragosi, S., Van Nieuwenhove, N., Rochon, A., Allan, E., De Schepper, S., Eynaud, F., Head, M.J., Limoges, A., Londeix, L., Marret, F., Matthiessen, J., Penaud, A., Pospelova, V., Price, A., Richerol, T.: Distribution of common modern dinoflagellate cyst taxa in surface sediments of the Northern Hemisphere in relation to environmental parameters: The new n=1968 database, *Mar. Micropaleontol.*, 159, 101796, <https://doi.org/10.1016/j.marmicro.2019.101796>, 2020.

Dorschel, B., Afanasyeva, V., Bender, M., Dreutter, S., Eisermann, H., Gebhardt, A.C., Hansen, K., Hebbeln, D., Jackson, R.: Past Greenland ice sheet dynamics, palaeoceanography and plankton ecology in the Northeast Baffin Bay - Cruise No. MSM44 "BAFFEAST" - June 30-July 30, 2015 - Nuuk (Greenland), *MARIA S. MERIAN-Berichte*, 51, [https://doi.org/10.2312/cr\\_msm2344](https://doi.org/10.2312/cr_msm2344), 2015.

Dray, S., Chessel, D., Thioulouse, J.: Co-inertia analysis and the linking of ecological data tables, *Ecology*, 84, 3078–3089, <https://doi.org/10.1890/03-0178>, 2003.

Efron, B., Gong, G.: A leisurely look at the bootstrap, the jackknife, and cross-validation, *Am. Stat.*, 37, 36–48, <https://doi.org/10.1080/00031305.1983.10483087>, 1983.

Escofier, B., Pagès, J.: Analyse factorielle multiple, *Cah. du Bur. Univ. Rech. opérationnelle Série Rech.*, 42, 3–68, 1984.

Escofier, B., Pagès, J.: Analyses factorielles simples et multiples: Objectifs, méthodes et interprétation, in: *Analyses factorielles simples et multiples: Objectifs, méthodes et interprétation*, Dunod, Paris, 1990.

Escofier, B., Pagès, J.: Multiple factor analysis (AFMULT package), *Comput. Stat. Data Anal.*, 18, 121–140, [https://doi.org/10.1016/0167-9473\(94\)90135-X](https://doi.org/10.1016/0167-9473(94)90135-X), 1994.

Fensome, R.A., Taylor, F.J.R., Norris, G., Sarjeant, W.A.S., Wharton, D.I., Williams, G.L.: A classification of living and fossil dinoflagellates, *Micropaleontol. Spec. Pap.*, 7, 1–351, 1993.

Fischer, G., Ratmeyer, V., Wefer, G.: Organic carbon fluxes in the Atlantic and the Southern Ocean: Relationship to primary production compiled from satellite radiometer data, *Deep Sea Res. Part II Top. Stud. Oceanogr.*, 47, 1961–1997, [https://doi.org/10.1016/S0967-0645\(00\)00013-8](https://doi.org/10.1016/S0967-0645(00)00013-8), 2000.

Gibb, O.T., Steinhauer, S., Frechette, B., de Vernal, A., Hillaire-Marcel, C.: Diachronous evolution of sea surface conditions in the Labrador Sea and Baffin Bay since the last deglaciation, *The Holocene*, 25, 1882–1897, <https://doi.org/10.1177/0959683615591352>, 2015.

Guiot, J., Gally, Y.: R Package: bioindic, 2014.

Head, M.J.: Modern dinoflagellate cysts and their biological affinities, in: *Palynology: Principles and Applications*, Jansonius, J., McGregor, D.C. (Eds.), American Association of Stratigraphic Palynologists Foundation, 1197–1248, 1996.

Hernández-Almeida, I., Cortese, G., Chen, M.-T., Kucera, M.: Environmental determinants of radiolarian assemblages in the western Pacific since the last deglaciation, *Paleoceanography*, 32, 830–847, <https://doi.org/10.1002/2017PA003159>, 2017.

Hohmann, S., Kucera, M., de Vernal, A.: Identifying the signature of sea-surface properties in dinocyst assemblages: Implications for quantitative palaeoceanographical reconstructions by transfer functions and analogue techniques, *Mar. Micropaleontol.*, 159, 101816, <https://doi.org/https://doi.org/10.1016/j.marmicro.2019.101816>, 2020.

Holzwarth, U., Esper, O., Zonneveld, K.A.F.: Distribution of organic-walled dinoflagellate cysts in shelf surface sediments of the Benguela upwelling system in relationship to environmental conditions, *Mar. Micropaleontol.*, 64, 91–119, <https://doi.org/10.1016/j.marmicro.2007.04.001>, 2007.

Imbrie, J., Kipp, N.G.: A new micropaleontological method for quantitative paleoclimatology: Application to a late Pleistocene Caribbean core, in: *The Late Cenozoic Glacial Ages*, Turekian, K.K. (Ed.), Yale University Press, New Haven, 71–181, 1971.

Josse, J., Pagès, J., Husson, F.: Testing the significance of the RV coefficient, *Comput. Stat. Data Anal.*, 53, 82–91, <https://doi.org/10.1016/j.csda.2008.06.012>, 2008.

Juggins, S.: *Rioja: Analysis of Quaternary science data*, 2017.

Kassambara, A., Mundt, F.: *Factoextra: Extract and visualize the results of multivariate data analyses*, R package version, 1, 2017.

- Kaufman, D., McKay, N., Routson, C., Erb, M., Dätwyler, C., Sommer, P.S., Heiri, O., Davis, B.: Holocene global mean surface temperature, a multi-method reconstruction approach, *Sci. Data*, 7, 201, <https://doi.org/10.1038/s41597-020-0530-7>, 2020.
- Koc, N., Jansen, E., Hafliðason, H.: Paleooceanographic reconstruction of surface ocean conditions in the Greenland, Iceland, and Norwegian seas through the last 14,000 years based on diatoms, *Quat. Sci. Rev.*, 12, 115–140, [https://doi.org/10.1016/0277-3791\(93\)90012-B](https://doi.org/10.1016/0277-3791(93)90012-B), 1993.
- Kokinos, J.P., Eglinton, T.I., Gon, M.A.: Characterization of a highly resistant biomacromolecular material in the cell wall of a marine dinoflagellate resting cyst, *Organic*, 28, 265–288, [https://doi.org/10.1016/S0146-6380\(97\)00134-4](https://doi.org/10.1016/S0146-6380(97)00134-4), 1998.
- Kucera, M., Weinelt, M., Kiefer, T., Pflaumann, U., Hayes, A., Weinelt, M., Chen, M., Mix, A.C., Barrows, T.T., Cortijo, E., Duprat, J., Juggins, S., Waelbroeck, C.: Reconstruction of sea-surface temperatures from assemblages of planktonic foraminifera: multi-technique approach based on geographically constrained calibration data sets and its application to glacial Atlantic and Pacific Oceans, *Quat. Sci. Rev.*, 24, 951–998, <https://doi.org/10.1016/j.quascirev.2004.07.014>, 2005.
- Lamentowicz, M., Lamentowicz, Ł., van der Knaap, W.O., Gabka, M., Mitchell, E.A.D.: Contrasting species-environment relationships in communities of testate amoebae, bryophytes and vascular plants along the Fen-Bog gradient, *Environ. Microbiol.*, 59, 499–510, <https://doi.org/10.1007/s00248-009-9617-6>, 2010.
- Lê, S., Josse, J., Husson, F.: FactoMineR: An R package for multivariate analysis, *J. Stat. Softw.*, 25, 1–18, <https://doi.org/10.18637/jss.v025.i01>, 2008.
- Legendre, P., Gallagher, E.D.: Ecologically meaningful transformations for ordination of species data, *Oecologia*, 129, 271–280, <https://doi.org/10.1007/s004420100716>, 2001.
- Lepš, J., Šmilauer, P. (Eds.): *Multivariate analysis of ecological data using CANOCO*, Cambridge university press, 2003.
- Levac, E., De Vernal, A., Blake, W.: Sea-surface conditions in northernmost Baffin Bay during the Holocene: Palynological evidence, *J. Quat. Sci.*, 16, 353–363, <https://doi.org/10.1002/jqs.614>, 2001.
- Lopes, C., Mix, A.C., Abrantes, F.: Environmental controls of diatom species in northeast Pacific sediments, *Palaeogeogr. Palaeoclimatol. Palaeoecol.*, 297, 188–200, <https://doi.org/10.1016/j.palaeo.2010.07.029>, 2010.
- Marcott, S.A., Shakun, J.D., Clark, P.U., Mix, A.C.: A Reconstruction of regional and global temperature for the past 11,300 years, *Science*, 339, 1198–1201, <https://doi.org/10.1126/science.1228026>, 2013.
- Marret, F.: Les effets de l'acétytolysé sur les assemblages de kystes de dinoflagelle's, *Palynosciences*, 2, 267–272, 1993.
- Matthiessen, J.: Distribution patterns of dinoflagellate cysts and other organic-walled microfossils in recent Norwegian-Greenland Sea sediments, *Mar. Micropaleontol.*, 24, 307–334, [https://doi.org/10.1016/0377-8398\(94\)00016-G](https://doi.org/10.1016/0377-8398(94)00016-G), 1995.
- Matthiessen, J., Baumann, K.H., Schröder-Ritzrau, A., Hass, C., Andruleit, H., Baumann, A., Jensen, S., Kohly, A., Pflaumann, U., Samtleben, C., Schäfer, P., Thiede, J.: Distribution of calcareous, siliceous and organic-walled planktic microfossils in surface sediments of the Nordic Seas and their relation to surface-water masses, in: *The Northern North Atlantic*, Schäfer, P., Ritzrau, W., Schlüter, M., Thiede, J. (Eds.), Springer, Berlin Heidelberg, 105–127, [https://doi.org/10.1007/978-3-642-56876-3\\_7](https://doi.org/10.1007/978-3-642-56876-3_7), 2001.
- McGarigal, K., Stafford, S., Cushman, S.: Discriminant analysis, in: *Multivariate statistics for wildlife and ecology research*, Springer, New York, 129–187, [https://doi.org/10.1007/978-1-4612-1288-1\\_4](https://doi.org/10.1007/978-1-4612-1288-1_4), 2000.
- Meyers, P.A.: Organic geochemical proxies of paleoceanographic, paleolimnologic, and paleoclimatic processes, *Org. Geochem.*, 27, 213–250, [https://doi.org/https://doi.org/10.1016/S0146-6380\(97\)00049-1](https://doi.org/https://doi.org/10.1016/S0146-6380(97)00049-1), 1997.
- Montresor, M., Sgroso, S., Procaccini, G., Wiebe, H.C.F.: Intraspecific diversity in *Scrippsiella trochoidea* (Dino-pbyceae): evidence for cryptic species, *Phycologia*, 42, 56–70, <https://doi.org/10.2216/i0031-8884-42-1-56.1>, 2003.

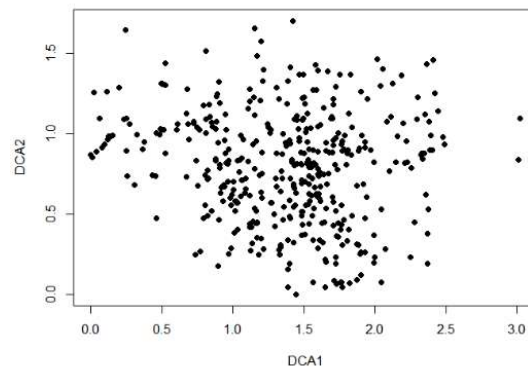
- Morey, A.E., Mix, A.C., Pisias, N.G.: Planktonic foraminiferal assemblages preserved in surface sediments correspond to multiple environment variables, *Quat. Sci. Rev.*, 24, 925–950, <https://doi.org/10.1016/j.quascirev.2003.09.011>, 2005.
- Mudie, P.J.: Circum-Arctic Quaternary and Neogene marine palynofloras: paleoecology and statistical analysis, *Neogene Quat. Dinoflag. cysts acritarchs*, 10, 347–390, 1992.
- Muller, P.J., Erlenkeuser, H., Von Grafenstein, R.: Glacial-interglacial cycles in oceanic productivity inferred from organic carbon contents in eastern north Atlantic sediment cores, in: *Coastal upwelling, its sediment record, part B: Sedimentary records of ancient coastal upwelling*, Thiede J., Suess, E. (Ed.), Plenum Press, New York, 65–398, 1983.
- Nooteboom, P.D., Bijl, P.K., Sebille, E. Van, Heydt, A.S. Von Der, Dijkstra, H.A.: Transport bias by ocean currents in sedimentary microplankton assemblages: Implications for paleoceanographic reconstructions, *Paleogeography and Paleoclimatology*, 34, 1178–1194, <https://doi.org/10.1029/2019PA003606>, 2019.
- Nychka, D., Furrer, R., Sain, S.: *fields: Tools for spatial data*, <https://doi.org/10.5065/D6W957CT>, 2017.
- Oksanen, J., Blanchet, F.G., Friendly, M., Kindt, R., Legendre, P., McGlinn, D., Minchin, P.R., O'Hara, R.B., Simpson, G.L., Solymos, P., Stevens, M.H.H., Szoecs, E., Wagner, H.: *Vegan: Community ecology package (version 2.5-6)*, The Comprehensive R Archive Network, 2019.
- Ouellet-Bernier, M.M., de Vernal, A., Hillaire-Marcel, C., Moros, M.: Paleocceanographic changes in the Disko Bugt area, West Greenland, during the Holocene, *Holocene*, 24, 1573–1583, <https://doi.org/10.1177/0959683614544060>, 2014.
- Parkinson, J.E., Baumgarten, S., Michell, C.T., Baums, I.B., Lajeunesse, T.C., Voolstra, C.R.: Gene expression variation resolves species and individual strains among coral-associated dinoflagellates within the genus *Symbiodinium*, *Genome Biol. Evol.*, 8, 665–680, <https://doi.org/10.1093/gbe/evw019>, 2016.
- Pebesma, E.J.: Multivariable geostatistics in S: the gstat package, *Comput. Geosci*, 30, 683–691, <https://doi.org/10.1016/j.cageo.2004.03.012>, 2004.
- Pebesma, E.J., Bivand, R.S.: S classes and methods for spatial data: the sp package, *R news*, 5, 9–13, 2005.
- Price, A.M., Pospelova, V., Coffin, M.R.S., Latimer, J.S., Chmura, G.L.: Biogeography of dinoflagellate cysts in northwest Atlantic estuaries, *Ecol. Evol.*, 6, 5648–5662, <https://doi.org/10.1002/ece3.2262>, 2016.
- Price, A.M., Baustian, M.M., Turner, R.E., Rabalais, N.N., Chmura, G.L.: Dinoflagellate cysts track eutrophication in the Northern Gulf of Mexico, *Estuaries and Coasts*, 41, 1322–1336, <https://doi.org/10.1007/s12237-017-0351-x>, 2018.
- R Core Team: *R: A language and environment for statistical computing*, 2017.
- Radi, T., de Vernal, A.: Dinocyst distribution in surface sediments from the northeastern Pacific margin (40–60°N) in relation to hydrographic conditions, productivity and upwelling, *Rev. Palaeobot. Palynol.*, 128, 169–193, [https://doi.org/10.1016/S0034-6667\(03\)00118-0](https://doi.org/10.1016/S0034-6667(03)00118-0), 2004.
- Radi, T., de Vernal, A.: Dinocysts as proxy of primary productivity in mid-high latitudes of the Northern Hemisphere, *Mar. Micropaleontol.*, 68, 84–114, <https://doi.org/10.1016/j.marmicro.2008.01.012>, 2008.
- Radi, T., de Vernal, A., Peyron, O.: Relationships between dinoflagellate cyst assemblages in surface sediment and hydrographic conditions in the Bering and Chukchi seas, *J. Quat. Sci.*, 16, 667–680, <https://doi.org/10.1002/jqs.652>, 2001.
- Rao, C.R.: A review of canonical coordinates and an alternative to correspondence analysis using Hellinger distance, *Questiú*, 19, 23–63, 1995.
- Ribeiro, S., Amorim, A.: Environmental drivers of temporal succession in recent dinoflagellate cyst assemblages from a coastal site in the North-East Atlantic (Lisbon Bay, Portugal), *Mar. Micropaleontol.*, 68, 156–178, <https://doi.org/10.1016/j.marmicro.2008.01.013>, 2008.
- Robert, P., Escoufier, Y.: A unifying tool for linear multivariate statistical methods: The RV-coefficient, *Appl. Stat.*, 25, 257–265, <https://doi.org/10.2307/2347233>, 1976.

- Rochon, A., de Vernal, A.: Palynomorph distribution in recent sediments from the Labrador Sea, *Can. J. Earth Sci.*, 31, 115–127, <https://doi.org/10.1139/e94-010>, 1994.
- Rochon, A., de Vernal, A., Turon, J.-L., Matthießen, J., Head, M.J.: Distribution of recent dinoflagellate cysts in surface sediments from the North Atlantic Ocean and adjacent seas in relation to sea-surface, *Am. Assoc. Stratigr. Palynol. Contrib. Ser.*, 35, 1–164, <https://doi.org/10013/epic.14283>, 1999.
- Rochon, A., Eynaud, F., de Vernal, A.: Dinocysts as tracers of hydrographical conditions and productivity along the ocean margins: Introduction, *Mar. Micropaleontol.*, 68, 1–5, <https://doi.org/10.1016/j.marmicro.2008.04.001>, 2008.
- Rühlemann, C., Müller, P.J., Schneider, R.R.: Organic carbon and carbonate as paleoproductivity proxies: Examples from high and low productivity areas of the tropical Atlantic, in: *Use of proxies in paleoceanography: Examples from the South Atlantic*, Fischer, G., Wefer, G. (Eds.), Springer, Berlin Heidelberg, 315–344, [https://doi.org/10.1007/978-3-642-58646-0\\_12](https://doi.org/10.1007/978-3-642-58646-0_12), 1999.
- Saini, J., Stein, R., Fahl, K., Weiser, J., Hebbeln, D., Hillaire, C., de Vernal, A.: Holocene variability in sea ice and primary productivity in the northeastern Baffin Bay, Arktos, <https://doi.org/10.1007/s41063-020-00075-y>, 2020.
- Sarnthein, M., Winn, K., Duplessy, J.-C., Fontugne, M.R.: Global variations of surface ocean productivity in low and mid latitudes: Influence on CO<sub>2</sub> reservoirs of the deep ocean and atmosphere during the last 21,000 years, *Paleoceanography*, 3, 361–399, <https://doi.org/10.1029/PA003i003p00361>, 1988.
- Schlitzer, R.: Ocean Data View, [odv.awi.de](http://odv.awi.de), 2018.
- Schröder-Adams, C.J., van Rooyen, D.: Response of recent benthic foraminiferal assemblages to contrasting environments in Baffin Bay and the northern Labrador Sea, Northwest Atlantic, Arctic, 64, 317–341, <https://doi.org/10.14430/arctic4122>, 2011.
- Seidenkrantz, M.S., Aagaard-Sørensen, S., Sulsbrück, H., Kuijpers, A., Jensen, K.G., Kunzendorf, H.: Hydrography and climate of the last 4400 years in a SW Greenland fjord: Implications for Labrador Sea palaeoceanography, *Holocene*, 17, 387–401, <https://doi.org/10.1177/0959683607075840>, 2007.
- Sha, L., Jiang, H., Seidenkrantz, M.S., Knudsen, K.L., Olsen, J., Kuijpers, A., Liu, Y.: A diatom-based sea-ice reconstruction for the Vaigat Strait (Disko Bugt, West Greenland) over the last 5000 yr, *Palaeogeogr. Palaeoclimatol. Palaeoecol.*, 403, 66–79, <https://doi.org/10.1016/j.palaeo.2014.03.028>, 2014.
- Taylor, F.J.R., Pollinger, U.: The ecology of dinoflagellate, in: *The biology of dinoflagellates*, Taylor, F.J.R. (Ed.), Blackwell Scientific Publications, Oxford, 398–529, 1987.
- Telford, R.J.: palaeoSig: Significance tests of quantitative palaeoenvironmental reconstructions, R package version, 1, 2015.
- Telford, R.J., Birks, H.J.B.: The secret assumption of transfer functions: Problems with spatial autocorrelation in evaluating model performance, *Quat. Sci. Rev.*, 24, 2173–2179, <https://doi.org/10.1016/j.quascirev.2005.05.001>, 2005.
- Telford, R.J., Birks, H.J.B.: Evaluation of transfer functions in spatially structured environments, *Quat. Sci. Rev.*, 28, 1309–1316, <https://doi.org/10.1016/j.quascirev.2008.12.020>, 2009.
- Telford, R.J., Birks, H.J.B.: A novel method for assessing the statistical significance of quantitative reconstructions inferred from biotic assemblages, *Quat. Sci. Rev.*, 30, 1272–1278, <https://doi.org/10.1016/j.quascirev.2011.03.002>, 2011.
- ter Braak, C.J.F.: Canonical correspondence analysis: A new eigenvector technique for multivariate direct gradient analysis, *Ecology*, 67, 1167–1179, <https://doi.org/10.2307/1938672>, 1986.
- ter Braak, C.J.F.: Ordination, in: *Data analysis in community and landscape ecology*, Jongman, R.H., ter Braak, C.J.F., van Tongeren, O.F.R. (Eds.), Center for Agricultural Publishing and Documentation, Wageningen, The Netherlands, 91–169, 1987.
- Trachsel, M., Telford, R.J.: Technical note: Estimating unbiased transfer-function performances in spatially structured environments, *Clim. Past*, 12, 1215–1223, <https://doi.org/10.5194/cp-12-1215-2016>, 2016.
- Turner, J.T.: Zooplankton fecal pellets, marine snow, phytodetritus and the ocean's biological pump, *Prog. Oceanogr.*, 130, 205–248, <https://doi.org/10.1016/j.pocean.2014.08.005>, 2015.

- Turner, J.T.: Zooplankton fecal pellets, marine snow and sinking phytoplankton blooms, *Aquat. Microb. Ecol.*, 27, 57–102, <https://doi.org/10.3354/ame027057>, 2002.
- van Nieuwenhove, N., Head, M.J., Limoges, A., Pospelova, V., Mertens, K.N., Matthiessen, J., De Schepper, S., de Vernal, A., Eynaud, F., Londeix, L., Marret, F., Penaud, A., Radi, T., Rochon, A.: An overview and brief description of common marine organic-walled dinoflagellate cyst taxa occurring in surface sediments of the Northern Hemisphere, *Mar. Micropaleontol.*, 159, 101814, <https://doi.org/10.1016/j.marmicro.2019.101814>, 2020.
- Wall, D., Dale, B.: Modern dinoflagellate cysts and evolution of the Peridinales, *Micropaleontology*, 14, 265–304, 1968.
- Wang, N., Mertens, K.N., Krock, B., Luo, Z., Derrien, A., Pospelova, V., Liang, Y., Bilien, G., Smith, K.F., De Schepper, S., Wietkamp, S., Tillmann, U., Gu, H.: Cryptic speciation in *Protoceratium reticulatum* (Dinophyceae): Evidence from morphological, molecular and ecophysiological data, *Harmful Algae*, 88, 101610, <https://doi.org/10.1016/j.hal.2019.05.003>, 2019.
- Wigley, T.M.L., Ingram, M.J., Farmer, G.: Past climates and their impact on man: A review, in: *Climate and History*, Cambridge University Press, New York, 3–50, 1981.
- Zamelczyk, K., Rasmussen, T.L., Husum, K., Hafliðason, H., de Vernal, A., Ravna, E.K., Hald, M., Hillaire-Marcel, C.: Paleoceanographic changes and calcium carbonate dissolution in the central Fram Strait during the last 20 ka, *Quat. Res.*, 78, 405–416, <https://doi.org/10.1016/j.yqres.2012.07.006>, 2012.
- Zonneveld, K.A.F., Siccha, M.: Dinoflagellate cyst based modern analogue technique at test - A 300 year record from the Gulf of Taranto (Eastern Mediterranean), *Palaeogeogr. Palaeoclimatol. Palaeoecol.*, 450, 17–37, <https://doi.org/10.1016/j.palaeo.2016.02.045>, 2016.
- Zonneveld, K.A.F., Versteegh, G.J.M., de Lange, G.J.: Preservation of organic-walled dinoflagellate cysts in different oxygen regimes: a 10,000 year natural experiment, *Mar. Micropaleontol.*, 29, 393–405, [https://doi.org/10.1016/S0377-8398\(96\)00032-1](https://doi.org/10.1016/S0377-8398(96)00032-1), 1997.
- Zonneveld, K.A.F., Versteegh, G., Kodrans-Nsiah, M.: Preservation and organic chemistry of Late Cenozoic organic-walled dinoflagellate cysts: A review, *Mar. Micropaleontol.*, 68, 179–197, <https://doi.org/10.1016/j.marmicro.2008.01.015>, 2008.
- Zonneveld, K.A.F., Versteegh, G.J.M., Kasten, S., Eglinton, T.I., Emeis, K., Huguet, C., Koch, B.P.: Selective preservation of organic matter in marine environments; processes and impact on the sedimentary record, *Biogeosciences*, 7, 483–511, <https://doi.org/10.5194/bg-7-483-2010>, 2010.
- Zonneveld, K.A.F., Gray, D., Kuhn, G., Versteegh, G.J.M.: Postdepositional aerobic and anaerobic particulate organic matter degradation succession reflected by dinoflagellate cysts: The Madeira Abyssal Plain revisited, *Mar. Geol.*, 408, 87–109, <https://doi.org/10.1016/j.margeo.2018.11.010>, 2019.

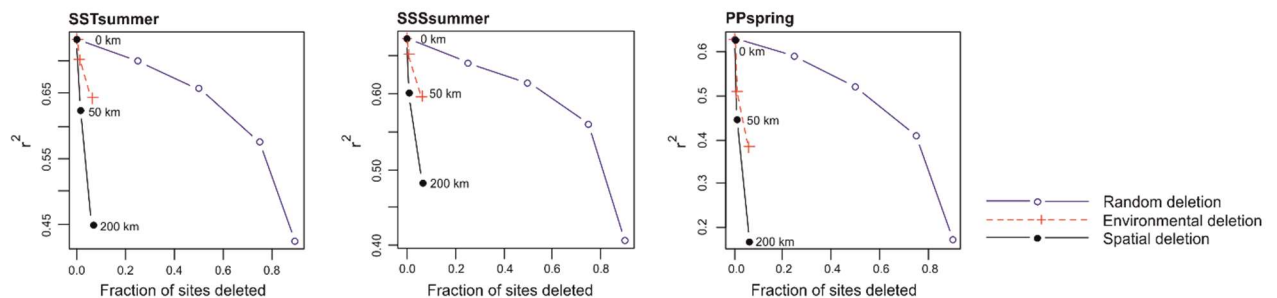
## 4.9 Supplementary material

**Dataset S4.1:** Dataset containing matrices of the local calibration dataset (n=421) including coordinates, taxa abundances and tested environmental variables (Excel-file). The dataset can be found at: will be available with publication.



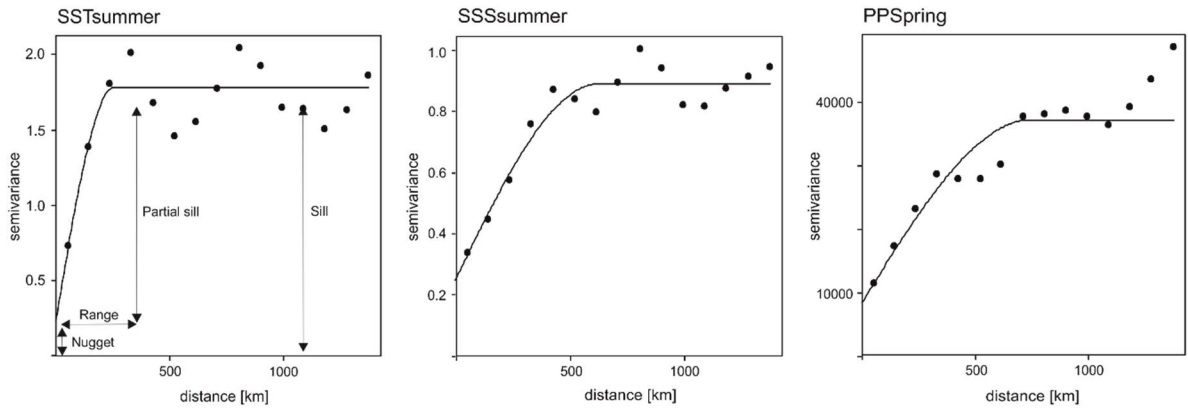
**Figure S4.2:** DCA analysis plot for the local dataset.

**Script S4.3:** R-Script explaining the variable selection procedure (manual forward selection) extricating independent variables in the local dataset (PDF-file). The script can be found at: will be available with publication.

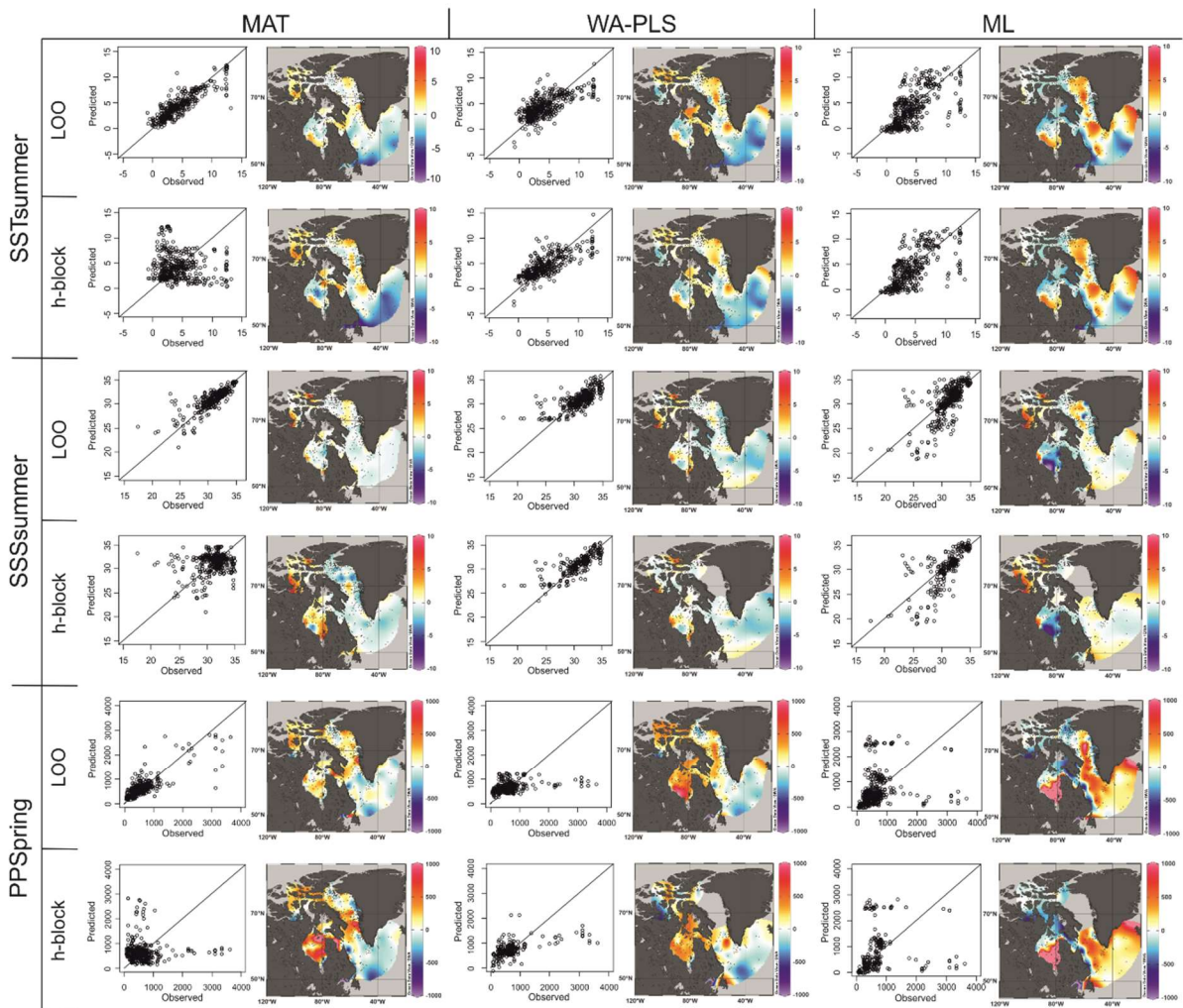


**Figure S4.4:** Spatial autocorrelation test. The effect of site deletion on the performance of a test transfer function (leaving-one-out  $r^2$  between observed and predicted values), comparing random site deletion, neighbourhood deletion (testing three distances) and environmental deletion for non-redundant variables. Note that the scale for  $r^2$  is different for each tested variable depending on its performance at the beginning.

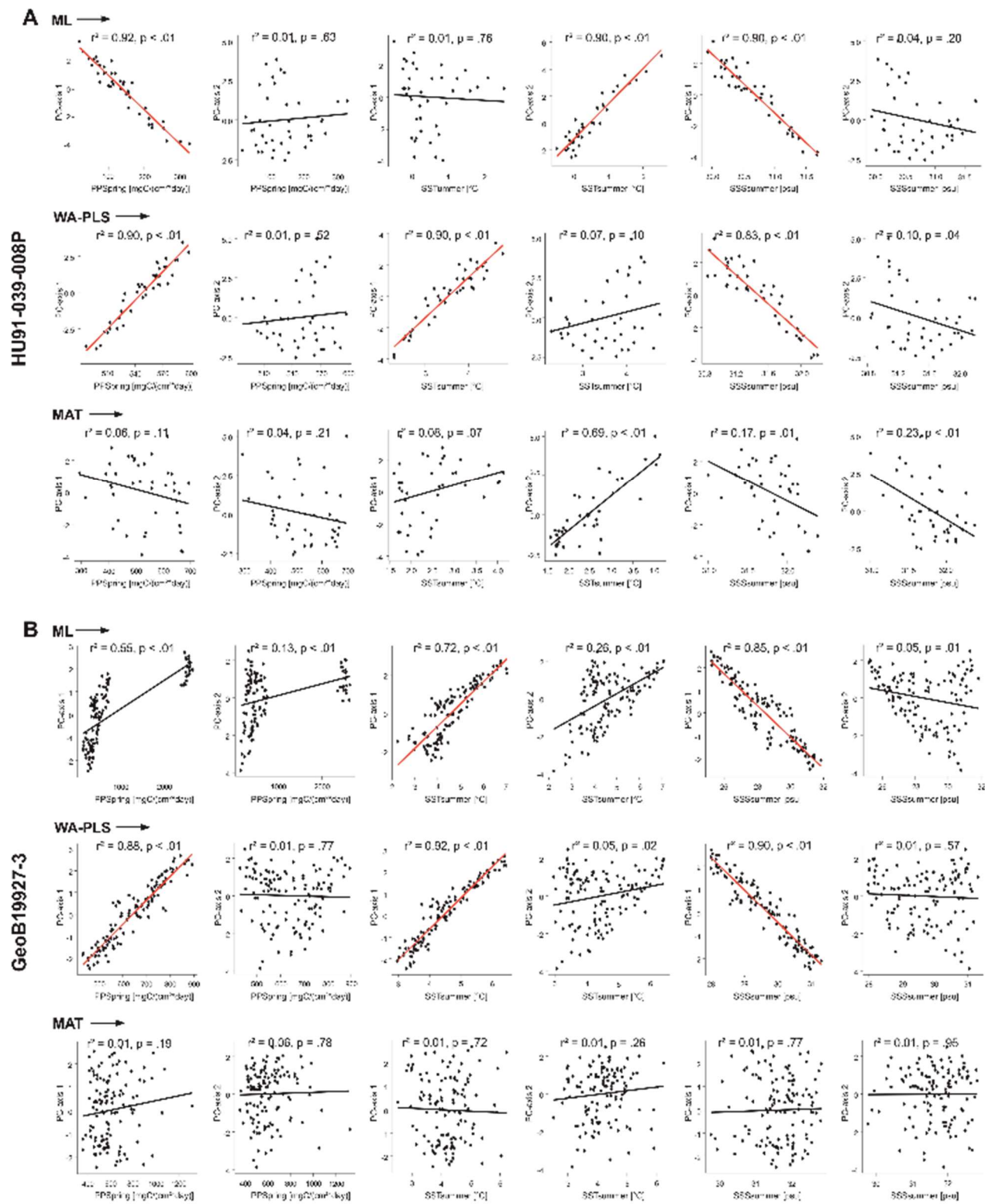




**Figure S4.5:** Variogram plots for the estimation of  $h$  in the  $h$ -block cross-validation.



**Figure S4.6:** Residuals from leave-one-out and  $h$ -block cross-validation for all tested transfer functions shown in cross-plots of predicted vs. observed environmental variables and in maps, indicating overestimation through red colours and underestimation through blue colours. White colour indicates none or little residuals.



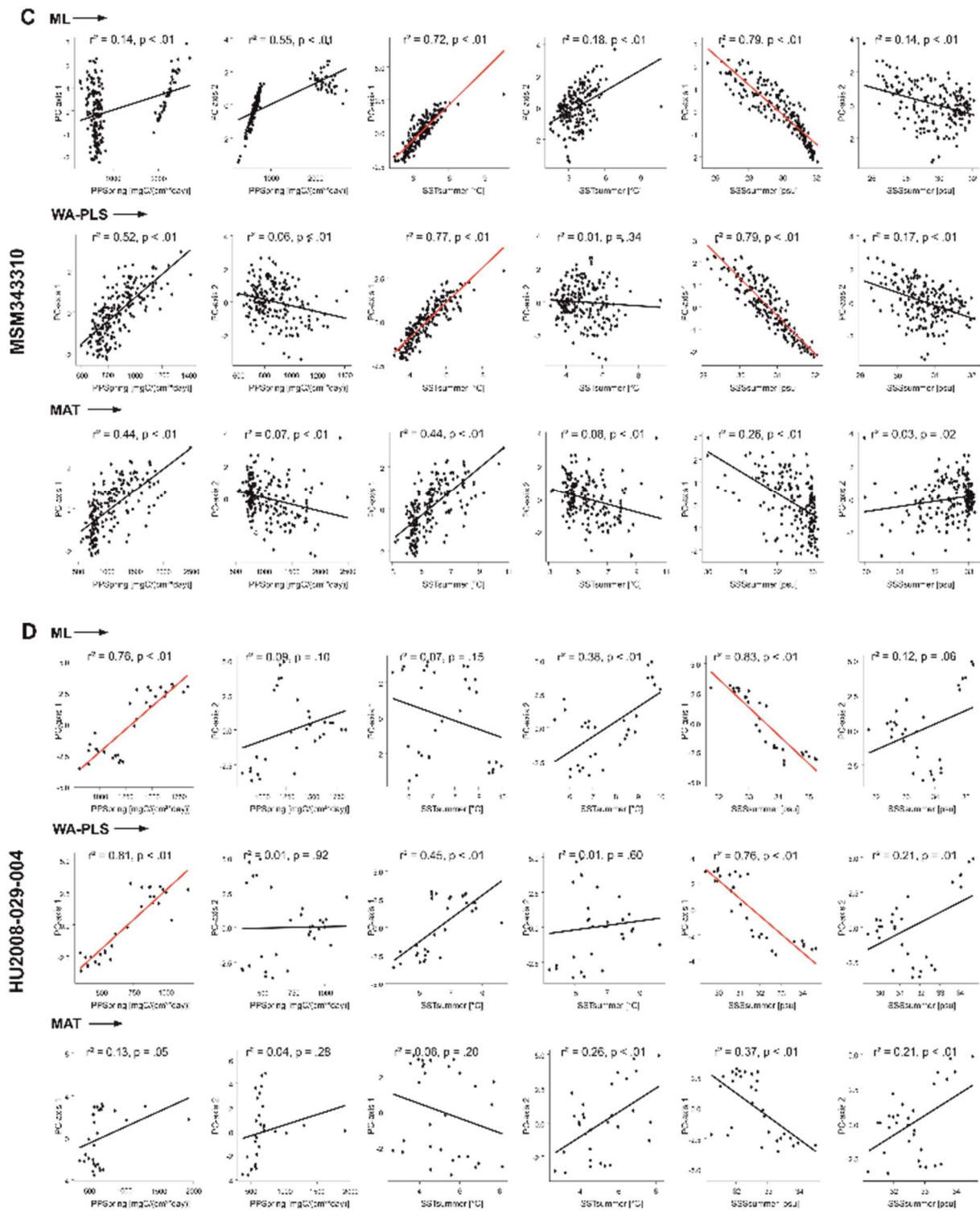


**Figure S4.7:** Correlation plots of downcore reconstructions vs PC-axis 1 and PC-axis 2 for all four cores from north to further south. a) HU91-039-008P, b) GeoB19927-3, c) MSM343310 and d) HU2008-029-004. Significant correlations with  $p \leq .01$  and  $r^2 \geq 0.70$  with red correlation line.

# Chapter 5

## **Holocene biogenic carbon production and deposition on the West Greenland margin of the Baffin Bay (Manuscript III)**

Sabrina Hohmann<sup>1\*</sup>, Michal Kucera<sup>1</sup>, Anne de Vernal<sup>2</sup>

<sup>1</sup>MARUM – Center for Marine Environmental Sciences, University of Bremen, Leobener Straße 8, D-28359 Bremen, Germany

<sup>2</sup>Centre Geotop, Université du Québec à Montréal, Geotop-UQAM, C.P. 8888, Succ. Centre-Ville, Montréal, QC, H3C 3P8, Canada

Submission planned to *Paleoceanography* in 2023

### **Abstract**

Understanding natural responses of processes driving the marine biological pump to the recent accelerating reduction in sea ice cover and ice sheet extent in the Arctic and Greenland areas is essential to advance model projections for future developments. Here, we used a middle to late Holocene sediment record of centennial-scale resolution from a sediment core (GeoB19927-3) of Baffin Bay (73°35.26' N, 58°05.66' W) as an equivalent for a warmer climate in the future. The record combines micropalaeontological counts (dinocysts, foraminifers), biomarkers (IP<sub>25</sub>, dinosterol, brassicasterol,  $\beta$ -sitosterol, campesterol), and bulk geochemical parameters (TOC, CaCO<sub>3</sub>). We compare estimates of marine primary productivity, export productivity, carbon burial, carbonate preservation and terrigenous input with reconstructed environmental parameters including sea-ice cover, sea surface salinity and sea surface temperature, with the aim to evaluate marine biological productivity processes happening within the biological carbon pump in the light of a changing environment. We show that the effect of interglacial warming continues until ~1.5 ka in Melville Bay. Continuous melt from land ice and reduction in sea-ice cover and sea surface salinity and increase in sea surface temperature characterised the study area until this time and led to an increase in primary productivity of about 65% and a decrease in organic carbon burial of about 89%. The increase in primary productivity is likely associated with a longer growing season due to sea-ice cover

reduction, meltwater-induced upwelling conditions and stronger surface water stratification. The decoupling between primary productivity and burial of marine organic carbon seems to be caused by changes in export efficiency, induced by a combination of an increase in the efficiency of organic matter recycling in the productive zone and a decrease in preservation due to longer oxygen exposure times induced by low sedimentation rates. Our results suggest a weakening of the marine organic carbon pump under meltwater-influenced warming conditions.

## 5.1 Introduction

Polar regions in the Northern Hemisphere, especially the Arctic Ocean and Greenland areas, are undergoing dramatic changes due to an accelerating reduction in sea ice cover and ice sheet extent for the past three to four decades supposedly due to the rising anthropogenic input of carbon dioxide (CO<sub>2</sub>) into the atmosphere (Kinnard et al., 2011; NSIDC, 2018). This has led to growing concerns about possible effects on the marine carbon cycle (e.g. Jones et al. 1987, IPCC 2013) as bio-production in the upper ocean, being a main driver of the cycle and accounting for about half of the global biosphere productivity, is largely affected by sea-ice cover reduction and the amount of dissolved carbon dioxide in the ocean water (Field et al., 1998; Behrenfeld et al., 2001).

The photosynthetic activity of marine algae fixes the dissolved CO<sub>2</sub> in the oceans, originating from the atmosphere, into biomass. After death, the remnants of marine microorganisms sink through the water column, transferring carbon from the upper waters to the deeper ocean. A fraction of this biomass is re-mineralised, and another fraction is buried in the sediment (Falkowski et al., 1998). Only a small amount of the organic matter produced in the surface ocean is thus exported to the deep ocean. Organic particles are mostly remineralised into inorganic forms within the upper 1000 m of the water column (Heinze et al., 1991). Remainders of the particle flux, however, that are not subject to degradation or dissolution within the water column, are incorporated in marine sediments. There, the material undergoes remineralisation in the sediment surface layers due to microbial oxidation or dissolution. Only about 0.4% to 1% of the material is subjected to burial and can be stored for millennia (Field et al., 1998; Behrenfeld et al., 2001; Ducklow et al., 2001). The efficiency of this process, known as the marine biological pump, may vary among ocean regions, geological timescales and hence environmental conditions (Raven and Falkowski, 1999; Lutz et al., 2002). As the biological pump plays a significant role for the marine carbon reservoir that withdraws and releases carbon dioxide from and into the atmosphere, alterations of its processes may affect the global carbon cycle (Berger et al., 1989; Sabine et al., 2004).

Arctic marine biological productivity was predominantly affected by changes in sea-ice cover duration (e.g. IPCC, 2013) prior to the last decades, during which nutrient supply becomes more important (Ardyna and Arrigo, 2020; Lewis et al., 2020; Randelhoff et al., 2020). Sea-ice cover duration has a profound effect on productivity as it controls light distribution and the timing of nutrient release to surface-water when it melts (e.g. Meir, 2011).

Given the magnitude of the ongoing reduction in the sea-ice cover in Arctic Ocean, subarctic seas and Greenland areas, information on its impact on biological productivity patterns over longer time scales is important. Ongoing changes in the sea-ice regime have profound effects on both the abundance and the species composition of Arctic microorganism communities (Loeng et al., 2005; Smetacek and Nicol, 2005; Tremblay et al., 2009; Arrigo, 2013; Boetius et al., 2013; Nöthig et al., 2015). This may have consequences for primary productivity patterns and hence the efficiency of the biological pump (Gradinger, 1995; Arrigo et al., 2008; Pabi et al., 2008; Kahru et al., 2011; Bélanger et al., 2013; Arrigo and van Dijken, 2015; Tremblay et al., 2015; Ardyna and Arrigo, 2020; Lewis et al., 2020; Randelhoff et al., 2020).

Understanding the responses of biological productivity, carbon export and carbon burial to changing environmental conditions in Arctic regions is essential for the testing of predictive Earth's system models to assess the future fate of the Arctic marine carbon reservoir and its consequences for the global carbon cycle.

Biogeochemical models can be used to predict future changes of the marine carbon cycle. However, their expediency depends on how they calculate primary and export productivity and remineralisation (Passow and Carlson, 2012). These models assume that changes in primary productivity, export productivity, and carbon burial in ocean sediments covary. Lopes et al. (2015) however, demonstrated that these processes are significantly decoupled under scenarios of large-scale climate change, implying the requirement for independent indicators to compare the state of photosynthesising plankton, export of carbon to the sea floor and rates of carbon burial in the sediment.

The geological sediment record provides an opportunity to assess the natural sensitivity of the biological pump to changing environmental conditions by posing the possibility to quantifying past parameters driving the biological pump under changing physical conditions in the past. The past may serve as an example to estimate the direction and magnitude of possible future developments. For the recent environmental changes leading to a warmer climate, the Holocene geological record may serve as an equivalent.

Marine microfossils from sediment sequences as tracers for past environmental conditions is a commonly used tool in palaeoceanography. Next to analyses of the chemical and isotopic



signals locked in microfossils skeletons, quantitative analyses of changes in the taxonomic composition of microfossil assemblages by means of ecological models is a widely used tool in palaeoceanography since Imbrie & Kipp (1971). Changes in bioproductivity related to sea-ice cover variability during the Holocene have been documented by several studies using microfossil tracers (e.g. de Vernal et al., 2000; Levac et al., 2001; de Vernal et al., 2013).

During the Holocene the eastern Baffin Bay and western coast off Greenland recorded a high variability of sea-ice cover duration, likely in response to changes in ocean circulation and interaction with the surrounding Greenland Ice Sheet (GIS) (e.g. Knudsen et al., 2008; Perner et al., 2013). The East Greenland Current (EGC) flows southward carrying cold polar waters along eastern Greenland, supplying the West Greenland Current (WGC) from the south. The Irminger Current (IC) transports warmer and saltier Atlantic waters northward into the Baffin Bay (Buch, 1981) (Fig. 5.1). The interaction of the colder EGC and the warmer IC feeding the WGC with the GIS meltwater discharge and cold Arctic water inflow from the North collectively affect local sea ice conditions and thus the light supply for surface waters.

While data from marine sediment cores indicate that ocean conditions in the Baffin Bay have been highly variable on millennial to decadal time scales (Briner et al., 2016) and data from satellites reveal a decrease in sea-ice over the last 50 years (Walsh and Chapman, 2001), the impact of changing ocean conditions on productivity and thus the local ecosystem still needs to be documented.

The West Greenland shelf area contains high-resolution sedimentary archives (Dorschel et al., 2016) providing the opportunity to assess the natural variability of marine biological productivity processes during the last millennia. In the present study, we reconstruct driving parameters of the biological carbon pump from a Holocene sediment core from Southern Melville Bay (GeoB19927-3), located in eastern Baffin Bay. In this region a shift toward modern postglacial conditions with warmer surface and sea-surface conditions occurred around 7.6 ka (e.g., Perner et al., 2013; Ouellet-Bernier et al., 2014; Jennings et al., 2014; Gibb et al., 2015; Caron et al., 2019). The coring site is located optimally to record changes in environmental conditions as an effect of the onset of the interglacial warming. It offers a high resolution and a continuous sedimentation (Dorschel et al., 2016). High-resolution radiocarbon-based chronology, organic biomarker proxies of sea-ice and bulk parameters are available from Saini et al. (2020).

Here, we estimated primary productivity, export productivity and carbon burial using independent indicators accounting for their potential decoupling as demonstrated by Lopes et al. (2015). We assess annual primary productivity (PP) quantitatively based on the assemblages of organic-walled dinoflagellate cysts (dinocysts) applying a local transfer

function developed in Hohmann et al. (2023). We estimate export productivity (EP) from benthic foraminifer accumulation rates (BFAR) (e.g. Coxall and Wilson, 2011). To assess biogenic carbonate dissolution, we use the ratio between linings and carbonate tests (OL-index) of benthic foraminifers (de Vernal et al., 1992) and the ratio between benthic and planktonic foraminifers (B/P-index) (Thunell, 1976). We assess organic carbon burial (OCB) from measurements of the total organic carbon content (TOC) in the bulk sediment, which have been presented in Saini et al. (2020). Finally, we calculate fluxes of biogenic carbonate from the shell weights of planktonic and benthic foraminifers, which allow us to estimate biogenic carbonate preservation and its amount within the whole carbonate content in the bulk sediment ( $\text{CaCO}_3$ ).

Based on all indicators mentioned above, we aim at evaluating the natural variability of processes within the biological carbon pump, from production to burial, in the eastern Baffin Bay area over the last millennial in the Holocene during which higher insolation and globally warmer than present day climate may serve as an analogue of future warming. Taking into consideration the regional palaeoceanographic and palaeoclimatic data (Briner et al., 2016; Axford et al., 2021), we examine the potential causes for changes in palaeoproductivity and the probable factors influencing export productivity and burial.

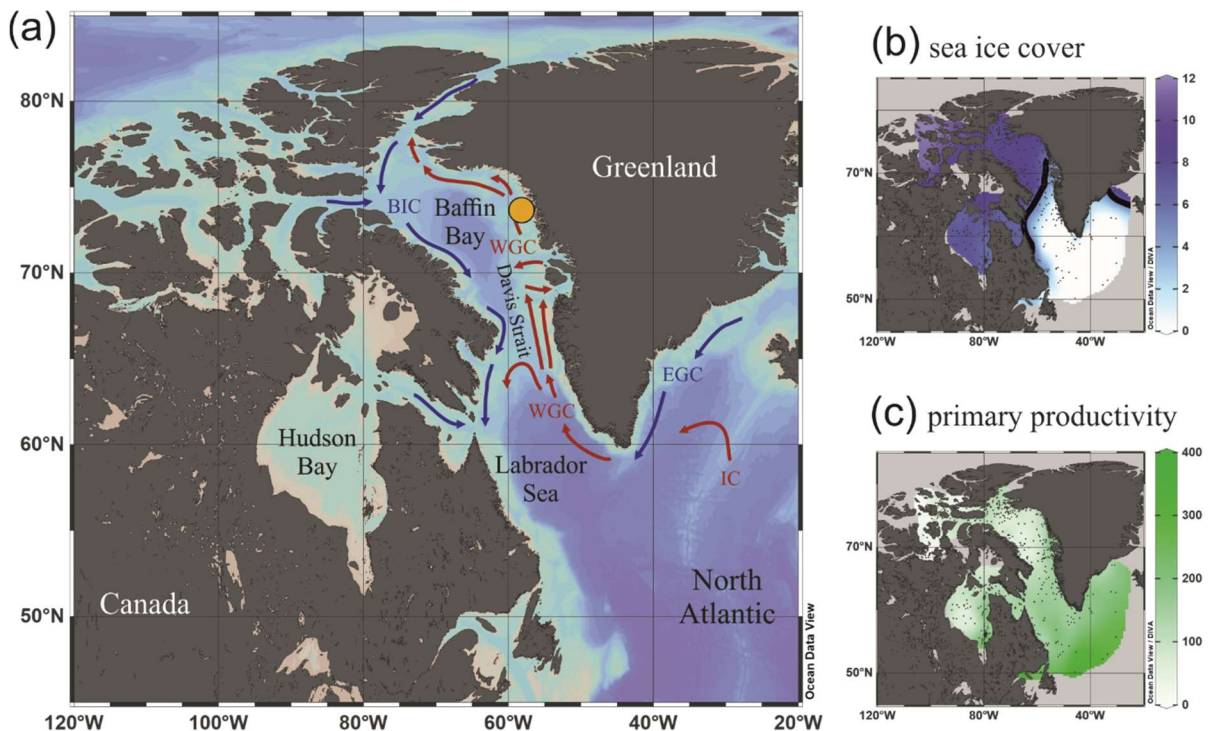


**Figure 5.1:** Location of the study area. a) Schematic modern surface circulation system in the Baffin Bay area and around Greenland and the sediment core GeoB19927-3 (orange dot). b) Modern sea-ice



cover duration in month  $\text{yr}^{-1}$ , the six-months sea-ice edge is indicated by the black cover line (Walsh et al., 2015). c) Modern annual primary productivity in  $\text{gC cm}^{-2}\text{kyrs}^{-1}$  (O'Malley, 2018). Modern environmental parameter gradients are gridded using DIVA gridding with Ocean Data View (Schlitzer, 2018).

## 5.2 Regional setting

The Baffin Bay is a narrow oceanic basin situated between Greenland and Canada (Fig. 5.1) characterised by strong seasonal sea ice variability and strong meltwater discharge from the Greenland Ice Sheet (GIS). It is a semi-enclosed basin, with connections to the North Atlantic through Davis Strait and Labrador Sea and connections to the Arctic Ocean through Nares Strait and Canadian Arctic Archipelago channels. The modern circulation in this area is anti-cyclonic and hydrographic conditions are dominated by the Baffin Island current (BIC), which consists of cold waters, and the West Greenland Current (WGC) which is fed by the East Greenland Current (EGC) and the Irminger Current (IC). The EGC consists of cold and fresh polar waters, which flow southward along the coast of East Greenland, and is mixed with the warmer and more saline IC off the coast of southern Greenland. It continues along the coastline of western Greenland as the WGC and enters into Baffin Bay (Tang et al., 2004). The WGC brings relatively warm waters from the North Atlantic via Labrador Sea and Davis Strait into the Baffin Bay and forms a subsurface water layer between 150-600 m (West Greenland Intermediate Water) capping the Baffin Bay Deep water which is a cool ( $0^{\circ}\text{C}$ ) and saline water mass occupying the deepest parts of Baffin Bay (Tang et al., 2004).

The discharge from glaciers of the West Greenland Ice Sheet together with the southward flow of low salinity polar waters via the BIC acts as freshwater supply resulting in a top layer (0-150 m) of cold and low saline waters in the Baffin Bay. The inflow of warmer water masses in the East and cooler waters in the West explains why sea-ice cover is more persistent and extensive in the western parts of Baffin Bay than along the west Greenland coast. However, sea-ice in general is persistent throughout most of the year in the whole region with the exception of the late summer months (Tang et al., 2004). The opening of Nares Strait at about 9 ka allowed the connection between Baffin Bay and the Arctic Ocean, which led to the establishment of the modern ocean circulations in the Baffin Bay (Jennings et al., 2011; Georgiadis et al., 2018).

At our study core location, the Melville Bay area off West Greenland, seasonal sea-ice variability is very high. In winter, this area is almost completely ice-covered as the sea-ice margin expands further southwards (Stern and Heide-Jørgensen, 2003; Tang et al., 2004). In summer, the area becomes almost ice-free. The Melville Bay is affected by outlet glaciers of the GIS as it collects about  $\sim 27\%$  of GIS drainage (Rignot and Kanagaratnam, 2006). Regional

wind stresses are highly seasonal being stronger in winter than summer (Tang et al., 2004). The sediments of Baffin Bay are predominantly derived from glacial erosion of the surrounding land masses. High sedimentation rates of 40–140 cm kyr<sup>-1</sup> render some areas of the Baffin Bay such as the Melville Bay, ideal for palaeoenvironmental studies (St-Onge and St-Onge, 2014).

## 5.3 Material and methods

### 5.3.1 Sediment core

Sediment core GeoB19927-3 (73°35,26' N, 58°05,66' W; water depth = 932 m) was taken by gravity coring during RV Maria S. Merian cruise MSM44 (BAFFEAST) in 2015 (Dorschel et al., 2016) (Fig. 5.2). 1147 cm of sediment were retrieved. The chronology has been provided by Saini et al. (2020) who used radiocarbon dates and <sup>210</sup>Pb measurements. We sub-sampled a total of 104 1 cm thick samples at intervals of 5 cm from 0 cm to 270 cm and at intervals of 10 cm from 270 cm to 760 cm. The sampled interval covers the last 7677 a. The average temporal resolution of our sampling is thus 74 years. In the upper 25 cm, the sampling for palynology was made at 1 cm interval, which corresponds to a temporal resolution of 30 years. The sedimentation rates vary between 32 and 172 cm kyr<sup>-1</sup>. High sedimentation rates of 100-150 cm kyr<sup>-1</sup> occur throughout the majority of the recovered intervals. A step-wise decrease in sedimentation rates to about ~ 80 cm kyr<sup>-1</sup> is observed at about 8-6 ka and to about ~ 30 cm kyr<sup>-1</sup> at about 3-1 ka, respectively. Excess lead is present down to 4.5 cm core depth, indicating that the core top is of recent age and only experienced minor disturbance during coring (cf. Saini et al., 2020).

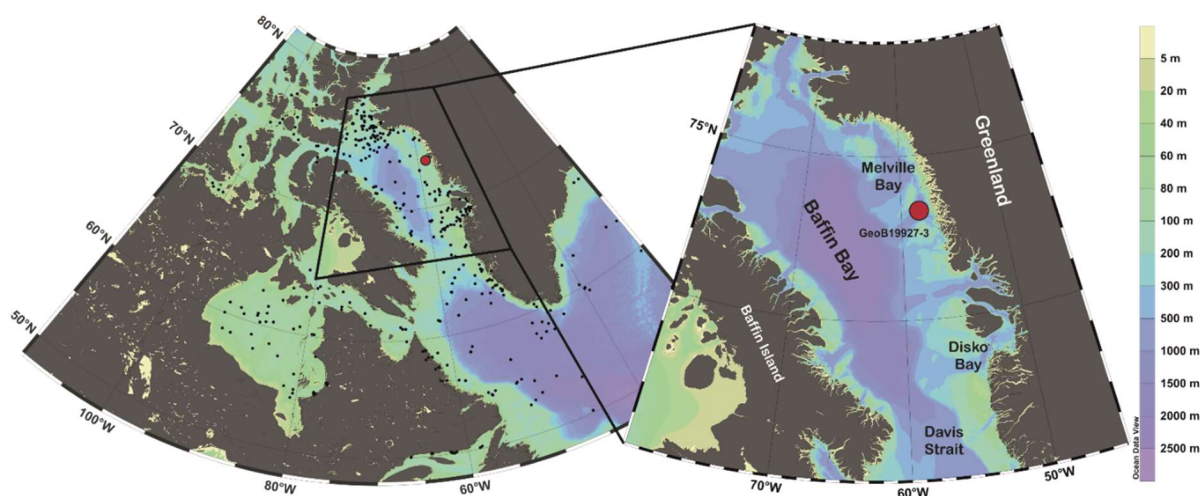


**Figure 5.2:** Study area. Location of sediment core GeoB19927-3 (red dot) and of surface sediment samples used for the local primary productivity dinocyst transfer function (black dots).

### 5.3.2 Proxy selection

We estimate annual primary productivity (PP<sub>annual</sub>) quantitatively based on the assemblage compositions of organic-walled dinoflagellate cysts (dinocysts) applying a local transfer function. Dinoflagellates form a major group of planktonic marine primary producers closely associated with carbon fixation (e.g. de Vernal and Marret, 2007). In settings with carbonate or opal dissolution, like high latitudes, dinocyst-based analyses are adequate for the reconstruction of environmental parameters as long as selective organic matter degradation does not alter dinocyst assemblage composition (e.g. Zonneveld et al., 2010). As selective organic matter degradation is not significant in eastern Baffin Bay (Hohmann et al., 2020), we adopt a previously developed local dinocyst transfer function, based on weighted averaging with partial-least square (WA-PLS, with 3 components) (cf. Hohmann et al., 2023). Reconstruction of PP<sub>annual</sub> and its significance test ( $p < .01$ ) was done with the calibrated (n=421) dataset with the software R (R Core Team, 2017) and packages palaeoSig (Telford, 2015) and rioja (Juggins, 2017). The significance test followed the method developed by Telford and Birks (2011), where a parameter reconstruction is deemed significant if the parameter explains a larger amount of the fossil species variance in the downcore data than most reconstructions derived from transfer functions trained on random environmental data. We determined dinocyst assemblage zones applying principal component analysis (PCA) on percentage data of the downcore dinocyst assemblages using the R vegan package (Oksanen et al., 2017).

Dinocyst assemblage data were reported in Hohmann et al. (2023) (see “data availability”). Organic linings of foraminifera were counted on the basis of the marker-grains method (Matthews, 1969) by adding a capsule of *Lycopodium clavatum* spores. Only complete linings were considered.

We assess export productivity (EP) based on the accumulative amount of benthic foraminifera (BFAR). BFAR represents the flux of organic matter to the seafloor (Gooday, 2003; Jorissen et al., 2007) as benthic foraminifera rely on the organic matter produced in surface layers and transported to the ocean floor. BFAR appears to correlate predictably with export production in a variety of modern locations (Herguera, 1992; Jorissen et al., 2007) if carbonate dissolution did not alter the shells of benthic foraminifers. The BFAR has already been applied in former studies (e.g. Coxall and Wilson, 2011).

We assess the preservation of biogenic carbonate and the amount of biogenic carbonate within the bulk carbonate (CaCO<sub>3</sub>) applying the accumulative shell weight of planktonic and benthic foraminifera. Foraminifera are single-celled, mostly calcite shell-bearing microorganisms, dwelling in all marine habitats (Hunt and Corliss, 1993; Wollenburg and Mackensen, 1998;

Jennings et al., 2004; Fontanier et al., 2008; Milker and Schmiedl, 2012; Müller-Navarra et al., 2016; Schiebel and Hemleben, 2017). Planktonic foraminifera dwell in the upper layers of the water column, belonging to the zooplankton. Benthic foraminifera live on (epibenthic) or in the sediment (endobenthic) (Hunt and Corliss, 1993; Łącka and Zajączkowski, 2016). Both, planktonic and benthic foraminifera are important producers and exporters of biogenic carbonate to marine sediments. Foraminifera shells are prone to carbonate dissolution which increases with depth in the oceans (Berger, 1970). The carbonate compensation depth (CCD) in the Baffin Bay area lies between 600-900 m (Aksu, 1983), resulting in carbonate dissolution and poor preservation of biogenic carbonate at deep core sites (e.g. Gibb et al., 2014).

For the estimation of carbonate dissolution we apply the ratio between planktonic and benthic foraminifera (B/P-index) (Thunell, 1976) and the OL-index (de Vernal et al., 1992). The OL-index is a quantitative measure based on the concentrations of organic and carbonate remains of benthic foraminifera and is expressed as the logarithm value of organic lining (OL) versus carbonate shell (CS) concentrations for the five benthic species (*Buliminella elegantissima* (d'Orbigny, 1839), *Melonis zandamee* (van Voorthuysen), *Elphidium excavatum* (Terquem, 1875), *Cibicides lobatulus* (Walker & Jacob, 1798), *Cibicides wuellerstorfi* (Schwager, 1866)) yielding acid-resistant palynomorphs ( $\log[OL/CS]$ ). For B/P-index, dissolution is marked by values  $>1$  while values between 0 and  $<1$  indicate preservation. For the OL-index, dissolution is marked by positive values approaching infinity in case of total dissolution. Negative values mark high preservation of biogenic carbonate.

We estimate organic carbon burial (OCB) considering measurements of the total organic carbon content (TOC) in the bulk sediment (e.g. Lopes et al., 2015), which have been presented in Saini et al. (2020).

Other data presented in Saini et al. (2021), including carbonate content from bulk sediment ( $\text{CaCO}_3$ ), dinosterol and brassicasterol biomarker fluxes and  $\beta$ -sito-campesterol fluxes, were used aiming to assess the amount of marine versus terrigenous input/ carbonate preservation.  $\text{CaCO}_3$ -concentration represents the amount of inorganic carbon (=carbonate) within the sediment consisting of biogenic carbonate such as foraminifera shells and detrital (abiotic) carbonate from terrigenous sources. Dinosterol (4-methyl sterol) is produced by most dinoflagellates and brassicasterol (24-methyl sterol) by diatom, algae and some plants (Volkman, 1986). Both dinosterols and brassicasterols have been used as indicators of open water phytoplankton productivity (Volkman, 1986; Meyers, 1997; Fahl and Stein, 1999; Saini, 2021) and led to track the contribution of plankton in marine organic matter (Mouradian et al., 2007). As dinosterol and brassicasterol are not exclusively produced by marine dinoflagellates

(Yunker et al., 1995) and diatoms (Thiel et al., 1997) respectively, they may be applied as tracers of export productivity and/or carbon burial.

The other biomarkers we used are  $\beta$ -sitosterol (24-ethylcholest-5-en-3 $\beta$ -ol) and campesterol (24-methylcholest-5-en-3 $\beta$ -ol), which are predominantly produced by land vascular plants (Stein and MacDonald, 2004) and have often been applied as proxies for land-derived terrigenous input (e.g. Fahl and Stein, 1997; Hörner et al., 2016; Syring et al., 2020).

To convert concentrations into fluxes, mass accumulation rates were calculated based on sedimentation rates and dry bulk density data following the equation after Ehrmann and Thiede (1985) following (Herguera and Berger, 1991) by multiplying the number of specimens or mass per gram sediment by the sample dry bulk density and by the linear sedimentation rate:

$$AR_x = LSR * DBD * BFN \quad (1)$$

with  $AR_x$  = accumulation rate of parameter x [specimens or mass of x  $\text{cm}^{-2}\text{kyrs}^{-1}$ ]; LSR = linear sedimentation rate [ $\text{cm kyr}^{-1}$ ]; DBD = density of dry sediment [ $\text{g cm}^{-3}$ ]; BFN = number or concentration of parameter x in one gram dry sediment [specimens or mass of x  $\text{g}^{-1}$ ].

### **5.3.3 Foraminifera analysis**

Between 4-16 grams of freeze-dried sediment samples were wet sieved over a 63  $\mu\text{m}$  mesh sieve and oven-dried at  $\sim 50$   $^{\circ}\text{C}$  for one day. The whole fraction  $> 63$   $\mu\text{m}$  was picked and counted for planktonic and benthic foraminifera, resulting in foraminifera counts between 0 and 1940. Most samples held counts between 50 and 200 specimens. Planktonic and benthic specimens and their fragments were sorted into two groups and separately weighed to six decimal places using a Sartorius microbalance. Each sample was weighed five times to determine the average weight of their accumulative shells. Benthic samples were analysed with attention given to the five species yielding acid-resistant organic linings (*B. elegantissima*, *M. zandamee*, *E. excavatum*, *C. lobatulus*, *C. wuellerstorfi*).

## **5.4 Results**

### **5.4.1 Dinocysts**

The samples analysed for dinocyst assemblages record dinocyst concentrations ranging from  $4.1 \cdot 10^3$  to  $5.2 \cdot 10^4$  cysts  $\text{cm}^{-3}$ . Using the respective sedimentation rates we calculate fluxes in the order of  $10^2$  to  $10^4$  cysts  $\text{cm}^{-2}\text{yr}^{-1}$  (Fig. 5.3).

A total of 15 dinocyst taxa were identified. Ten of these species represent about 99% of the assemblages: *Operculodinium centrocarpum*, *Spiniferites elongatus*, *Spiniferites ramosus*, *Nematosphaeropsis labyrinthus*, the cysts of *Pentaparsodinium dalei*, *Brigantedinium* spp., *Islandinium minutum*, *Echinidinium karaense*, *Echinidinium* spp. and *Selenopemphix quanta* (Fig. 5.4).

We performed multivariate analyses to characterise the dinocyst assemblage composition. Detrended correspondence analysis (DCA) (Birks, 1995) resulted in an ordination axis of 1.0 standard deviation, suggesting a linear relationship and principal components analysis (PCA) to analyse the species variance of core GeoB19927-3 (Lepš and Šmilauer, 2003).

The first PCA axis opposes *O. centrocarpum* on the negative side and the cyst of *P. dalei* on the positive side, explaining 76.6% of the total taxa variance and represents the variance of autotrophic cysts in general (Fig. 5.5). The autotrophic taxa include mostly *O. centrocarpum*, cysts of *P. dalei* and *S. elongatus*. In the West Greenland region, the occurrence of these taxa is supposedly related to the late summer bloom due to meltwater input (e.g. Boertmann et al., 2013; Juul-pedersen et al., 2015). In the Arctic *O. centrocarpum* occurs in areas that can be covered by sea-ice for up to 12 months a year whereby a negative relationship exists between its relative abundance and annual ice cover (e.g. Radi and de Vernal, 2008). The cyst of *P. dalei* is commonly linked to high stratification and large seasonal temperature gradients (Rochon et al., 1999; Allan et al., 2018). In the core region specifically it is linked to low summer salinity (Hohmann et al., 2023), linking the first PCA axis predominantly to salinity/stratification and temperature.

The second PCA axis is characterised by the distance between *Brigantedinium* spp. and the other dominant species, explaining 17.0% of the taxa variance. *Brigantedinium* spp. is reported from all studied regions and high relative abundances may occur anywhere within its broad environmental gradients (cf. Marret and Zonneveld, 2003). *I. minutum* is typically common in environments characterised by seasonal sea-ice (e.g. Rochon et al., 1999; Hamel et al., 2002; Radi and de Vernal, 2008; de Vernal et al., 2013). The second axis in general however, is affected by variances of heterotrophic taxa. Heterotrophic dinoflagellates are generally associated with high primary productivity in seasonal sea-ice edge environments (Hamel et al., 2002; Radi and de Vernal, 2008; de Vernal et al., 2013). At sea-ice edges, heterotrophic taxa take advantage of a high diatom biomass during the spring bloom, whereas phototrophic dinoflagellates cannot compete with the diatoms (e.g. Gosselin et al., 1997; Poulin et al., 2011). Hence, the second axis corresponds predominantly to changes in seasonal sea-ice cover.

PCA analysis of the dinocyst assemblages led to identify two assemblage zones mirrored in PCA-axis 1 and three assemblage zones mirrored in PCA-axis 2. Assemblage zone shifts occur around 640 cm (6.3 ka), 220 cm (3.1 ka) and 20 cm (0.7 ka). The first zone shift (6.3 ka) corresponds to a shift from negative to positive PCA 2 marked by a decrease in heterotrophic taxa suggesting changes in sea-ice edge conditions. The corresponding increase in *O. centrocarpum* suggests a retreating sea-ice edge in the core region.

A change in the first PCA axis from negative to positive around 3.1 ka marks the second and major zone shift and is affected by a large increase of cysts of *P. dalei* and a decrease in *O. centrocarpum* supposedly due to increasing stratification induced by increasing meltwater input. The last zone shift occurring around 0.7 ka indicated by a change from positive to negative values in PCA axis 2 and corresponding increases in heterotrophic cysts, predominantly *I. minutum* and *S. quanta*, suggests increasing sea-ice cover.

We reconstructed annual primary productivity adopting a local transfer function from Hohmann et al. (2023) for dinocyst assemblages. The PPannual reconstruction from the data of core GeoB19927-3 based on WA-PLS has been tested significant ( $p < .01$ ) following the test of Telford and Birks (2011). Until 300 cm (3.9 ka) primary productivity estimates display relatively low rates around  $170 \text{ gC cm}^{-2}\text{kyrs}^{-1}$ , which subsequently increase up to around  $250 \text{ gC cm}^{-2}\text{kyrs}^{-1}$  between 130 and 70 cm (around 1.9 ka) (Fig. 5.3). In the upper part of the core, primary productivity declines to about  $200 \text{ gC cm}^{-2}\text{kyrs}^{-1}$ . PPannual reconstructions mostly correspond to variations in PCA-axis 1, rendering it a function of stratification and temperature in the Melville Bay area during the Holocene.

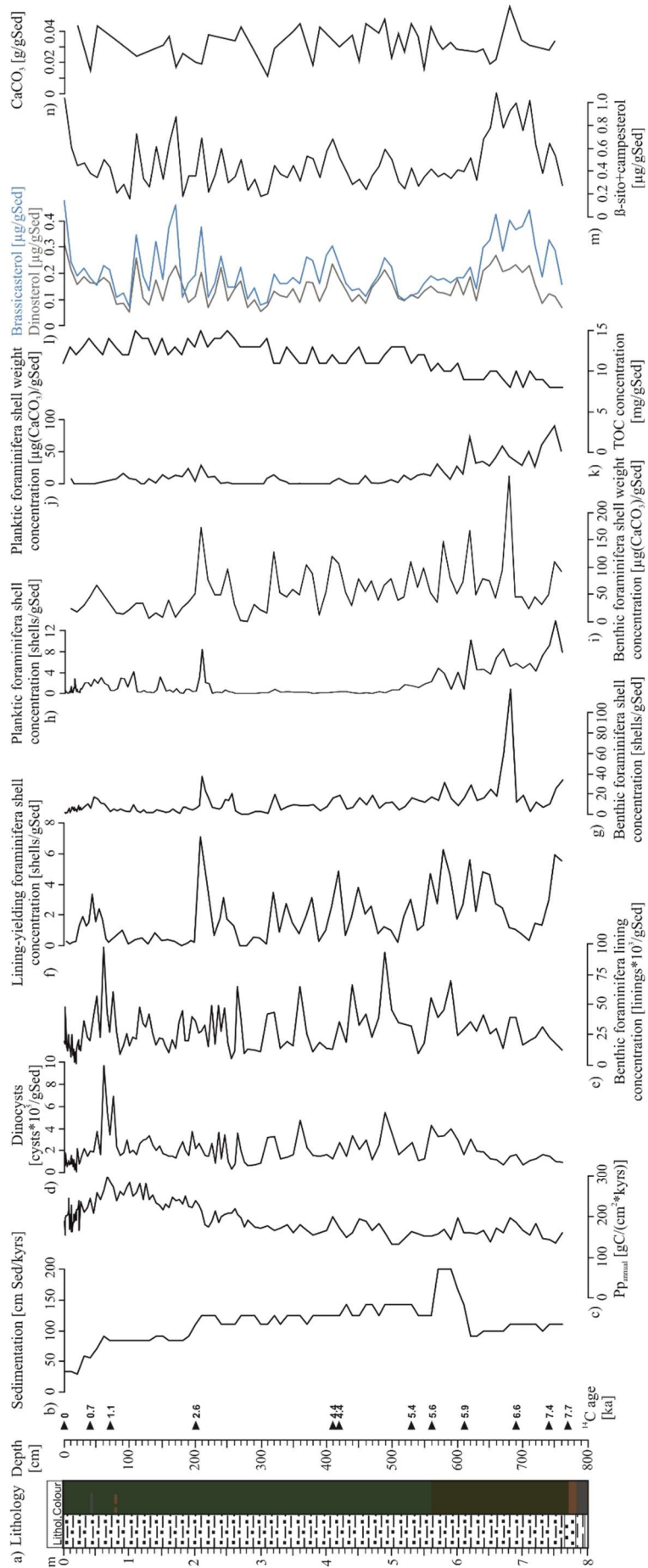




**Figure 5.3:** Summarised results from sedimentological and micropalaeontological analyses in core GeoB19927-3. a) Lithology (after Dorschel et al., 2015), b) Sedimentation rate [ $\text{cmSed kyr}^{-1}$ ] (Saini et al., 2020), palynological parameters - c) Reconstructed annual primary productivity [ $\text{gC cm}^{-2}\text{kyrs}^{-1}$ ], d) Dinocyst concentration [ $\text{cysts} \cdot 10^5 \text{gSed}^{-1}$ ], e) Benthic foraminifera lining concentration [ $\text{linings} \cdot 10^3 \text{gSed}^{-1}$ ], foraminiferal parameters - f) Lining-yielding foraminifera shell concentration [ $\text{shells gSed}^{-1}$ ], g) Benthic foraminifera shell concentration [ $\text{shells gSed}^{-1}$ ], h) Planktic foraminifera shell concentration, i) Benthic foraminifera shell weight concentration [ $\mu\text{g}(\text{CaCO}_3) \text{gSed}^{-1}$ ], j) Planktic foraminifera shell weight concentration [ $\mu\text{g}(\text{CaCO}_3) \text{gSed}^{-1}$ ] - and from Saini et al. (2020) k) TOC concentration [ $\text{mg gSed}^{-1}$ ], l) Brassicasterol and dinosterol concentration [ $\mu\text{g gSed}^{-1}$ ], m)  $\beta$ -sitosterol+campesterol concentration [ $\mu\text{g gSed}^{-1}$ ], n)  $\text{CaCO}_3$  concentration [ $\text{g gSed}^{-1}$ ]. Black solid triangles mark the AMS  $^{14}\text{C}$  datings (Saini, 2021).

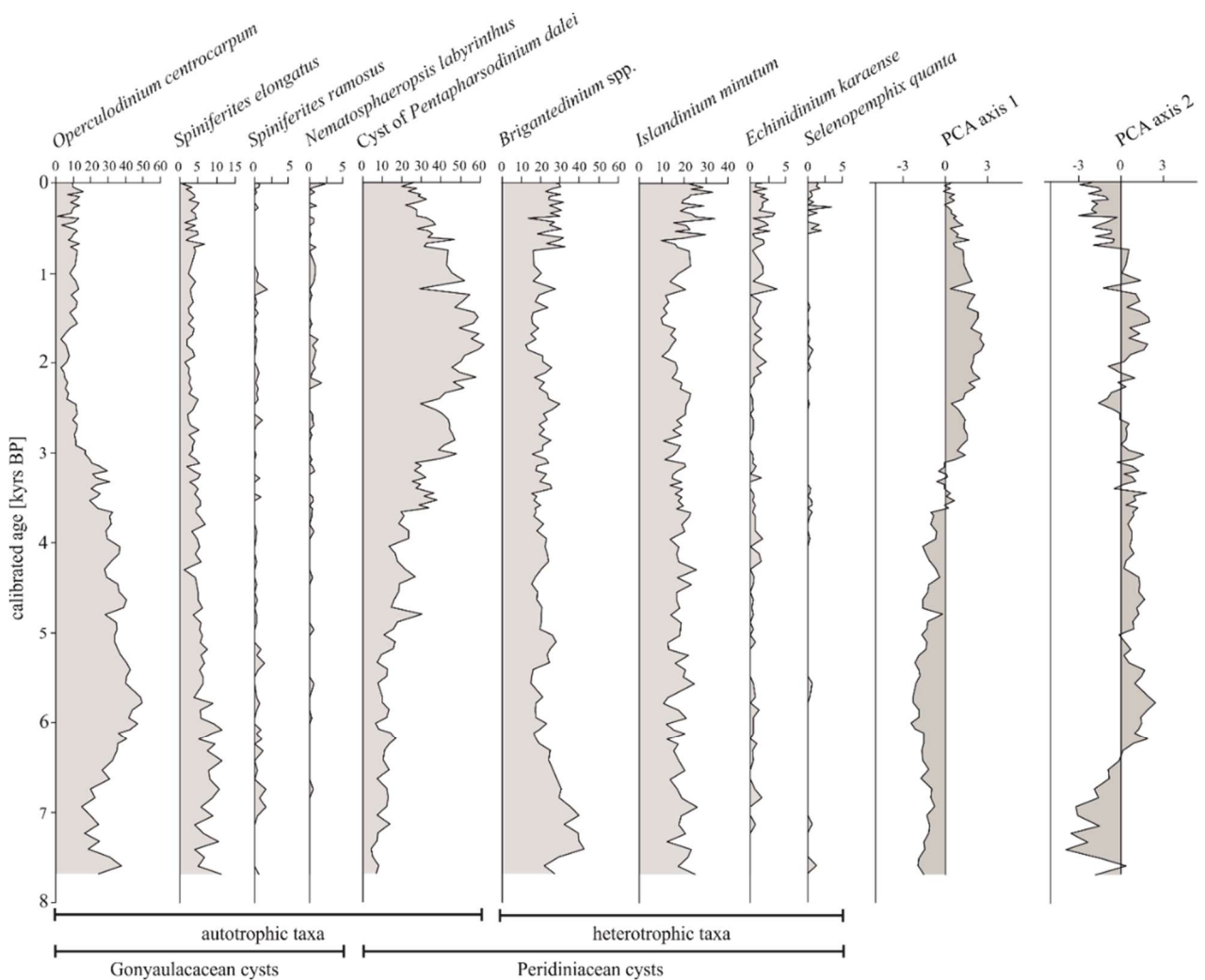


**Figure 5.4:** Percentages of the main dinocyst taxa (>2%) and scores of PCA axes 1 (proportion explained 76.6%) and 2 (proportion explained 17%) in core GeoB19927-3.

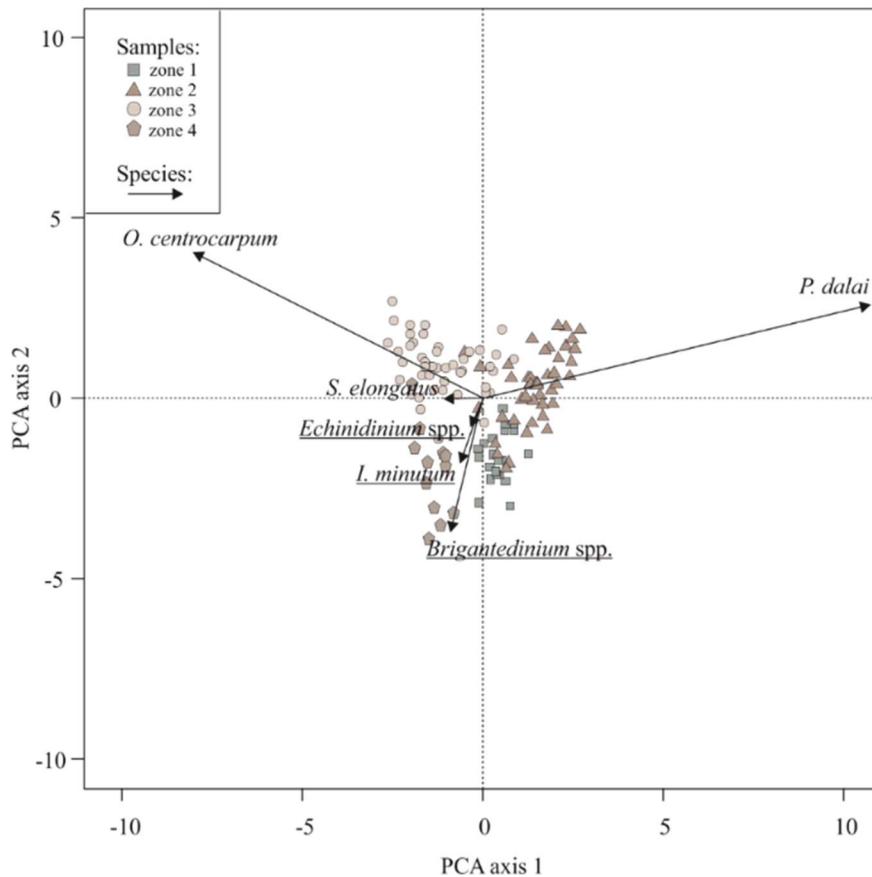


**Figure 5.5:** Ordination diagram of the six highest scoring dinocyst taxa from the downcore assemblages of core GeoB19927-3, according to the two main axes, PCA 1 and PCA 2. Other taxa score in the centre of the diagram. The symbols correspond to the assemblage zones. The names of heterotrophic taxa are underlined, those of autotrophic taxa not.

#### 5.4.2 Foraminifera

The majority of calcareous benthic foraminifera in the samples are well preserved and show only sporadic signs of dissolution. Planktonic foraminifera are rare or absent in most samples, with a few exceptions of samples yielding about 14 planktonic shells/gSed. Their percentages range between 0 and 67% of the foraminifera fauna. From the five species yielding acid-resistant organic linings, we identified *C. lobatulus* and *Elphidium excavatum* subsp. *clavatum* (Cushman, 1930). Their shells record 0-24% and 0-37% of the benthic foraminifer assemblages, which represent concentrations of 0-4.8 and 0-6.2 shells/gSed, respectively. *C. lobatulus* is a cosmopolitan species, while *E. clavatum* is commonly found in Arctic waters (Jennings and Helgadottir, 1994; Hald and Korsun, 1997). *B. elegantissima*, *M. zandamee* and *C. wuellerstorfi* are absent. While *C. wuellerstorfi* shows a cosmopolitan distribution (Gooday and Jorissen, 2012), *B. elegantissima* inhabits deep waters and high productivity environments

(Risdal, 1964). *M. zandamee* is associated with the influence of intermediate North-Atlantic waters (Mackensen et al., 1985).

The overall benthic foraminifera shell concentrations range between 0 and 20 shells/gSed apart from two peaks around 690 cm and 210 cm with concentration >100 and >40 shells/gSed, respectively. Concentrations are less variable in the upper 200 centimetres. Carbonate concentrations measured by benthic foraminifera shell weights follow the trend of benthic shell concentrations with alterations between 0 and 250 µg carbonate per gram sediment. Planktonic foraminifera shell weight concentrations are relatively high with values ranging around 50 µg/gSed in the lower part of the core below 520 cm. Above 510 cm values range around 10 µg/gSed with many samples barren in planktonic foraminifera. Concentrations of benthic foraminifera linings are relatively low in the lower part of the core between 760 and 610 cm (< 40,000 linings/gSed), and highly variable above with values ranging from 5,000 to 90,000 linings/gSed.

#### **5.4.3 Bulk parameters and biomarkers**

TOC concentrations range from 8-15 mg/gSed with minimum but increasing values in the lower part of the core and high values in the upper part (Fig. 5.3 k). The phytoplankton biomarkers brassicasterol and dinosterol show a very similar trend in their concentration record with fluctuations ranging from 0.07-0.48 µg/gSed and 0.05-0.31 µg/gSed, respectively (Fig. 5.3 l). Intervals of enhanced brassicasterol and dinosterol concentrations are observed from about 7.4-6.3 ka and from about 2.6-1.1 ka. The terrigenous biomarkers (β-sitosterol+campesterol) concentrations range from 0.15-1.08 µg/gSed (Fig. 5.3 m). They show a very similar trend in their concentration record like brassicasterol and dinosterol. CaCO<sub>3</sub> concentrations range from 0.01-0.06 g/gSed throughout the record (Fig. 5.3 n) (cf. Saini, 2021).

## **5.5 Discussion**

### **5.5.1 Primary productivity**

PPannual reconstructions based on dinocyst assemblage changes and variations in PCA-axis 1 are highly correlated ( $r = 0.89$ ;  $p < .01$ ). This combined with the significance of the estimate ( $p < .01$ ; test after Telford and Birks, 2011), suggests that dinocyst assemblages in the core region were driven by changes in annual primary productivity. This is congruent with results from Hohmann et al. (2023) for spring primary productivity. The assumption above that the first PCA-axis is linked to salinity and stratification supports this suggestion. Studies from the West

Greenland region link the occurrences of *O. centrocarpum* and the cysts of *P. dalei* to the late summer bloom productivity (e.g. Boertmann et al., 2013; Juul-pedersen et al., 2015), which is presumably induced by sea ice retreat and increased meltwater input, resulting in decreased salinity and strengthened stratification.

However, when using dinocyst assemblages, selective organic matter degradation can be an issue (e.g. Zonneveld et al., 1997; Zonneveld and Brummer, 2000; Zonneveld et al., 2007; 2008; 2010). Although Hohmann et al. (2020) demonstrated from a calibration dataset covering the study region that selective degradation of dinocysts by oxidation has no impact, we cannot rule out that the fossil record from core GeoB19927-3 was not altered by selective degradation. Zonneveld et al. (2007) suggested from sediment trap studies that the production rates of resistant and sensitive dinocysts are linearly related when organic matter in surface sediments is not affected by aerobic degradation, thus strengthening the assumption that proportional fluxes of resistant and sensitive cysts suggest no selective preservation (Versteegh and Zonneveld, 2002). The correlations between resistant and sensitive cyst abundances in core GeoB19927-3 suggest limited impact of selective degradation, if any ( $r = 0.94$ ;  $p \leq .01$ ). Moreover, *Echinidinium* spp. and *Brigantedinium* spp., which are both highly sensitive to aerobic degradation, are abundant in all samples. Hence, the reconstructed PPannual flux presumably provides reliable production rates of organic carbon in surface waters.

Based on the PCA results, the dinocyst record can be subdivided into four zones, with main shifts occurring around 0.7, 3.1 and 6.3 ka (Fig. 5.6). Shifts in dinocyst assemblages around 1.0 ka in the Disco Bay and around 4.0 and 6.7 ka in the central Baffin Bay area have been described by Allan et al. (2018) and Hohmann et al. (2023), which is in line with our new data set.

Alongside the positive relationship between reconstructed PP and the first PCA axis, we find a positive relationship with the abundance of cysts of *P. dalei* ( $r = 0.91$ ;  $p < .01$ ). *P. dalei* is a phototrophic taxon often described as being associated with primary productivity and sea surface temperature changes in Arctic environments (Radi and de Vernal, 2008; de Vernal and Rochon, 2011; Hohmann et al., 2023). The relative abundance (percentage) of *P. dalei* correlates with PPannual, suggesting this parameter as an indicator of productivity. However, the accumulation rates of *P. dalei* do not covary with PPannual ( $r = 0.46$ ). The total dinocyst flux also shows no correlation with PPannual reconstructions (Fig. 5.6 g.). While the transfer function reconstruction and relative abundances of *P. dalei* within the whole dinocyst assemblage seem to represent organic carbon production, accumulation rates of *P. dalei* and dinocysts in general, rather seem to represent their respective biogenic fluxes and their preservation in the water column and sediments.

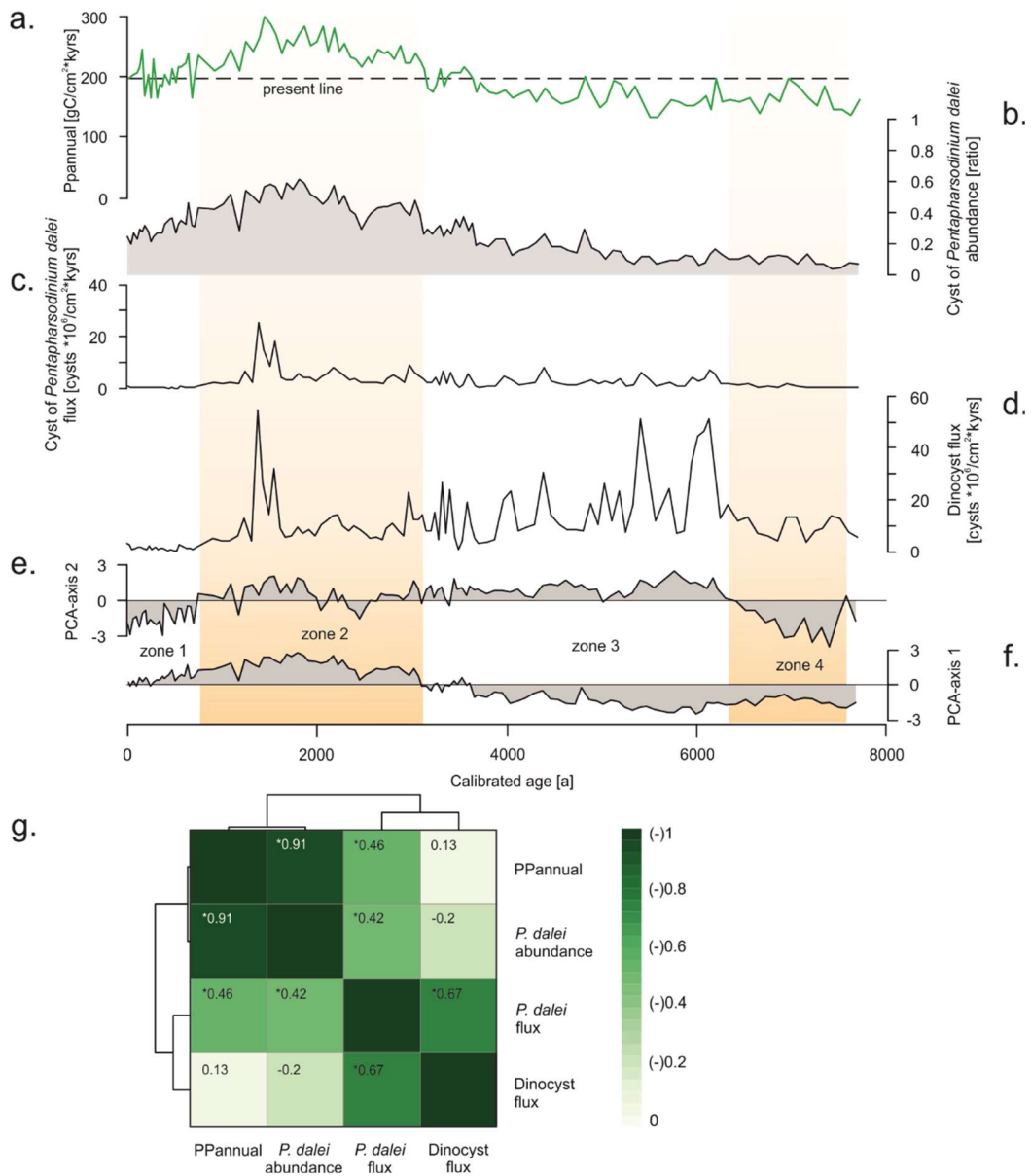


**Figure 5.6:** Estimated productivity and selected dinocyst parameters. a) Reconstructed annual primary productivity [ $\text{gC cm}^{-2} \text{kyrs}^{-1}$ ], b) Relative abundance of *P. dalei* [ratio], c) Accumulation rate of *P. dalei* [ $\text{cysts} \cdot 10^6 \text{ cm}^{-2} \text{kyrs}^{-1}$ ], d) Accumulation rate of dinocysts [ $\text{cysts} \cdot 10^6 \text{ cm}^{-2} \text{kyrs}^{-1}$ ], e) PCA-axis 2 and f) PCA-axis 1. Zones 1-4 defined from assemblage composition changes as shown by PCA 1 and 2 axes shifts are highlighted through orange shading. g) Clustering heatmap indicating correlations between parameters (done with R package pheatmap (Kolde, 2019)). Asterisks indicate significant correlations after Bonferroni correction ( $p < .013$ ).

### **5.5.2 Export productivity**

One of the most important parameters of the carbon cycle impacting climate on time scales of thousands of years is the carbon export to the deep ocean (e.g. Broecker, 1982; Berger et al., 1989). Here, we tentatively estimated the export productivity from the BFAR (e.g. Gooday, 2003; Jorissen et al., 2007).

Benthic foraminiferal accumulation rates are high but variable in the lower part of the core and relatively low in the upper part of the core, thus suggesting a reduction of benthic foraminiferal production and hence export productivity after 3.0 ka (Fig. 5.7). However, the carbonate compensation depth (CCD), the depth below which >90% of calcium carbonate is dissolved (Lisitzin, 1972), presently lies between 600 and 900 m water depth in the Baffin Bay (Aksu, 1983), suggesting extensive carbonate dissolution may have affected the preservation of foraminiferal shells in the sediment.

Generally higher benthic foraminifera accumulation rates in samples older than 3.0 ka is recorded from the fluxes of benthic foraminifer linings, which are composed of organic matter and are not altered by carbonate dissolution. However, there is no correlation between the BFAR and organic lining fluxes (Fig. 5.7 b and e), which is not surprising as only a few benthic foraminifera species yield organic linings resistant to palynological treatments (de Vernal et al., 1992).

Dissolution indices confirm continuous dissolution during the Holocene and imply two intervals with higher dissolution rates between 5.7 and 2.7 ka and between 0.7 ka and present day (Fig. 5.7 c-d). Dissolution rates within these intervals are erratic and extensive, rendering interpretations of BFAR difficult. Nevertheless, continuous but moderate dissolution rates in an upper and a lower part of the core comfort us with our interpretation of higher BFAR fluxes before 5.7 ka and reduced fluxes after 2.7 ka.

The estimation of carbon export from BFAR is based on the assumption that the benthic foraminifer community is mainly controlled by organic input from the surface waters. In general however, accumulation rates of elements, minerals or microfossils in sediment, are not reliable parameters if they are a function of their respective (primary) productivity, their (biogenic) fluxes and their preservation in the water column and in sediments (e.g. Henson et al., 2012; Arndt et al., 2013). Only a small fraction of exported carbon from the surface waters is eventually buried and preserved in the sediment due to remineralisation and dissolution within the water column and in sediments (e.g. Heinze et al., 1991; Falkowski et al., 1998; Field et al., 1998; Behrenfeld et al., 2001), not mentioning the potential impact of bottom currents. Hence, fluxes estimated from sediments, including benthic foraminifera accumulation rates

may rather represent burial rates, a parameter that does not always correlate with export productivity (Lopes et al., 2015), recommending caution with interpretations.

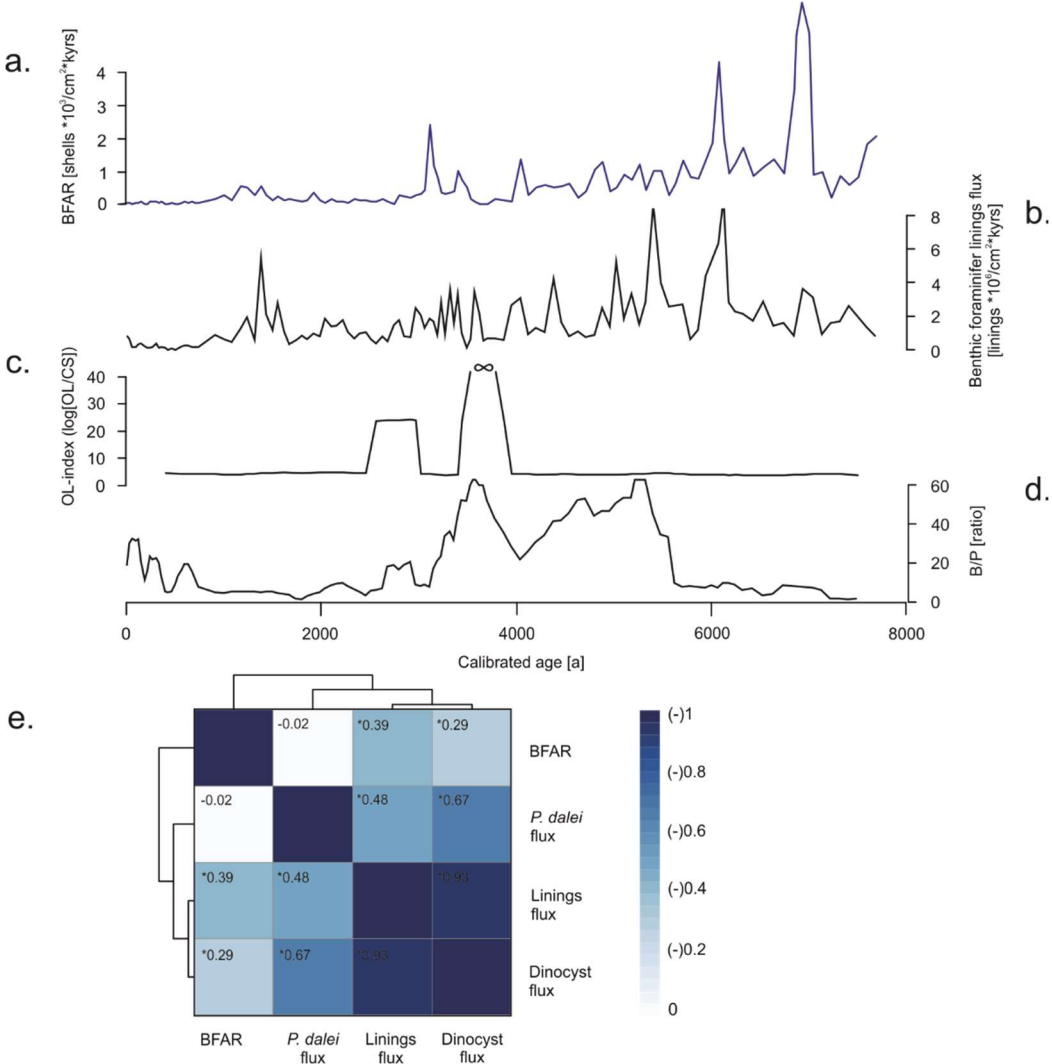


**Figure 5.7:** Foraminifer and carbonate dissolution parameters. a) Accumulation rate of benthic foraminifera shells [shells  $\cdot 10^3 \text{ cm}^{-2} \text{kyrs}^{-1}$ ], b) Accumulation rate of benthic foraminifera linings [linings  $\cdot 10^6 \text{ cm}^{-2} \text{kyrs}^{-1}$ ], c) OL-index [log(OL/CS)], d) B/P-index. Dissolution indices are shown as 5-point-moving-averages, calculated with R package zoo (Zeileis and Grothendieck, 2005). e) Clustering heatmap indicating correlations between parameters (done with R package pheatmap (Kolde, 2019)). Asterisks indicate significant correlations after Bonferroni correction ( $p < .013$ ).

### 5.5.3 Burial flux

We estimated organic carbon burial (OCB) considering measurements of the total organic carbon content (TOC) in the bulk sediment (e.g. Lopes et al., 2015). TOC fluxes suggest lower rates of carbon burial before 6.2 ka and higher burial rates between 6.2 and 3.0 ka, followed by a decrease until present day (Fig. 5.8 a).

The TOC content in marine sediment, however, may include both marine and terrestrial carbon. In Arctic regions like Baffin Bay, terrigenous input to continental shelves takes place via river discharge and coastal erosion prior to being further redistributed by ocean currents, icebergs, sea ice and aeolian processes (Wegner et al., 2015). During the Holocene, terrigenous organic matter released from sea ice may have accounted for a major fraction of TOC flux in the Arctic Ocean and in Greenland Seas (Hebbeln and Wefer, 1991; Stein and MacDonald, 2004). While marine organic carbon burial may become more important in areas with higher primary productivity, no detailed data were available for the estimation of the marine carbon fraction in the Baffin Bay region until the work by Saini (2021).

Saini (2021) used  $\beta$ -sitosterol (24-ethylcholest-5-en-3 $\beta$ -ol) and campesterol (24-methylcholest-5-en-3 $\beta$ -ol), two specific biomarkers predominantly produced by land vascular plants (Stein and MacDonald, 2004), to estimate terrigenous input in the Melville Bay region. Higher concentration of  $\beta$ -sito+campesterol per gram TOC until 6.0 ka, followed by lower values after 6.0 ka suggest that a larger fraction of the organic carbon flux was of terrestrial origin in the lower core section (Saini, 2021). Fluxes of  $\beta$ -sito+campesterol also show higher values before 6.0 ka, followed by a continuous slow decrease until present day (Fig. 5.8 d).

Additionally, Saini (2021) found that heavier  $\delta^{13}\text{C}_{\text{org}}$  values ( $> -23\text{‰}$ ) and low TOC/ $N_{\text{corr}}$  ratio ( $< 10$ ) support an increased proportion of marine organic matter relative to terrestrial organic matter in younger sediments. In general, fluxes of marine organic carbon are controlled by sedimentation rates. Hence, the findings of Saini (2021) are congruent with other studies demonstrating increasing marine organic carbon fluxes during interglacial times when sedimentation rates were lower (Chang et al., 2014).

Dinosterol and brassicasterol fluxes, previously used as biomarkers for the estimation of marine phytoplankton productivity (e.g. Volkman, 1986; Meyers, 1997; Saini, 2021) and the contribution of plankton in marine organic matter (Mouradian et al., 2007), show no collinearity with PP<sub>annual</sub> (Fig. 5.6 a) and no conformity with the pattern illustrated by Saini (2021) for the amount of marine organic matter in TOC (Fig. 8). We find high correlations between  $\beta$ -sito+campesterol, dinosterol and brassicasterol (all  $r > 0.89$ ;  $p < 0.01$ ) (Fig. 5.8 e). This implies that dino- and brassicasterol fluxes in Melville Bay may illustrate terrigenous input, as they can



be produced by freshwater dinoflagellates (Yunker et al., 1995) and diatoms (Thiel et al., 1997). Since,  $\beta$ -sito+campesterol, dino- and brassicasterol fluxes likely reflect terrestrial input but show no correlation with TOC (Fig. 5.8 e) we can assume that the TOC contains varying proportions from marine origin.

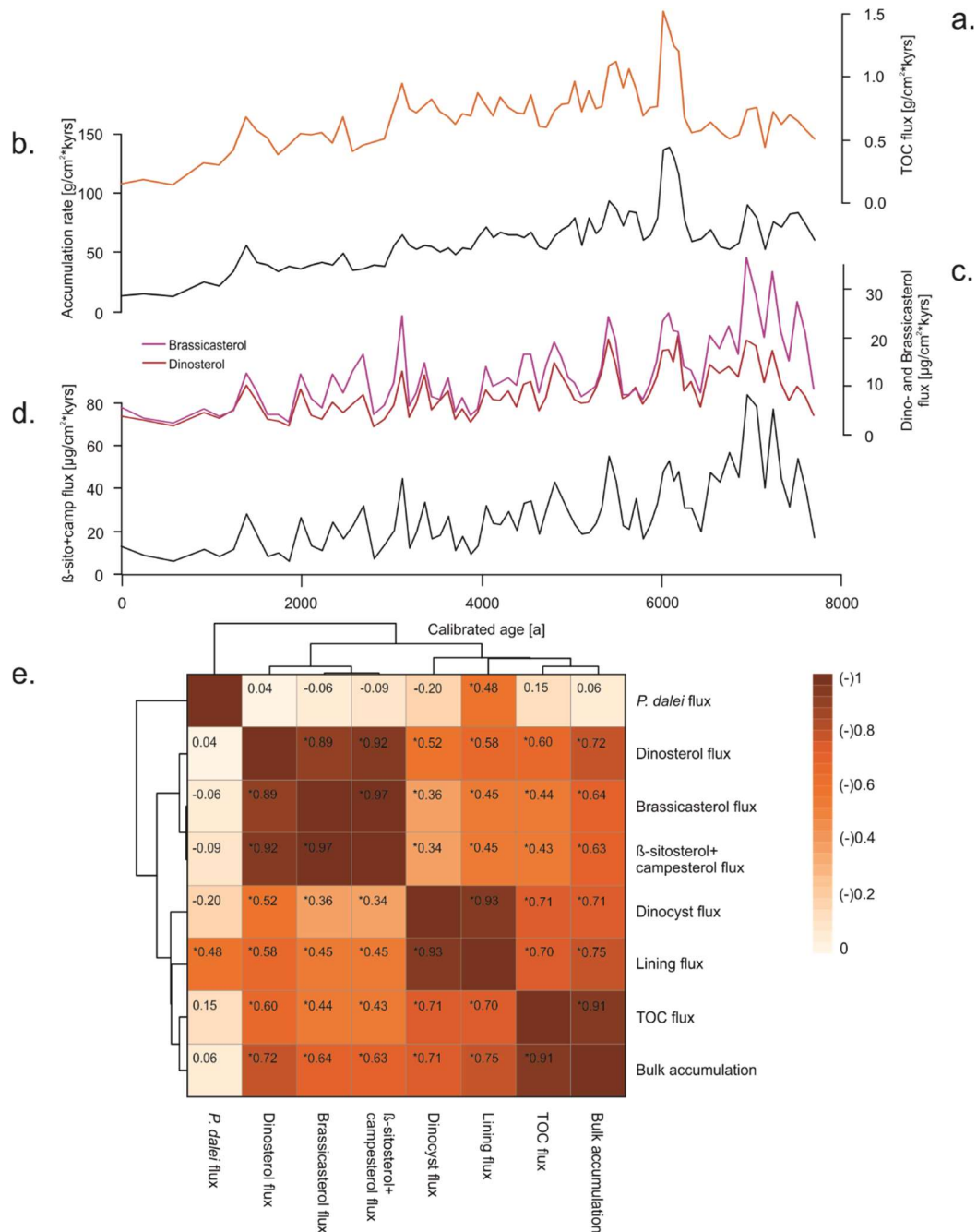


**Figure 5.8:** Burial parameters. a) Total organic carbon accumulation rate [g cm<sup>-2</sup>kyrs<sup>-1</sup>], b) Bulk accumulation rate [g cm<sup>-2</sup>kyrs<sup>-1</sup>], c) Dinosterol (red) and brassicasterol (pink) accumulation rate [μg cm<sup>-2</sup>kyrs<sup>-1</sup>], d) β-sito+campesterol accumulation rate [μg cm<sup>-2</sup>kyrs<sup>-1</sup>]. e) Clustering heatmap indicating correlations between parameters (done with R package pheatmap (Kolde, 2019)). Asterisks indicate significant correlations after Bonferroni correction ( $p < .006$ ).

We found that fluxes of benthic foraminifera linings do not correlate with benthic foraminifera shell fluxes, and that dinocyst fluxes do not correlate with PP<sub>annual</sub>. However, the lining fluxes show collinearity with dinocyst accumulation rates ( $r = 0.93$ ) (Fig. 5.7 e) and both are significantly correlated with the TOC flux ( $r > 0.7$ ;  $p < .01$ ) (Fig. 5.8 e). As only a fraction of the dinoflagellate population produces cysts, dinocyst accumulation rates do not mirror organic carbon production. Similarly, as only a few benthic foraminifer species yield acid-treatment-resistant linings, lining accumulation rates do not mirror organic carbon export. Our results suggest that both parameters may nevertheless relate to organic carbon burial in the Baffin Bay region in terms of acting as marine markers reflecting the marine fraction of the TOC content in the sediment. This strengthens the assumption that the TOC record after 6.0 ka reflects marine organic carbon burial.

#### **5.5.4 Burial efficiency**

Our results provide estimations for primary productivity (PP) and organic carbon burial (OCB) from dinocyst-based reconstruction of PP<sub>annual</sub> and TOC accumulation rates. Our results imply that, especially after 6.0 ka, TOC reflects marine organic carbon burial thus allowing us to evaluate the burial efficiency (OCB/PP) in Melville Bay during the Holocene. Burial efficiency was about 0.4% before 6 ka, followed by a maximum of about 0.6 – 0.8% between 6.0 and 5.0 ka, and a decrease to only 0.1% of the produced carbon being buried in the sediment at present day (Fig. 5.9 a). We find a general opposite trend of primary productivity and organic carbon burial ( $r = -0.4$ ,  $p < .01$ ; when only samples <6.0 ka are considered:  $r = -0.53$ ,  $p < .01$ ) (Fig. 5.9 b). This implies that less marine organic matter was buried in the sediment at times when the overall annual productivity appears to have been higher. This situation is reminiscent of the discovery by Lopes et al. (2015), who ascribed it to a decoupling between primary productivity and burial flux due to changes in export efficiency.

Burial efficiency increased around 6 ka when primary productivity was lowest (Fig. 5.6 a). A better preservation due to shorter oxygen exposure time (Emerson and Hedges, 1988; Hartnett et al., 1998) or sorption to mineral surfaces (Keil et al., 1994; Mayer, 1994) is probable as sedimentation rates also increased around 6 ka. (Fig. 5.8 b). A peak in export productivity around the same time (Fig. 5.7 a) supports the hypothesis of an additional decreased recycling within the water column and more organic matter reaching the ocean floor. Between 2.2 and 1.4 ka however, when primary productivity peaked, organic carbon burial, sedimentation rate and export productivity were low and still decreasing and burial efficiency was the lowest recorded during the Holocene. This implies that organic carbon burial was decoupled from

primary productivity due to a high amount of organic carbon recycling within the productive zone.

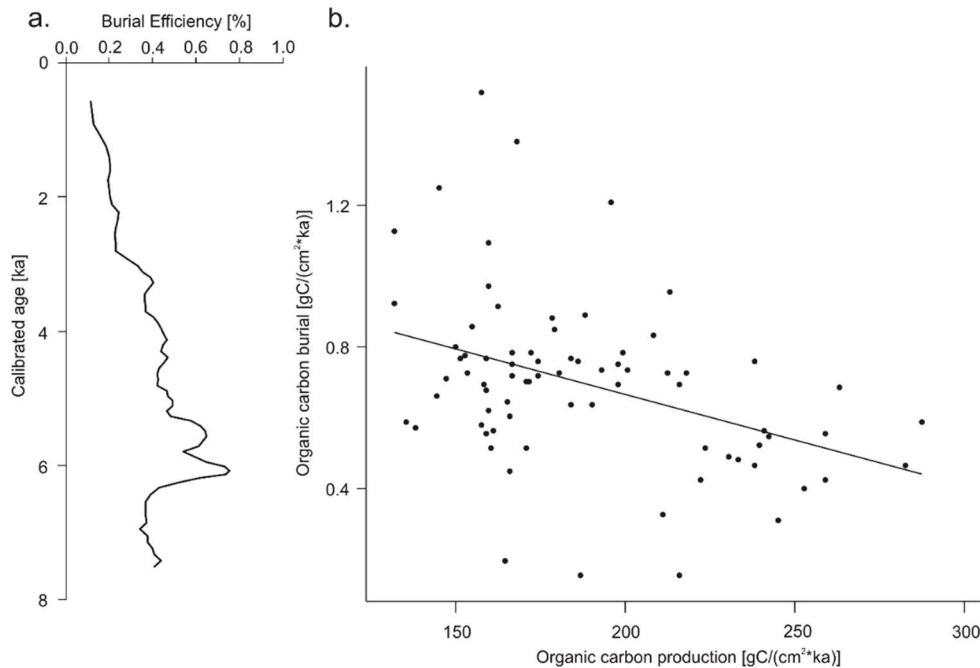


**Figure 5.9:** Burial efficiency. a) Burial efficiency (OCB/PP) estimated from TOC flux (OCB) and PP annual reconstruction (PP). Burial efficiency is shown as 5-point-moving-averages, calculated with R package zoo (Zeileis and Grothendieck, 2005). b) Carbon burial decreases with increasing carbon production ( $r = -0.4$ ,  $p < .01$ ).

### 5.5.5 Carbonate preservation

The bulk carbonate content in marine sediment is composed of marine carbonate and terrigenous carbonate, either biogenic (i.e. produced by (micro)organisms) or abiotic (i.e. from alteration). In high-latitude marine basins like the Melville Bay where sedimentation is largely controlled by detrital input and where the planktonic biogenic production is dominated by organic (dinoflagellate) or siliceous (diatom) microorganisms, only a very small fraction of the bulk sediment consists of biogenic carbonate from marine sources. We estimated the amount of marine biogenic carbonate applying accumulation rates of planktonic and benthic foraminifera accumulated shell weights (Fig. 5.10 a and b) and compared them with bulk carbonate fluxes (Fig. 5.10 c).

We find higher fluxes of planktonic foraminifera carbonate before 6.0 ka, suggesting either enhanced productivity of planktonic foraminifera or a better preservation of carbonate in the sediment. Carbonate dissolution was relatively low before 6.0 ka (Fig. 5.7 c and d) but it was

not much lower than during other phases and therefore do not provide an explanation for enhanced planktonic carbonate fluxes. Burial efficiency before 6.0 ka was also relatively low (Fig. 5.9 a), not promoting increased fluxes. Additionally, bulk carbonate accumulation rates show no correlation with planktonic carbonate fluxes ( $r = 0.32$ ) (Fig. 5.10 f). However, terrigenous input increased (Fig. 5.8 d), thus suggesting a faster burial of marine planktonic carbonate due to an increased amount of terrestrial detrital material, reducing the time of exposure to dissolving waters.

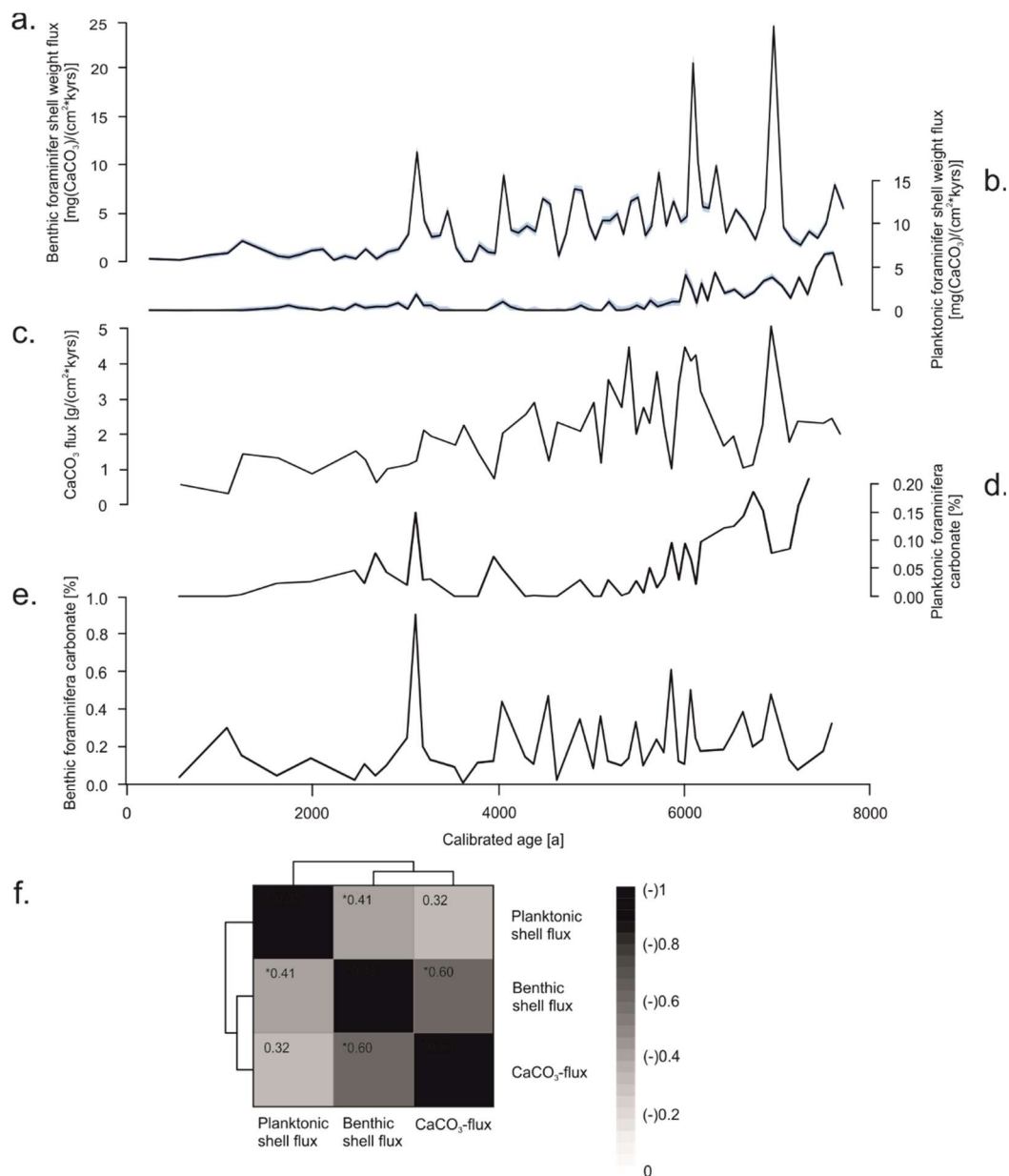


**Figure 5.10:** Carbonate parameters. a) Accumulation rate of benthic foraminifera carbonate [ $\text{mg CaCO}_3 \text{ cm}^{-2}\text{kyrs}^{-1}$ ], b) Accumulation rate of planktonic foraminifera carbonate [ $\text{mg CaCO}_3 \text{ cm}^{-2}\text{kyrs}^{-1}$ ], c) Bulk  $\text{CaCO}_3$  accumulation rate [ $\text{g cm}^{-2}\text{kyrs}^{-1}$ ], d) Planktonic foraminifera carbonate within bulk carbonate [%],

e) Benthic foraminifera carbonate within bulk carbonate [%]. f) Clustering heatmap indicating correlations between parameters (done with R package pheatmap (Kolde, 2019)). Asterisks indicate significant correlations after Bonferroni correction ( $p < .017$ ).

In our results, there is an increased fraction of planktonic carbonate within the bulk carbonate before 6.0 ka (Fig. 5.10 d). During that interval, we observe high ratios of planktonic carbonate coinciding with low accumulation rates of bulk carbonate, supporting the assumption of fast-deposited larger amounts of terrestrial non-carbonate material.

After 6.0 ka, two peaks of marine carbonate around 4.0 and 3.1 ka visible within both, planktonic and benthic fluxes and ratios, indicating an enhanced preservation or export productivity. Export productivity peaks around the same time (Fig. 5.7 a) while dissolution shows decreased values (Fig. 5.7 c and d), thus suggesting a combination of both.

## **5.5.6 Palaeoceanography**

### **5.5.6.1 Zone 4 (7.6 – 6.3 ka)**

Between 7.6 and 6.3 ka Baffin Bay was still a region of marginal ice zones (Fig. 5.11 g) (Saini et al., 2020), while the Laurentide and the Greenland ice sheets retreated (Fig. 5.11 c and d) (Dyke et al., 2003; Larsen et al., 2015). In the lowermost part of the core, a low primary productivity and moderate organic carbon burial rate led us to calculate a burial efficiency of about 0.3 % (Fig. 5.11 k). Export shows a peak around 7.0 ka coinciding with peaks in terrestrial input, bulk carbonate burial, biogenic marine carbonate burial, Greenland air temperature and a slight dip in sea surface salinity (Fig. 5.11 grey shaded area within zone 4). This suggests that a high air temperature fostered increased meltwater discharges. As sea ice and icebergs are important contributors of detrital particles in the Arctic (Wegner et al., 2015), high meltwater discharge likely resulted in enhanced terrigenous input, which in turn might have fostered faster deposition of carbonate and hence better preservation due to faster covering of deposited matter at the sea floor preventing long exposure to bottom waters and hence decomposition and dissolution (Emerson and Hedges, 1988; Hartnett et al., 1998). However, sedimentation rates during this interval have been low (Fig. 5.8 b) and a better preservation is not mirrored by organic carbon burial (Fig. 5.11 j). The combination of low organic carbon burial rates and enhanced terrestrial input suggests that most of the buried organic carbon is not of marine origin but terrestrial.

### 5.5.6.2 Zone 3 (6.3 – 3.1 ka)

After 6.3 ka the shift towards mild postglacial conditions was supposedly completed in Melville Bay (Gibb et al., 2015; Caron et al., 2019). This interval corresponds to optimal conditions in Greenland where surface temperatures were higher than today (Axford et al., 2013; Axford et al., 2021; Andresen et al., 2022).

Primary productivity slowly increased as indicated by dinocyst-based estimates, while export slowly decreased (Fig. 5.11). A rising primary productivity may result from continuously melting sea-ice after 6.5 ka (Fig. 5.11 f and g) and the resulting decrease in sea surface salinity after 5.0 ka (Fig. 5.11 e) in the study area. For southern Melville Bay, other records also propose a slow salinity decrease (Gibb et al., 2015; Caron et al., 2019), a continuous decrease in sea-ice cover (Gibb et al., 2015; Caron et al., 2019; Saini et al., 2020) and an increase in primary productivity (Caron et al., 2019) after ~6.0 ka. The adoption of warmer conditions in this area is likely a result of the reinforcement of the warmer component (IC) of the WGC and linked with the final retreat of the Laurentide and the Greenland Ice Sheet (Lloyd et al., 2005; Ouellet-Bernier et al., 2014; Gibb et al., 2015). Perner et al. (2013) recorded a higher influence of the IC between 6.2 and 3.5 ka.

At the Southwest Greenland margin dinoflagellate blooms in summer-fall have been associated with freshwater inputs due to meltwater runoff from the GIS, which triggers upwelling of nutrient-rich waters and high productivity (Juul-Pedersen et al., 2015; Krawczyk et al., 2015, 2018). Along most of the West Greenland margin, sea-ice melt and meltwater runoff from the GIS result in seasonal stratification of surface waters, which is amplified in summer by solar heat leading to relatively mild conditions (Juul-Pedersen et al., 2015; Tremblay et al., 2015) also enhancing primary productivity. While melting of sea-ice and icebergs in the near vicinity of the core site before 6.3 ka may have led to increased terrigenous input through ice rafted debris (IRD), the terrigenous influence after 6.3 ka decreased, fostering an increase in relative marine input. In other words, more distal detrital sediment sources inland (Giraudeau et al., 2020) resulted in less supply via IRD (Jennings et al., 2014). This is supported by the further retreat in Greenland ice sheet area (Fig. 5.11 c).

Enhanced burial of carbonate and organic carbon after 6.3 ka might have resulted from high export productivity (Fig. 5.11 i) and sedimentation rate (Fig. 5.8 b) resulting in a higher burial efficiency (Fig. 5.11 k). After 5.5 ka export productivity, carbonate burial and burial efficiency continuously declined, which may be attributed, at least in part, to enhanced carbonate dissolution. Two short intervals of better carbonate preservation around 4.0 and 3.2 ka coincide with peaks of increased biogenic carbonate burial and export productivity (Fig. 5.7 c-d and Fig.

5.11). As export productivity was estimated from the accumulation rate of benthic foraminifera shells, this led us to suppose that export rates were actually not decreasing during this interval but that the decrease is an artefact of dissolution rates.

#### 5.5.6.3 Zone 2 (3.1 – 0.7 ka)

During the late Holocene we observe maximum values for primary productivity and sea surface temperature and minimum values of sea-ice cover and sea surface salinity in southern Melville Bay (Fig. 5.11). Although other records from the West Greenland coast observe the beginning of subsurface cooling and glacier advances (e.g. Perner et al. 2013; Briner et al., 2016; Schweinsberg et al., 2017), known as the Neoglacial cooling trend (Weidick et al., 2012) since the last 4.0 ka (e.g. Knudsen et al., 2008; Seidenkrantz et al., 2008; Krawczyk et al., 2010; Andresen et al., 2010), we seem to see the continuing effect of the earlier interglacial warming until ~1.5 ka in records from Melville Bay (Fig. 5.11).

The Neoglacial cooling trend is marked by climate oscillations, including the short warming phases of the Roman Warm Period (2250-1600 a) (Lamb, 2002) and the Medieval Climatic Optimum (1100-700 a) (Lamb, 1965; Mann, 2002). Regional cooling accompanied by decreasing summer solar insolation (Berger and Loutre, 1991), fostering regrowth of the GIS (Briner et al., 2010; Weidick and Bennike, 2007; Young et al., 2011), as well as cooling over the GIS (Dahl-Jensen et al., 1998) led to more extensive sea-ice, which was accompanied by increasing sea surface salinity and a decline in primary productivity.

The increase in primary productivity until 1.5 ka is likely associated with a longer growing season due to sea-ice cover reduction, meltwater induced upwelling conditions (Juul-Pedersen et al., 2015; Krawczyk et al., 2015, 2018) and stratification leading to mild surface water conditions enhancing phytoplankton productivity. The dinocyst of *P. dalei* is the dominant dinocyst taxa between 3.0 and 1.0 ka (Fig. 5.4), suggesting a large seasonal gradient of sea surface temperature caused by stratified surface waters (Rochon et al., 1999; Solignac et al., 2006; Gibb et al., 2015) as cysts of *P. dalei* in the Arctic are associated with sea surface temperatures higher than 4°C and stratified, highly productive waters (Rochon et al., 1999; Matthiessen et al., 2005; Ribeiro et al., 2012).

The increase in primary productivity until 1.5 ka is in accordance to the increase in Caron et al. (2019). Caron et al. (2019) also observes a decrease in “polar” dinocyst taxa abundances until this time, supporting the assumption of the continuing effect of interglacial warming after

4.0 ka. Indeed, Gibb et al. (2015) observed warmer sea surface temperatures (increase by  $\sim 1.5^{\circ}\text{C}$ ) after  $\sim 3.1$  ka, which was attributed to enhanced strength of the IC in Baffin Bay.

Despite an increase in primary productivity of  $\sim 65\%$ , export productivity was low and organic carbon burial was even decreasing further (Fig. 5.11 i and j). This may be attributed to the strongly stratified surface waters, which held the organic matter in the upper layers and caused a longer residence time, leading to a more efficient organic matter recycling in the productive zone. This indicates that primary productivity, export productivity and burial were decoupled during the Holocene in Melville Bay.

The decrease in burial flux is strongly correlated to the decrease in sedimentation rate during this time ( $r = 0.91$ ;  $p < .01$ ), suggesting that a faster burial of organic matter due to a higher sedimentation rate had a stronger influence on the amount of buried organic carbon than the amount of produced or exported organic matter had.

After the Roman Climatic Optimum  $\sim 1.5$  ka, regional cooling and the continued regrowth of the Greenland Ice Sheet led to more extensive sea-ice, which was accompanied by high sea surface salinity and a decline in primary productivity (Fig 5.11). We also observe a decline in the abundance of autotrophic taxa, which were dominant before 1.5 ka, indicating warmer conditions, towards a codominance of the heterotrophic taxa *Brigantedinium* spp. and *I. minutum*, which is associated with harsh ice-covered conditions (Rochon et al., 1999; de Vernal et al., 2001, 2013; Zonneveld et al., 2013).

#### 5.5.6.4 Zone 1 (0.7 ka – present)

The recent period may illustrate the Little Ice Age conditions (700 – 150 a) (Mann, 2002a; Matthews and Briffa, 2005), with low temperatures over Greenland and glacier advances. Through the whole period, primary productivity was relatively low, and salinity and sea-ice increased. Export productivity, sedimentation rate, organic carbon burial, burial efficiency and terrigenous input showed the lowest values considering the last 8.0 ka (Fig. 5.11). This suggests that cooling conditions, although leading to an increase in salinity and hence reduced stratification and less organic matter recycling in the surface layers, caused a reduction in export productivity because primary productivity also decreased. In addition environmental cooling led to decreased terrigenous input due to less melting ice, causing the sedimentation rate to even decrease more, which in combination with low export seems to have resulted in extremely low burial rates of organic carbon and hence a minimum burial efficiency.



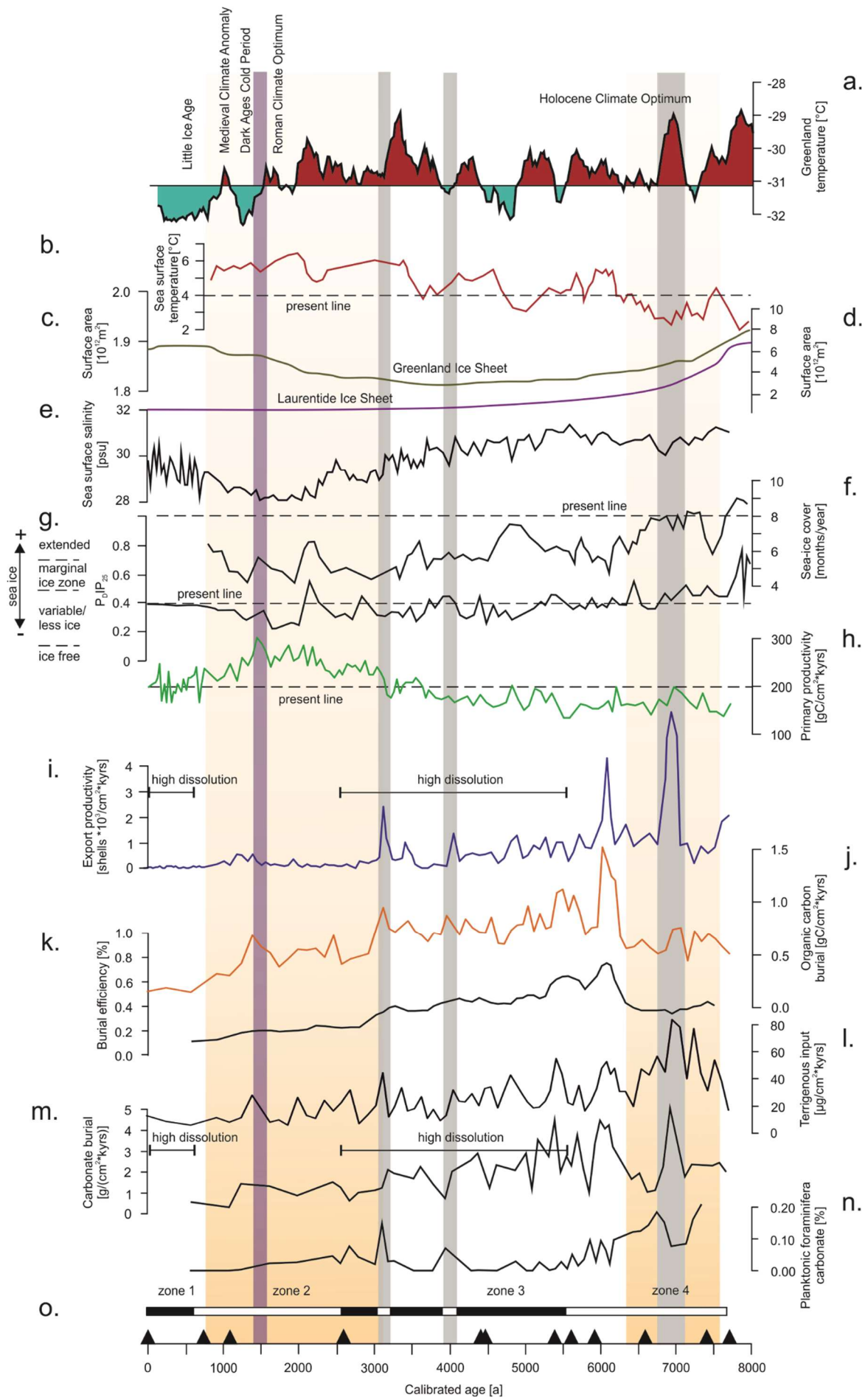


**Figure 5.11:** Time series in core GeoB19927-3. a) Greenland temperatures based on  $\delta^{18}\text{O}$  from the GISP ice core (Alley et al., 2010), b) Summer sea surface temperature in Melville Bay based on dinocyst assemblages (Caron et al., 2019), c) Greenland Ice Sheet area (Larsen et al., 2015), d) Laurentide Ice Sheet area (Dyke et al., 2003), e) Sea surface salinity based on a WA-PLS reconstruction from dinocyst assemblages (Hohmann et al., 2023), f) Sea-ice coverage in Melville Bay based on dinocyst assemblages (Caron et al., 2019), g) Sea-ice coverage in Melville Bay based on a PIP<sub>25</sub> index using dinosterol (Saini et al., 2020), classification of different sea-ice scenarios based on (Müller et al., 2011), h) Annual primary productivity estimates from dinocyst assemblages, i) Export productivity based on BFAR, j) Organic carbon burial based on TOC accumulation rates, k) Burial efficiency (OCB/PP), l) Terrigenous input based on  $\beta$ -sito+campesterol accumulation rates, m) Carbonate burial based on bulk  $\text{CaCO}_3$ , n) Planktonic foraminifera carbonate ratio within bulk  $\text{CaCO}_3$ , o) Intensity of dissolution based on OL- and B/P-indices, white indicates continuous and relatively low dissolution, black indicates high and erratic dissolution. Ecozones based on dinocyst assemblages are shaded in orange/white. Grey shaded areas represent events during zones 3 and 4. Violet shaded area represents environmental shift around 1.5 ka.

## 5.6 Conclusion

We aimed to evaluate the natural variability of marine biological productivity processes driving the marine biological carbon pump in the eastern Baffin Bay during the Holocene.

The terrestrial component of organic carbon burial before 6.3 ka was too high to allow a solid interpretation of the data in terms of the biological carbon pump. After 6.3 ka terrigenous input decreased and suggested that the buried organic carbon is predominantly of marine origin, which rendered reliable interpretations possible.

Between 6.3 and 1.5 ka we observed the ongoing effects of interglacial warming mirrored by continuous melting conditions with reduction in ice cover and sea surface salinity and increase in sea surface temperature and primary productivity. Melting processes supposedly fostered longer growth seasons, upwelling conditions and mild surface waters due to enhanced stratification.

Despite increased primary productivity, we observed low export productivity and a decreasing organic carbon burial, which might be attributed to strongly stratified surface waters, holding the organic matter in the upper layers and causing a longer residence time, leading to a more efficient organic matter recycling in the productive zone. We additionally found a strong correlation between organic carbon burial and sedimentation rate, which suggested that a fast burial induced by high sedimentation had a stronger influence on the amount of buried organic carbon than the amount of produced or exported organic matter had.

Our results indicate that primary productivity, export productivity and organic carbon burial were decoupled during the Holocene in Melville Bay, which was probably caused by changes in export efficiency, induced by a combination of an increase in the efficiency of organic matter recycling in the productive zone and a decrease in preservation due to longer oxygen exposure times induced by low sedimentation rates. Our results suggest that during meltwater-influenced warming conditions the efficiency of the organic carbon pump decreases.

## 5.7 Data availability

New data from core GeoB19927-3 used in this manuscript were uploaded to PANGAEA and will be available soon.

## 5.8 Acknowledgements

This study is a contribution of the International Research Training Group “Processes and Impacts of Climate Change in the North Atlantic Ocean and the Canadian Arctic” (ArcTrain), which was supported jointly by the German Research Foundation (DFG) (IRTG 1904) and by the Natural Sciences and Engineering Research Council of Canada (NSERC). We also acknowledge the support from the *Fonds de recherche du Québec – Nature et Technologies* (FRQNT).

## 5.9 References (Chapter 5)

Aksu, A. E. (1983) ‘Holocene and Pleistocene dissolution cycles in deep-sea cores of Baffin Bay and Davis Strait: Palaeoceanographic implications’, *Marine Geology*, 53(4), pp. 331–348. doi: 10.1016/0025-3227(83)90049-X.

Allan, E. et al. (2018) ‘Late Holocene sea-surface instabilities in the Disko Bugt area, west Greenland, in phase with  $\delta^{18}\text{O}$ -oscillations at Camp Century’, *Paleogeography and Paleoclimatology*, 33, pp. 227–243. doi: 10.1002/2017PA003289.

Alley, R. B. et al. (2010) ‘History of the Greenland Ice Sheet: paleoclimatic insights’, *Quaternary Science Reviews*. Elsevier Ltd, 29, pp. 1728–1756. doi: 10.1016/j.quascirev.2010.02.007.

Andresen, C.S., McCarthy, D.J., Dylmer, C.V., Seidenkrantz, M., Kuijpers, A., Lloyd, J.M. (2010) ‘Interaction between subsurface ocean waters and calving of the Jakobshavn Isbræ during the late Holocene’, *The Holocene*, 21, pp. 211–224. doi: 10.1177/0959683610378877.

Andresen, C. S. et al. (2022) ‘Early Holocene palaeoceanographic and glaciological changes in southeast Greenland’, *Holocene*, 32(6), pp. 501–514. doi: 10.1177/09596836221080758.

Ardyna, M. and Arrigo, K. R. (2020) ‘Phytoplankton dynamics in a changing Arctic Ocean’, *Nature Climate Change*. Springer US, 10(October), pp. 892–903. doi: 10.1038/s41558-020-0905-y.

- Arndt, S. et al. (2013) 'Quantifying the degradation of organic matter in marine sediments: A review and synthesis', *Earth-Science Reviews*. Elsevier B.V., 123, pp. 53–86. doi: 10.1016/j.earscirev.2013.02.008.
- Arrigo, K. R. (2013) 'The changing Arctic Ocean', *Elementa: Science of the Anthropocene*, 1. doi: 10.12952/journal.elementa.000010.
- Arrigo, K. R. and van Dijken, G. L. (2015) 'Continued increases in Arctic Ocean primary production', *Progress in Oceanography*. Elsevier Ltd, 136, pp. 60–70. doi: 10.1016/j.pocean.2015.05.002.
- Arrigo, K. R., van Dijken, G. and Pabi, S. (2008) 'Impact of a shrinking Arctic ice cover on marine primary production', *Geophysical Research Letters*, 35(19), pp. 1–6. doi: 10.1029/2008GL035028.
- Axford, Y. et al. (2013) 'Holocene temperature history at the western Greenland Ice Sheet margin reconstructed from lake sediments', *Quaternary Science Reviews*. Elsevier Ltd, 59, pp. 87–100. doi: 10.1016/j.quascirev.2012.10.024.
- Axford, Y., De Vernal, A. and Osterberg, E. C. (2021) 'Past warmth and its impacts during the holocene thermal maximum in greenland', *Annual Review of Earth and Planetary Sciences*, 49, pp. 279–307. doi: 10.1146/annurev-earth-081420-063858.
- Behrenfeld, M. J. et al. (2001) 'Biospheric Primary Production During an ENSO Transition', *Science*, 291(5513), pp. 2594–2597. doi: 10.1016/j.cognition.2008.05.007.
- Bélanger, S., Babin, M. and Tremblay, J.-É. (2013) 'Increasing cloudiness in Arctic damps the increase in phytoplankton primary production due to sea ice receding', *Biogeosciences*, 10(6), pp. 4087–4101. doi: 10.5194/bg-10-4087-2013.
- Berger, W. H. (1970) 'Planktonic Foraminifera: Selective Solution and the Lysocline', *Marine Geology*, 8, pp. 111–138.
- Berger, W. H., Smetacek, V. and Wefer, G. (1989) 'Ocean productivity and paleoproductivity - an overview', in *Productivity of the Ocean: Present and Past*, John Wiley & Sons Limited, pp. 1–34.
- Birks, J. B. (1995) 'Quantitative palaeoenvironmental reconstructions', in Maddy, D. and Brew, I. S. (eds) *Statistical Modelling of Quaternary Science Data*. Technical. Cambridge: Quaternary Research Association, p. 271 pp.
- Boertmann, D. et al. (2013) 'Disko West. A strategic environmental impact assessment of hydrocarbon activities', Aarhus University, DCE–Danish Centre for Environment and Energy, 71, p. 306.
- Boetius, A. et al. (2013) 'Supplementary material for: Export of Algal Biomass from the Melting Arctic Sea Ice', *Science*, 339(6126), pp. 1430–1432. doi: 10.1126/science.1231346.
- Briner, J. P. et al. (2016) 'Holocene climate change in Arctic Canada and Greenland', *Quaternary Science Reviews*, 147, pp. 340–364. doi: 10.1016/j.quascirev.2016.02.010.
- Broecker, W. S. (1982) 'Glacial to interglacial changes in ocean chemistry', *Progress in Oceanography*, 11(2), pp. 151–197. doi: 10.1016/0079-6611(82)90007-6.
- Buch, E. (1981) 'A review of the oceanographic conditions in subarea O and 1 in the decade 1970–1979'.
- Caron, M., Rochon, A., Carlos, J., Serrano, M., Onge, G.S.T. (2019) 'Evolution of sea - surface conditions on the northwestern Greenland margin during the Holocene', *J. Quat. Sci.*, 34, pp. 569–580. doi: 10.1002/jqs.3146.

- Caron, M. et al. (2020) 'Quantifying Provenance and Transport Pathways of Holocene Sediments From the Northwestern Greenland Margin', *Paleoceanography and Paleoclimatology*, 35(5), pp. 1–23. doi: 10.1029/2019PA003809.
- Chang, A. S., Pedersen, T. F. and Hendy, I. L. (2014) 'Effects of productivity, glaciation, and ventilation on late Quaternary sedimentary redox and trace element accumulation on the Vancouver Island margin, western Canada', *Paleoceanography*, 29(7), pp. 730–746. doi: 10.1002/2013PA002581.
- Coxall, H. K. and Wilson, P. A. (2011) 'Early Oligocene glaciation and productivity in the eastern equatorial Pacific: Insights into global carbon cycling', *Paleoceanography*, 26(2), pp. 1–18. doi: 10.1029/2010PA002021.
- Dorschel, B. et al. (2015) 'Past Greenland Ice Sheet dynamics, Palaeoceanography and Plankton Ecology in the Northeast Baffin Bay - Cruise No. MSM44 "BAFFEAST" - June 30-July 30, 2015 - Nuuk (Greenland)', *MARIA S. MERIAN-Berichte*, p. 51. doi: 10.2312/cr\_msm2344.
- Ducklow, H.W., Steinberg, D.K., Buch, E. (2001) 'Upper ocean carbon export and the biological pump', *Oceanography*, 14, pp. 50–58. doi: 10.5670/oceanog.2001.06.
- Dyke, A. S., Moore, A. and Robertson, L. (2003) 'Deglaciation of North America', *Geol. Surv. Can., Open File*.
- Ehrmann, W. and Thiede, J. (1985) 'History of Mesozoic and Cenozoic sediment fluxes to the North Atlantic Ocean', *Contributions to Sedimentology*, 15, pp. 1–109.
- Emerson, S. and Hedges, J. I. (1988) 'Processes controlling the organic carbon content of open ocean sediments', *Paleoceanography*, 3(5), pp. 621–634.
- Fahl, K. and Stein, R. (1997) 'Modern organic carbon deposition in the Laptev Sea and the adjacent continental slope: Surface water productivity vs. terrigenous input', *Organic Geochemistry*, 26(5–6), pp. 379–390. doi: 10.1016/S0146-6380(97)00007-7.
- Fahl, K. and Stein, R. (1999) 'Biomarkers as organic-carbon-source and environmental indicators in the Late Quaternary Arctic Ocean: problems and perspectives', *Marine Chemistry*, 63, pp. 293–309. doi: 10.1016/S0304-4203(98)00068-1.
- Falkowski, P. G., Barber, R. T. and Smetacek, V. (1998) 'Biogeochemical controls and feedbacks on ocean primary production', *Science*, 281(1998), pp. 200–206. doi: 10.1126/science.281.5374.200.
- Field, C. B. et al. (1998) 'Primary production of the biosphere: integrating terrestrial and oceanic components', *Science*, 281(5374), pp. 237–240. doi: 10.1016/j.cognition.2008.05.007.
- Fontanier, C. et al. (2008) 'Live foraminifera from the open slope between Grand Rhône and Petit Rhône Canyons (Gulf of Lions, NW Mediterranean)', *Deep-Sea Research Part I: Oceanographic Research Papers*, 55(11), pp. 1532–1553. doi: 10.1016/j.dsr.2008.07.003.
- Georgiadis, E. et al. (2018) 'Deglacial to postglacial history of Nares Strait ,Northwest Greenland: a marine perspective from Kane Basin', *Climate of the Past*, 14(12), pp. 1991–2010. doi: 10.5194/cp-14-1991-2018.
- Gibb, O. T., Hillaire-Marcel, C. and de Vernal, A. (2014) 'Oceanographic regimes in the northwest Labrador Sea since Marine Isotope Stage 3 based on dinocyst and stable isotope proxy records', *Quaternary Science Reviews*, 92(April), pp. 269–279. doi: 10.1016/j.quascirev.2013.12.010.
- Gibb, O.T., Steinhauer, S., Frechette, B., de Vernal, A., Hillaire-Marcel, C. (2015) 'Diachronous evolution of sea surface conditions in the Labrador Sea and Baffin Bay since the last deglaciation', *The Holocene*, 25, pp. 1882–1897. doi: 10.1177/0959683615591352.

- Giraudeau, J. et al. (2020) A high-resolution elemental record of post-glacial lithic sedimentation in Upernavik Trough, western Greenland: History of ice-sheet dynamics and ocean circulation changes over the last 9100 years, *Global and Planetary Change*. doi: 10.1016/j.gloplacha.2020.103217.
- Gooday, A. J. (2003) 'Benthic foraminifera (protista) as tools in deep-water palaeoceanography: Environmental influences on faunal characteristics', in: Academic Press (*Advances in Marine Biology*), pp. 1–90. doi: [https://doi.org/10.1016/S0065-2881\(03\)46002-1](https://doi.org/10.1016/S0065-2881(03)46002-1).
- Gooday, A. J. and Jorissen, F. J. (2012) 'Benthic foraminiferal biogeography: Controls on global distribution patterns in deep-water settings', *Annual Review of Marine Science*, 4, pp. 237–262. doi: 10.1146/annurev-marine-120709-142737.
- Gosselin, M. et al. (1997) 'New measurements of phytoplankton and ice algal production in the Arctic Ocean', *Deep-Sea Research II*, 44(8), pp. 1623–1644. Available at: <http://www.sciencedirect.com/science/article/pii/S0967064597000544%5Cnpapers2://publication/uuid/6E70D9B9-2D57-4A2C-89A5-80B54F5B3DCC>.
- Gradinger, R. (1995) 'Climate change and biological oceanography of the Arctic Ocean', *Philosophical Transactions: Physical Sciences and Engineering*, 352(1699), pp. 277–286. doi: <https://doi.org/10.1098/rsta.1995.0070>.
- Hald, M. and Korsun, S. (1997) 'Distribution of modern benthic foraminifera from fjords of Svalbard, European Arctic', *Journal of Foraminiferal Research*, 27(2), pp. 101–122. doi: 10.2113/gsjfr.27.2.101.
- Hamel, D. et al. (2002) 'Organic-walled microfossils and geochemical tracers: Sedimentary indicators of productivity changes in the North Water and northern Baffin Bay during the last centuries', *Deep-Sea Research Part II: Topical Studies in Oceanography*, 49(22–23), pp. 5277–5295. doi: 10.1016/S0967-0645(02)00190-X.
- Hartnett, H. E. et al. (1998) 'Influence of oxygen exposure time on organic carbon preservation in continental margin sediments', *Nature*, 391(6667), pp. 572–574.
- Hebbeln, D. and Wefer, G. (1991) 'Effects of ice coverage and ice-rafted material on sedimentation in the Fram Strait', *Nature*, 350, pp. 409–411. doi: 10.1038/350409a0.
- Heinze, C., Maier-Reimer, E. and Winn, K. (1991) 'Glacial pCO<sub>2</sub> Reduction by the World Ocean: Experiments With the Hamburg Carbon Cycle Model', *Paleoceanography*, 6(4), pp. 395–430.
- Henson, S., Lampitt, R. and Johns, D. (2012) 'Variability in phytoplankton community structure in response to the North Atlantic Oscillation and implications for organic carbon flux', *Limnology and Oceanography*, 57(6), pp. 1591–1601. doi: 10.4319/lo.2012.57.6.1591.
- Herguera, J. C. (1992) 'Deep-sea benthic foraminifera and biogenic opal: Glacial to postglacial productivity changes in the western equatorial Pacific', *Marine Micropaleontology*, 19(1–2), pp. 79–98. doi: 10.1016/0377-8398(92)90022-C.
- Herguera, J. C. and Berger, W. H. (1991) 'Paleoproductivity from benthic foraminifera abundance : Glacial to postglacial change in the west-equatorial Pacific', *Geology*, 19, pp. 1173–1176.
- Hohmann, S., Kucera, M. and de Vernal, A. (2023) 'Disentangling environmental drivers of Subarctic dinocyst assemblage compositional change during the Holocene', *EGUsphere*, 2023, pp. 1-46. doi: 10.5194/egusphere-2023-561.
- Hohmann, S., Kucera, M. and de Vernal, A. (2020) 'Identifying the signature of sea-surface properties in dinocyst assemblages: Implications for quantitative palaeoceanographical reconstructions by transfer functions and analogue techniques', *Marine Micropaleontology*, 159, p. 101816. doi: <https://doi.org/10.1016/j.marmicro.2019.101816>.

Hörner, T. et al. (2016) 'Post-glacial variability of sea ice cover , river run-off and biological production in the western Laptev Sea ( Arctic Ocean ) e A high- resolution biomarker study', *Quaternary Science Reviews*, 143, pp. 133–149. doi: 10.1016/j.quascirev.2016.04.011.

Hunt, A. S. and Corliss, B. H. (1993) 'Distribution and microhabitats of living (stained) benthic foraminifera from the Canadian Arctic Archipelago', *Marine Micropaleontology*, 20(3–4), pp. 321–345. doi: 10.1016/0377-8398(93)90041-U.

Imbrie, J. and Kipp, N. G. (1971) 'A new micropaleontological method for quantitative paleoclimatology: application to a late Pleistocene Caribbean core', in Turekian, K. K. (ed.) *The late Cenozoic glacial ages*. New Haven: Yale University Press, pp. 71–181.

IPCC (2013) *Climate Change 2013: The Physical Science Basis. Contribution of Working Group I to the Fifth Assessment Report of the Intergovernmental Panel on Climate Change*. doi: 10.1017/CBO9781107415324.Summary.

Jennings, A. et al. (2011) 'The Holocene history of Nares Strait: transition from Glacial Bay to Arctic-Atlantic throughflow', *Oceanography*, 24(3), pp. 26–41.

Jennings, A. E. et al. (2004) 'Modern foraminiferal faunas of the southwestern to northern Iceland Shelf: Oceanographic and environmental controls', *Journal of Foraminiferal Research*, 34(3), pp. 180–207. doi: <https://doi.org/10.2113/34.3.180>.

Jennings, A. E. et al. (2014) 'Paleoenvironments during Younger Dryas-Early Holocene retreat of the Greenland Ice Sheet from outer Disko Trough, central west Greenland', *Journal of Quaternary Science*, 29(1), pp. 27–40. doi: 10.1002/jqs.2652.

Jennings, A. E. and Helgadottir, G. (1994) 'Foraminiferal assemblages from the fjords and shelf of eastern Greenland', *Journal of Foraminiferal Research*, 24(2), pp. 123–144. doi: <https://doi.org/10.2113/gsjfr.24.2.123>.

Jones, P. D., Wigley, T. M. L. and Raper, S. C. B. (1987) 'The Rapidity of CO<sub>2</sub>-Induced Climatic Change: Observations, Model Results and Palaeoclimatic Implications', in Berger, W. H. and Labeyrie, L. D. (eds) *Abrupt Climatic Change: Evidence and Implications*. Dordrecht: Springer Netherlands, pp. 47–55. doi: 10.1007/978-94-009-3993-6\_4.

Jorissen, F. J., Fontanier, C. and Thomas, E. (2007) 'Chapter Seven Paleooceanographical Proxies Based on Deep-Sea Benthic Foraminiferal Assemblage Characteristics', in Hillaire–Marcel, C. and de Vernal, A. (eds) *Proxies in Late Cenozoic Paleooceanography*. Developmen. Elsevier, pp. 263–325. doi: 10.1016/S1572-5480(07)01012-3.

Juggins, S. (2017) 'rioja: Analysis of Quaternary Science Data'. Available at: <http://cran.r-project.org/package=rioja>.

Juul-pedersen, T. et al. (2015) 'Seasonal and interannual phytoplankton production in a sub-Arctic tidewater outlet glacier fjord, SW Greenland', *Marine Ecology Progress Series*, 524, pp. 27–38. doi: 10.3354/meps11174.

Kahru, M. et al. (2011) 'Are phytoplankton blooms occurring earlier in the Arctic?', *Global Change Biology*, 17(4), pp. 1733–1739. doi: 10.1111/j.1365-2486.2010.02312.x.

Keil, R. G. et al. (1994) 'Sorptive preservation of labile organic matter in marine sediments', *Nature*, 370, pp. 549–552.

Kinnard, C. et al. (2011) 'Reconstructed changes in Arctic sea ice over the past 1,450 years', *Nature*, 479, pp. 509–512. doi: <https://doi.org/10.1038/nature10581>.

- Knudsen, K. L. et al. (2008) 'Deglacial and Holocene conditions in northernmost Baffin Bay: Sediments, foraminifera, diatoms and stable isotopes', *Boreas*, 37(3), pp. 346–376. doi: 10.1111/j.1502-3885.2008.00035.x.
- Kolde, R. (2019) 'pheatmap: Pretty Heatmaps. R package version 1.0.12'. Available at: <https://cran.r-project.org/package=pheatmap>.
- Krawczyk, D., Witkowski, A., Moros, M., Lloyd, J., Kuijpers, A., Kierzek, A. (2010) 'Late-Holocene diatom-inferred reconstruction of temperature variations of the West Greenland Current from Disko Bugt, Central West Greenland', *The Holocene*, 20, pp. 659–666. doi: 10.1177/0959683610371993.
- Krawczyk, D. W. et al. (2015) 'Microplankton succession in a SW Greenland tidewater glacial fjord influenced by coastal inflows and run-off from the Greenland Ice Sheet', *Polar Biology*. Springer Berlin Heidelberg, 38(9), pp. 1515–1533. doi: 10.1007/s00300-015-1715-y.
- Krawczyk, D. W. et al. (2018) 'Seasonal succession, distribution, and diversity of planktonic protists in relation to hydrography of the Godthåbsfjord system (SW Greenland)', *Polar Biology*, 41(10), pp. 2033–2052. doi: 10.1007/s00300-018-2343-0.
- Łącka, M. and Zajączkowski, M. (2016) 'Does the recent pool of benthic foraminiferal tests in fjordic surface sediments reflect interannual environmental changes? The resolution limit of the foraminiferal record', *Annales Societatis Geologorum Poloniae*, 86(1), pp. 59–71. doi: 10.14241/asgp.2015.019.
- Lamb, H. H. (1965) 'The early medieval warm epoch and its sequel', *Palaeogeography, Palaeoclimatology, Palaeoecology*, 1, pp. 13–37. doi: 10.1016/0031-0182(65)90004-0.
- Lamb, H. H. (2002) *Climate, history and the modern world*. Routledge.
- Larsen, N. K. et al. (2015) 'The response of the southern Greenland ice sheet to the Holocene thermal maximum', *Geology*, 43(4), pp. 291–294. Available at: <http://dx.doi.org/10.1130/G36476.1>.
- Lepš, J. and Šmilauer, P. (2003) *Multivariate analysis of ecological data using CANOCO*. Cambridge university press.
- Levac, E., De Vernal, A. and Blake, W. (2001) 'Sea-surface conditions in northernmost Baffin Bay during the Holocene: Palynological evidence', *Journal of Quaternary Science*, 16(4), pp. 353–363. doi: 10.1002/jqs.614.
- Lewis, K. M., Dijken, G. L. Van and Arrigo, K. R. (2020) 'Changes in phytoplankton concentration now drive increased Arctic Ocean primary production', *Science*, 202(July), pp. 198–202.
- Lisitzin, A. P. (1972) 'Sedimentation in the world ocean', *Soc. Econ. Paleontol. Mineral., Spec. Publ.*, 17, p. 218 pp.
- Lloyd JM, Park LA, Kuijpers A, et al. (2005) 'Early Holocene palaeoceanography and deglacial chronology of Disko Bugt, west Greenland', *Quaternary Science Reviews*, 24 (14-15), pp. 1741–1755.
- Loeng, H. et al. (2005) 'Marine systems', in Symon, C., Arris, L., and Heal, B. (eds) *Arctic climate impact assessment*. New York: Cambridge University Press, pp. 453–538.
- Lopes, C., Kucera, M. and Mix, A. C. (2015) 'Climate change decouples oceanic primary and export productivity and organic carbon burial.', *Proceedings of the National Academy of Sciences of the United States of America*, 112(2), pp. 332–5. doi: 10.1073/pnas.1410480111.
- Lutz, M., Dunbar, R. and Caldeira, K. (2002) 'Regional variability in the vertical flux of particulate organic carbon in the ocean interior', *Global biogeochemical cycles*, 16(3), pp. 11–18. doi: 10.1029/2000gb001383.



- Mackensen, A., Sejrup, H. P. and Jansen, E. (1985) 'The distribution of living benthic foraminifera in the continental slope and rise off Southwest Norway', *Marine Micropaleontology*, 9, pp. 275–306.
- Mann, M. E. (2002a) 'Little Ice Age', *Encyclopedia of Global Environmental Change*, 1, pp. 504–509. doi: 10.1007/1-4020-3266-8\_127.
- Mann, M. E. (2002b) 'Medieval Climatic Optimum', *Encyclopedia of Global Environmental Change*, 1, pp. 514–516.
- Marret, F. and Zonneveld, K. a. F. (2003) 'Atlas of modern organic-walled dinoflagellate cyst distribution', *Review of Palaeobotany and Palynology*, 125(1–2), pp. 1–200. doi: 10.1016/S0034-6667(02)00229-4.
- Matthews, B. Y. J. (1969) 'The Assessment of a Method for the Determination of Absolute Pollen Frequencies', *New Phytologist*, 68, pp. 161–166. doi: 10.1111/j.1469-8137.1969.tb06429.x.
- Matthews, J. A. and Briffa, K. R. (2005) 'The "little ice age": re-evaluation of an evolving concept', *Geografiska Annaler: Series A, Physical Geography*, 87(1), pp. 17–36. doi: 10.1111/j.0435-3676.2005.00242.x.
- Matthiessen, J., de Vernal, A., Head, M., et al. (2005) 'Modern organic-walled dinoflagellate cysts in Arctic marine environments and their (paleo-) environmental significance', *Paläontologische Zeitschrift*, 79 (1), pp. 3–51.
- Mayer, L. M. (1994) 'Surface area control of organic carbon accumulation in continental shelf sediments', *Geochimica et Cosmochimica Acta*, 58(4), pp. 1271–1284. doi: 10.1016/0016-7037(94)90381-6.
- Meir, W. N. (2011) 'Sea ice', in *Snow, Water, Ice and Permafrost in the Arctic: Climate Change and the Cryosphere*. Oslo, Norway: Arctic Monitoring and Assessment Program (AMAP), pp. 1–82.
- Meyers, P. A. (1997) 'Organic geochemical proxies of paleoceanographic, paleolimnologic, and paleoclimatic processes', *Organic Geochemistry*, 27(5), pp. 213–250. doi: [https://doi.org/10.1016/S0146-6380\(97\)00049-1](https://doi.org/10.1016/S0146-6380(97)00049-1).
- Milker, Y. and Schmiedl, G. (2012) 'A taxonomic guide to modern benthic shelf foraminifera of the western Mediterranean sea', *Palaeontologia Electronica*, 15(2). doi: 10.26879/271.
- Mouradian, M. et al. (2007) 'Dinosterols or dinocysts to estimate dinoflagellate contributions to marine sedimentary organic matter?', *Limnology and Oceanography*, 52(6), pp. 2569–2581. doi: 10.4319/lo.2007.52.6.2569.
- Müller-Navarra, K., Milker, Y. and Schmiedl, G. (2016) 'Natural and anthropogenic influence on the distribution of salt marsh foraminifera in the Bay of Tümlau, German North Sea', *Journal of Foraminiferal Research*, 46(1), pp. 61–74. doi: <https://doi.org/10.2113/gsjfr.46.1.61>.
- Müller, J. et al. (2011) 'Towards quantitative sea ice reconstructions in the northern North Atlantic: A combined biomarker and numerical modelling approach', *Earth and Planetary Science Letters*. Elsevier B.V., 306, pp. 137–148. doi: 10.1016/j.epsl.2011.04.011.
- Nöthig, E.-M. et al. (2015) 'Summertime plankton ecology in Fram Strait—a compilation of long- and short-term observations', *Polar Research*. Routledge, 34(1), p. 23349. doi: 10.3402/polar.v34.23349.
- NSIDC (2018) National Snow and Ice Data Center (NSIDC) - Arctic Sea Ice News and Analysis.
- O'Malley, R. (2018) Online Data: Standard VGPM, Ocean Productivity. Available at: <http://orca.science.oregonstate.edu/2160.by.4320.monthly.xyz.vgpm.m.chl.m.sst.php> (Accessed: 20 November 2018).

- Oksanen, J. et al. (2017) 'vegan: Community Ecology Package'. Available at: <https://cran.r-project.org/package=vegan>.
- Ouellet-Bernier, M. M. et al. (2014) 'Paleoceanographic changes in the Disko Bugt area, West Greenland, during the Holocene', *Holocene*, 24(11), pp. 1573–1583. doi: 10.1177/0959683614544060.
- Pabi, S., Dijken, G. L. Van and Arrigo, K. R. (2008) 'Primary production in the Arctic Ocean , 1998 – 2006', *Journal of Geophysical Research*, 113(2008), pp. 1998–2006. doi: 10.1029/2007JC004578.
- Passow, U. and Carlson, C. A. (2012) 'The biological pump in a high CO<sub>2</sub> world', *Marine Ecology Progress Series*, 470(2), pp. 249–271. doi: 10.3354/meps09985.
- Perner, K. et al. (2013) 'Holocene palaeoceanographic evolution off West Greenland', *The Holocene*, 23(3), pp. 374–387. doi: 10.1177/0959683612460785.
- Poulin, M. et al. (2011) 'The pan-Arctic biodiversity of marine pelagic and sea-ice unicellular eukaryotes: A first-attempt assessment', *Marine Biodiversity*, 41, pp. 13–28. doi: 10.1007/s12526-010-0058-8.
- R Core Team (2017) 'R: A Language and Environment for Statistical Computing'. Vienna, Austria. Available at: <http://www.r-project.org/>.
- Radi, T. and de Vernal, A. (2008) 'Dinocysts as proxy of primary productivity in mid-high latitudes of the Northern Hemisphere', *Marine Micropaleontology*, 68(1–2), pp. 84–114. doi: 10.1016/j.marmicro.2008.01.012.
- Randelhoff, A. et al. (2020) 'Pan-Arctic Ocean primary production constrained by turbulent nitrate fluxes', *Frontiers in Marine Science*, 7. doi: Achim Randelhoff<sup>1,2\*</sup>, Johnna Holding<sup>3,4</sup>, Markus Janout<sup>5</sup>, Mikael Kristian Sejr<sup>3,4</sup>, Marcel Babin<sup>1,2</sup>, Jean-Éric Tremblay<sup>1,2</sup> and Matthew B. Alkire<sup>6†</sup>.
- Raven, J. A. and Falkowski, P. G. (1999) 'Oceanic sinks for atmospheric CO<sub>2</sub>', *Plant, Cell and Environment*, 22(6), pp. 741–755. doi: 10.1046/j.1365-3040.1999.00419.x.
- Ribeiro, S., Moros, M., Ellegaard, M., et al. (2012) 'Climate variability in West Greenland during the past 1500 years: Evidence from a high-resolution marine palynological record from Disko Bay', *Boreas*, 41, pp. 68–83.
- Rignot, E. and Kanagaratnam, P. (2006) 'Changes in the Velocity Structure of the Greenland Ice Sheet', *Science*, 311(5763), pp. 986–991. doi: 10.1126/science.1121381.
- Risdal, D. (1964) 'The bathymetrical relation of récent foraminiferal faunas in the Oslo fjord, with a discussion of the foraminiferal zones from late Quaternary time', *Norges Geologiske Under søkelser*, 226, pp. 1–142.
- Rochon, A. et al. (1999) 'Distribution of recent dinoflagellate cysts in surface sediments from the North Atlantic Ocean and adjacent seas in relation to sea-surface parameters', *American Association of Stratigraphic Palynologists Contribution Series*, 35, pp. 1–146.
- Sabine, C. L. et al. (2004) 'The oceanic sink for anthropogenic CO<sub>2</sub>.', *Science (New York, N.Y.)*, 305(5682), pp. 367–71. doi: 10.1126/science.1097403.
- Saini, J. et al. (2020) 'Holocene variability in sea ice and primary productivity in the northeastern Baffin Bay', *Arktos*. Springer International Publishing. doi: 10.1007/s41063-020-00075-y.
- Saini, J. (2021) 'Holocene variability in sea ice, primary productivity and terrigenous input in Baffin Bay-Labrador Sea: A biomarker approach'. Universität Bremen.

- Schiebel, R. and Hemleben, C. (2017) *Planktic Foraminifers in the Modern Ocean: Ecology, Biogeochemistry, and Application*. Springer.
- Schlitzer, R. (2018) 'Ocean Data View'. Available at: <https://odv.awi.de>.
- Schweinsberg, A.D., Briner, J.P., Miller, G.H., Bennike, O., Thomas, E.K. (2017) 'Local glaciation in West Greenland linked to North Atlantic ocean circulation during the Holocene', *Geology*, 45, pp. 195–198. doi:10.1130/G38114.1.
- Seidenkrantz, M.S., Roncaglia, L., Fischel, A., Heilmann-Clausen, C., Kuijpers, A., Moros, M. (2008) 'Variable North Atlantic climate seesaw patterns documented by a late Holocene marine record from Disko Bugt, West Greenland', *Mar. Micropaleontol.*, 68, pp. 66–83. doi: 10.1016/j.marmicro.2008.01.006.
- Smetacek, V. and Nicol, S. (2005) 'Polar ocean ecosystems in a changing world', *Nature*, 437(7057), pp. 362–368. doi: 10.1038/nature04161.
- Solignac, S., Giraudeau, J. and de Vernal, A. (2006) 'Holocene sea surface conditions in the western North Atlantic: Spatial and temporal heterogeneities', *Paleoceanography*, 21 (2), PA2004.
- St-Onge, M. P. and St-Onge, G. (2014) 'Environmental changes in Baffin Bay during the Holocene based on the physical and magnetic properties of sediment cores', *Journal of Quaternary Science*, 29(1), pp. 41–56. doi: 10.1002/jqs.2674.
- Stein, R. and MacDonald, R. W. (2004) *The Organic Carbon Cycle in the Arctic Ocean*. Edited by R. Stein and R. W. Macdonald. Berlin: Springer-Verlag.
- Stern, H. L. and Heide-Jørgensen, M. P. (2003) 'Trends and variability of sea ice in Baffin Bay and Davis Strait, 1953–2001', *Polar Research*, 22(1), pp. 11–18. doi: <https://doi.org/10.1111/j.1751-8369.2003.tb00090.x>.
- Syring, N. et al. (2020) 'Holocene changes in sea-ice cover and polynya formation along the eastern North Greenland shelf: New insights from biomarker records', *Quaternary Science Reviews*. The Authors, 231, p. 106173. doi: 10.1016/j.quascirev.2020.106173.
- Tang, C. C. L. et al. (2004) 'The circulation, water masses and sea-ice of Baffin Bay', *Progress in Oceanography*, 63(4), pp. 183–228. doi: <https://doi.org/10.1016/j.pocean.2004.09.005>.
- Telford, R. J. (2015) 'palaeoSig: Significance Tests of Quantitative Palaeoenvironmental Reconstructions'. Available at: <http://cran.r-project.org/package=palaeoSig>.
- Telford, R. J. and Birks, H. J. B. (2011) 'A novel method for assessing the statistical significance of quantitative reconstructions inferred from biotic assemblages', *Quaternary Science Reviews*. Elsevier Ltd, 30(9–10), pp. 1272–1278. doi: 10.1016/j.quascirev.2011.03.002.
- Thiel, V. et al. (1997) 'Unusual distributions of long-chain alkenones and tetrahymanol from the highly alkaline Lake Van, Turkey', *Geochimica et Cosmochimica Acta*, 61(10), pp. 2053–2064. doi: 10.1016/S0016-7037(97)00038-0.
- Thunell, R. C. (1976) 'Optimum indices of calcium carbonate dissolution in deep-sea sediments', *Geology*, 4(9), pp. 525–528.
- Tremblay, G. et al. (2009) 'Late summer phytoplankton distribution along a 3500 km transect in Canadian Arctic waters: Strong numerical dominance by picoeukaryotes', *Aquatic Microbial Ecology*, 54(1), pp. 55–70. doi: 10.3354/ame01257.
- Tremblay, J. É. et al. (2015) 'Global and regional drivers of nutrient supply, primary production and CO<sub>2</sub> drawdown in the changing Arctic Ocean', *Progress in Oceanography*, 139, pp. 171–196. doi: 10.1016/j.pocean.2015.08.009.

- de Vernal, A. et al. (2000) 'Reconstruction of sea-surface temperature, salinity, and sea-ice cover in the northern North Atlantic during the last glacial maximum based on dinocyst assemblages', *Canadian Journal of Earth Sciences*. NRC Research Press, 37(5), pp. 725–750.
- de Vernal, A. et al. (2013) 'Reconstructing past sea ice cover of the Northern Hemisphere from dinocyst assemblages: Status of the approach', *Quaternary Science Reviews*, 79, pp. 122–134. doi: 10.1016/j.quascirev.2013.06.022.
- de Vernal, A. et al. (1992) 'Quantitative assessment of carbonate dissolution in marine sediments from foraminifer linings vs. shell ratios: Davis Strait, northwest North Atlantic', *Geology*, 20(6), pp. 527–530. doi: 10.1130/0091-7613(1992)020<0527:QAOCDI>2.3.CO;2.
- de Vernal, A., Henry, M., Matthiessen, J., et al. (2001) 'Dinoflagellate cyst assemblages as tracers of sea-surface conditions in the Northern North Atlantic, Arctic and sub-Arctic seas: The new "n = 677" data base and its application for quantitative palaeoceanographic reconstruction', *Journal of Quaternary Science*, 16, pp. 681–698.
- de Vernal, A., Hillaire-Marcel, C., et al. (2013) 'Dinocyst-based reconstructions of sea ice cover concentration during the Holocene in the Arctic Ocean, the northern North Atlantic Ocean and its adjacent seas', *Quaternary Science Reviews*, 79(September 2016), pp. 111–121. doi: 10.1016/j.quascirev.2013.07.006.
- de Vernal, A., Rochon, A., et al. (2013) 'Reconstructing past sea ice cover of the Northern Hemisphere from dinocyst assemblages: Status of the approach', *Quaternary Science Reviews*, 79(July), pp. 122–134. doi: 10.1016/j.quascirev.2013.06.022.
- de Vernal, A. and Marret, F. (2007) 'Organic-walled dinoflagellate cysts: Tracers of sea-surface conditions', in *Developments in Marine Geology*. Elsevier B.V., pp. 371–408. doi: 10.1016/S1572-5480(07)01014-7.
- de Vernal, A. and Rochon, A. (2011) 'Dinocysts as tracers of sea-surface conditions and sea-ice cover in polar and subpolar environments', *IOP Conference Series: Earth and Environmental Science*, 14, p. 012007. doi: 10.1088/1755-1315/14/1/012007.
- Versteegh, G. J. M. and Zonneveld, K. A. F. (2002) 'Use of selective degradation to separate preservation from productivity', *Geology*, 30(7), pp. 615–618.
- Volkman, J. K. (1986) 'A review of sterol markers for marine and terrigenous organic matter', *Organic Geochemistry*, 9(2), pp. 83–99. doi: 10.1016/0146-6380(86)90089-6.
- Walsh, J. E. and Chapman, W. L. (2001) '20th-century sea-ice variations from observational data', *Annals of Glaciology*, 33(1).
- Walsh, J. E., Chapman, W. L. and Fetterer, F. (2015) 'Gridded Monthly Sea Ice Extent and Concentration, 1850 Onward, Version 1'. Boulder, Colorado USA: NSIDC: National Snow and Ice Data Center, p. updated 2016. doi: <https://doi.org/10.7265/N5833PZ5>.
- Wegner, C. et al. (2015) 'Variability in transport of terrigenous material on the shelves and the deep Arctic Ocean during the Holocene Variability in transport of terrigenous material on the shelves and', *Polar Research*, 34(1). doi: 10.3402/polar.v34.24964.
- Weidick, A. et al. (2012) Neoglacial and historical glacier changes around Kangarsuneq fjord in southern West Greenland, Geological Survey of Denmark and Greenland Bulletin. doi: 10.34194/geusb.v27.4694.
- Wollenburg, J. E. and Mackensen, A. (1998) 'Living benthic foraminifers from the central Arctic Ocean: Faunal composition, standing stock and diversity', *Marine Micropaleontology*, 34(3–4), pp. 153–185. doi: 10.1016/S0377-8398(98)00007-3.

- Yunker, M. B. et al. (1995) 'Terrestrial and marine biomarkers in a seasonally ice-covered Arctic estuary - integration of multivariate and biomarker approaches', *Marine Chemistry*, 49(1), pp. 1–50. doi: 10.1016/0304-4203(94)00057-K.
- Zeileis, A. and Grothendieck, G. (2005) 'zoo: S3 Infrastructure for Regular and Irregular Time Series', *Journal of Statistical Software*, 14(6), pp. 1–27. doi: 10.18637/jss.v014.i06.
- Zonneveld, K. A. F. et al. (2010) 'Selective preservation of organic matter in marine environments; processes and impact on the sedimentary record', *Biogeosciences*, 7, pp. 483–511.
- Zonneveld, K. A. F., Bockelmann, F. and Holzwarth, U. (2007) 'Selective preservation of organic-walled dinoflagellate cysts as a tool to quantify past net primary production and bottom water oxygen concentrations', *Marine Geology*, 237(3–4), pp. 109–126. doi: 10.1016/j.margeo.2006.10.023.
- Zonneveld, K. A. F. and Brummer, G. A. (2000) '( Palaeo- ) ecological signi " cance , transport and preservation of organic-walled dino # agellate cysts in the Somali Basin , NW Arabian Sea', 47, pp. 2229–2256.
- Zonneveld, K. A. F., Versteegh, G. J. M. and Lange, G. J. De (1997) 'Preservation of organic-walled dinoflagellate cysts in different oxygen regimes : a 10 , 000 year natural experiment', *Marine Micropaleontology*, 29, pp. 393–405.
- Zonneveld, K. A. F., Versteegh, G. and Kodrans-Nsiah, M. (2008) 'Preservation and organic chemistry of Late Cenozoic organic-walled dinoflagellate cysts: A review', *Marine Micropaleontology*, 68(1–2), pp. 179–197. doi: 10.1016/j.marmicro.2008.01.015.
- Zonneveld, K.A.F., Marret, F., Versteegh, G.J.M., et al. (2013) 'Atlas of modern dinoflagellate cyst distribution based on 2405 data points', *Review of Palaeobotany and Palynology*, 191, pp. 1–197.

# Chapter 6

## Conclusions and outlook

### 6.1 Conclusion

The Earth's climate and the ocean's carbon reservoir interact through the marine carbon cycle. Its driving factors have a substantial impact on carbon storage and atmospheric CO<sub>2</sub> concentrations. Especially in the Arctic realm, the increased input of atmospheric CO<sub>2</sub> led to rapid changes in the physical environment and biogeochemical processes within the water column.

Aiming to contribute to the understanding of the Arctic marine carbon cycle, the main objective of this thesis was to estimate the sensitivity of the cycle to changing environmental boundary conditions by quantifying its key components like primary productivity, export productivity and carbon burial throughout the Holocene as an equivalent for the recent warming conditions, and provide observational constraints.

By constraining the key components of the marine carbon cycle, model projections of its future behavior in the light of a changing climate can be advanced and lead to more sustainable predictions.

As primary productivity being one of the most important drivers of the marine carbon cycle is difficult to quantify, the main prerequisite of this thesis was to establish a method for a nuisance free quantification of past primary productivity.

In the first study (chapter 3) the regional impact of sea surface properties on dinocyst assemblage compositions were re-evaluated. Transfer functions and the modern analogue technique were tested for their abilities to reconstruct past sea surface properties and the impact of diagenetically induced nuisance variables on the assemblage compositions was addressed. Region specific primary drivers for assemblage compositions (including primary productivity) were identified with only a negligible amount of diagenetic or other parameter nuisances affecting the estimates. The quantification of primary productivity seems to be reliable if the assemblage composition is driven by this parameter in the area of interest. This implies the benefit of a local dinocyst assemblage calibration dataset for the region of interest to verify if the composition is driven by primary productivity and if a reliable reconstruction is possible.

In the second study (chapter 4) a locally calibrated dinocyst dataset was applied to test if the assemblage compositions in the Baffin Bay area are driven by primary productivity. By applying

four Holocene sediment cores from a North-South transect throughout the Baffin Bay area this study also evaluated if primary productivity drove the composition of fossil dinocyst assemblages and if significant Holocene reconstructions of productivity are possible. Results imply that primary productivity is a less important driver for modern and Holocene assemblages in the Baffin Bay area as they are/were primarily driven by hydrography changes. In Southern Melville Bay off the coast of West Greenland however, primary productivity played a major role in driving dinocyst compositions, posing the opportunity to reconstruct a nuisance-depleted primary productivity record for the Holocene in Southern Melville Bay.

In the third study (chapter 5) the sensitivity of key components (primary productivity, export productivity and burial) driving the marine carbon cycle to changing environmental boundary conditions was evaluated. A sediment core from Southern Melville Bay (GeoB19927-3), where a significant primary productivity quantification seems to be possible, served as generalisation to evaluate what drove these key components' variability in time, conjecturing that this is what drives the variability across space and to provide constraints for future model projections.

Results imply that during the ongoing effects of interglacial warming primary productivity, export productivity and organic carbon burial were decoupled during the Holocene in Melville Bay. This was probably caused by changes in export efficiency, induced by a combination of an increase in the efficiency of organic matter recycling in the productive zone and a decrease in preservation due to longer oxygen exposure times induced by low sedimentation rates. These results suggest that during meltwater-influenced warming conditions the efficiency of the organic carbon pump is decreasing.

## 6.2 Implications and outlook

Collectively, these results advance the understanding of parameter quantification through the application of dinocyst assemblage compositions and can be used to refine palaeoceanographic reconstructions and interpretations. They also enhance the understanding of the Arctic marine carbon cycle and can help to improve projections of its future behaviour and future climate change.

In this thesis, the Holocene Southern Melville Bay (Baffin Bay) served as a benchmark for the Arctic proper as its climate varied between mostly ice-covered to seasonally ice-free conditions. Recent measurements of chlorophyll from this area provide values of  $153 \text{ gC/cm}^2\text{kyrs}^{-1}$  for today's annual primary productivity (O'Malley, 2018). Values reconstructed for the Holocene in this thesis vary between  $120\text{-}300 \text{ gC/cm}^2\text{kyrs}^{-1}$ , implying plausible estimations for the past.

Between 2003 and 2021 the mean annual primary productivity in Baffin Bay changed about 15.7% reflecting  $1.17 \text{ gC/cm}^2\text{kyrs}^{-1}$  change per decade (Source:

<https://www.arctic.noaa.gov/Report-Card/Report-Card-2021>). These values suggest an increase of  $117 \text{ gC/cm}^2\text{kyrs}^{-1}$  over the next thousand years with possible values up to  $270 \text{ gC/cm}^2\text{kyrs}^{-1}$ , which would be in accordance to Holocene variabilities in this region (this thesis and e.g. Allan et al. (2021)).

The current trend for annual primary productivity for the whole Arctic region is about  $1.53 \text{ gC/cm}^2\text{kyrs}^{-1}$  per decade, suggesting an average increase in primary productivity of up to  $\sim 330 \text{ gC/cm}^2\text{kyrs}^{-1}$  within the next thousand years (Fig. 6.1 b) (Source: <https://www.arctic.noaa.gov/Report-Card/Report-Card-2021>). These observations and projections suggest that the results in this study for the Holocene can be treated as an equivalent for the current changes.

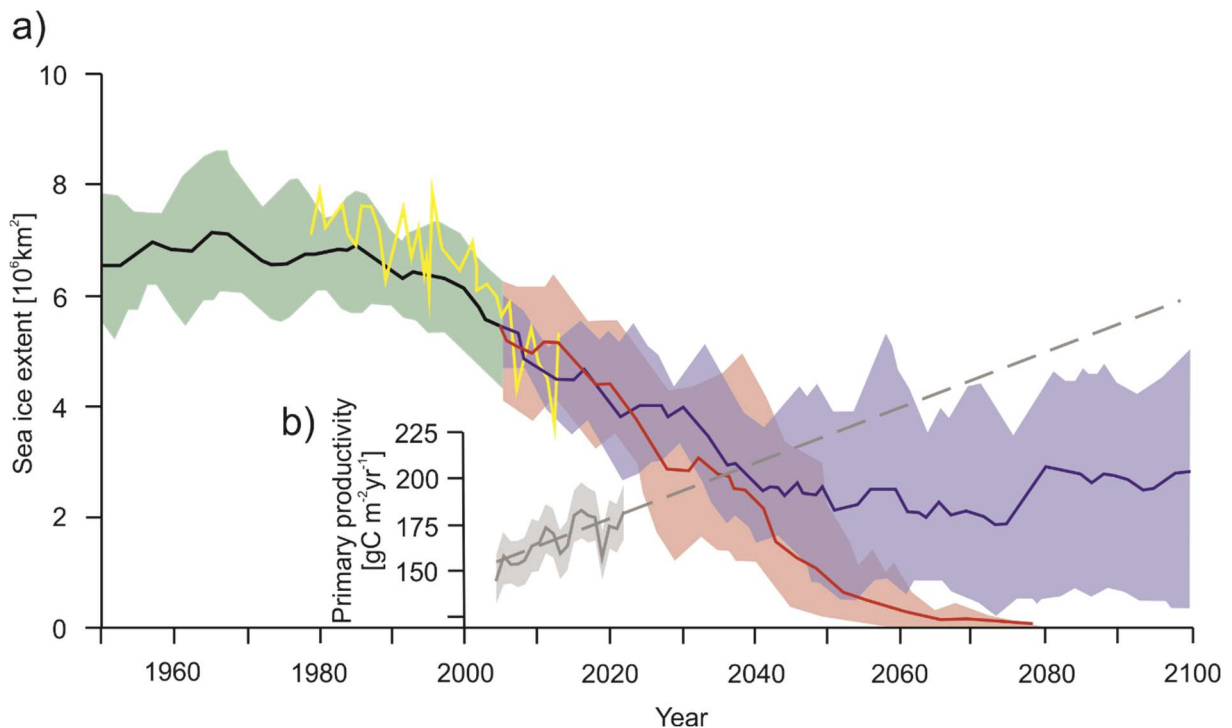


**Figure 6.1:** Projections for changes in the Arctic. a) Projections of Northern Hemisphere sea ice extent in September for this century based on 5<sup>th</sup> assessment of IPCC AR5 report that best captures recent sea ice changes until 2013 (yellow). High (red) and very low emissions (blue) scenarios are shown as shaded bands with solid as mean. b) Average primary productivity (2003-2021, March-September) from nine Arctic and Subarctic regions (grey) (Sources: website accessed in 2023: <https://arctic.noaa.gov/Report-card /Report-Card-2021>), the dashed line is the extension of the current trend.

In general, between 0.4 and 1 % of the net primary production is subjected to burial in the sediment and can be stored for millennia (Field et al., 1998; Behrenfeld et al., 2001; Ducklow et al. 2001), while more than 99% of the organic matter is hydrolysed, remineralised and utilised in the water column (e.g. Iversen, 2023). Reconstructed values for the Holocene of the fraction of organic matter buried in the sediment, commonly known as burial efficiency, vary



between 0.1 and 0.8 % and are in unison with standard values. Intriguing are the changes in burial efficiency, as marine primary productivity and marine organic carbon burial counteract, implying that under meltwater-influenced warming conditions less organic matter was buried, although primary productivity was high. These findings are partly in accordance with the discoveries of Lopes et al. (2015) for the Northeast Pacific, revealing that burial of organic matter increased while primary productivity decreased. However, in the study from Lopes et al. (2015) during the transition phase from Glacial to Interglacial, productivity decreased and burial increased, while in this study productivity increased and burial decreased during the transition from colder to warmer conditions. Considering that the observation in Lopes et al. (2015) are from the Northeast Pacific at  $\sim 45^\circ\text{N}$  and from the glacial-interglacial transition, this suggests that the conditions changed from a meltwater-influenced warming towards a meltwater-free warming implying that meltwater is an important factor for the direction of change. This strengthens the conclusion in chapter 5 that a **meltwater-influenced warming** results in enhanced primary productivity and diminished organic carbon burial.

The increased burial efficiency between 6.0 – 3.0 ka when productivity was low, is supposedly caused by better preservation due to shorter oxygen exposure time (Emerson and Hedges, 1988; Hartnett et al., 1998) or sorption to mineral surfaces (Keil et al., 1994; Mayer, 1994) as sedimentation rates in this phase are also high. Decreased burial efficiency between 3.0 and 1.4 ka when primary productivity peaked was accompanied by low export productivity and low sedimentation rate suggesting increased organic carbon recycling within the productive zone possibly supported by enhanced meltwater induced stratification and a resulting prolonging in residence time of organic matter within the productive zone.

Paying attention to biological processes that attenuate and transform organic matter as it sinks through the water column is potentially important to understand the interaction between organic carbon production and organic carbon storage. Organic matter is transported through the water column in many forms, including single phytoplankton cells, small aggregates, marine snow, fecal pellets, and dead animals (Turner, 2015). As described by Iversen (2023) preferential export of zooplankton fecal pellets and carbon-rich aggregates will increase the amount of carbon that is exported per unit nitrogen compared to when single phytoplankton cells or marine snow dominate export productivity. Mayor et al. (2014) pointed out that aggregate fragmentation by zooplankton in the upper water column, causes a reduction in the amount of exported carbon as smaller aggregates sink more slowly causing increased residence time in the water column. Both findings imply that the composition of producers and the abundance of zooplankton in the productive zone plays an important role for carbon export and storage. Results in chapter 5 show that during times with higher organic carbon burial the flux of planktonic foraminifera was higher as low fluxes depicted in the data are supposedly an artefact of extensive dissolution during this time interval (Fig. 5.7, 5.10, 5.11). In contrast,

during the late Holocene when burial was lowest, the flux of planktonic foraminifera was also lowest, supporting the assumptions in Mayor et al. (2014) and Iversen et al. (2023). Attention should also be given to the effect of redistribution and drift deposition on the pathway of particles to the burial site. Traditionally, particle fluxes are considered to decrease exponentially with depth due to ongoing recycling processes (Martin et al., 1987). However, lateral transport may substantially affect the linkage between primary productivity and organic carbon burial as it decouples sources and sinks (e.g. Rogge et al., 2023).

Yamamoto et al. (2018) suggested that circulation changes and lower nutrient supply to the surface ocean will decrease the efficiency of carbon burial and that this would be the main driver for a decrease in the uptake of atmospheric CO<sub>2</sub> by the ocean in the future. In Baffin Bay continuous melting processes seem to enhance nutrient supply and stratification, benefiting primary productivity and hence the uptake of CO<sub>2</sub>, although seeming to reduce carbon storage. Similar developments can be seen southwest off Greenland (Oksman et al., 2022). The results from this study suggest that the currently happening meltwater-influenced warming of the Arctic leads to a decreased carbon burial efficiency and hence a weakening of the organic carbon pump, with an increased uptake of atmospheric CO<sub>2</sub> in short-terms and a reduction in the uptake in long-terms as the storage decreases.

In a possible future ice-free scenario, nutrient supply and stratification would decrease leading possibly to decreased primary productivity as suggested by Yamamoto et al. (2018). The observation in Lopes et al. (2015) suggest that when conditions change from a meltwater-influenced warming towards a meltwater-free warming, a decrease in primary productivity will lead to higher burial rates, increasing the burial efficiency and hence a strengthening of the organic carbon pump. This proposes a possible future increase in carbon storage and hence long-term uptake of atmospheric CO<sub>2</sub> when the meltwater-influence becomes too weak to enhance primary productivity.

Despite the contributions of this study to the understanding of the Arctic marine carbon cycle and the attempt to constrain its key components, certainly one location serving as generalisation is not representative, although being not entirely irrelevant. The perspective for future research should be the clarification if the observations made in this study are also true for other regions undergoing melting processes. If this were the case, it would be important to determine if there is a tipping point after which the burial efficiency increases due to a decrease in organic matter recycling in the productive zone. Holocene sediment cores that are further away from sea-ice and ice sheets than the core studied here, may serve this cause. A possible change between meltwater-influenced and meltwater-free warming may have already occurred during the Holocene.

The marine biological pump remains a challenging topic to work at with many possibilities of potential future research.

# Acknowledgements

First, I would like to bow to the turn of events, that this PhD project was advertised at the right time and at the right place, making it possible for me to choose this path.

I most of all thank Prof. Dr. Michal Kucera, for offering me this perfect PhD position, for being my supervisor, for his patient guidance, for trusting me and granting me the freedom and responsibility to organise my work and get things done all these years! Thank you Michal!

I further thank the graduate college ArcTrain ("Processes and impacts of climate change in the North Atlantic Ocean and the Canadian Arctic"), funded by the Deutsche Forschungsgemeinschaft (DFG; IRTG 1904 ArcTrain), for the possibility of conference trips, annual meetings and research stays abroad. Above all, the possibility to include my family and take my children with me on my research stay in Montréal, Canada.

I thank Prof. Dr. Anne de Vernal for being my second supervisor, for her feedbacks and for welcoming me at the Université du Québec à Montréal, Canada and I thank the GEOTOP institute at UQÀM for sharing their labs and hosting my research stay. I would like to express special thanks to Maryse Henry who has not only been incredibly supportive and welcoming but also lend me a kind ear once in a while.

I am also thankful for the possibility to take part in some extraordinary courses with great lecturers within the graduate school GLOMAR. I especially thank Werner Große (Science Presentation – Improve your Style) and Natalie A. Peter (Sketchnotes for Scientists) who provided me with the tools and the knowledge on how to visually convey ANY topic to ANYone.

I thank all the members of the micropaleontology group at Marum for their welcoming, the friendly environment and the extraordinary positive atmosphere! I enjoyed working there! I especially thank Birgit Lübben for her help and for always being there when I needed anything.

Thanks also to my fellow ArcTrain PhD students in Germany for the nice atmosphere in the group.

Last but not least, I thank the circumstances in life for providing me with the time it required to take the path I needed!

Finally, I would like to acknowledge myself for keeping on and believing in myself when other paths would have been easier. I walked that path!

# Datasets

**Dataset 1:** “Record of dinocyst assemblage compositions from sediment core GeoB19927-3 during the Holocene”

The dataset contains abundances of dinoflagellate cysts (dinocysts) from sediment samples from sediment core GeoB19927-3 (73°35,26' N, 58°05,66' W) located in Southern Melville Bay (Baffin Bay). The dataset covers the depth interval between 760-0 cm top depths, corresponding to 7.7 ka BP – present. The core was taken at 932 meters of water depth by gravity coring during cruise MSM44 in 2015 (Dorschel et al., 2015). The core consists of 1147 cm of sediment. For dinocyst analysis, it was sub-sampled every centimetre within the top 25 cm, every 5 cm within the 25 cm to 280 cm interval and every 10 cm within the 280 cm to 760 cm interval, including 124 samples. Sample processing followed the procedure for palynological preparation described in Vernal et al. (2010). The taxonomy of dinocysts used here was based on Rochon et al. (1999) and de Vernal et al. (2020). At least 300 dinocyst specimens were counted per sample when possible. For samples with low dinocyst abundance as many specimens as possible were enumerated. In the sample with lowest dinocyst abundance, 89 specimens were counted. The chronology has been provided by Saini et al. (2020).

The dataset will be uploaded to PANGAEA and will be available soon.

**Dataset 2:** “Records of biogenic carbon parameters from sediment core GeoB19927-3 during the Holocene”

The dataset contains bioproductivity parameter fluxes from sediment samples from sediment core GeoB19927-3 (73°35,26' N, 58°05,66' W) located in Southern Melville Bay (Baffin Bay). The dataset covers the depth interval between 760-0 cm top depths, corresponding to 7.7 ka BP – present. The core was taken at 932 meters of water depth by gravity coring during cruise MSM44 in 2015 (Dorschel et al., 2015). The core consists of 1147 cm of sediment. The chronology has been provided by Saini et al. (2020). Excess lead is present down to 4.5 cm core depth, indicating that the core top is of recent age and only experienced minor disturbance during coring. In the upper 25 cm, the sampling for palynology was made at 1 cm interval, which corresponds to a temporal resolution of 30 years. Within the 25 cm to 280 cm interval

every 5 cm and within the 280 cm to 760 cm interval every 10 cm were sub-sampled for palynology and all other analysis.

Palynology sample processing followed the procedure for palynological preparation described in Vernal et al. (2010). The taxonomy of dinocysts used here was based on Rochon et al. (1999) and de Vernal et al. (2020). Organic linings of foraminifera were counted on the basis of the marker-grains method (Matthews, 1969) by adding a capsule of *Lycopodium clavatum* spores. Only complete linings were considered.

For foraminifera analysis between 4-16 grams of freeze-dried sediment samples were wet sieved over a 63 µm mesh sieve and oven-dried at ~50 °C for one day. The whole fraction > 63 µm was picked and counted for planktonic and benthic foraminifers. Planktonic and benthic specimens and their fragments were sorted into two groups and separately weighed to six decimal places using a Sartorius microbalance. Each sample was weighed five times to determine the average weight of their accumulative shells. Benthic samples were analysed with attention given to the five species yielding acid-resistant organic linings (*B. elegantissima*, *M. zandamee*, *E. excavatum*, *C. lobatulus*, *C. wuellerstorfi*).

Estimations of primary productivity are based on dinocyst assemblage compositions available in the dataset “Record of dinocyst assemblage compositions from sediment core GeoB19927-3 during the Holocene” and the method described in Hohmann et al. (this thesis, chapter 4).

The dataset will be uploaded to PANGAEA and will be available soon.

# References (Chapters 1, 2, 6)

- Abrantes, F., Winn, K., Sarnthein, M., 1994. Late Quaternary Paleoproductivity Variations in the NE and Equatorial Atlantic: Diatom and Corg Evidence, in: Zahn, R., Pedersen, T.F., Kaminski, M.A., Labeyrie, L. (Eds.), *Carbon Cycling in the Glacial Ocean: Constraints on the Ocean's Role in Global Change: Quantitative Approaches in Paleoceanography*. Springer Berlin Heidelberg, Berlin, Heidelberg, pp. 425–441. [https://doi.org/10.1007/978-3-642-78737-9\\_19](https://doi.org/10.1007/978-3-642-78737-9_19)
- Aksu, A.E., 1983. Holocene and Pleistocene dissolution cycles in deep-sea cores of Baffin Bay and Davis Strait: Palaeoceanographic implications. *Mar. Geol.* 53, 331–348. [https://doi.org/10.1016/0025-3227\(83\)90049-X](https://doi.org/10.1016/0025-3227(83)90049-X)
- Albright, R., Caldeira, L., Hosfelt, J., Kwiatkowski, L., Maclaren, J.K., Mason, B.M., Nebuchina, Y., Ninokawa, A., Pongratz, J., Ricke, K.L., Rivlin, T., Schneider, K., Sesboüé, M., Shamberger, K., Silverman, J., Wolfe, K., Zhu, K., Caldeira, K., 2016. Reversal of ocean acidification enhances net coral reef calcification. *Nature* 531, 362–365. <https://doi.org/10.1038/nature17155>
- Allan, E., de Vernal, A., Seidenkrantz, M. -S., Briner, J.P., Hillaire-Marcel, C., Pearce, C., Meire, L., Røy, H., Mathiasen, A.M., Nielsen, M.T., Plesner, J.L., Perner, K., 2021. Insolation vs . meltwater control of productivity and sea surface conditions off SW Greenland during the Holocene. *Boreas*. <https://doi.org/10.1111/bor.12514>
- Alley, R.B., Agustsdottir, A.M., 2005. The 8k event: cause and consequences of a major Holocene abrupt climate change. *Quat. Sci. Rev.* 24, 1123–1149. <https://doi.org/10.1016/j.quascirev.2004.12.004>
- Alley, R.B., Andrews, J.T., Brigham-Grette, J., Clarke, G.K.C., Cuffey, K.M., Fitzpatrick, J.J., Funder, S., Marshall, S.J., Miller, G.H., Mitrovica, J.X., Muhs, D.R., Otto-Bliesner, B.L., Polyak, L., White, J.W.C., 2010. History of the Greenland Ice Sheet: paleoclimatic insights. *Quat. Sci. Rev.* 29, 1728–1756. <https://doi.org/10.1016/j.quascirev.2010.02.007>
- Almogi-Labin, A., Schmiedl, G., Hemleben, C., Siman-Tov, R., Segl, M., Meischner, D., 2000. The influence of the NE winter monsoon on productivity changes in the Gulf of Aden, NW Arabian Sea, during the last 530ka as recorded by foraminifera. *Mar. Micropaleontol.* 40, 295–319. [https://doi.org/https://doi.org/10.1016/S0377-8398\(00\)00043-8](https://doi.org/https://doi.org/10.1016/S0377-8398(00)00043-8)
- Andresen, C.S., Sha, L., Seidenkrantz, M.S., Dyke, L.M., Jiang, H., 2022. Early Holocene palaeoceanographic and glaciological changes in southeast Greenland. *Holocene* 32, 501–514. <https://doi.org/10.1177/09596836221080758>
- Ardyna, M., Babin, M., Devred, E., Forest, A., Gosselin, M., 2017. Shelf-basin gradients shape ecological phytoplankton niches and community composition in the coastal Arctic Ocean (Beaufort Sea). *Limnol. Oceanogr.* 62, 2113–2132. <https://doi.org/10.1002/lno.10554>
- Arrigo, K.R., Perovich, D.K., Pickart, R.S., Brown, Z.W., Van Dijken, G.L., Lowry, K.E., Mills, M.M., Palmer, M.A., Balch, W.M., Bahr, F., Bates, N.R., Benitez-Nelson, C., Bowler, B., Brownlee, E., Ehn, J.K., Frey, K.E., Garley, R., Laney, S.R., Lubelczyk, L., Mathis, J., Matsuoka, A., Mitchell, B.G., Moore, G.W.K., Ortega-Retuerta, E., Pal, S., Polashenski, C.M., Reynolds, R.A., Schieber, B., Sosik, H.M., Stephens, M., Swift, J.H., 2012. Massive phytoplankton blooms under arctic sea ice. *Science* (80-. ). 336, 1408. <https://doi.org/10.1126/science.1215065>
- Axford, Y., De Vernal, A., Osterberg, E.C., 2021. Past warmth and its impacts during the holocene thermal maximum in greenland. *Annu. Rev. Earth Planet. Sci.* 49, 279–307. <https://doi.org/10.1146/annurev-earth-081420-063858>
- Axford, Y., Losee, S., Briner, J.P., Francis, D.R., Langdon, P.G., Walker, I.R., 2013. Holocene temperature history at the western Greenland Ice Sheet margin reconstructed from lake sediments. *Quat. Sci. Rev.* 59, 87–100. <https://doi.org/10.1016/j.quascirev.2012.10.024>
- Baes, C.F.J., 1982. Effects of ocean chemistry and biology on atmospheric carbon dioxide. *Carbon dioxide Rev.*
- Bamberg, A., Rosenthal, Y., Paul, A., Heslop, D., Mulitza, S., Rühlemann, C., Schulz, M., 2010. Reduced North Atlantic central water formation in response to early Holocene ice-sheet melting. *Geophys. Res. Lett.* 37, 1–5. <https://doi.org/10.1029/2010GL043878>

- Barnola, J.M., Raynaud, D., Korotkevich, Y.S., Lorius, C., 1987. Vostok ice core provides 160,000-year record of atmospheric CO<sub>2</sub>. *Nature* 329, 408–414.
- Bates, N.R., Mathis, J.T., 2009. The Arctic Ocean marine carbon cycle: Evaluation of air-sea CO<sub>2</sub> exchanges, ocean acidification impacts and potential feedbacks. *Biogeosciences* 6, 2433–2459. <https://doi.org/10.5194/bg-6-2433-2009>
- Beaufort, L., Bassinot, F., Vincent, E., 1999. Primary production response to orbitally induced variations of the southern oscillations in the equatorial Indian Ocean, in: Abrantes, F., Mix, A.C. (Ed.), *Reconstructing Ocean History: A Window into the Future*. Kluwer Academic/Plenum Publishers, New York, pp. 245–272.
- Beaufort, L., de Garidel-Thoron, T., Mix, A.C., Pisias, N.G., 2001. ENSO-like Forcing on Oceanic Primary Production During the Late Pleistocene. *Science* (80-. ). 293, 2440–2444. <https://doi.org/10.1126/science.293.5539.2440>
- Beaufort, L., Lancelot, Y., Camberlin, P., Cayre, O., Vincent, E., Bassinot, F., Labeyrie, L., 1997. Insolation Cycles as a Major Control of Equatorial Indian Ocean Primary Production. *Science* (80-. ). 278, 1451–1454. <https://doi.org/10.1126/science.278.5342.1451>
- Bednarsek, N., Tarling, G.A., Bakker, D.C.E., Fielding, S., Feely, R.A., 2014. Dissolution dominating calcification process in polar pteropods close to the point of aragonite undersaturation. *PLoS One* 9. <https://doi.org/10.1371/journal.pone.0109183>
- Behrenfeld, M.J., Falkowski, P.G., 1997. Photosynthetic rates derived from satellite-based chlorophyll concentration. *Limnol. Oceanogr.* 42, 1–20. <https://doi.org/10.4319/lo.1997.42.1.0001>
- Behrenfeld, M.J., Randerson, J.T., McClain, C.R., Feldman, G.C., Los, S.O., Tucker, C.J., 2001. Biospheric Primary Production During an ENSO Transition. *Science* (80-. ). 291, 2594–2597. <https://doi.org/10.1016/j.cognition.2008.05.007>
- Bender, M., Grande, K., Johnson, K., Marra, J., Williams, P.J.L., Sieburth, J., Pilson, M., Langdon, C., Hitchcock, G., Orchardo, J., Blunt, C., Donaghay, P., Heinemann, K., 1987. A comparison of four methods for determining planktonic community production. *Limnologica* 32, 1085–1098.
- Berger, W.H., Smetacek, V., Wefer, G., 1989. Ocean productivity and paleoproductivity - an overview, in: *Productivity of the Ocean: Present and Past*, John Wiley & Sons Limited. pp. 1–34.
- Berner, W., Oeschger, H., Stauffer, B., 1980. Information on the CO<sub>2</sub> cycle from ice core studies. *Radiocarbon* 22, 227–235.
- Birks, J.B., 1995. Quantitative palaeoenvironmental reconstructions, in: Maddy, D., Brew, I.S. (Eds.), *Statistical Modelling of Quaternary Science Data*. Quaternary Research Association, Cambridge, p. 271 pp.
- Bradtmiller, L.I., Anderson, R.F., Fleisher, M.Q., Burckle, L.H., 2006. Diatom productivity in the equatorial Pacific Ocean from the last glacial period to the present: A test of the silicic acid leakage hypothesis. *Paleoceanography* 21, n/a--n/a. <https://doi.org/10.1029/2006PA001282>
- Briner, J.P., McKay, N.P., Axford, Y., Bennike, O., Bradley, R.S., de Vernal, A., Fisher, D., Francus, P., Fréchette, B., Gajewski, K., Jennings, A., Kaufman, D.S., Miller, G., Rouston, C., Wagner, B., 2016. Holocene climate change in Arctic Canada and Greenland. *Quat. Sci. Rev.* 147, 340–364. <https://doi.org/10.1016/j.quascirev.2016.02.010>
- Bringué, M., Pospelova, V., Calvert, S.E., Enkin, R.J., Lacourse, T., Ivanochko, T., 2016. High resolution dinoflagellate cyst record of environmental change in Effingham Inlet (British Columbia, Canada) over the last millennium. *Palaeogeogr. Palaeoclimatol. Palaeoecol.* 441, 787–810. <https://doi.org/10.1016/j.palaeo.2015.10.026>
- Buch, E., 1981. A review of the oceanographic conditions in subarea O and 1 in the decade 1970–1979.
- Burrows, M.T., Schoeman, D.S., Buckley, L.B., Moore, P., Poloczanska, E.S., Brander, K.M., Brown, C., Bruno, J.F., Duarte, C.M., Halpern, B.S., Holding, J., Kappel, C. V., Kiessling, W., O'Connor, M.I., Pandolfi, J.M., Parmesan, C., Schwing, F.B., Sydeman, W.J., Richardson, A.J., 2011. The Pace of Shifting Climate in Marine and Terrestrial Ecosystems. *Science* 334, 652–655. <https://doi.org/10.1126/science.1210288>
- Carmack, E., Wassmann, P., 2006. Food webs and physical-biological coupling on pan-Arctic shelves:

- Unifying concepts and comprehensive perspectives. *Prog. Oceanogr.* 71, 446–477.  
<https://doi.org/10.1016/j.pocean.2006.10.004>
- Cayre, O., Beaufort, L., Vincent, E., 1999. Paleoproductivity in the Equatorial Indian Ocean for the last 260,000yr: A transfer function based on planktonic foraminifera. *Quat. Sci. Rev.* 18, 839–857.  
[https://doi.org/https://doi.org/10.1016/S0277-3791\(98\)00036-5](https://doi.org/https://doi.org/10.1016/S0277-3791(98)00036-5)
- Cofaigh, Ó.C., Dowdeswell, J.A., Jennings, A.E., Hogan, K.A., Kilfeather, A., Hiemstra, J.F., Noormets, R., Evans, J., McCarthy, D.J., Andrews, J.T., Lloyd, J.M., Moros, M., 2013. An extensive and dynamic ice sheet on the west greenland shelf during the last glacial cycle. *Geology* 41, 219–222.  
<https://doi.org/10.1130/G33759.1>
- Cormier, M.A., Rochon, A., de Vernal, A., Gélinas, Y., 2016. Multi-proxy study of primary production and paleoceanographical conditions in northern Baffin Bay during the last centuries. *Mar. Micropaleontol.* 127, 1–10. <https://doi.org/10.1016/j.marmicro.2016.07.001>
- Dale, B., 1992. Dinoflagellate contributions to the open ocean sediment flux, in: Dale, B., Dale, A.L. (Eds.), *Dinoflagellate Contributions to the Deep Sea. Ocean Biocoenosis Ser.*, pp. 1–31.
- Dale, B., 1983. *Dinoflagellate resting cysts: “benthic plankton,” Survival Strategies of the Algae.* Cambridge University Press.
- Dale, B., Dale, A.L., 1992. Dinoflagellate contributions to the sediment flux of the Nordic Seas, in: Dale, B., Dale, A.L. (Eds.), *Dinoflagellate Contributions to the Deep Sea. Ocean Biocoenosis Ser.*, pp. 45–75.
- de Vernal, A., Henry, M., Matthiessen, J., Mudie, P.J., Rochon, A., Boessenkool, K., Eynaud, F., Grøsfjeld, K., Guiot, J., Hamel, D., Harland, R., Head, M.J., Kunz-Pirrung, M., Levac, E., Loucheur, V., Peyron, O., Pospelova, V., Radi, T., Turon, J.-L., Voronina, E., 2001. Dinoflagellate cyst assemblages as tracers of sea-surface conditions in the northern North Atlantic, Arctic and sub-Arctic seas: the new “n= 677” data base and its application for quantitative palaeoceanographic reconstruction. *J. Quat. Sci.* 16, 681–698. <https://doi.org/10.1002/jqs.659>
- de Vernal, A., Hillaire-Marcel, C., Rochon, A., Fréchette, B., Henry, M., Solignac, S., Bonnet, S., 2013. Dinocyst-based reconstructions of sea ice cover concentration during the Holocene in the Arctic Ocean, the northern North Atlantic Ocean and its adjacent seas. *Quat. Sci. Rev.* 79, 111–121.  
<https://doi.org/10.1016/j.quascirev.2013.07.006>
- de Vernal, A., Hillaire-Marcel, C., Turon, J.-L., Matthiessen, J., 2000. Reconstruction of sea-surface temperature, salinity, and sea-ice cover in the northern North Atlantic during the last glacial maximum based on dinocyst assemblages. *Can. J. Earth Sci.* 37, 725–750.
- de Vernal, A., Marret, F., 2007. Organic-walled dinoflagellate cysts: Tracers of sea-surface conditions, in: *Developments in Marine Geology.* Elsevier B.V., pp. 371–408. [https://doi.org/10.1016/S1572-5480\(07\)01014-7](https://doi.org/10.1016/S1572-5480(07)01014-7)
- de Vernal, A., Radi, T., Zaragosi, S., Van Nieuwenhove, N., Rochon, A., Allan, E., De Schepper, S., Eynaud, F., Head, M.J., Limoges, A., Londeix, L., Marret, F., Matthiessen, J., Penaud, A., Pospelova, V., Price, A., Richerol, T., 2020. Distribution of common modern dinoflagellate cyst taxa in surface sediments of the Northern Hemisphere in relation to environmental parameters: The new n=1968 database. *Mar. Micropaleontol.* 159, 101796.  
<https://doi.org/https://doi.org/10.1016/j.marmicro.2019.101796>
- de Vernal, A., Rochon, A., Fréchette, B., Henry, M., Radi, T., Solignac, S., 2013. Reconstructing past sea ice cover of the Northern Hemisphere from dinocyst assemblages: Status of the approach. *Quat. Sci. Rev.* 79, 122–134. <https://doi.org/10.1016/j.quascirev.2013.06.022>
- de Vernal, A., Rochon, A., Turon, J.-L., Matthiessen, J., 1997. Organic-walled dinoflagellate cysts: Palynological tracers of sea-surface conditions in middle to high latitude marine environments. *Geobios* 30, 905–920. [https://doi.org/10.1016/S0016-6995\(97\)80215-X](https://doi.org/10.1016/S0016-6995(97)80215-X)
- Delmas R.J., Ascencio J.M., Legrand M., 1980. Polar ice evidence that atmospheric CO<sub>2</sub> 20,000 yr BP was 50% of present. *Nature.* <https://doi.org/10.1034/j.1600-0889.1999.t01-1-00005.x>
- Doney, S.C., Schimel, D.S., 2007. Carbon and climate system coupling on timescales from the Precambrian to the anthropocene. *Annu. Rev. Environ. Resour.* 32, 31–66.  
<https://doi.org/10.1146/annurev.energy.32.041706.124700>
- Dorschel, B., Afanasyeva, V., Bender, M., Dreutter, S., Eisermann, H., Gebhardt, A.C., Hansen, K.,



- Hebbeln, D., Jackson, R., 2015. Past Greenland Ice Sheet dynamics, *Palaeoceanography and Plankton Ecology in the Northeast Baffin Bay - Cruise No. MSM44 "BAFFEAST" - June 30-July 30, 2015 - Nuuk (Greenland). MARIA S. MERIAN-Berichte* 51. [https://doi.org/10.2312/cr\\_msm2344](https://doi.org/10.2312/cr_msm2344)
- Ducklow, H.W., Steinberg, D.K., Buch, E., 2001. Upper ocean carbon export and the biological pump. *Oceanography* 14, 50–58. <https://doi.org/10.5670/oceanog.2001.06>
- Dymond, J., Suess, E., Lyle, M., 1992. Barium in Deep-Sea Sediment: A Geochemical Proxy for Paleoproductivity. *Paleoceanography* 7, 163–181. <https://doi.org/10.1029/92PA00181>
- Emerson, S., Hedges, J., 2003. Sediment Diagenesis and Benthic Flux. *Treatise on Geochemistry* 6, 625. <https://doi.org/10.1016/B0-08-043751-6/06112-0>
- Emerson, S., Hedges, J.I., 1988. Processes controlling the organic carbon content of open ocean sediments. *Paleoceanography* 3, 621–634.
- Fabry, V.J., McClintock, J.B., Mathis, J.T., Grebeier, J.M., 2009. Ocean acidification at high latitudes: The Bellwether. *Oceanography* 22, 160–171. <https://doi.org/10.5670/oceanog.2009.105>
- Falkowski, P.G., Barber, R.T., Smetacek, V., 1998. Biogeochemical controls and feedbacks on ocean primary production. *Science (80-. )*. 281, 200–206. <https://doi.org/10.1126/science.281.5374.200>
- Field, C.B., Behrenfeld, M.J., Randerson, J.T., Falkowski, P., 1998. Primary production of the biosphere: integrating terrestrial and oceanic components. *Science (80-. )*. 281, 237–240. <https://doi.org/10.1016/j.cognition.2008.05.007>
- Fischer, G., Ratmeyer, V., Wefer, G., 2000. Organic carbon fluxes in the Atlantic and the Southern Ocean: relationship to primary production compiled from satellite radiometer data. *Deep Sea Res. Part II Top. Stud. Oceanogr.* 47, 1961–1997. [https://doi.org/https://doi.org/10.1016/S0967-0645\(00\)00013-8](https://doi.org/https://doi.org/10.1016/S0967-0645(00)00013-8)
- Fischer, G., Wefer, G., 1999. *Use of Proxies in Paleoceanography: Examples from the South Atlantic*. Springer Verlag, Berlin.
- Francois, R., Frank, M., van der Loeff, M.M., Bacon, M.P., 2004. 230Th normalization: An essential tool for interpreting sedimentary fluxes during the late Quaternary. *Paleoceanography* 19, n/a--n/a. <https://doi.org/10.1029/2003PA000939>
- Francois, R., Honjo, S., Manganini, S.J., Ravizza, G.E., 1995. Biogenic barium fluxes to the deep sea: Implications for paleoproductivity reconstruction. *Global Biogeochem. Cycles* 9, 289–303. <https://doi.org/10.1029/95GB00021>
- Gallinari, M., Ragueneau, O., Corrin, L., DeMaster, D.J., Tréguer, P., 2002. The importance of water column processes on the dissolution properties of biogenic silica in deep-sea sediments I. Solubility. *Geochim. Cosmochim. Acta* 66, 2701–2717. [https://doi.org/https://doi.org/10.1016/S0016-7037\(02\)00874-8](https://doi.org/https://doi.org/10.1016/S0016-7037(02)00874-8)
- Gibb, O.T., Steinhauer, S., Frechette, B., de Vernal, A., Hillaire-Marcel, C., 2015. Diachronous evolution of sea surface conditions in the Labrador Sea and Baffin Bay since the last deglaciation. *The Holocene* 25, 1882–1897. <https://doi.org/10.1177/0959683615591352>
- Gooday, A.J., 2003. Benthic foraminifera (protista) as tools in deep-water palaeoceanography: Environmental influences on faunal characteristics, in: *Advances in Marine Biology*. Academic Press, pp. 1–90. [https://doi.org/https://doi.org/10.1016/S0065-2881\(03\)46002-1](https://doi.org/https://doi.org/10.1016/S0065-2881(03)46002-1)
- Guiot, J., 1990. Methodology of the last climatic cycle reconstruction in France from pollen data. *Palaeogeogr. Palaeoclimatol. Palaeoecol.* 80, 49–69. [https://doi.org/10.1016/0031-0182\(90\)90033-4](https://doi.org/10.1016/0031-0182(90)90033-4)
- Guiot, J., de Vernal, A., 2007. Chapter Thirteen Transfer Functions: Methods for Quantitative Paleoceanography Based on Microfossils. *Dev. Mar. Geol.* 1, 523–563. [https://doi.org/10.1016/S1572-5480\(07\)01018-4](https://doi.org/10.1016/S1572-5480(07)01018-4)
- Hartnett, H.E., Keil, R.G., Hedges, J.I., Devol, A.H., 1998. Influence of oxygen exposure time on organic carbon preservation in continental margin sediments. *Nature* 391, 572–574.
- Haugan, P.M., Drange, H., 1996. Effects of CO<sub>2</sub> on the ocean environment. *Energy Convers. Manag.* 37, 1019–1022. [https://doi.org/10.1016/0196-8904\(95\)00292-8](https://doi.org/10.1016/0196-8904(95)00292-8)
- Heinze, C., Maier-Reimer, E., Winn, K., 1991. Glacial pCO<sub>2</sub> Reduction by the World Ocean: Experiments With the Hamburg Carbon Cycle Model. *Paleoceanography* 6, 395–430.

- Helama, S., Jones, P.D., Briffa, K.R., 2017. Dark Ages Cold Period: A literature review and directions for future research. *The Holocene* 27, 1600–1606. <https://doi.org/10.1177/0959683617693898>
- Hill, V., Ardyna, M., Lee, S.H., Varela, D.E., 2018. Decadal trends in phytoplankton production in the Pacific Arctic Region from 1950 to 2012. *Deep Sea Res. Part II Top. Stud. Oceanogr.* 152, 82–94.
- Hohmann, S., Kucera, M., de Vernal, A., n.d. Disentangling environmental drivers of Subarctic dinocyst assemblage compositional change during the Holocene. in prep.
- IPCC, 2013. *Climate Change 2013: The Physical Science Basis. Contribution of Working Group I to the Fifth Assessment Report of the Intergovernmental Panel on Climate Change.* <https://doi.org/10.1017/CBO9781107415324.Summary>
- Ivanova, E., Schiebel, R., Singh, A.D., Schmiedl, G., Niebler, H.-S., Hemleben, C., 2003. Primary production in the Arabian Sea during the last 135 000 years. *Palaeogeogr. Palaeoclimatol. Palaeoecol.* 197, 61–82. [https://doi.org/https://doi.org/10.1016/S0031-0182\(03\)00386-9](https://doi.org/https://doi.org/10.1016/S0031-0182(03)00386-9)
- Iversen, M.H., 2023. Carbon Export in the Ocean : A Biologist ' s Perspective. *Annu. Rev. Mar. Sci. Mar. Sci.* 15, 357–381. <https://doi.org/10.1146/annurev-marine-032122-035153>
- Jeandel, C., Tachikawa, K., Bory, A., Dehairs, F., 2000. Biogenic barium in suspended and trapped material as a tracer of export production in the tropical NE Atlantic (EUMELI sites). *Mar. Chem.* 71, 125–142. [https://doi.org/https://doi.org/10.1016/S0304-4203\(00\)00045-1](https://doi.org/https://doi.org/10.1016/S0304-4203(00)00045-1)
- Jones, P.D., Wigley, T.M.L., Raper, S.C.B., 1987. The Rapidity of CO<sub>2</sub>-Induced Climatic Change: Observations, Model Results and Palaeoclimatic Implications, in: Berger, W.H., Labeyrie, L.D. (Eds.), *Abrupt Climatic Change: Evidence and Implications.* Springer Netherlands, Dordrecht, pp. 47–55. [https://doi.org/10.1007/978-94-009-3993-6\\_4](https://doi.org/10.1007/978-94-009-3993-6_4)
- Jorissen, F.J., Fontanier, C., Thomas, E., 2007. Chapter Seven Paleooceanographical Proxies Based on Deep-Sea Benthic Foraminiferal Assemblage Characteristics, in: Hillaire-Marcel, C., de Vernal, A. (Eds.), *Proxies in Late Cenozoic Paleooceanography.* Elsevier, pp. 263–325. [https://doi.org/10.1016/S1572-5480\(07\)01012-3](https://doi.org/10.1016/S1572-5480(07)01012-3)
- Juul-pedersen, T., Arendt, K.E., Mortensen, J., Blicher, M.E., Søgaard, D.H., Rysgaard, S., 2015. Seasonal and interannual phytoplankton production in a sub-Arctic tidewater outlet glacier fjord, SW Greenland. *Mar. Ecol. Prog. Ser.* 524, 27–38. <https://doi.org/10.3354/meps11174>
- Kaufman, D.S., Ager, T.A., Anderson, N.J., Anderson, P.M., Andrews, J.T., Bartlein, P.J., Brubaker, L.B., Coats, L.L., Cwynar, L.C., Duvall, M.L., Dyke, A.S., Edwards, M.E., Eisner, W.R., Gajewski, K., Geirsdóttir, A., Hu, F.S., Jennings, A.E., Kaplan, M.R., Kerwin, M.W., Lozhkin, A. V., MacDonald, G.M., Miller, G.H., Mock, C.J., Oswald, W.W., Otto-Bliesner, B.L., Porinchu, D.F., Rühland, K., Smol, J.P., Steig, E.J., Wolfe, B.B., 2004. Holocene thermal maximum in the western Arctic (0-180°W). *Quat. Sci. Rev.* 23, 529–560. <https://doi.org/10.1016/j.quascirev.2003.09.007>
- Keil, R.G., Montlucon, D.B., Prahl, F.G., Hedges, J.I., 1994. Sorptive preservation of labile organic matter in marine sediments. *Nature* 370, 549–552.
- Klump, J., Hebbeln, D., Wefer, G., 2000. The impact of sediment provenance on barium-based productivity estimates. *Mar. Geol.* 169, 259–271. [https://doi.org/https://doi.org/10.1016/S0025-3227\(00\)00092-X](https://doi.org/https://doi.org/10.1016/S0025-3227(00)00092-X)
- Knudsen, K.L., Stabell, B., Seidenkrantz, M.S., Eiríksson, J., Blake, W., 2008. Deglacial and Holocene conditions in northernmost Baffin Bay: Sediments, foraminifera, diatoms and stable isotopes. *Boreas* 37, 346–376. <https://doi.org/10.1111/j.1502-3885.2008.00035.x>
- Koc, N., Jansen, E., Hafliðason, H., 1993. Paleooceanographic reconstruction of surface ocean conditions in the Greenland, Iceland, and Norwegian seas through the last 14,000 years based on diatoms. *Quat. Sci. Rev.* 12, 115–140.
- Kokinos, J.P., Eglinton, T.I., Gon, M.A., 1998. Characterization of a highly resistant biomacromolecular material in the cell wall of a marine dino<sup>+</sup> agellate resting cyst. *Organic* 28, 265–288.
- Krawczyk, D.W., Meire, L., Lopes, C., Juul-Pedersen, T., Mortensen, J., Li, C.L., Krogh, T., 2018. Seasonal succession, distribution, and diversity of planktonic protists in relation to hydrography of the Godthåbsfjord system (SW Greenland). *Polar Biol.* 41, 2033–2052. <https://doi.org/10.1007/s00300-018-2343-0>
- Krawczyk, D.W., Witkowski, A., Juul-Pedersen, T., Arendt, K.E., Mortensen, J., Rysgaard, S., 2015.

- Microplankton succession in a SW Greenland tidewater glacial fjord influenced by coastal inflows and run-off from the Greenland Ice Sheet. *Polar Biol.* 38, 1515–1533. <https://doi.org/10.1007/s00300-015-1715-y>
- Kroeker, K.J., Kordas, R.L., Crim, R.N., Singh, G.G., 2010. Meta-analysis reveals negative yet variable effects of ocean acidification on marine organisms. *Ecol. Lett.* 13, 1419–1434. <https://doi.org/10.1111/j.1461-0248.2010.01518.x>
- Lafrenière, M.J., Lamoureux, S.F., 2019. Effects of changing permafrost conditions on hydrological processes and fluvial fluxes. *Earth-Science Rev.* 191, 212–223. <https://doi.org/10.1016/j.earscirev.2019.02.018>.
- Lamb, H.H., 2002. *Climate, history and the modern world*. Routledge.
- Lamb, H.H., 1965. The early medieval warm epoch and its sequel. *Palaeogeogr. Palaeoclimatol. Palaeoecol.* 1, 13–37. [https://doi.org/10.1016/0031-0182\(65\)90004-0](https://doi.org/10.1016/0031-0182(65)90004-0)
- Langdon, C., Atkinson, M.J., 2005. Effect of elevated pCO<sub>2</sub> on photosynthesis and calcification of corals and interactions with seasonal change in temperature/ irradiance and nutrient enrichment. *J. Geophys. Res. Ocean.* 110, 1–16. <https://doi.org/10.1029/2004JC002576>
- Le Quéré, C., Takahashi, T., Buitenhuis, E.T., Rödenbeck, C., Sutherland, S.C., 2010. Impact of climate change and variability on the global oceanic sink of CO<sub>2</sub>. *Global Biogeochem. Cycles* 24, 1–10. <https://doi.org/10.1029/2009GB003599>
- Leu, E., Mundy, C.J., Assmy, P., Campbell, K., Gabrielsen, T.M., Gosselin, M., Juul-pedersen, T., Gradinger, R., 2015. Progress in Oceanography Arctic spring awakening – Steering principles behind the phenology of vernal ice algal blooms. *Prog. Oceanogr.* 139, 151–170. <https://doi.org/10.1016/j.pocean.2015.07.012>
- Lewis, K.M., Dijken, G.L. Van, Arrigo, K.R., 2020. Changes in phytoplankton concentration now drive increased Arctic Ocean primary production. *Science* (80- ). 202, 198–202.
- Ljungqvist, F.C., 2010. A new reconstruction of temperature variability in the extra - tropical northern hemisphere during the last two millennia VARIABILITY IN THE EXTRA-TROPICAL NORTHERN. *Geogr. Ann. Ser. A, Phys. Geogr.* 92, 339–351. <https://doi.org/10.1111/j.1468-0459.2010.00399.x>
- Lopes, C., Kucera, M., Mix, A.C., 2015. Climate change decouples oceanic primary and export productivity and organic carbon burial. *Proc. Natl. Acad. Sci. U. S. A.* 112, 332–5. <https://doi.org/10.1073/pnas.1410480111>
- Lopes, C., Mix, A.C., Abrantes, F., 2010. Environmental controls of diatom species in northeast Pacific sediments. *Palaeogeogr. Palaeoclimatol. Palaeoecol.* 297, 188–200. <https://doi.org/10.1016/j.palaeo.2010.07.029>
- Loubere, P., 1999. A multiproxy reconstruction of biological productivity and oceanography in the eastern equatorial Pacific for the past 30,000 years. *Mar. Micropaleontol.* 37, 173–198.
- Loubere, P., 1994. Quantitative estimation of surface ocean productivity and bottom water oxygen concentration using benthic water oxygen values purposes in this case ). This procedure water oxygen range. *Paleoceanography* 9, 723–737.
- Loubere, P., 1991. Deep-Sea Benthic Foraminiferal Assemblage Response to a Surface Ocean Productivity Gradient: A Test. *Paleoceanography* 6, 193–204.
- Loubere, P., Fariduddin, M., 1999. Quantitative estimation of global patterns of surface ocean biological productivity and its seasonal variation. *Global Biogeochem. Cycles* 13, 115–133.
- Lüthi, D., Le Floch, M., Bereiter, B., Blunier, T., Barnola, J.-M., Siegenthaler, U., Raynaud, D., Jouzel, J., Fischer, H., Kawamura, K., Stocker, T.F., 2008. High-resolution carbon dioxide concentration record 650,000-800,000 years before present. *Nature* 453, 379–382. <https://doi.org/10.1038/nature06949>
- Mackensen, A., Schumacher, S., Radke, J., Schmidt, D.N., 2000. Microhabitat preferences and stable carbon isotopes of endobenthic foraminifera: Clue to quantitative reconstruction of oceanic new production? *Mar. Micropaleontol.* 40, 233–258. [https://doi.org/10.1016/S0377-8398\(00\)00040-2](https://doi.org/10.1016/S0377-8398(00)00040-2)
- Mann, M.E., 2002a. Medieval Climatic Optimum. *Encycl. Glob. Environ. Chang.* 1, 514–516.
- Mann, M.E., 2002b. Little Ice Age. *Encycl. Glob. Environ. Chang.* 1, 504–509.

[https://doi.org/10.1007/1-4020-3266-8\\_127](https://doi.org/10.1007/1-4020-3266-8_127)

Marret, F., Zonneveld, K. a. F., 2003. Atlas of modern organic-walled dinoflagellate cyst distribution. *Rev. Palaeobot. Palynol.* 125, 1–200. [https://doi.org/10.1016/S0034-6667\(02\)00229-4](https://doi.org/10.1016/S0034-6667(02)00229-4)

Martin, J.H., Knauer, G.A., Karl, D.M., Broenkow, W.W., 1987. VERTEX: carbon cycling in the northeast Pacific. *Deep Sea Res. Part A, Oceanogr. Res. Pap.* 34, 267–285. [https://doi.org/10.1016/0198-0149\(87\)90086-0](https://doi.org/10.1016/0198-0149(87)90086-0)

Matishov, G.G., 1999. Oceanic periglacial in the evolution of the Arctic marine ecosystem. *World Resour. Rev.* 11, 190–195.

Matthews, B.Y.J., 1969. The Assessment of a Method for the Determination of Absolute Pollen Frequencies. *New Phytol.* 68, 161–166. <https://doi.org/10.1111/j.1469-8137.1969.tb06429.x>

Matthews, J.A., Briffa, K.R., 2005. The 'little ice age': re-evaluation of an evolving concept. *Geogr. Ann. Ser. A, Phys. Geogr.* 87, 17–36. <https://doi.org/10.1111/j.0435-3676.2005.00242.x>

Matthiessen, J., 1995. Distribution patterns of dinoflagellate cysts and other organic-walled microfossils in recent Norwegian-Greenland Sea sediments. *Mar. Micropaleontol.* 24, 307–334. [https://doi.org/10.1016/0377-8398\(94\)00016-G](https://doi.org/10.1016/0377-8398(94)00016-G)

Matthiessen, J., Baumann, K.H., Schröder-Ritzrau, A., Hass, C., Andruleit, H., Baumann, A., Jensen, S., Kohly, A., Pflaumann, U., Samtleben, C., Schäfer, P., Thiede, J., 2001. Distribution of Calcareous, Siliceous and Organic-Walled Planktic Microfossils in Surface Sediments of the Nordic Seas and their Relation to Surface-Water Masses, in: Schäfer, P., Ritzrau, W., Schlüter, M., Thiede, J. (Eds.), *The Northern North Atlantic*. Springer Berlin Heidelberg, pp. 105–127.

Matthiessen, J., de Vernal, a., Head, M., Okolodkov, Y., Zonneveld, K., Harland, R., 2005. Modern organic-walled dinoflagellate cysts in Arctic marine environments and their (paleo-) environmental significance. *Paläontologische Zeitschrift* 79, 3–51. <https://doi.org/10.1007/BF03021752>

Mayer, L.M., 1994. Surface area control of organic carbon accumulation in continental shelf sediments. *Geochim. Cosmochim. Acta* 58, 1271–1284. [https://doi.org/10.1016/0016-7037\(94\)90381-6](https://doi.org/10.1016/0016-7037(94)90381-6)

Mayor, D.J., Sanders, R., Giering, S.L.C., Anderson, T.R., 2014. Microbial gardening in the ocean's twilight zone: Detritivorous metazoans benefit from fragmenting, rather than ingesting, sinking detritus. *Bioessays* 36, 1132–1137. <https://doi.org/10.1002/bies.201400100>

McCorkle, D.C., Martin, P.A., Lea, D.W., Klinkhammer, G.P., 1995. Evidence of a dissolution effect on benthic foraminiferal shell chemistry:  $\delta^{13}\text{C}$ , Cd/Ca, Ba/Ca, and Sr/Ca results from the Ontong Java Plateau. *Paleoceanography* 10, 699–714. <https://doi.org/10.1029/95PA01427>

Meier, W.N., Hovelsrud, G.K., van Oort, B.E.H., Key, J.R., Kovacs, K.M., Michel, C., Haas, C., Granskog, M.A., Gerland, S., Perovich, D.K., Makshtas, A., Reist, J.D., 2014. Arctic sea ice in transformation: A review of recent observed changes and impacts on biology and human activity. *Rev. Geophys.* 52, 185–217. <https://doi.org/10.1002/2013RG000431>

Meir, W N, 2011. Sea ice, in: *Snow, Water, Ice and Permafrost in the Arctic: Climate Change and the Cryosphere*. Arctic Monitoring and Assessment Program (AMAP), Oslo, Norway, pp. 1–82.

Meir, W.N., 2011. Sea Ice. In *Snow, Water, Ice and Permafrost in the Arctic: Climate Change and the Cryosphere*. Arct. Monit. Assess. Pro- gram (AMAP), Oslo, Norway, 1–82.

Meyers, P.A., 1997. Organic geochemical proxies of paleoceanographic, paleolimnologic, and paleoclimatic processes. *Org. Geochem.* 27, 213–250. [https://doi.org/https://doi.org/10.1016/S0146-6380\(97\)00049-1](https://doi.org/https://doi.org/10.1016/S0146-6380(97)00049-1)

Mikaloff Fletcher, S.E., Gruber, N., Jacobson, A.R., Doney, S.C., Dutkiewicz, S., Gerber, M., Follows, M., Joos, F., Lindsay, K., Menemenlis, D., Mouchet, A., Müller, S.A., Sarmiento, J.L., 2006. Inverse estimates of anthropogenic CO<sub>2</sub> uptake, transport, and storage by the ocean. *Global Biogeochem. Cycles* 20, 1–16. <https://doi.org/10.1029/2005GB002530>

Mudie, P.J., 1992. Circum-Arctic Quaternary and Neogene marine palynofloras: paleoecology and statistical analysis. *Neogene Quat. Dinoflag. cysts acritarchs* 10, 347–390.

Muller, P.J., Erlenkeuser, H., Von Grafenstein, R., 1983. Glacial– interglacial cycles in oceanic productivity inferred from organic carbon contents in eastern north Atlantic sediment cores, in: Thiede J., Suess, E. (Ed.), *Coastal Upwelling, Its Sediment Record, Part B: Sedimentary Records of Ancient*

Coastal Upwelling. Plenum Press, New York, pp. 65–398.

Müller, P.J., Suess, E., 1979. Productivity, sedimentation rate, and sedimentary organic matter in the oceans—I. Organic carbon preservation. *Deep. Res.* 26, 1347–1362.

Naidu, P.D., Malmgren, B.A., 1996. A High-resolution record of Late Quaternary upwelling along the Oman Margin, Arabian Sea based on planktonic foraminifera. *Paleoceanography* 11, 129–140. <https://doi.org/10.1029/95PA03198>

Nelson, D.M., Tréguer, P., Brzezinski, M.A., Leynaert, A., Quéguiner, B., 1995. Production and dissolution of biogenic silica in the ocean: Revised global estimates, comparison with regional data and relationship to biogenic sedimentation. *Global Biogeochem. Cycles* 9, 359–372. <https://doi.org/10.1029/95GB01070>

Nooteboom, P.D., Bijl, P.K., Sebille, E. Van, Heydt, A.S. Von Der, Dijkstra, H.A., 2019. Transport bias by ocean currents in sedimentary microplankton assemblages: Implications for paleoceanographic reconstructions. *Paleogeography and Paleoclimatology*. <https://doi.org/10.1029/2019PA003606>

O'Malley, R., 2018. Online Data: Standard VGPM [WWW Document]. Ocean Product. URL <http://orca.science.oregonstate.edu/2160.by.4320.monthly.xyz.vgpm.m.chl.m.sst.php> (accessed 11.20.18).

Oksman, M., Kvorning, A.B., Larsen, S.H., Kjeldsen, K.K., Mankoff, K.D., Colgan, W., Andersen, T.J., Nørgaard-Pedersen, N., Seidenkrantz, M.-S., Mikkelsen, N., Ribeiro, S., 2022. Impact of freshwater runoff from the southwest Greenland Ice Sheet on fjord productivity since the late 19th century. *Cryosph.* 16, 2471–2491. <https://doi.org/doi.org/10.5194/tc-16-2471-2022>

Orr, J.C., Fabry, V.J., Aumont, O., Bopp, L., Doney, S.C., Feely, R.A., Gnanadesikan, A., Gruber, N., Ishida, A., Joos, F., Key, R.M., Lindsay, K., Maier-Reimer, E., Matear, R., Monfray, P., Mouchet, A., Najjar, R.G., Plattner, G.-K., Rodgers, K.B., Sabine, C.L., Sarmiento, J.L., Schlitzer, R., Slater, R.D., Totterdell, I.J., Weirig, M.-F., Yamanaka, Y., Yool, A., 2005. Anthropogenic ocean acidification over the twenty-first century and its impact on calcifying organisms. *Nature* 437, 681–6. <https://doi.org/10.1038/nature04095>

Paytan, A., Kastner, M., Chavez, F.P., 1996. Glacial to interglacial fluctuations in productivity in the equatorial Pacific as indicated by marine barite. *Science* (80-. ). 274, 1355–1357.

Perner, K., Moros, M., Jennings, A.E., Lloyd, J.M., Knudsen, K.L., 2013. Holocene palaeoceanographic evolution off West Greenland. *The Holocene* 23, 374–387. <https://doi.org/10.1177/0959683612460785>

Pospelova, V., de Vernal, A., Pedersen, T.F., 2008. Distribution of dinoflagellate cysts in surface sediments from the northeastern Pacific Ocean (43-25°N) in relation to sea-surface temperature, salinity, productivity and coastal upwelling. *Mar. Micropaleontol.* 68, 21–48. <https://doi.org/10.1016/j.marmicro.2008.01.008>

Radi, T., de Vernal, A., 2008. Dinocysts as proxy of primary productivity in mid-high latitudes of the Northern Hemisphere. *Mar. Micropaleontol.* 68, 84–114. <https://doi.org/10.1016/j.marmicro.2008.01.012>

Radi, T., de Vernal, A., 2004. Dinocyst distribution in surface sediments from the northeastern Pacific margin (40-60°N) in relation to hydrographic conditions, productivity and upwelling. *Rev. Palaeobot. Palynol.* 128, 169–193. [https://doi.org/10.1016/S0034-6667\(03\)00118-0](https://doi.org/10.1016/S0034-6667(03)00118-0)

Radi, T., de Vernal, A., Peyron, O., 2001. Relationships between dinoflagellate cyst assemblages in surface sediment and hydrographic conditions in the Bering and Chukchi seas. *J. Quat. Sci.* 16, 667–680. <https://doi.org/10.1002/jqs.652>

Ragueneau, O., Tréguer, P., Leynaert, A., Anderson, R.F., Brzezinski, M.A., DeMaster, D.J., Dugdale, R.C., Dymond, J., Fischer, G., François, R., Heinze, C., Maier-Reimer, E., Martin-Jézéquel, V., Nelson, D.M., Quéguiner, B., 2000. A review of the Si cycle in the modern ocean: recent progress and missing gaps in the application of biogenic opal as a paleoproductivity proxy. *Glob. Planet. Change* 26, 317–365. [https://doi.org/https://doi.org/10.1016/S0921-8181\(00\)00052-7](https://doi.org/https://doi.org/10.1016/S0921-8181(00)00052-7)

Rasmussen, S.O., Andersen, K.K., Svensson, A.M., Steffensen, J.P., Vinther, B.M., Clausen, H.B., Johnsen, S.J., Larsen, L.B., Bigler, M., Ro, R., Fischer, H., 2006. A new Greenland ice core chronology for the last glacial termination. *J. Geophys. Res. Atmos.* 111, 1–16. <https://doi.org/10.1029/2005JD006079>

- Renssen, H., Seppä, H., Crosta, X., Goosse, H., Roche, D.M., 2012. Global characterization of the Holocene Thermal Maximum. *Quat. Sci. Rev.* 48, 7–19. <https://doi.org/10.1016/j.quascirev.2012.05.022>
- Rochon, A., de Vernal, A., 1994. Palynomorph distribution in recent sediments from the Labrador Sea. *Can. J. Earth Sci.* 31, 115–127.
- Rochon, A., de Vernal, A., Turon, J.-L., Matthießen, J., Head, M.J., 1999a. Distribution of recent dinoflagellate cysts in surface sediments from the North Atlantic Ocean and adjacent seas in relation to sea-surface parameters. *Am. Assoc. Stratigr. Palynol. Contrib. Ser.* 35, 1–146.
- Rochon, A., de Vernal, A., Turon, J.-L., Matthießen, J., Head, M.J., 1999b. Distribution of recent dinoflagellate cysts in surface sediments from the North Atlantic Ocean and adjacent seas in relation to sea-surface. *Am. Assoc. Stratigr. Palynol. Contrib. Ser.* 35, 1–164.
- Rochon, A., Eynaud, F., de Vernal, A., 2008. Dinocysts as tracers of hydrographical conditions and productivity along the ocean margins: Introduction. *Mar. Micropaleontol.* 68, 1–5. <https://doi.org/10.1016/j.marmicro.2008.04.001>
- Rogge, A., Janout, M., Loginova, N., Trudnowska, E., Hörstmann, C., Wekerle, C., Oziel, L., Schourup-kristensen, V., Ruiz-castillo, E., Schulz, K., Povazhnyy, V. V., Iversen, M.H., 2023. Carbon dioxide sink in the Arctic Ocean from cross-shelf transport of dense Barents Sea water. *Nat. Geosci.* 16, 82–88. <https://doi.org/10.1038/s41561-022-01069-z>
- Rühlemann, C., Müller, P.J., Schneider, R.R., 1999. Organic Carbon and Carbonate as Paleoproductivity Proxies: Examples from High and Low Productivity Areas of the Tropical Atlantic, in: Fischer, G., Wefer, G. (Eds.), *Use of Proxies in Paleoceanography: Examples from the South Atlantic*. Springer Berlin Heidelberg, Berlin, Heidelberg, pp. 315–344. [https://doi.org/10.1007/978-3-642-58646-0\\_12](https://doi.org/10.1007/978-3-642-58646-0_12)
- Ruscio, B.A., Brubaker, M., Glasser, J., Hueston, W., Hennessy, T.W., 2015. One Health – a strategy for resilience in a changing arctic. *Int. J. Circumpolar Health* 74, 27913. <https://doi.org/10.3402/ijch.v74.27913>
- Sabine, C.L., Feely, R.A., Gruber, N., Key, R.M., Lee, K., Bullister, J.L., Wanninkhof, R., Wong, C.S., Wallace, D.W.R., Tilbrook, B., Millero, F.J., Peng, T.-H., Kozyr, A., Ono, T., Rios, A.F., 2004. The oceanic sink for anthropogenic CO<sub>2</sub>. *Science* 305, 367–71. <https://doi.org/10.1126/science.1097403>
- Saini, J., 2021. Holocene variability in sea ice, primary productivity and terrigenous input in Baffin Bay-Labrador Sea: A biomarker approach. Universität Bremen.
- Saini, J., Stein, R., Fahl, K., Weiser, J., Hebbeln, D., Hillaire, C., de Vernal, A., 2020. Holocene variability in sea ice and primary productivity in the northeastern Baffin Bay. *Arktos*. <https://doi.org/10.1007/s41063-020-00075-y>
- Sarnthein, M., Pflaumann, U., Ross, R., Tiedemann, R., Winn, K., 1992. Transfer functions to reconstruct ocean palaeoproductivity: a comparison. *Geol. Soc. London, Spec. Publ.* 64, 411–427. <https://doi.org/10.1144/GSL.SP.1992.064.01.27>
- Schlitzer, R., 2018. Ocean Data View.
- Schröder-Adams, C.J., van Rooyen, D., 2011. Response of recent benthic foraminiferal assemblages to contrasting environments in baffin bay and the northern labrador sea, Northwest Atlantic. *Arctic* 64, 317–341. <https://doi.org/10.14430/arctic4122>
- Seidenkrantz, M.S., Aagaard-Sørensen, S., Sulsbrück, H., Kuijpers, A., Jensen, K.G., Kunzendorf, H., 2007. Hydrography and climate of the last 4400 years in a SW Greenland fjord: Implications for Labrador Sea palaeoceanography. *Holocene* 17, 387–401. <https://doi.org/10.1177/0959683607075840>
- Sigman, D.M., Hain, M.P., Education, N., 2012. The Biological Productivity of the Ocean. *Nat. Educ.* 3, 1–16.
- Steinacher, M., Joos, F., Frölicher, T.L., Plattner, G.-K., Doney, S.C., 2009. Imminent ocean acidification in the Arctic projected with the NCAR global coupled carbon cycle-climate model. *Biogeosciences* 6, 515–533. <https://doi.org/10.5194/bg-6-515-2009>
- Susek, E., Zonneveld, K.A.F., Fischer, G., Versteegh, G.J.M., Willems, H., 2005. Organic-walled dinoflagellate cyst production in relation to upwelling intensity and lithogenic influx in the Cape Blanc

region (off north-west Africa). *Phycol. Res.* 53, 97–112. <https://doi.org/10.1111/j.1440-183.2005.00377.x>

Svendsen, J.I., Alexanderson, H., Astakhov, V.I., Demidov, I., Dowdeswell, J.A., Funder, S., Gataullin, V., Henriksen, M., Hjort, C., Houmark-Nielsen, M., Hubberten, H.W., Ingolfsson, O., Jakobsson, M., Kjaer, K.H., Larsen, E., Lokrantz, H., Lunkka, J.P., Lysa, A., Mangerud, J., Matiouchkov, A., Murray, A., Moller, P., Niessen, F., Nikolskaya, O., Polyak, L., Saarnisto, M., Siegert, C., Siegert, M.J., Spielhagen, R.F., Stein, R., 2004. Late Quaternary ice sheet history of northern Eurasia. *Quat. Sci. Rev.* 23, 1229–1271. <https://doi.org/10.1016/j.quascirev.2003.12.008>

Tang, C.C.L., Ross, C.K., Yao, T., Petrie, B., Detracey, B.M., Dunlap, E., 2004. The circulation, water masses and sea-ice of Baffin Bay. *Prog. Oceanogr.* 63, 183–228. <https://doi.org/10.1016/j.pocean.2004.09.005>

Taylor, F.J.R., 1987. The biology of dinoflagellates. *Bot. Monogr.* 21, 723–731.

ter Braak, C.J.F., 1986. Canonical Correspondence Analysis: A New Eigenvector Technique for Multivariate Direct Gradient Analysis. *Ecology* 67, 1167–1179.

Terhaar, J., Kwiatkowski, L., Bopp, L., 2020. Emergent constraint on Arctic Ocean acidification in the twenty-first century. *Nature* 582, 379–383. <https://doi.org/10.1038/s41586-020-2360-3>

Tremblay, J.É., Anderson, L.G., Matrai, P., Coupel, P., Bélanger, S., Michel, C., Reigstad, M., 2015. Global and regional drivers of nutrient supply, primary production and CO<sub>2</sub> drawdown in the changing Arctic Ocean. *Prog. Oceanogr.* 139, 171–196. <https://doi.org/10.1016/j.pocean.2015.08.009>

Turner, J.T., 2015. Zooplankton fecal pellets, marine snow, phytodetritus and the ocean's biological pump. *Prog. Oceanogr.* 130, 205–248.

Vénec-Peyré, M.-T., Caulet, J.-P., 2000. Paleoproductivity changes in the upwelling system of Socotra (Somali Basin, NW Indian Ocean) during the last 72,000 years: evidence from biological signatures. *Mar. Micropaleontol.* 40, 321–344. [https://doi.org/https://doi.org/10.1016/S0377-8398\(00\)00044-X](https://doi.org/https://doi.org/10.1016/S0377-8398(00)00044-X)

Vernal, A. De, Henry, M., Bilodeau, G., 2010. Micropaleontological preparation techniques and analyses, *Les Cahiers du GEOTOP*.

Volk, T., Hoffert, M.I., 1985. Ocean Carbon Pumps: Analysis of Relative Strength and Efficiencies in Ocean-Driven Atmospheric CO<sub>2</sub> Changes, in: *The Carbon Cycle and Atmospheric CO<sub>2</sub>: Natural Variations Archean to Present*. pp. 99–110.

von Breymann, M.T., Emeis, K.C., Suess, E., 1992. Water depth and diagenetic constraints on the use of barium as a palaeoproductivity indicator, in: Summerhayes, C.P., Prell, W.L., Emeis, K.C. (Eds.), *Upwelling Systems: Evolution since the Early Miocene*. Special Publication. Geological Society of London, London, pp. 273–284.

Wall, D., Dale, B., 1968. Modern Dinoflagellate Cysts and Evolution of the Peridiniales. *Micropaleontology* 14, 265–304.

Walsh, J.E., Chapman, W.L., 2001. 20th-century sea-ice variations from observational data. *Ann. Glaciol.* 33.

Wanner, H., Solomina, O., Grosjean, M., Ritz, S.P., Jetel, M., 2011. Structure and origin of Holocene cold events. *Quat. Sci. Rev.* 30, 3109–3123. <https://doi.org/10.1016/j.quascirev.2011.07.010>

Wassmann, P., Carmack, E.C., Bluhm, B.A., Duarte, C.M., Berge, J., Brown, K., Grebmeier, J.M., Holding, J., K. Kosobokova, R.K., Matrai, P., Agusti, S., Babin, M., Bhatt, U., Eicken, H., Polyakov, I., Rysgaard, S., Huntington, H.P., 2020. Towards a unifying pan-arctic perspective: A conceptual modelling toolkit. *Prog. Oceanogr.* 189. <https://doi.org/https://doi.org/10.1016/j.pocean.2020.102455>

Wassmann, P., Duarte, C.M., Agusti, S., Sejr, M.K., 2011. Footprints of climate change in the Arctic marine ecosystem. *Glob. Chang. Biol.* 17, 1235–1249. <https://doi.org/10.1111/j.1365-2486.2010.02311.x>

Wefer, G., Berger, W.H., Bijma, J., Fischer, G., 1999. Clues to Ocean History: a Brief Overview of Proxies, in: Fischer, Gerhard, Wefer, Gerold (Eds.), *Use of Proxies in Paleoceanography: Examples from the South Atlantic*. Springer Berlin Heidelberg, Berlin, Heidelberg, pp. 1–68. [https://doi.org/10.1007/978-3-642-58646-0\\_1](https://doi.org/10.1007/978-3-642-58646-0_1)

Weidick, A., Bennike, O., Citterio, M., Nørgaard-Pedersen, N., 2012. Neoglacial and historical glacier changes around Kangarsuneq fjord in southern West Greenland, Geological Survey of Denmark and

Greenland Bulletin. <https://doi.org/10.34194/geusb.v27.4694>

Yamamoto, A., Abe-Ouchi, A., Yamanaka, Y., 2018. Long-term response of oceanic carbon uptake to global warming via physical and biological pumps. *Biogeosciences* 15, 4163–4180. <https://doi.org/10.5194/bg-15-4163-2018>

Zamelczyk, K., Rasmussen, T.L., Husum, K., Hafliðason, H., de Vernal, A., Ravna, E.K., Hald, M., Hillaire-Marcel, C., 2012. Paleoceanographic changes and calcium carbonate dissolution in the central Fram Strait during the last 20ka. *Quat. Res. (United States)* 78, 405–416. <https://doi.org/10.1016/j.yqres.2012.07.006>

Zonneveld, K.A.F., Brummer, G.A., 2000. ( Palaeo- ) ecological signi " cance , transport and preservation of organic-walled dino # agellate cysts in the Somali Basin , NW Arabian Sea 47, 2229–2256.

Zonneveld, K.A.F., Siccha, M., 2016. Dinoflagellate cyst based modern analogue technique at test - A 300 year record from the Gulf of Taranto (Eastern Mediterranean). *Palaeogeogr. Palaeoclimatol. Palaeoecol.* 450, 17–37. <https://doi.org/10.1016/j.palaeo.2016.02.045>

Zonneveld, K.A.F., Versteegh, G., Kodrans-Nsiah, M., 2008. Preservation and organic chemistry of Late Cenozoic organic-walled dinoflagellate cysts: A review. *Mar. Micropaleontol.* 68, 179–197. <https://doi.org/10.1016/j.marmicro.2008.01.015>

Zonneveld, K.A.F., Versteegh, G.J.M., Kasten, S., Eglinton, T.I., Emeis, K., Huguet, C., Koch, B.P., 2010. Selective preservation of organic matter in marine environments; processes and impact on the sedimentary record. *Biogeosciences* 7, 483–511.